

World Journal of *Gastroenterology*

World J Gastroenterol 2024 August 7; 30(29): 3456-3540



EDITORIAL

- 3456 Effective roles of exercise and diet adherence in non-alcoholic fatty liver disease
Zhu W
- 3461 Gastroesophageal reflux following peroral endoscopic myotomy for achalasia: Bumps in the road to success
Itskoviz D, Malnick SDH

ORIGINAL ARTICLE**Observational Study**

- 3465 Diagnostic delay in inflammatory bowel diseases in a German population
Blüthner E, Dehe A, Büning C, Siegmund B, Prager M, Maul J, Krannich A, Preiß J, Wiedenmann B, Rieder F, Khedraki R, Tacke F, Sturm A, Schirbel A
- 3479 Prevalence of *Helicobacter pylori* infection among patients with esophageal carcinoma
López-Gómez M, Morales M, Fuerte R, Muñoz M, Delgado-López PD, Gómez-Cerezo JF, Casado E

Basic Study

- 3488 Leech *Poecilobdella manillensis* protein extract ameliorated hyperuricemia by restoring gut microbiota dysregulation and affecting serum metabolites
Liu X, Liang XQ, Lu TC, Feng Z, Zhang M, Liao NQ, Zhang FL, Wang B, Wang LS
- 3511 *Calculus bovis* inhibits M2 tumor-associated macrophage polarization via Wnt/ β -catenin pathway modulation to suppress liver cancer
Huang Z, Meng FY, Lu LZ, Guo QQ, Lv CJ, Tan NH, Deng Z, Chen JY, Zhang ZS, Zou B, Long HP, Zhou Q, Tian S, Mei S, Tian XF

LETTER TO THE EDITOR

- 3534 Defining failure of endoluminal biliary drainage in the era of endoscopic ultrasound and lumen apposing metal stents
Ali FS, Guha S
- 3538 Evaluating the role of large language models in inflammatory bowel disease patient information
Gong EJ, Bang CS

ABOUT COVER

Editorial Board Member of *World Journal of Gastroenterology*, Fabio Grizzi, PhD, Head, Histology Core, IRCCS Humanitas Research Hospital, Via Manzoni 56, Rozzano 20089, Milan, Italy. fabio.grizzi@humanitasresearch.it

AIMS AND SCOPE

The primary aim of *World Journal of Gastroenterology* (WJG, *World J Gastroenterol*) is to provide scholars and readers from various fields of gastroenterology and hepatology with a platform to publish high-quality basic and clinical research articles and communicate their research findings online. WJG mainly publishes articles reporting research results and findings obtained in the field of gastroenterology and hepatology and covering a wide range of topics including gastroenterology, hepatology, gastrointestinal endoscopy, gastrointestinal surgery, gastrointestinal oncology, and pediatric gastroenterology.

INDEXING/ABSTRACTING

The WJG is now abstracted and indexed in Science Citation Index Expanded (SCIE), MEDLINE, PubMed, PubMed Central, Scopus, Reference Citation Analysis, China Science and Technology Journal Database, and Superstar Journals Database. The 2024 edition of Journal Citation Reports® cites the 2023 journal impact factor (JIF) for WJG as 4.3; Quartile: Q1. The WJG's CiteScore for 2023 is 7.8.

RESPONSIBLE EDITORS FOR THIS ISSUE

Production Editor: *Hua-Ge Yu*; Production Department Director: *Xu Guo*; Cover Editor: *Jia-Ru Fan*.

NAME OF JOURNAL

World Journal of Gastroenterology

ISSN

ISSN 1007-9327 (print) ISSN 2219-2840 (online)

LAUNCH DATE

October 1, 1995

FREQUENCY

Weekly

EDITORS-IN-CHIEF

Andrzej S Tarnawski

EXECUTIVE ASSOCIATE EDITORS-IN-CHIEF

Xian-Jun Yu (Pancreatic Oncology), Jian-Gao Fan (Chronic Liver Disease), Hou-Bao Liu

EDITORIAL BOARD MEMBERS

<http://www.wjgnet.com/1007-9327/editorialboard.htm>

PUBLICATION DATE

August 7, 2024

COPYRIGHT

© 2024 Baishideng Publishing Group Inc

PUBLISHING PARTNER

Shanghai Pancreatic Cancer Institute and Pancreatic Cancer Institute, Fudan University
Biliary Tract Disease Institute, Fudan University

INSTRUCTIONS TO AUTHORS

<https://www.wjgnet.com/bpg/gcrinfo/204>

GUIDELINES FOR ETHICS DOCUMENTS

<https://www.wjgnet.com/bpg/GerInfo/287>

GUIDELINES FOR NON-NATIVE SPEAKERS OF ENGLISH

<https://www.wjgnet.com/bpg/gcrinfo/240>

PUBLICATION ETHICS

<https://www.wjgnet.com/bpg/GerInfo/288>

PUBLICATION MISCONDUCT

<https://www.wjgnet.com/bpg/gcrinfo/208>

POLICY OF CO-AUTHORS

<https://www.wjgnet.com/bpg/GerInfo/310>

ARTICLE PROCESSING CHARGE

<https://www.wjgnet.com/bpg/gcrinfo/242>

STEPS FOR SUBMITTING MANUSCRIPTS

<https://www.wjgnet.com/bpg/GerInfo/239>

ONLINE SUBMISSION

<https://www.f6publishing.com>

PUBLISHING PARTNER'S OFFICIAL WEBSITE

<https://www.shca.org.cn>
<https://www.zs-hospital.sh.cn>



Effective roles of exercise and diet adherence in non-alcoholic fatty liver disease

Wei Zhu

Specialty type: Gastroenterology and hepatology

Provenance and peer review: Invited article; Externally peer reviewed.

Peer-review model: Single blind

Peer-review report's classification

Scientific Quality: Grade C

Novelty: Grade C

Creativity or Innovation: Grade C

Scientific Significance: Grade B

P-Reviewer: Khayyat YM

Received: March 7, 2024

Revised: June 22, 2024

Accepted: July 1, 2024

Published online: August 7, 2024

Processing time: 143 Days and 15.4 Hours



Wei Zhu, School of Life Sciences and Technology, Tongji University, Shanghai 200092, China

Wei Zhu, Shanghai Xirong Information Science and Technology Co., Ltd., National Science and Technology Park, Tongji University, Shanghai 200092, China

Corresponding author: Wei Zhu, PhD, CEO, Postdoctoral Fellow, Researcher, School of Life Sciences and Technology, Tongji University, No. 1239 Siping Road, Yangpu District, Shanghai 200092, China. zhuwei8247@aliyun.com

Abstract

Non-alcoholic fatty liver disease (NAFLD) is characterized by symptoms of excessive fat accumulation and steatosis in the liver without alcohol intake in patients. The associated pathogenic mechanism is not completely understood and there are no specific drugs for patients with NAFLD. Exercise and diet adherence are the best options for the management of NAFLD patients. Questionnaire associated analysis models of adherence to these interventions are used to assess their effectiveness in the management of NAFLD patients using specificity, sensitivity, and so on. Studies have indicated that the relative ratio of NAFLD can be reduced by physical activity with diet control. In the future, the pathogenesis of NAFLD should be clarified with stratified efforts to develop appropriate drugs, and both exercise and diet adherence should be optimized using better questionnaire design and evaluation models for patients with NAFLD.

Key Words: Exercise and diet adherence; Non-alcoholic fatty liver disease; Delphi; Mediterranean diet; Physical lifestyle

©The Author(s) 2024. Published by Baishideng Publishing Group Inc. All rights reserved.

Core Tip: It is essential to reverse pathogenic syndromes before fibrosis occurs in patients with non-alcoholic fatty liver disease (NAFLD). Early diagnosis and appropriate interventions are important in NAFLD patients. Exercise and diet adherence may provide an effective treatment in patients with NAFLD.

Citation: Zhu W. Effective roles of exercise and diet adherence in non-alcoholic fatty liver disease. *World J Gastroenterol* 2024; 30(29): 3456-3460

URL: <https://www.wjgnet.com/1007-9327/full/v30/i29/3456.htm>

DOI: <https://dx.doi.org/10.3748/wjg.v30.i29.3456>

INTRODUCTION

Non-alcoholic fatty liver disease (NAFLD) affects approximately one third of the adult population worldwide, and is associated with a high risk of mortality when in combination with other serious syndromes such as cardiovascular diseases[1]. It is important to clarify various factors including environment, microbiome, metabolism, and genetics in predicting the progression and treatment outcome of NAFLD[2]. Obesity and insulin resistance can easily result in metabolic syndrome and inflammation, which could initiate the chronic progression of NAFLD to cirrhosis, and even hepatocellular carcinoma[3]. There are no specific drugs for NAFLD; therefore, it is meaningful to investigate the pathogenesis of NAFLD in order to provide information for drug development and other interventions. Hence, Zeng *et al*[4] evaluated the positive effect of exercise and diet adherence in patients with NAFLD as acceptable interventions.

The normal liver has the capacity to metabolize carbohydrates and fatty acids; however, fatty acids are commonly supplied or eliminated under abnormal conditions which results in endoplasmic reticulum stress and hepatocyte injury [5]. However, there is an important gap in the pathogenic mechanism between lipid metabolism symptoms and activated inflammatory progression of NAFLD[6]. One common explanation has indicated that gut microbiota disorder could trigger an abnormal immune microenvironment to mediate inflammatory responses in the liver in the presence of NAFLD. The lack of knowledge on the specific mechanism initiating NAFLD is hindering the development of effective drugs.

PATHOGENESIS OF NAFLD

NAFLD with insulin resistance has been shown to produce excessive fat accumulation and steatosis in the liver, which are classified as non-alcoholic fatty liver and non-alcoholic steatohepatitis (NASH), two distinct pathological conditions [7]. NAFLD is different from alcoholic liver disease which is associated with daily alcohol intake in patients. These diseases involve several different factors including costs, low predictive parameters, and risky liver biopsy, especially in patients aged > 50 years and those with type 2 diabetes mellitus[8]. In Figure 1, it can be seen that in hepatic steatosis, the uptake of free fatty acids, *de novo* lipogenesis, and fatty acid oxidation can result in excessive lipid accumulation in the liver. The outcomes of these metabolic syndromes in the liver can result in the export of very low-density lipoproteins into the blood circulation and the activation of inflammatory responses. In NAFLD, compensatory fatty acid oxidation and high lipid levels appear to damage subcellular functions of mitochondria, peroxisomes, and cytochromes, which also adversely affect other organs[9]. Additionally, liver oxidant/antioxidant imbalance can impair mitochondrial metabolism and possibly induce subsequent inflammation in NAFLD without a clear mechanism[10]. Despite advances in the pathogenesis of NAFLD being incomplete, one hypothesis of multiple hits is considered to explain the multiple insults in the development of NAFLD[11].

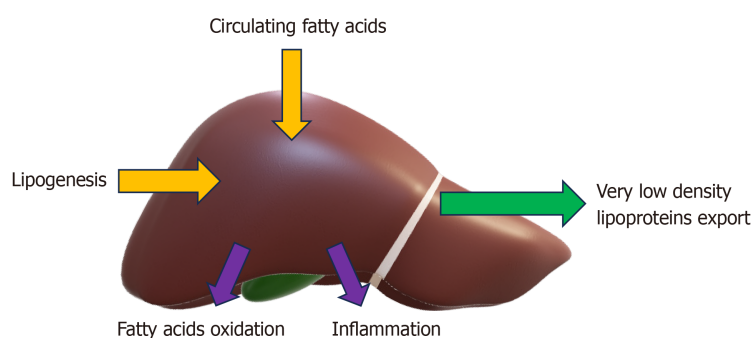


Figure 1 Dysregulation of liver function in non-alcoholic fatty liver disease.

EXERCISE AND DIET ADHERENCE IN NAFLD

Modifications of both physical activity and cognitive behavior were found to be beneficial in assisting patients with chronic diseases to overcome uncomfortable symptoms, and more than 60% of syndromes were inactive[12]. Urbanization in many Asian countries has promoted the prevalence of NAFLD due to sedentary lifestyle and overnutrition in around 25% of the population similar to many Western countries[13]. Zeng *et al*[4] reported that NAFLD

patients needed a positive change in their lifestyle, but few patients achieve improvements in weight reduction and persistent exercise and diet adherence. Therefore, the determination and perseverance in persistent exercise and diet adherence are critical in patients with NAFLD and chronic complications. Besides the role of exercise in these chronic diseases, an unhealthy diet such as excessive eating, smoking, and alcohol intake have a negative effect on life-expectancy and all-cause mortality rates[14]. Nutrition research has demonstrated that biological constituents have synergistic and/or antagonistic actions in human health beyond individual components[15]. An example is the Mediterranean diet which can prevent chronic diseases and premature mortality due to the dietary pattern and lifestyle in Mediterranean countries [16]. Clinically, many diseases including cardiovascular and neurodegenerative diseases and cancer have been associated with increasing age[16,17]. Similar to emerging non-communicative diseases, NAFLD commonly appears in diverse age groups especially in adults.

Although the accurate pathogenesis and standard treatment of NAFLD are not yet available, associated factors such as an unhealthy lifestyle is considered to elevate liver lipogenesis and microenvironment dysfunction. Hence, both the American Association for the Study of Liver Diseases and the National Institute for Health and Care Excellence guidelines recommended lifestyle modifications as the first choice for weight loss in patients with NAFLD[18,19]. Based on the results of Zeng *et al*[4], the efficacy of both exercise and diet adherence was high but only the specificity of diet adherence remained when compared to the control group. It is possible that diet adherence was easy to quantify and maintain, but sustaining exercise was difficult in patients aged > 50 years. In addition, instability of the composition of unsaturated fats could be improved by the high quantities of antioxidant compounds in foods. This study supported that complex food compositions were more beneficial than single or purified nutrients in the diet. The Mediterranean diet is recommended for NAFLD patients due to the presence of antioxidant compounds including polyphenols, carotenoids, fiber, and polyunsaturated fatty acids, which should be combined with physical activity[7]. It was reported that high adherence to the Mediterranean diet was associated with less liver damage and lower insulin resistance in patients with NAFLD[20]. Zeng *et al*[4] presented a similar conclusion on the effects of Mediterranean diet adherence, where exercise and diet adherence could greatly improve the clinical syndromes of patients with NAFLD.

REDUCED RATIO ANALYSIS OF NAFLD DUE TO MANAGEMENT

The Delphi method was used to collect opinions from experts with pooled intelligence and promote individual judgement on a particular field of research *via* a series of questionnaires[21]. In Table 1, this survey *via* different styles besides online interview was widely applied to gather primary data on patients with NAFLD and was displayed by Zeng *et al*[4] in their presentations[4,22-25]. The Pearson and Spearman correlation coefficients were used to analyze test-retest interval reliability, while exercise steps and reduced calorie intake were evaluated using the areas under the receiver operating characteristic curves. Different from these analysis methods, models of logistic, linear regression, and Cox proportional hazard were respectively applied to examine the odds, risk, and hazard ratios of combinations between physical activity and dietary adherence in NAFLD patients (Table 1). These ratios with confidence intervals were generally found to decrease after exercise and diet adherence in NAFLD patients. Hence, the establishment and validation of questionnaires with an appropriate analysis model are important for complete evaluation of the management of NAFLD patients.

Table 1 Reduced ratios of non-alcoholic fatty liver disease *via* exercise and diet adherence

Ref.	Period	Data	Management	Model	Index
Heredia <i>et al</i> [22]	2017-2018	Online interview	Physical activity; dietary intervention	Multivariable logistic regression	Odds ratio (OR) = 0.65, 95% confidence interval (CI): 0.42-0.99; OR = 0.60, 95%CI: 0.44-0.84
George <i>et al</i> [23]	2002-2012	Questionnaire survey	Mediterranean diet	Binary logistic regression	OR = 0.99, 95%CI: 0.85-0.94; OR = 0.87, 95%CI: 0.80-0.96
Bullón-Vela <i>et al</i> [24]	55-75 years	Questionnaire survey	Mediterranean diet (high legume) + physical activity	Linear regression analyses (tertiles 2, 3)	Relative risk ratio = 0.45, 95%CI: 0.22-0.92; Relative risk ratio = 0.48, 95%CI: 0.24-0.97
Petermann-Rocha <i>et al</i> [25]	10.2 years	Questionnaire survey	Mediterranean diet	Cox proportional hazard	Hazard ratio = 0.76, 95%CI: 0.62-0.94

FUTURE PERSPECTIVES

The spectrum of NAFLD ranges from early steatosis to both inflammation and fibrosis in liver disease, while the stage of NAFLD is critical in diagnosis and treatment planning. Currently, liver biopsy is the standard method for diagnosis, but this is invasive and expensive for patients with NAFLD. It was reported that serum markers and a scoring system have been identified for determination of NAFLD and NASH[26]. Therefore, the investigation of novel serum markers should be encouraged *via* multi-omics techniques for the diagnosis of NAFLD.

Lifestyle modification involving diet and exercise is the first choice in the management of NAFLD patients. Questionnaires can be optimized by stratifying and subgrouping according to the diverse characteristics of patients with NAFLD in the clinic. In addition to these efforts, there are several drugs for both diabetes and obesity, and antioxidants such as

vitamin E, pioglitazone, and metformin that could be used to prevent the progression of steatosis and fibrosis may be beneficial in patients with NAFLD[27,28]. Also, several signaling molecules are considered to be involved in the progression of NAFLD by mediating lipid and sugar metabolism. One example is the transforming growth factor-beta 1 signaling pathway, which was found to be associated with the pathogenic progression of NAFLD[26,29]. Hence, molecules associated with signaling pathways are potentially important candidates in the diagnosis and treatment of NAFLD in the future.

CONCLUSION

The pathogenesis of NAFLD from early steatosis to fibrosis is critical for treatment of the disease, but has not yet been completely elucidated. As the underlying mechanism of NAFLD is incompletely understood, this has resulted in a lack of appropriate drug treatment. Exercise and diet adherence have become an effective lifestyle modification and will hopefully improve the optimization of NAFLD treatment.

FOOTNOTES

Author contributions: Zhu W designed the study, wrote the manuscript, and prepared the figure and table, in addition to other associated work.

Supported by Natural Science Foundation of Shanghai, No. 17ZR1431400; and National Key R&D Program of China, No. 2017YFA0103902.

Conflict-of-interest statement: The authors have no competing interests related to this study.

Open-Access: This article is an open-access article that was selected by an in-house editor and fully peer-reviewed by external reviewers. It is distributed in accordance with the Creative Commons Attribution NonCommercial (CC BY-NC 4.0) license, which permits others to distribute, remix, adapt, build upon this work non-commercially, and license their derivative works on different terms, provided the original work is properly cited and the use is non-commercial. See: <https://creativecommons.org/licenses/by-nc/4.0/>

Country of origin: China

ORCID number: Wei Zhu 0000-0001-7523-7203.

S-Editor: Qu XL

L-Editor: Wang TQ

P-Editor: Zhao YQ

REFERENCES

- 1 Targher G, Byrne CD, Tilg H. NAFLD and increased risk of cardiovascular disease: clinical associations, pathophysiological mechanisms and pharmacological implications. *Gut* 2020; **69**: 1691-1705 [PMID: 32321858 DOI: 10.1136/gutjnl-2020-320622]
- 2 Friedman SL, Neuschwander-Tetri BA, Rinella M, Sanyal AJ. Mechanisms of NAFLD development and therapeutic strategies. *Nat Med* 2018; **24**: 908-922 [PMID: 29967350 DOI: 10.1038/s41591-018-0104-9]
- 3 Guo X, Yin X, Liu Z, Wang J. Non-Alcoholic Fatty Liver Disease (NAFLD) Pathogenesis and Natural Products for Prevention and Treatment. *Int J Mol Sci* 2022; **23** [PMID: 36555127 DOI: 10.3390/ijms232415489]
- 4 Zeng MH, Shi QY, Xu L, Mi YQ. Establishment and validation of an adherence prediction system for lifestyle interventions in non-alcoholic fatty liver disease. *World J Gastroenterol* 2024; **30**: 1393-1404 [PMID: 38596499 DOI: 10.3748/wjg.v30.i10.1393]
- 5 Mota M, Banini BA, Cazanave SC, Sanyal AJ. Molecular mechanisms of lipotoxicity and glucotoxicity in nonalcoholic fatty liver disease. *Metabolism* 2016; **65**: 1049-1061 [PMID: 26997538 DOI: 10.1016/j.metabol.2016.02.014]
- 6 Rong L, Zou J, Ran W, Qi X, Chen Y, Cui H, Guo J. Advancements in the treatment of non-alcoholic fatty liver disease (NAFLD). *Front Endocrinol (Lausanne)* 2022; **13**: 1087260 [PMID: 36726464 DOI: 10.3389/fendo.2022.1087260]
- 7 European Association for the Study of the Liver (EASL); European Association for the Study of Diabetes (EASD); European Association for the Study of Obesity (EASO). EASL-EASD-EASO Clinical Practice Guidelines for the management of non-alcoholic fatty liver disease. *J Hepatol* 2016; **64**: 1388-1402 [PMID: 27062661 DOI: 10.1016/j.jhep.2015.11.004]
- 8 Chalasani N, Younossi Z, Lavine JE, Diehl AM, Brunt EM, Cusi K, Charlton M, Sanyal AJ. The diagnosis and management of non-alcoholic fatty liver disease: practice Guideline by the American Association for the Study of Liver Diseases, American College of Gastroenterology, and the American Gastroenterological Association. *Hepatology* 2012; **55**: 2005-2023 [PMID: 22488764 DOI: 10.1002/hep.25762]
- 9 Ipsen DH, Lykkesfeldt J, Tveden-Nyborg P. Molecular mechanisms of hepatic lipid accumulation in non-alcoholic fatty liver disease. *Cell Mol Life Sci* 2018; **75**: 3313-3327 [PMID: 29936596 DOI: 10.1007/s00018-018-2860-6]
- 10 Barrea L, Verde L, Savastano S, Colao A, Muscogiuri G. Adherence to Mediterranean Diet: Any Association with NAFLD? *Antioxidants (Basel)* 2023; **12** [PMID: 37507858 DOI: 10.3390/antiox12071318]
- 11 Buzzetti E, Pinzani M, Tsochatzis EA. The multiple-hit pathogenesis of non-alcoholic fatty liver disease (NAFLD). *Metabolism* 2016; **65**:

- 1038-1048 [PMID: 26823198 DOI: 10.1016/j.metabol.2015.12.012]
- 12 **Marcus BH**, Dubbert PM, Forsyth LH, McKenzie TL, Stone EJ, Dunn AL, Blair SN. Physical activity behavior change: issues in adoption and maintenance. *Health Psychol* 2000; **19**: 32-41 [PMID: 10709946 DOI: 10.1037/0278-6133.19.suppl1.32]
 - 13 **Fan JG**, Kim SU, Wong VW. New trends on obesity and NAFLD in Asia. *J Hepatol* 2017; **67**: 862-873 [PMID: 28642059 DOI: 10.1016/j.jhep.2017.06.003]
 - 14 **Janssen F**, Trias-Llimós S, Kunst AE. The combined impact of smoking, obesity and alcohol on life-expectancy trends in Europe. *Int J Epidemiol* 2021; **50**: 931-941 [PMID: 33432332 DOI: 10.1093/ije/dyaa273]
 - 15 **Jacobs DR Jr**, Gross MD, Tapsell LC. Food synergy: an operational concept for understanding nutrition. *Am J Clin Nutr* 2009; **89**: 1543S-1548S [PMID: 19279083 DOI: 10.3945/ajcn.2009.26736B]
 - 16 **Dominguez LJ**, Di Bella G, Veronese N, Barbagallo M. Impact of Mediterranean Diet on Chronic Non-Communicable Diseases and Longevity. *Nutrients* 2021; **13** [PMID: 34204683 DOI: 10.3390/nu13062028]
 - 17 **Lynch J**, Smith GD. A life course approach to chronic disease epidemiology. *Annu Rev Public Health* 2005; **26**: 1-35 [PMID: 15760279 DOI: 10.1146/annurev.publhealth.26.021304.144505]
 - 18 **Chalasan N**, Younossi Z, Lavine JE, Charlton M, Cusi K, Rinella M, Harrison SA, Brunt EM, Sanyal AJ. The diagnosis and management of nonalcoholic fatty liver disease: Practice guidance from the American Association for the Study of Liver Diseases. *Hepatology* 2018; **67**: 328-357 [PMID: 28714183 DOI: 10.1002/hep.29367]
 - 19 **Glen J**, Floros L, Day C, Pryke R; Guideline Development Group. Non-alcoholic fatty liver disease (NAFLD): summary of NICE guidance. *BMJ* 2016; **354**: i4428 [PMID: 27605111 DOI: 10.1136/bmj.i4428]
 - 20 **Kontogianni MD**, Tileli N, Margariti A, Georgoulis M, Deutsch M, Tiniakos D, Fragopoulou E, Zafiropoulou R, Manios Y, Papatheodoridis G. Adherence to the Mediterranean diet is associated with the severity of non-alcoholic fatty liver disease. *Clin Nutr* 2014; **33**: 678-683 [PMID: 24064253 DOI: 10.1016/j.clnu.2013.08.014]
 - 21 **de Villiers MR**, de Villiers PJ, Kent AP. The Delphi technique in health sciences education research. *Med Teach* 2005; **27**: 639-643 [PMID: 16332558 DOI: 10.1080/13611260500069947]
 - 22 **Heredia NI**, Zhang X, Balakrishnan M, Daniel CR, Hwang JP, McNeill LH, Thrift AP. Physical activity and diet quality in relation to non-alcoholic fatty liver disease: A cross-sectional study in a representative sample of U.S. adults using NHANES 2017-2018. *Prev Med* 2022; **154**: 106903 [PMID: 34861339 DOI: 10.1016/j.ypmed.2021.106903]
 - 23 **George ES**, Georgousopoulou EN, Mellor DD, Chrysohoou C, Pitsavos C, Panagiotakos DB. Exploring the Path of Mediterranean Diet, Non-Alcoholic Fatty Liver Disease (NAFLD) and Inflammation towards 10-Year Cardiovascular Disease (CVD) Risk: The ATTICA Study 10-Year Follow-Up (2002-2012). *Nutrients* 2022; **14** [PMID: 35745097 DOI: 10.3390/nu14122367]
 - 24 **Bullón-Vela V**, Abete I, Tur JA, Pintó X, Corbella E, Martínez-González MA, Toledo E, Corella D, Macías M, Tinahones F, Fitó M, Estruch R, Ros E, Salas-Salvadó J, Daimiel L, Zulet MA, Martínez JA; PREDIMED Plus investigators. Influence of lifestyle factors and staple foods from the Mediterranean diet on non-alcoholic fatty liver disease among older individuals with metabolic syndrome features. *Nutrition* 2020; **71**: 110620 [PMID: 31838461 DOI: 10.1016/j.nut.2019.110620]
 - 25 **Petermann-Rocha F**, Carrasco-Marin F, Boonpor J, Parra-Soto S, Shannon O, Malcomson F, Phillips N, Jain M, Deo S, Livingstone KM, Dingle SE, Mathers JC, Forrest E, Ho FK, Pell JP, Celis-Morales C. Association of five diet scores with severe NAFLD incidence: A prospective study from UK Biobank. *Diabetes Obes Metab* 2024; **26**: 860-870 [PMID: 37997550 DOI: 10.1111/dom.15378]
 - 26 **Zhang C**, Yang M. Current Options and Future Directions for NAFLD and NASH Treatment. *Int J Mol Sci* 2021; **22** [PMID: 34299189 DOI: 10.3390/ijms22147571]
 - 27 **Sumida Y**, Yoneda M. Current and future pharmacological therapies for NAFLD/NASH. *J Gastroenterol* 2018; **53**: 362-376 [PMID: 29247356 DOI: 10.1007/s00535-017-1415-1]
 - 28 **Clayton-Chubb D**, Kemp W, Majeed A, Lubel JS, Hodge A, Roberts SK. Understanding NAFLD: From Case Identification to Interventions, Outcomes, and Future Perspectives. *Nutrients* 2023; **15** [PMID: 36771394 DOI: 10.3390/nu15030687]
 - 29 **Liu D**, Wang K, Li K, Xu R, Chang X, Zhu Y, Sun P, Han X. Ets-1 deficiency alleviates nonalcoholic steatohepatitis via weakening TGF-β1 signaling-mediated hepatocyte apoptosis. *Cell Death Dis* 2019; **10**: 458 [PMID: 31189885 DOI: 10.1038/s41419-019-1672-4]

Gastroesophageal reflux following peroral endoscopic myotomy for achalasia: Bumps in the road to success

David Itskoviz, Stephen David Howard Malnick

Specialty type: Gastroenterology and hepatology

Provenance and peer review: Invited article; Externally peer reviewed.

Peer-review model: Single blind

Peer-review report's classification

Scientific Quality: Grade D

Novelty: Grade C

Creativity or Innovation: Grade C

Scientific Significance: Grade C

P-Reviewer: Kawahara H

Received: March 10, 2024

Revised: May 16, 2024

Accepted: July 10, 2024

Published online: August 7, 2024

Processing time: 140 Days and 19.3 Hours



David Itskoviz, Kaplan Medical Center, Institute of Gastroenterology and Hepatology, Hebrew University Medical School of Jerusalem, Rehovot 76100, Israel

Stephen David Howard Malnick, Kaplan Medical Center, Department of Internal Medicine C, Hebrew University Medical School of Jerusalem, Rehovot 76100, Israel

Corresponding author: David Itskoviz, MD, Doctor, Kaplan Medical Center, Institute of Gastroenterology and Hepatology, Hebrew University Medical School of Jerusalem, Pasternak Street, Rehovot 76100, Israel. dudyi@clalit.org.il

Abstract

Achalasia can significantly impair the quality of life. The clinical presentation typically includes dysphagia to both solids and liquids, chest pain, and regurgitation. Diagnosis can be delayed in patients with atypical presentations, and they might receive a wrong diagnosis, such as gastroesophageal reflux disease (GERD), owing to overlapping symptoms of both disorders. Although the cause of achalasia is poorly understood, its impact on the motility of the esophagus and gastroesophageal junction is well established. Several treatment modalities have been utilized, with the most common being surgical Heller myotomy with concomitant fundoplication and pneumatic balloon dilatation. Recently, peroral endoscopic myotomy (POEM) has gained popularity as an effective treatment for achalasia, despite a relatively high incidence of GERD occurring after treatment compared to other modalities. The magnitude of post-POEM GERD depends on its definition and is influenced by patient and procedure-related factors. The long-term sequelae of post-POEM GERD are yet to be determined, but it appears to have a benign course and is usually manageable with clinically available modalities. Identifying risk factors for post-POEM GERD and modifying the POEM procedure in selected patients may improve the overall success of this technique.

Key Words: Achalasia; Per-oral endoscopic myotomy; Gastroesophageal reflux; Pneumatic dilatation; Heller myotomy; Proton pump inhibitor; Acidic fermentation

©The Author(s) 2024. Published by Baishideng Publishing Group Inc. All rights reserved.

Core Tip: Peroral endoscopic myotomy (POEM) is a valuable treatment for achalasia, although the occurrence of gastroesophageal reflux disease (GERD) following this procedure is a major concern among patients and caregivers. In this editorial, we will address the true meaning of acidic reflux after POEM, discuss the factors that need to be taken into account to prevent post-POEM GERD, and outline the treatment options available when it occurs.

Citation: Itskoviz D, Malnick SDH. Gastroesophageal reflux following peroral endoscopic myotomy for achalasia: Bumps in the road to success. *World J Gastroenterol* 2024; 30(29): 3461-3464

URL: <https://www.wjgnet.com/1007-9327/full/v30/i29/3461.htm>

DOI: <https://dx.doi.org/10.3748/wjg.v30.i29.3461>

INTRODUCTION

Achalasia is a rare esophageal motility disorder, with a reported incidence of approximately 1 per 100000 persons per year. The clinical presentation typically includes dysphagia to both solids and liquids, chest pain, and regurgitation. Diagnosis may also be delayed or mistaken as gastroesophageal reflux disease (GERD) owing to atypical presentations or overlapping symptoms.

DIAGNOSIS AND TREATMENT

The etiology of achalasia is still unknown, but the pathophysiology is characterized by impaired lower esophageal sphincter relaxation with concomitant peristalsis dysfunction in the esophageal smooth muscles. The diagnosis involves careful consideration of the clinical scenario, together with the results of esophagogastroduodenoscopy, contrast esophagogram, and high-resolution manometry (HRM). The gold standard for diagnosing achalasia is HRM, as it allows an objective and reproducible measurement of dynamic esophageal pressure over time and space. This technique also enables the subcategorization of patients with achalasia into different subtypes according to the Chicago Classification 4.0.

Functional lumen imaging probe (FLIP or endoFLIP) is a high-resolution impedance system that measures esophageal distensibility and has a good correlation with HRM. FLIP is performed during sedated esophagogastroduodenoscopy. It has the advantage of aiding diagnosis in patients intolerant of HRM and providing immediate feedback on the effectiveness of treatment.

Treatment goals for achalasia center on the main pathophysiological issue: impaired relaxation of the lower esophageal sphincter. Pharmacological treatment options have proven to be ineffective, except for endoscopic botulinum toxin injections at the lower esophageal sphincter, which have only short-lived effectiveness. The classic treatment for achalasia has been either pneumatic dilatation of the esophagus or Heller myotomy performed surgically, usually with concomitant creation of a gastric fundoplication[1-4].

In 2010, Inoue and Kudo[5] published their experience with 43 achalasia patients treated with peroral endoscopic myotomy (POEM). Since then, this approach has gained popularity as a treatment modality for achalasia patients. POEM is performed under endoscopic guidance by creating a submucosal tunnel in the esophagus and stomach cardia and selectively dissecting the muscle fibers in that tunnel. While POEM is considered an effective and safe procedure, the development of post-POEM GERD remains a challenge. In surgical myotomy, the anti-reflux mechanism is partially restored by creating a fundoplication, but this is not the case in the classical POEM procedure.

POST-POEM GERD

Nabi *et al*[1] have comprehensively reviewed the clinical significance and approach to post-POEM GERD. The first question addressed is how to define post-POEM GERD. Should we rely on patient-reported symptoms, objectively look for esophagitis and measure esophageal exposure to acid, or perhaps combine all of the above outcomes?

A significant number of post-POEM patients show evidence of esophageal acid exposure, but most remain asymptomatic. Moreover, even in patients with proven esophageal acid exposure, the incidence of severe esophagitis is relatively low[6,7]. Dewitt *et al*[8] recently described a cohort of 149 patients who underwent POEM and were followed up after at least 6 months with pH-metry. They found that a positive reflux symptom association was as low as 17.1%-20.9% in symptomatic patients. Karyampudi *et al*[9] compared 50 patients with post-POEM GERD to those with non-achalasia-related GERD and found a positive reflux symptom association in only 6% of post-POEM GERD patients compared to 56% in the control group. It is also important to note that the documentation of an acidic environment in the post-POEM esophagus can be related to acidic fermentation secondary to motility disturbances and food stasis and not to actual acid reflux from the stomach. The incidence of actual acid reflux is significantly less evident when we examine the acid exposure pattern in these patients[10,11].

The second question that arises is regarding the clinical significance of post-POEM GERD besides the patients' symptoms. Given that POEM is a relatively new procedure, the available data are limited, and yet, it appears that the development of GERD-related complications, such as Barrett's esophagus and peptic strictures, is infrequent. It is estimated that even these uncommon complications can be avoided with readily available drugs such as proton pump inhibitors and, possibly, potassium-competitive acid blockers[6,12].

Shiwaku *et al*[13] found a 7.5% incidence of severe reflux esophagitis in a cohort of 2905 patients who underwent POEM. They found an association between the development of severe reflux esophagitis and older age (> 65 years), previous achalasia treatments, an Eckardt score ≥ 7 , sigmoid-type achalasia, and long (> 10 cm) myotomy. Another retrospective study involving 183 post-POEM patients reported an incidence of severe GERD in 19.5% of patients[14]. A recent systematic review and meta-analysis of 11 studies, including 2342 post-POEM patients with a median follow-up of 48 months, reported only 3 cases of significant reflux-related consequences, such as Barrett's esophagus and peptic stricture[15].

The third question is whether we can predict which patients are prone to develop post-POEM GERD, and, if so, whether we can offer them any preventive measures. Nabi *et al*[1] address several risk factors in their review, such as obesity, female sex, and the presence of a hiatal hernia. In addition, they discuss several technical aspects of the procedure that might mitigate the risk of post-POEM GERD, such as limiting the length of the gastric myotomy, preserving the sling fibers during myotomy, and even combining the creation of a gastric fundoplication during the POEM procedure *via* the natural orifice transluminal endoscopic surgery approach, which appears to be safe and effective in experienced hands, although its generalizability is yet to be determined[16-18].

The fourth and last question is how easily we can treat patients with post-POEM GERD. It appears that the primary treatment regimen is similar to that for any other GERD patients, involving proton pump inhibitors. This well-known class of drugs seems to work well in post-POEM GERD patients. Other more instrumental methods to treat GERD are also effective and available. A recent review of eight studies including 3568 patients found that treatment using proton pump inhibitors is effective and leads to complete resolution of symptoms in most post-POEM patients dealing with GERD[19].

CONCLUSION

POEM is an effective treatment for achalasia patients, but GERD remains an important side effect of this procedure. Defining the true incidence and impact of GERD in post-POEM patients can be challenging. However, by identifying specific risk factors in our patients and refining the POEM procedure accordingly, we can make the road to success in treating achalasia a little smoother.

FOOTNOTES

Author contributions: Itskoviz D reviewed the literature and wrote the editorial draft; Malnick SDH reviewed the literature, and reviewed and edited the manuscript.

Conflict-of-interest statement: The authors do not have any conflicts of interest to declare.

Open-Access: This article is an open-access article that was selected by an in-house editor and fully peer-reviewed by external reviewers. It is distributed in accordance with the Creative Commons Attribution NonCommercial (CC BY-NC 4.0) license, which permits others to distribute, remix, adapt, build upon this work non-commercially, and license their derivative works on different terms, provided the original work is properly cited and the use is non-commercial. See: <https://creativecommons.org/licenses/by-nc/4.0/>

Country of origin: Israel

ORCID number: David Itskoviz 0000-0001-5776-5643; Stephen David Howard Malnick 0000-0003-1865-8313.

S-Editor: Fan JR

L-Editor: Filipodia

P-Editor: Yu HG

REFERENCES

- 1 Nabi Z, Inavolu P, Duvvuru NR. Prediction, prevention and management of gastroesophageal reflux after per-oral endoscopic myotomy: An update. *World J Gastroenterol* 2024; **30**: 1096-1107 [PMID: 38577183 DOI: 10.3748/wjg.v30.i9.1096]
- 2 Vaezi MF, Pandolfino JE, Yadlapati RH, Greer KB, Kavitt RT. ACG Clinical Guidelines: Diagnosis and Management of Achalasia. *Am J Gastroenterol* 2020; **115**: 1393-1411 [PMID: 32773454 DOI: 10.14309/ajg.0000000000000731]
- 3 Khashab MA, Vela MF, Thosani N, Agrawal D, Buxbaum JL, Abbas Fehmi SM, Fishman DS, Gurudu SR, Jamil LH, Jue TL, Kannadath BS, Law JK, Lee JK, Naveed M, Qumseya BJ, Sawhney MS, Yang J, Wani S. ASGE guideline on the management of achalasia. *Gastrointest Endosc* 2020; **91**: 213-227.e6 [PMID: 31839408 DOI: 10.1016/j.gie.2019.04.231]

- 4 **Oude Nijhuis RAB**, Zaninotto G, Roman S, Boeckxstaens GE, Fockens P, Langendam MW, Plumb AA, Smout A, Targarona EM, Trukhmanov AS, Weusten B, Bredenoord AJ. European guidelines on achalasia: United European Gastroenterology and European Society of Neurogastroenterology and Motility recommendations. *United European Gastroenterol J* 2020; **8**: 13-33 [PMID: [32213062](#) DOI: [10.1177/2050640620903213](#)]
- 5 **Inoue H**, Kudo SE. [Per-oral endoscopic myotomy (POEM) for 43 consecutive cases of esophageal achalasia]. *Nihon Rinsho* 2010; **68**: 1749-1752 [PMID: [20845759](#)]
- 6 **Modayil RJ**, Zhang X, Rothberg B, Kollarus M, Galibov I, Peller H, Taylor S, Brathwaite CE, Halwan B, Grendell JH, Stavropoulos SN. Peroral endoscopic myotomy: 10-year outcomes from a large, single-center U.S. series with high follow-up completion and comprehensive analysis of long-term efficacy, safety, objective GERD, and endoscopic functional luminal assessment. *Gastrointest Endosc* 2021; **94**: 930-942 [PMID: [33989646](#) DOI: [10.1016/j.gie.2021.05.014](#)]
- 7 **Abu-Nuwar MR**, Eriksson S, Zheng P, Jobe B, Ayazi S. Gastroesophageal Reflux after Peroral Endoscopic Myotomy: An Assessment of Incidence and Predisposing Factor. *J Am Coll Surg* 2022; **235**: S22-S22 [DOI: [10.1097/01.xcs.0000893056.72245.c2](#)]
- 8 **DeWitt JM**, Kessler WR, Wo JM, Stainko S, Perkins A, Dickason D, Al-Haddad MA, Siwec R. Symptom Association for Gastroesophageal Reflux Disease by pH Monitoring After Peroral Endoscopic Myotomy. *Am J Gastroenterol* 2022; **117**: 1316-1319 [PMID: [35467562](#) DOI: [10.14309/ajg.0000000000001801](#)]
- 9 **Karyampudi A**, Nabi Z, Ramchandani M, Darisetty S, Goud R, Chavan R, Kalapala R, Rao GV, Reddy DN. Gastroesophageal reflux after per-oral endoscopic myotomy is frequently asymptomatic, but leads to more severe esophagitis: A case-control study. *United European Gastroenterol J* 2021; **9**: 63-71 [PMID: [32723068](#) DOI: [10.1177/2050640620947645](#)]
- 10 **Ramchandani M**, Pal P, Singla N, Reddy DN. Post-per-oral endoscopic myotomy heartburn: It's not always reflux: Expert review. *Dig Endosc* 2022; **34**: 325-333 [PMID: [34390053](#) DOI: [10.1111/den.14106](#)]
- 11 **Singh AP**, Singla N, Budhwani E, Januszewicz W, Memon SF, Inavolu P, Nabi Z, Jagtap N, Kalapala R, Lakhtakia S, Darisetty S, Reddy DN, Ramchandani M. Defining "true acid reflux" after peroral endoscopic myotomy for achalasia: a prospective cohort study. *Gastrointest Endosc* 2024; **99**: 166-173.e3 [PMID: [37598862](#) DOI: [10.1016/j.gie.2023.08.008](#)]
- 12 **Nabi Z**, Ramchandani M, Kotla R, Tandan M, Goud R, Darisetty S, Rao GV, Reddy DN. Gastroesophageal reflux disease after peroral endoscopic myotomy is unpredictable, but responsive to proton pump inhibitor therapy: a large, single-center study. *Endoscopy* 2020; **52**: 643-651 [PMID: [32208499](#) DOI: [10.1055/a-1133-4354](#)]
- 13 **Shiwaku H**, Sato H, Shimamura Y, Abe H, Shiota J, Sato C, Ominami M, Sakae H, Hata Y, Fukuda H, Ogawa R, Nakamura J, Tatsuta T, Ikebuchi Y, Yokomichi H, Hasegawa S, Inoue H. Risk factors and long-term course of gastroesophageal reflux disease after peroral endoscopic myotomy: A large-scale multicenter cohort study in Japan. *Endoscopy* 2022; **54**: 839-847 [PMID: [35172368](#) DOI: [10.1055/a-1753-9801](#)]
- 14 **Rassoul Abu-Nuwar M**, Eriksson SE, Sarici IS, Zheng P, Hoppo T, Jobe BA, Ayazi S. GERD after Peroral Endoscopic Myotomy: Assessment of Incidence and Predisposing Factors. *J Am Coll Surg* 2023; **236**: 58-70 [PMID: [36519909](#) DOI: [10.1097/XCS.000000000000448](#)]
- 15 **Vespa E**, Pellegatta G, Chandrasekar VT, Spadaccini M, Patel H, Maselli R, Galtieri PA, Cariani E, Sharma P, Hassan C, Repici A. Long-term outcomes of peroral endoscopic myotomy for achalasia: a systematic review and meta-analysis. *Endoscopy* 2023; **55**: 167-175 [PMID: [35798336](#) DOI: [10.1055/a-1894-0147](#)]
- 16 **Gu L**, Ouyang Z, Lv L, Liang C, Zhu H, Liu D. Safety and efficacy of peroral endoscopic myotomy with standard myotomy versus short myotomy for treatment-naïve patients with type II achalasia: a prospective randomized trial. *Gastrointest Endosc* 2021; **93**: 1304-1312 [PMID: [33058884](#) DOI: [10.1016/j.gie.2020.10.006](#)]
- 17 **Tanaka S**, Toyonaga T, Kawara F, Watanabe D, Hoshi N, Abe H, Ariyoshi R, Ohara Y, Takao T, Morita Y, Umegaki E, Kodama Y. Novel per-oral endoscopic myotomy method preserving oblique muscle using two penetrating vessels as anatomic landmarks reduces postoperative gastroesophageal reflux. *J Gastroenterol Hepatol* 2019; **34**: 2158-2163 [PMID: [31373050](#) DOI: [10.1111/jgh.14814](#)]
- 18 **Attaar M**, Su B, Wong HJ, Kuchta K, Denham W, Haggerty SP, Linn J, Ujiki MB. Intraoperative impedance planimetry (EndoFLIP™) results and development of esophagitis in patients undergoing peroral endoscopic myotomy (POEM). *Surg Endosc* 2021; **35**: 4555-4562 [PMID: [32789722](#) DOI: [10.1007/s00464-020-07876-y](#)]
- 19 **Nagi TK**, Suarez ZK, Haider MA, Holder SS, Vallejo C, Chaudhari SS. Per-Oral Endoscopic Myotomy-Induced Gastroesophageal Reflux Disease and Review of the Efficacy of Proton Pump Inhibitors as a Management Strategy: Review of the Literature. *Cureus* 2023; **15**: e50324 [PMID: [38205455](#) DOI: [10.7759/cureus.50324](#)]

Observational Study

Diagnostic delay in inflammatory bowel diseases in a German population

Elisabeth Blüthner, Annalena Dehe, Carsten Büning, Britta Siegmund, Matthias Prager, Jochen Maul, Alexander Krannich, Jan Preiß, Bertram Wiedenmann, Florian Rieder, Raneem Khedraki, Frank Tacke, Andreas Sturm, Anja Schirbel

Specialty type: Gastroenterology and hepatology

Provenance and peer review: Unsolicited article; Externally peer reviewed.

Peer-review model: Single blind

Peer-review report's classification
Scientific Quality: Grade C, Grade C

Novelty: Grade B, Grade B

Creativity or Innovation: Grade B, Grade B

Scientific Significance: Grade B, Grade B

P-Reviewer: Tang G; Xu L

Received: February 10, 2024

Revised: April 28, 2024

Accepted: June 18, 2024

Published online: August 7, 2024

Processing time: 169 Days and 16.1 Hours



Elisabeth Blüthner, Annalena Dehe, Carsten Büning, Britta Siegmund, Matthias Prager, Jochen Maul, Alexander Krannich, Jan Preiß, Bertram Wiedenmann, Florian Rieder, Raneem Khedraki, Frank Tacke, Andreas Sturm, Anja Schirbel, Department of Hepatology and Gastroenterology, Campus Virchow-Klinikum and Campus Charité Mitte, Charité-Universitätsmedizin Berlin, Berlin 10117, Germany

Annalena Dehe, Department of Gastroenterology, Vivantes Klinikum im Friedrichshain, Berlin 10249, Germany

Carsten Büning, Department of Internal Medicine, Krankenhaus Waldfriede, Berlin 14163, Germany

Britta Siegmund, Department of Gastroenterology, Infectious Diseases and Rheumatology, Charité-Universitätsmedizin Berlin, Berlin 12203, Germany

Matthias Prager, Praxis für Gastroenterologie Berlin Zehlendorf, Berlin 14195, Germany

Jochen Maul, Gastroenterologie am Bayrischen Platz, Berlin 10825, Germany

Alexander Krannich, Clinical Trial Office, Charité-Universitätsmedizin Berlin, Berlin 10117, Germany

Jan Preiß, Department of Gastroenterology, Diabetology and Hepatology, Vivantes Klinikum Neukölln, Berlin 10117, Germany

Florian Rieder, Raneem Khedraki, Department of Gastroenterology, Hepatology and Nutrition, Digestive Diseases and Surgery Institute, The Cleveland Clinic Foundation, Cleveland, OH 44195, United States

Andreas Sturm, Department of Internal Medicine, DRK Kliniken Berlin Westend, Berlin 14050, Germany

Anja Schirbel, Gastroenterologie im Havelland, Straße der Einheit, Falkensee 14612, Germany

Corresponding author: Anja Schirbel, MD, Doctor, Research Scientist, Department of Hepatology and Gastroenterology, Campus Virchow-Klinikum and Campus Charité Mitte, Charité-Universitätsmedizin Berlin, Charitéplatz 1, Berlin 10117, Germany.

Abstract

BACKGROUND

Early diagnosis is key to prevent bowel damage in inflammatory bowel disease (IBD). Risk factor analyses linked with delayed diagnosis in European IBD patients are scarce and no data in German IBD patients exists.

AIM

To identify risk factors leading to prolonged diagnostic time in a German IBD cohort.

METHODS

Between 2012 and 2022, 430 IBD patients from four Berlin hospitals were enrolled in a prospective study and asked to complete a 16-item questionnaire to determine features of the path leading to IBD diagnosis. Total diagnostic time was defined as the time from symptom onset to consulting a physician (patient waiting time) and from first consultation to IBD diagnosis (physician diagnostic time). Univariate and multivariate analyses were performed to identify risk factors for each time period.

RESULTS

The total diagnostic time was significantly longer in Crohn's disease (CD) compared to ulcerative colitis (UC) patients (12.0 *vs* 4.0 mo; $P < 0.001$), mainly due to increased physician diagnostic time (5.5 *vs* 1.0 mo; $P < 0.001$). In a multivariate analysis, the predominant symptoms diarrhea ($P = 0.012$) and skin lesions ($P = 0.028$) as well as performed gastroscopy ($P = 0.042$) were associated with longer physician diagnostic time in CD patients. In UC, fever was correlated ($P = 0.020$) with shorter physician diagnostic time, while fatigue ($P = 0.011$) and positive family history ($P = 0.046$) were correlated with longer physician diagnostic time.

CONCLUSION

We demonstrated that CD patients compared to UC are at risk of long diagnostic delay. Future efforts should focus on shortening the diagnostic delay for a better outcome in these patients.

Key Words: Diagnostic time; Diagnostic delay; Crohn's disease; Ulcerative colitis; Germany

©The Author(s) 2024. Published by Baishideng Publishing Group Inc. All rights reserved.

Core tip: Early diagnosis is key to reducing complications and improving response to medical therapy. This prospective questionnaire-based study aimed to identify risk factors impairing diagnostic time. We demonstrated that diagnostic delay was significantly longer in Crohn's disease than in ulcerative colitis and was mainly physician dependent. The multivariate analysis showed that disease-specific symptoms and rapidly available diagnostic tools resulted in reduction of physician diagnostic time.

Citation: Blüthner E, Dehe A, Büning C, Siegmund B, Prager M, Maul J, Krannich A, Preiß J, Wiedenmann B, Rieder F, Khedraki R, Tacke F, Sturm A, Schirbel A. Diagnostic delay in inflammatory bowel diseases in a German population. *World J Gastroenterol* 2024; 30(29): 3465-3478

URL: <https://www.wjgnet.com/1007-9327/full/v30/i29/3465.htm>

DOI: <https://dx.doi.org/10.3748/wjg.v30.i29.3465>

INTRODUCTION

Crohn's disease (CD) and ulcerative colitis (UC) are the most common forms of inflammatory bowel disease (IBD). IBD is defined as destructive inflammatory disorder of the gastrointestinal tract resulting in chronic relapsing–remitting disease courses. IBD manifests primarily in the intestine but may also have extraintestinal manifestation (EIM). IBD has been shown to be associated with various autoimmune diseases that impact other organs or systems[1,2]. Due to its heterogeneous, nonspecific clinical presentation, and poor diagnostic precision of existing biomarker tests, diagnosis of IBD can be challenging and often results in a prolonged time from symptom onset to an established and correct diagnosis[3,4]. The median delay in diagnosis ranges from 5.0 to 9.5 months for CD and 3.1 to 4.0 months for UC, likely due to different medical standards and regional differences in disease behavior[4-7].

However, prompt diagnosis and treatment of these patients is critical. Recently published studies showed that early therapeutic intervention reduced the need for surgery, as well as severe disease progression with complications[5,8]. Early intensive treatment has been associated with improved responses to immunomodulators or targeted biologic

therapy[9]. Diagnostic delay affects patients' quality of life and the burden on the healthcare system[10]. Therefore, awareness of risk factors for delayed diagnosis in IBD patients is imperative.

It is noteworthy that most of the studies have evaluated the total diagnostic delay, whereas studies that systematically evaluate the time patients spend before consulting a physician as well as the time the physician takes to establish an IBD diagnosis separately are scarce[4,11]. Most of the studies were performed in countries with different medical provider systems and hence lack generalizability. Results from Central Europe are lacking [4,6,8,11,12]. Considering the east-west gradient in the incidence of IBD, more research is required on this clinical problem[13]. Therefore, we aimed to comprehensively assess risk factors for delayed diagnosis in a German IBD cohort to enhance our management of IBD patients.

MATERIALS AND METHODS

Study design

From May 2012 to May 2022, 513 patients with IBD were enrolled in this descriptive cross-sectional, questionnaire-based evaluation study at the IBD outpatient clinic.

The patients were recruited at the three hospital sites at the Charité-Universitätsmedizin Berlin (42.3% at Charité-Campus Mitte, 28.4% at Charité-Virchow Klinikum, 26.0% at Charité-Benjamin Franklin) and at Krankenhaus Waldfriede Berlin-Zehlendorf (18%). We included adult patients (no upper age limit) with confirmed CD or UC diagnosis for at least 6 months with completed questionnaires and excluded patients who were unable to consent due to mental incapacity or language barriers as well as the diagnosis of indeterminate colitis. Study participants were interviewed once after written informed consent was obtained. A total of 430 patients were enrolled in the study. Fifty-four patients did not complete the questionnaire, 15 were excluded because of a diagnosis of indeterminate colitis, three were excluded because of a diagnosis of irritable bowel syndrome (IBS), four did not sign the informed consent form correctly, and seven were excluded because of duplicate entries. A total of 430 (83.3%) adult patients were analyzed for this study.

The study was approved by the local ethics committee (EA2/170/11) and was conducted in accordance with the ethical standards of the Declaration of Helsinki of 1964 and its latest revision of 2013. The study protocol is also compliant with the STROBE criteria[14].

Questionnaire

The administered questionnaire contained 16 questions that investigated demographic and disease-specific factors, which may directly or indirectly play a role for the delay of diagnosis. In addition to patient age and gender, urban or rural residence, medical history (predominant symptoms and general symptoms at diagnosis), severity of symptoms, location of disease, method of IBD diagnosis, and whether the patient had affected family members or had ever heard of IBD, were recorded. EIMs were defined as the presence of ankylosing spondylitis, aphthous stomatitis, erythema nodosum, peripheral arthritis, primary sclerosing cholangitis, psoriasis, pyoderma gangrenosum, or uveitis. Medication was categorized as basic (rectal treatment, mesalazine, budesonide) or advanced (cortisone, azathioprine, methotrexate, infliximab, adalimumab).

Three different time intervals were assessed in patient questionnaires (Figure 1). Patient waiting time was defined as time from onset of symptoms to first physician contact. Physician time to diagnosis was defined as time from first physician contact to the diagnosis of IBD. Total diagnostic time was the sum of both time periods and was defined as the time from IBD symptom onset to diagnosis.

Statistical analysis

Statistical analysis was performed using SPSS Statistics 22 (SPSS Inc., Chicago, IL, USA). Figures were created using Prism 6 software (GraphPad Software, La Jolla, CA, USA). We used the Kolmogorov-Smirnov test to determine the distribution of our data. Continuous variables were presented as median and interquartile range (IQR), differences were compared by the Kruskal-Wallis test or Mann-Whitney *U* test. Categorical data were expressed in the form of numbers and percentages and were compared by the χ^2 test. Univariate analysis of the different clinically relevant factors associated with diagnostic time was performed using the Kaplan-Meier survival method and the differences were compared using the log-rank test. We also presented hazard ratios (HR) for the univariate analysis. HRs exceeding unity (HR > 1) represented a better chance for early diagnosis. All variables with a $P < 0.1$ in univariate analysis were further used for multivariate analyses using Cox's proportional hazard model in a backward stepwise manner. $P < 0.05$ was considered statistically significant.

RESULTS

Patient characteristics

Patient characteristics for IBD are summarized in Table 1. We analyzed 223 patients with CD and 207 with UC. Patients were mainly female (54.4%) with a median age at diagnosis of 26 (20–25) years for CD and 28 (21–39) years for UC. The most common reported symptoms were diarrhea in CD (43.5%) and UC (48.8%), followed by abdominal pain in CD (33.2%) and blood in the stool in UC (33.8%). The predominant site of disease at the time of diagnosis was the terminal ileum in CD (68.6%) and the colon in UC (74.4%). Most UC and CD patients were diagnosed based on colonoscopy (78.5 vs 96.1%; $P < 0.001$) compared with computed tomography (3.1 vs 0.5%; $P = 0.037$) or magnetic resonance imaging (2.2 vs

Table 1 Patient characteristics, n (%)

Parameter	CD (n = 223)	UC (n = 207)	P value
Sex, M/F	95/128	101/106	0.198
Age at enrolment (yr)	40 (30-50)	41 (32-52)	0.509
Age at diagnosis (yr)	26 (20-35)	28 (21-39)	0.565
Residence at diagnosis			0.554
Village	12 (5.4)	14 (6.8)	0.537
Small-town	18 (8.1)	18 (8.7)	0.801
Medium-sized town	24 (10.8)	14 (6.8)	0.149
Large city	165 (74.0)	152 (73.9)	0.977
Abroad	1 (0.4)	5 (2.4)	0.081
Patient waiting time (mo)	2.0 (0.5-6.0)	1.0 (0.5-4.0)	0.051
Physician time to diagnosis (mo)	5.5 (0.75-23.5)	1.0 (0-5.0)	< 0.001
Total diagnostic time (mo)	12.0 (6.0-24.0)	4.0 (1.5-12.0)	< 0.001
Predominant symptom			
Diarrhea	97 (43.5)	101 (48.8)	0.239
Constipation	1 (0.4)	1 (0.5)	0.954
Abdominal pain	74 (33.2)	16 (7.7)	< 0.001
Heartburn	1 (0.4)	0 (0)	0.336
Bloating	0 (0)	3 (1.4)	0.070
Blood in stool	11 (4.9)	70 (33.8)	< 0.001
Nausea/vomiting	9 (4.0)	0 (0)	0.004
Skin	1 (0.4)	1 (0.5)	0.954
Joint pain	4 (1.8)	0 (0)	0.054
Fistula	5 (2.2)	0 (0)	0.031
Weight loss	1 (0.4)	0 (0)	0.336
Fever	1 (0.4)	1 (0.5)	0.954
Fatigue	5 (2.2)	5 (2.4)	0.897
Other symptoms	8 (3.6)	3 (1.4)	0.164
Location			
Upper GI	19 (8.5)	2 (1.0)	< 0.001
Small bowel	73 (32.7)	16 (7.7)	< 0.001
Terminal ileum	153 (68.6)	21 (10.1)	< 0.001
Colon	101 (45.3)	154 (74.4)	< 0.001
Rectum	49 (22.0)	111 (53.6)	< 0.001
Severity			
Very mild	7 (3.1)	9 (4.3)	0.519
Mild	11 (4.9)	23 (11.1)	0.019
Moderate	38 (17.0)	55 (26.6)	0.018
Strong	88 (39.5)	69 (33.3)	0.187
Very strong	75 (33.6)	49 (23.7)	0.023
Physician			
Gastroenterologist	85 (38.1)	97 (46.9)	0.066

Hospital	104 (46.6)	73 (35.3)	0.017
General practitioner	18 (8.1)	19 (9.2)	0.682
Expert in IBD	9 (4.0)	9 (4.3)	0.871
Another consultant	4 (1.8)	8 (3.9)	0.187
Others	2 (0.9)	2 (0.9)	0.172
Diagnostic tests			
Colonoscopy	175 (78.5)	199 (96.1)	< 0.001
Gastroscopy	5 (2.2)	1 (0.5)	0.111
Sonography	4 (1.8)	1 (0.5)	0.193
Computed tomography	7 (3.1)	1 (0.5)	0.037
Magnetic resonance imaging	5 (2.2)	1 (0.5)	0.028
Diagnosis change			
Positive family history	35 (15.7)	35 (16.9)	0.808
Parents	13 (37.1)	10 (28.6)	0.445
Siblings	12 (5.4)	8 (22.9)	0.290
Aunt/uncle	2 (0.9)	8 (22.9)	0.040
Grandparents	4 (1.8)	9 (25.7)	0.124
Knowledge of IBD	49 (22.0)	39 (18.8)	0.437
Affected person	27 (55.1)	20 (51.3)	0.721
Media	10 (20.4)	7 (17.9)	0.772
Internet	8 (16.3)	6 (15.4)	0.904
Profession	6 (12.2)	9 (23.1)	0.179
Medication			
Mesalazine	149 (66.8)	180 (87.0)	< 0.001
Budesonide	68 (30.5)	24 (11.6)	< 0.001
Cortisone	54 (24.2)	115 (55.6)	< 0.001
Azathioprine	2 (0.9)	29 (14.0)	0.007
Methotrexate	7 (3.1)	1 (0.5)	0.607
Infliximab	7 (3.1)	5 (2.4)	0.649
Adalimumab	17 (7.6)	1 (0.5)	0.042
Local treatment	13 (5.8)	64 (30.9)	< 0.001

CD: Crohn's disease; IBD: Inflammatory bowel disease; UC: Ulcerative colitis; GI: Gastrointestinal tract.

0.5 %; $P = 0.028$). The CD diagnosis was mainly made in hospital (46.6% CD *vs* 35.5% UC). UC diagnosis was predominantly made by private practice gastroenterologists (38.1% CD *vs* 46.9% UC). The CD patients reported more severe symptoms compared with UC patients (33.6% CD *vs* 23.7% UC; $P = 0.023$) and had more EIMs (26.0% CD *vs* 12.1% UC; $P < 0.001$).

Diagnostic time

Total diagnostic time was longer for CD (12.0 months; IQR 6.0–24.0) than UC (4.0 months; IQR 1.5–12.0; $P < 0.001$). While the patient waiting time was comparable between CD and UC (2.0 months; IQR 0.5–6.0) *vs* 1.0 month; IQR 0.5–4.0; $P = 0.051$), the physician diagnostic time was longer in CD patients (5.5 months; IQR 0.75–23.5) than UC patients (1.0 month; IQR 0–5.0; $P < 0.001$). Time to event analysis for all three intervals for CD and UC, separately, are depicted as Kaplan–Meier curves (Figure 2).

CD

Patient waiting time: In the univariate analysis, patient waiting time was shorter with female sex ($P = 0.089$), living abroad ($P = 0.020$), the predominant symptoms of abdominal pain ($P = 0.038$), fistula ($P = 0.032$), nausea/vomiting ($P =$

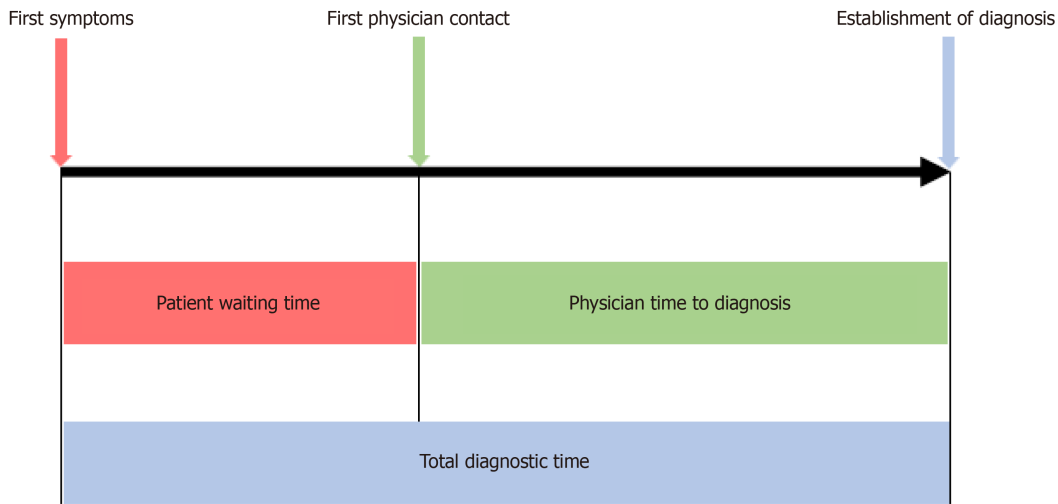


Figure 1 Diagnostic time intervals. Based on the patients' questionnaires, three relevant time intervals were calculated: (1) patient waiting time [interval from the first inflammatory bowel disease (IBD) symptoms till consulting a physician]; (2) physician diagnostic time (interval from first physician contact to IBD diagnosis); and (3) total diagnostic time (interval from the first IBD symptoms till establishment of IBD diagnosis).

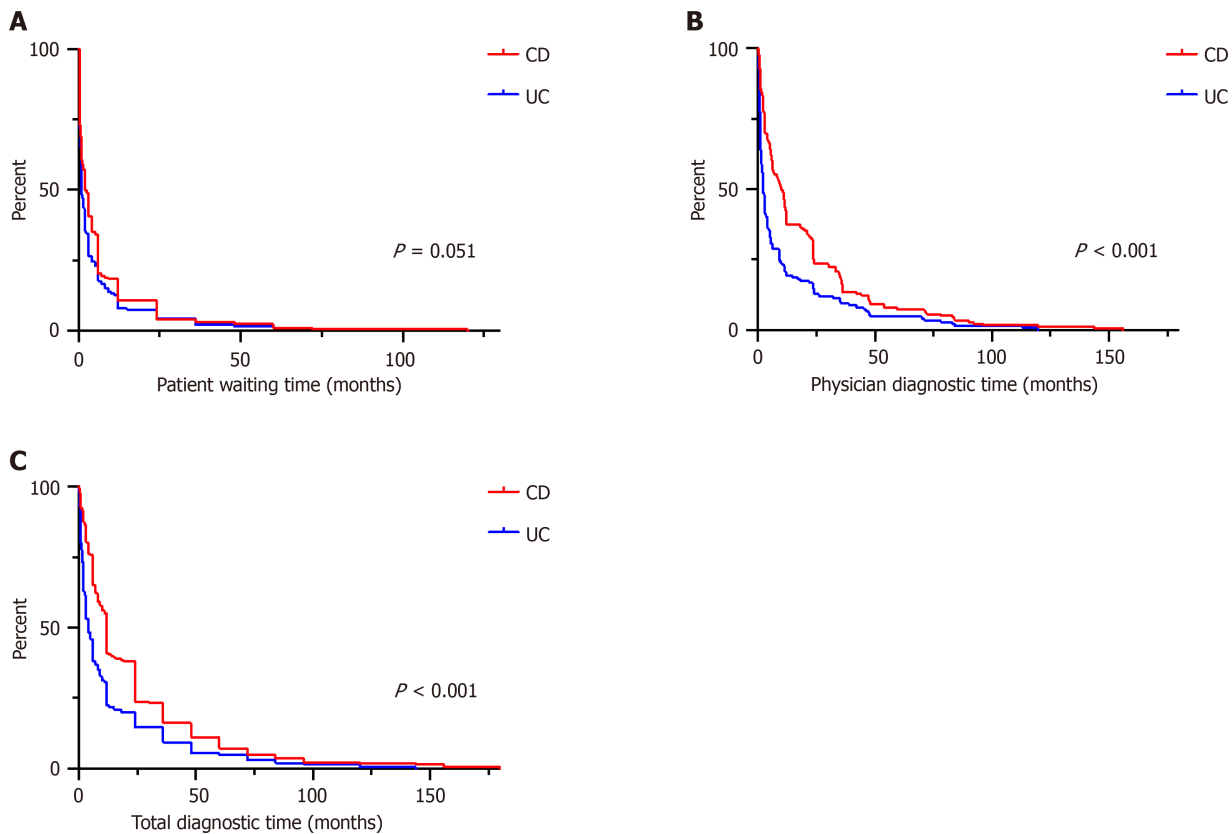


Figure 2 Diagnostic time in Crohn's disease versus ulcerative colitis patients. A: Patient waiting time almost equals in Crohn's disease (CD) and ulcerative colitis patients; B: Significantly prolonged physician diagnostic time in CD patients; C: Significantly prolonged total diagnostic time in these patients. CD: Crohn's disease; UC: Ulcerative colitis.

0.075), strong disease severity ($P = 0.023$), and positive family history of IBD ($P = 0.005$). Longer patient waiting time was associated with blood in stool ($P = 0.069$) and diarrhea ($P < 0.001$). The clinical factors influencing patient waiting time in CD are summarized in [Table 2](#).

Multivariate analysis determined the predominant symptoms of abdominal pain (HR 1.428; $P = 0.018$), fistula (HR = 2.841; $P = 0.027$) and positive family history (HR = 1.734; $P = 0.004$) were associated with shorter patient waiting time ([Table 3](#)).

Physician diagnostic time: Univariate analysis of physician diagnostic time revealed that the predominant symptoms of diarrhea ($P = 0.003$), skin lesions ($P = 0.044$), joint pain ($P = 0.066$), and weight loss ($P = 0.044$), as well as the common

Table 2 Univariate analysis

Parameter		Patient waiting time		Physician diagnostic time	
		HR	P value	HR	P value
Sex, female <i>vs</i> male	CD	1.235	0.089	0.852	0.222
	UC	0.954	0.714	0.897	0.407
Age, ≤ 40 <i>vs</i> > 40 yr	CD	1.071	0.654	1.176	0.329
	UC	1.407	0.031	1.109	0.508
Year of diagnosis, ≤ 2000 <i>vs</i> > 2000	CD	1.081	0.520	0.975	0.846
	UC	0.947	0.666	0.976	0.856
Predominant symptom					
Diarrhea, yes <i>vs</i> no	CD	0.826	0.116	1.484	0.003
	UC	1.141	0.305	1.065	0.640
Constipation, yes <i>vs</i> no	CD	2.045	0.440	1.835	0.517
	UC	1.011	0.991	0.882	0.893
Abdominal pain, yes <i>vs</i> no	CD	1.307	0.038	0.834	0.191
	UC	1.096	0.701	0.708	0.167
Heartburn, yes <i>vs</i> no	CD	0.975	0.979	0.826	0.844
Bloating, yes <i>vs</i> no	UC	0.218	0.010	0.789	0.664
Blood in stool, yes <i>vs</i> no	CD	0.609	0.069	1.272	0.419
	UC	1.014	0.916	0.999	0.993
Nausea/vomiting, yes <i>vs</i> no	CD	1.216	0.520	0.675	0.233
Skin, yes <i>vs</i> no	CD	1.164	0.872	5.178	0.044
	UC	0.295	0.138	3.637	0.108
Joint pain, yes <i>vs</i> no	CD	0.844	0.703	0.323	0.039
Fistula, yes <i>vs</i> no	CD	2.450	0.032	0.656	0.334
Weight loss, yes <i>vs</i> no	CD	0.387	0.236	5.178	0.044
Fever, yes <i>vs</i> no	CD	0.387	0.236	0.620	0.619
	UC	6.191	0.026	1.207	0.838
Fatigue, yes <i>vs</i> no	CD	1.482	0.335	1.452	0.390
	UC	1.652	0.225	1.937	0.101
Symptoms					
Diarrhea, yes <i>vs</i> no	CD	0.590	< 0.001	0.947	0.732
	UC	1.331	0.068	1.028	0.867
Constipation, yes <i>vs</i> no	CD	1.103	0.644	0.747	0.209
	UC	1.031	0.921	0.808	0.513
Abdominal pain, yes <i>vs</i> no	CD	0.988	0.934	0.963	0.812
	UC	1.018	0.889	0.952	0.708
Heartburn, yes <i>vs</i> no	CD	0.988	0.947	0.735	0.110
	UC	0.697	0.140	1.014	0.955
Bloating, yes <i>vs</i> no	CD	0.827	0.150	0.842	0.235
	UC	0.814	0.132	0.960	0.770
Blood in stool, yes <i>vs</i> no	CD	0.932	0.572	0.889	0.393
	UC	0.970	0.856	0.913	0.586

Nausea/vomiting, yes vs no	CD	1.264	0.075	1.082	0.574
	UC	1.210	0.334	0.966	0.864
Skin, yes vs no	CD	0.801	0.261	0.628	0.036
	UC	0.663	0.157	0.947	0.859
Joint pain, yes vs no	CD	0.882	0.403	0.733	0.066
	UC	0.780	0.309	0.836	0.478
Fistula, yes vs no	CD	1.280	0.231	0.937	0.770
	UC	0.694	0.421	0.766	0.574
Weight loss, yes vs no	CD	1.019	0.875	0.900	0.416
	UC	1.400	0.016	0.893	0.429
Fever, yes vs no	CD	1.196	0.239	1.142	0.420
	UC	1.381	0.150	1.654	0.026
Fatigue, yes vs no	CD	1.094	0.457	0.959	0.746
	UC	0.961	0.757	0.767	0.045
EIM, yes vs no	CD	0.902	0.450	0.784	0.104
	UC	0.745	0.129	0.913	0.651
Location					
Upper GI, yes vs no	CD	1.198	0.400	1.256	0.323
	UC	0.813	0.748	0.668	0.545
Small bowel, yes vs no	CD	0.910	0.461	0.929	0.594
	UC	1.007	0.976	0.818	0.411
Terminal ileum, yes vs no	CD	0.964	0.778	1.183	0.237
	UC	0.849	0.432	1.087	0.700
Colon, yes vs no	CD	1.135	0.292	0.927	0.565
	UC	1.014	0.924	1.012	0.934
Rectum, yes vs no	CD	1.075	0.616	1.043	0.791
	UC	0.864	0.251	0.907	0.457
Disease severity, strong vs mild	CD	1.359	0.023	1.240	0.154
	UC	1.098	0.469	1.247	0.096
Diagnosis made in hospital, yes vs no	CD	0.915	0.464	0.992	0.952
	UC	1.314	0.039	1.013	0.923
Diagnosis made by gastroscopy, yes vs no	CD	1.059	0.891	2.857	0.011
	UC	1.520	0.644	0.804	0.815
Family history, positive vs negative	CD	1.587	0.005	1.073	0.697
	UC	0.767	0.120	0.708	0.053
Medication, strong vs mild	CD	1.067	0.647	0.965	0.816
	UC	0.967	0.794	0.991	0.944

The bold binary parameter denotes to what the hazard ratio is referring to. Items with P -value < 0.1 in univariate analysis were entered into the multivariate model. CD: Crohn's disease; EIM: Extraintestinal manifestation; GI: Gastrointestinal tract; UC: Ulcerative colitis.

symptoms of skin lesions ($P = 0.036$), joint pain ($P = 0.066$), and performance of diagnostic gastroscopy ($P = 0.011$) were linked with shorter physician diagnostic time. The univariate analysis of risk factors for physician diagnostic time are presented in [Table 2](#).

Table 3 Multivariate analysis for Crohn's disease

Parameter	Patient waiting time		
	HR	95%CI	P value
Abdominal pain ¹	1.428	1.062-1.919	0.018
Fistula ¹	2.841	1.125-7.175	0.027
Positive family history	1.734	1.196-2.514	0.004

¹Predominant symptom.

CI: Confidence interval; HR: Hazard ratio.

The predominant symptoms of diarrhea (HR = 1.438, $P = 0.012$), skin lesions (HR = 9.746, $P = 0.028$), and performance of diagnostic gastroscopy (HR = 2.570, $P = 0.042$) were associated with shorter physician diagnostic time in the multivariate analysis (Table 4).

Total diagnostic time: In patients with CD, total diagnostic time was longer with the symptom of joint pain (HR = 0.696, $P = 0.048$) and shorter with performance of diagnostic gastroscopy (HR = 3.019, $P = 0.018$; data not shown). Location of disease, place of residence at time of diagnosis or year of diagnosis (≤ 2000 vs > 2000) had no effect on the three relevant time intervals shown in Table 2 and were therefore not included in the multivariate model.

UC

Patient waiting time: Univariate analysis of UC patients showed that age ≤ 40 years ($P = 0.031$), predominant symptoms of fever ($P = 0.026$), diarrhea ($P = 0.068$) and weight loss ($P = 0.016$), and diagnosis made in a hospital setting ($P = 0.039$) were associated with shorter patient waiting time. The predominant symptom of bloating ($P = 0.010$) was associated with longer patient waiting time.

In the multivariate analysis, the predominant symptom of bloating was associated with longer patient waiting time (HR = 0.207; $P = 0.029$), whereas diarrhea was associated with shorter patient waiting time (HR = 1.463, $P = 0.034$) (Table 5).

Physician diagnostic time: In UC, fever ($P = 0.026$), fatigue ($P = 0.045$), strong disease severity ($P = 0.096$) and negative family history of IBD ($P = 0.053$) were associated with shorter physician diagnostic time (Table 2). In the multivariate analysis, fever was associated with shorter physician diagnostic time (HR = 1.813; $P = 0.020$) and fatigue (HR = 0.685; $P = 0.011$) was associated with longer physician diagnostic time. Surprisingly, a positive family history for IBD (HR = 0.681; $P = 0.046$) was also associated with longer physician diagnostic time (Table 6).

Total diagnostic time: On multivariate analysis, fever was associated with shorter total diagnostic time (HR = 0.743, $P = 0.032$) and the predominant symptom of fatigue with longer total diagnostic time (HR = 0.285, $P = 0.007$; data not shown). Location of disease, place of residence at diagnosis, or year of diagnosis were not linked with any of the three diagnostic intervals.

DISCUSSION

This is the first study in an adult German IBD population to evaluate diagnostic delay, which in addition provides further focus on patient-related and physician-related risk factors. We confirmed the previous observations of markedly longer total diagnostic time in CD patients, which in our study was shown to be mainly physician related[4,5,8]. Disease-specific symptoms and easily available diagnostics led to a reduction in physician diagnostic time. A positive family history decreased patient waiting time, whereas it had no effect on the physician diagnostic time in CD patients. Positive family history increased physician diagnostic time in UC patients. Inexplicably, no significant improvement in diagnostic time has been observed over the last 50 years, as demonstrated by comparing diagnostic time from before and after the turn of the millennium.

The IBD incidence has markedly increased worldwide over the last several decades[15,16]. However, regional differences in care patterns are well described and make cross-comparisons difficult due to differences in access and utilization of healthcare services, socioeconomic status, environmental factors, and varying degrees of implementation of clinical guidelines[8,13]. Previously there were no data on diagnostic delay from a German national cohort. However, knowledge of risk factors for diagnostic delay is crucial to reduce time to diagnosis and improve patient outcomes. Previous studies have extensively demonstrated that diagnostic delay is associated with an increased risk of IBD-related complications and need for colorectal surgery, as well as significantly reduced quality of life and lack of response to medical therapy[7,8,12,17]. However, identified risk factors may not be applicable in patients of different background and in different healthcare systems and evaluation in a German cohort hence is critical.

In our German CD patients, the total diagnostic time was on average 12 months, which was longer in UC with only 4 months (Figure 2C). This finding is consistent with previously published data regarding diagnostic time in CD versus UC

Table 4 Multivariate analysis of physician diagnostic time in Crohn's disease

Parameter	Physician diagnostic time		
	HR	95%CI	P value
Diarrhea ¹	1.438	1.085-1.906	0.012
Skin lesions ¹	9.746	1.273-74.609	0.028
Gastroscopy	2.570	1.037-6.371	0.042

¹Predominant symptom.

CI: Confidence interval; HR: Hazard ratio.

Table 5 Multivariate analysis for ulcerative colitis

Parameter	Patient waiting time		
	HR	95%CI	P value
Bloating ¹	0.207	0.050-0.848	0.029
Diarrhea	1.463	1.030-2.079	0.034

¹Predominant symptom.

CI: Confidence interval; HR: Hazard ratio.

Table 6 Multivariate analysis of physician diagnostic time in ulcerative colitis

Parameter	Physician diagnostic time		
	HR	95%CI	P value
Fatigue	0.685	0.512-0.917	0.011
Fever	1.813	1.096-2.999	0.020
Positive family history	0.681	0.466-0.994	0.046

CI: Confidence interval; HR: Hazard ratio.

patients. Cantoro *et al*[18] reported a median diagnostic time of 7.1 *vs* 2.0 months in Italian patients, Vavricka *et al*[6] reported 9 *versus* 4 months in Swiss patients, and Nguyen *et al*[5] described 9.5 *versus* 3.1 months in American patients. This marked difference between CD and UC could be attributed to a higher frequency of nonspecific symptoms, such as abdominal pain, in CD compared with UC.

Studies that systematically evaluate the reasons for diagnostic delay are scarce. In this study we also differentiated between patient-related and physician-related causes for the delay. Of note, the diagnostic delay in CD patients was mainly attributed to increased physician diagnostic delay (5.5 months in CD *vs* 1.0 month in UC). In UC patients, the patient-related time interval was almost equal to the physician-related time interval (2.0 months *vs* 1.0 month). This finding compares favorably with the previously reported data[5]. One explanation is the marked symptom variance of patients with CD compared to patients with UC, with a large symptom overlap between IBD and functional disease complaints. In our study, nonspecific symptoms such as abdominal pain or nausea/vomiting were increased in CD (Table 1). CD patients were 2.2 times more likely than UC patients to have an EIM of IBD at the time of disease onset. The effect of atypical *versus* typical IBD symptoms on time to diagnosis is again demonstrated by the time interval to physician diagnosis. In our study, the presence of prolonged diarrhea and skin manifestations was independently associated with early physician diagnosis in CD patients (Table 3). High symptom severity was linked with faster diagnosis, likely due to triggering further investigation. In UC patients, fever shortened the physician's diagnostic time, whereas the nonspecific symptom, fatigue, prolonged the diagnostic interval. Surprisingly, rectal bleeding was more commonly reported in our UC patients but was not associated with faster diagnosis (Table 2). In our study a performance of gastroscopy was associated with decreased physician diagnostic time in CD patients, possibly being a surrogate marker indicating better access to diagnostic endoscopy (Table 3).

In the context of diagnostic delay in CD patients, the impact of a positive family history should also be noted. Surprisingly, a positive family history was independently associated with shorter patient waiting time in CD patients, but did not influence physician diagnostic time (Figure 3). Even when patients are aware of their genetic predisposition, the diagnosis is not easily made by the physician. This could be attributed to lack of knowledge, delayed referral or long

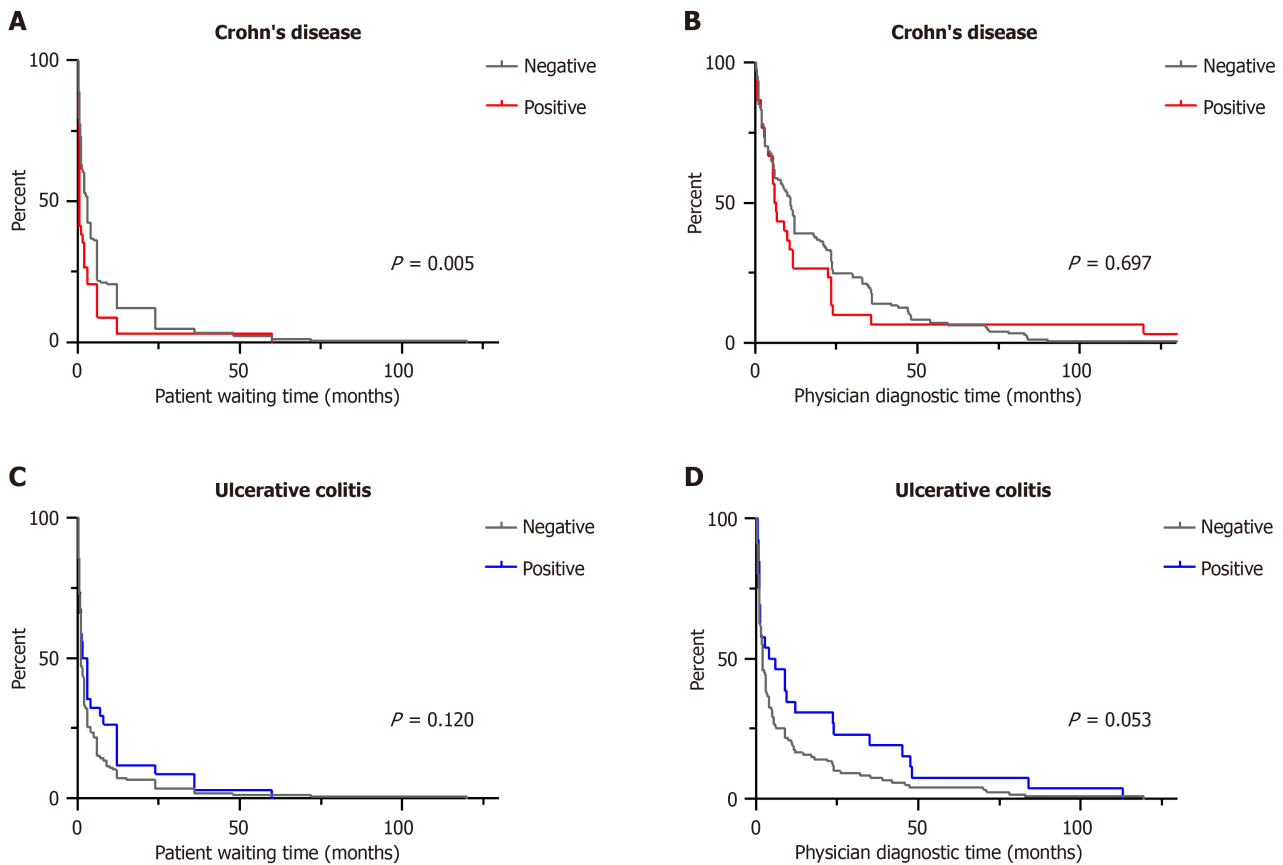


Figure 3 Diagnostic time depending on family history for inflammatory bowel disease. A: A positive family history of inflammatory bowel disease was associated with reduced patient waiting time in Crohn's disease (CD); B: But did not affect physician diagnostic time in CD patients; C: A positive family history did not affect patient waiting time in ulcerative colitis (UC) patients; D: But delayed physician diagnostic time in UC patients.

waiting times for relevant diagnostic procedures. In Germany, health insurance is universal and includes all relevant diagnostic procedures. Moreover, adults receive routine preventive medical care from a general practitioner. The time between the primary care visit and the specialist appointment may be a crucial period to intervene and prevent disease complications. The prevalence of general gastrointestinal complaints (5%–11%) is markedly higher compared to IBD (0.2%) in primary care[19,20]. Functional bowel disorders like IBS often mimic early manifestations of CD, which may delay referral to a gastroenterologist. Moon *et al*[11] demonstrated comparable results regarding the negative impact of family history on time to diagnosis. However, conflicting results have been reported in the literature[12]. This inconsistency might be partly explained by different patient populations in different regions. In summary, the significance of patients' symptoms and family history should not be underestimated. Our results emphasize the importance of the medical history especially when IBD is suspected.

As therapies continue to advance and the incidence of IBD has steadily increased in recent years, IBD continues to gain more attention[13]. Despite these advances, recent studies have shown no change in time to diagnosis over the past few decades[18]. In line with these data, we discovered that the total diagnostic time in CD and UC has not changed between 1964 to 2021. It is clear, that clinicians' lack of knowledge and patients' access to specialists including dedicated diagnostics, outweighs the advancement of diagnostic modalities. This lack of change has been a persistent problem for the last 57 years with a huge impact on the quality of life of patients, and as a result, warrants further action. Knowing that early treatment improves disease outcome, it is important to focus our awareness on this lack of rigor in the existing literature.

Firstly, we want to emphasize the importance of screening tools in primary care. Clinical routine is increasingly determined by time constraints and expanding knowledge about rare diseases. The "Red Flags Index for Suspected CD" by Danese *et al*[21] has established method of diagnostic accuracy to discriminate healthy controls from IBS and early CD. Easily accessible tools, such as the 8-item questionnaire (CalproQuest) can help to identify potential IBD patients[20]. Questions for perianal fistula, first-degree relatives, weight loss, chronic abdominal pain (not after meals), nocturnal diarrhea, mild fever and rectal urgency can help to screen patients for IBD, especially CD. Implementation of these screening tools in early clinical practice might be the first step to meet the requirements of a timely diagnosis in CD. In addition, the noninvasive biomarker, fecal calprotectin, is a sensitive marker for gut inflammation and is now widely established to distinguish between IBS and IBD[22]. However, it must be noted that calprotectin can also be elevated in other differential diagnoses such as gastritis, polyps, diverticulitis or during the use of proton pump inhibitors.

Secondly, educational programs for general practitioners should specifically target early symptoms, signs, and characteristics of IBD with difficult-to-predict courses, and diverse complications. The respective practitioner level of knowledge about disease symptoms as well as the diagnostic workup are important factors regarding disease identification.

Thirdly, public awareness programs and patient educational training focusing on disease heredity, empower patients to become active participants in a patient-centered care model. Additionally, direct access to specialist appointments for patients may also be helpful to reduce the diagnostic delay. Utilizing these tools can improve patients' quality of life, disease outcome and diagnostic delay[23].

Our study had several limitations. This study focused on the course of IBD diagnosis and did not include well-known disease-modifying factors such as smoking habits or educational level. We did not include disease-related complications, but recognize the influence and relevance they may have on disease outcome. In our analysis we could not find a significant correlation of the type of initial medication as a surrogate marker of disease severity and the diagnostic time periods. However, we did not consider this to be a weakness of our study because the primary focus was on the time to diagnosis. This study was not designed as a longitudinal study. Our study design was patient-reported questionnaire-based, which may have led to recall bias. Our Berlin patients do not represent a population-based cohort for Germany. Finally, our population was composed of patients from tertiary referral centers, which may have introduced relevant selection bias.

CONCLUSION

Despite these limitations, we present in the first German adult IBD cohort that CD patients, more than UC patients, are at risk of a long diagnostic delay, which is mainly physician dependent. Disease-specific symptoms and readily available diagnostics resulted in a reduction in physician diagnostic time. We conclude that good interdisciplinary collaboration, physicians' awareness, and screening tools are imperative to reduce diagnostic delay and therefore improve treatment starting position, course of disease and patient satisfaction.

ACKNOWLEDGEMENTS

We thank all the patients who participated in this study. The data underlying this article will be shared on reasonable request to the corresponding author.

FOOTNOTES

Author contributions: Blüthner E analyzed and interpreted data, drafted and submitted the manuscript; Dehe A designed and performed research; Büning C performed research; Siegmund B interpreted the data; Prager M performed research; Maul J performed research; Krannich A analyzed data; Preiß J performed research; Wiedenmann B interpreted the data; Rieder F and Khedraki R reviewed and edited the manuscript, Tacke F interpreted the data; Sturm A performed research; Schirbel A designed and performed research as well as interpreted the data; all authors have revised and approved the final manuscript.

Institutional review board statement: The study was approved by the local ethics committee (EA2/170/11) and was conducted in accordance with the ethical standards of the Declaration of Helsinki of 1964 and its latest revision of 2013.

Informed consent statement: Study participants were interviewed once after written informed consent was obtained.

Conflict-of-interest statement: All authors declare that they have no conflicts of interest related to this paper.

Data sharing statement: Data available on request from the authors.

STROBE statement: The authors have read the STROBE Statement-checklist of items, and the manuscript was prepared and revised according to the STROBE Statement-checklist of items.

Open-Access: This article is an open-access article that was selected by an in-house editor and fully peer-reviewed by external reviewers. It is distributed in accordance with the Creative Commons Attribution NonCommercial (CC BY-NC 4.0) license, which permits others to distribute, remix, adapt, build upon this work non-commercially, and license their derivative works on different terms, provided the original work is properly cited and the use is non-commercial. See: <https://creativecommons.org/licenses/by-nc/4.0/>

Country of origin: Germany

ORCID number: Elisabeth Blüthner 0000-0002-7008-8795; Britta Siegmund 0000-0002-0055-958X; Anja Schirbel 0009-0001-7686-8450.

Corresponding Author's Membership in Professional Societies: DGVS, No. 08051; ESPEN, No. 75794; DGEM, No. 6024.

S-Editor: Qu XL

L-Editor: Kerr C

P-Editor: Zhao YQ

REFERENCES

- 1 **de Souza HSP**, Fiocchi C, Iliopoulos D. The IBD interactome: an integrated view of aetiology, pathogenesis and therapy. *Nat Rev Gastroenterol Hepatol* 2017; **14**: 739-749 [PMID: 28831186 DOI: 10.1038/nrgastro.2017.110]
- 2 **Chang JT**. Pathophysiology of Inflammatory Bowel Diseases. *N Engl J Med* 2020; **383**: 2652-2664 [PMID: 33382932 DOI: 10.1056/NEJMra2002697]
- 3 **Talley NJ**, Phillips SF, Melton LJ, Mulvihill C, Wiltgen C, Zinsmeister AR. Diagnostic value of the Manning criteria in irritable bowel syndrome. *Gut* 1990; **31**: 77-81 [PMID: 2318433 DOI: 10.1136/gut.31.1.77]
- 4 **Nahon S**, Lahmek P, Lesgourgues B, Poupardin C, Chaussade S, Peyrin-Biroulet L, Abitbol V. Diagnostic delay in a French cohort of Crohn's disease patients. *J Crohns Colitis* 2014; **8**: 964-969 [PMID: 24529604 DOI: 10.1016/j.crohns.2014.01.023]
- 5 **Nguyen VQ**, Jiang D, Hoffman SN, Guntaka S, Mays JL, Wang A, Gomes J, Sorrentino D. Impact of Diagnostic Delay and Associated Factors on Clinical Outcomes in a U.S. Inflammatory Bowel Disease Cohort. *Inflamm Bowel Dis* 2017; **23**: 1825-1831 [PMID: 28885229 DOI: 10.1097/MIB.0000000000001257]
- 6 **Vavricka SR**, Spigaglia SM, Rogler G, Pittet V, Michetti P, Felley C, Mottet C, Braegger CP, Rogler D, Straumann A, Bauerfeind P, Fried M, Schoepfer AM; Swiss IBD Cohort Study Group. Systematic evaluation of risk factors for diagnostic delay in inflammatory bowel disease. *Inflamm Bowel Dis* 2012; **18**: 496-505 [PMID: 21509908 DOI: 10.1002/ibd.21719]
- 7 **Schoepfer AM**, Dehlavi MA, Fournier N, Safroneeva E, Straumann A, Pittet V, Peyrin-Biroulet L, Michetti P, Rogler G, Vavricka SR; IBD Cohort Study Group. Diagnostic delay in Crohn's disease is associated with a complicated disease course and increased operation rate. *Am J Gastroenterol* 2013; **108**: 1744-53; quiz 1754 [PMID: 23978953 DOI: 10.1038/ajg.2013.248]
- 8 **Zaharie R**, Tantau A, Zaharie F, Tantau M, Gheorghe L, Gheorghe C, Gologan S, Cijevschi C, Trifan A, Dobru D, Goldis A, Constantinescu G, Iacob R, Diculescu M; IBDPROSPECT Study Group. Diagnostic Delay in Romanian Patients with Inflammatory Bowel Disease: Risk Factors and Impact on the Disease Course and Need for Surgery. *J Crohns Colitis* 2016; **10**: 306-314 [PMID: 26589956 DOI: 10.1093/ecco-jcc/jjv215]
- 9 **D'Haens G**, Baert F, van Assche G, Caenepeel P, Vergauwe P, Tuynman H, De Vos M, van Deventer S, Stitt L, Donner A, Vermeire S, Van De Mierop FJ, Coche JR, van der Woude J, Ochsenkühn T, van Bodegraven AA, Van Hooitegem PP, Lambrecht GL, Mana F, Rutgeerts P, Feagan BG, Hommes D; Belgian Inflammatory Bowel Disease Research Group; North-Holland Gut Club. Early combined immunosuppression or conventional management in patients with newly diagnosed Crohn's disease: an open randomised trial. *Lancet* 2008; **371**: 660-667 [PMID: 18295023 DOI: 10.1016/S0140-6736(08)60304-9]
- 10 **De Boer AG**, Bennebroek Evertsz F, Stokkers PC, Bockting CL, Sanderman R, Hommes DW, Sprangers MA, Frings-Dresen MH. Employment status, difficulties at work and quality of life in inflammatory bowel disease patients. *Eur J Gastroenterol Hepatol* 2016; **28**: 1130-1136 [PMID: 27340897 DOI: 10.1097/MEG.0000000000000685]
- 11 **Moon CM**, Jung SA, Kim SE, Song HJ, Jung Y, Ye BD, Cheon JH, Kim YS, Kim YH, Kim JS, Han DS; CONNECT study group. Clinical Factors and Disease Course Related to Diagnostic Delay in Korean Crohn's Disease Patients: Results from the CONNECT Study. *PLoS One* 2015; **10**: e0144390 [PMID: 26647084 DOI: 10.1371/journal.pone.0144390]
- 12 **Li Y**, Ren J, Wang G, Gu G, Wu X, Ren H, Hong Z, Hu D, Wu Q, Li G, Liu S, Anjum N, Li J. Diagnostic delay in Crohn's disease is associated with increased rate of abdominal surgery: A retrospective study in Chinese patients. *Dig Liver Dis* 2015; **47**: 544-548 [PMID: 25840874 DOI: 10.1016/j.dld.2015.03.004]
- 13 **Burisch J**, Pedersen N, Čuković-Čavka S, Brinar M, Kaimakliotis I, Duricova D, Shonová O, Vind I, Avnstrøm S, Thorsgaard N, Andersen V, Krabbe S, Dahlerup JF, Salupere R, Nielsen KR, Olsen J, Manninen P, Collin P, Tsianos EV, Katsanos KH, Ladefoged K, Lakatos L, Björnsson E, Ragnarsson G, Bailey Y, Odes S, Schwartz D, Martinato M, Lupinacci G, Milla M, De Padova A, D'Inca R, Beltrami M, Kupcinskis L, Kiudelis G, Turcan S, Tighineanu O, Mihu I, Magro F, Barros LF, Goldis A, Lazar D, Belousova E, Nikulina I, Hernandez V, Martinez-Ares D, Almer S, Zhulina Y, Halfvarson J, Arebi N, Sebastian S, Lakatos PL, Langholz E, Munkholm P; EpiCom-group. East-West gradient in the incidence of inflammatory bowel disease in Europe: the ECCO-EpiCom inception cohort. *Gut* 2014; **63**: 588-597 [PMID: 23604131 DOI: 10.1136/gutjnl-2013-304636]
- 14 **von Elm E**, Altman DG, Egger M, Pocock SJ, Gøtzsche PC, Vandenbroucke JP; STROBE Initiative. The Strengthening the Reporting of Observational Studies in Epidemiology (STROBE) Statement: guidelines for reporting observational studies. *Int J Surg* 2014; **12**: 1495-1499 [PMID: 25046131 DOI: 10.1016/j.ijsu.2014.07.013]
- 15 **Molodecky NA**, Soon IS, Rabi DM, Ghali WA, Ferris M, Chernoff G, Benchimol EI, Panaccione R, Ghosh S, Barkema HW, Kaplan GG. Increasing incidence and prevalence of the inflammatory bowel diseases with time, based on systematic review. *Gastroenterology* 2012; **142**: 46-54.e42; quiz e30 [PMID: 22001864 DOI: 10.1053/j.gastro.2011.10.001]
- 16 **van den Heuvel TRA**, Jeurings SFG, Zeegers MP, van Dongen DHE, Wolters A, Masclee AAM, Hameeteman WH, Romberg-Camps MJL, Oostenbrug LE, Pierik MJ, Jonkers DM. A 20-Year Temporal Change Analysis in Incidence, Presenting Phenotype and Mortality, in the Dutch IBD Cohort-Can Diagnostic Factors Explain the Increase in IBD Incidence? *J Crohns Colitis* 2017; **11**: 1169-1179 [PMID: 28430884 DOI: 10.1093/ecco-jcc/jjx055]
- 17 **Lee DW**, Koo JS, Choe JW, Suh SJ, Kim SY, Hyun JJ, Jung SW, Jung YK, Yim HJ, Lee SW. Diagnostic delay in inflammatory bowel disease increases the risk of intestinal surgery. *World J Gastroenterol* 2017; **23**: 6474-6481 [PMID: 29085197 DOI: 10.3748/wjg.v23.i35.6474]
- 18 **Cantoro L**, Di Sabatino A, Papi C, Margagnoni G, Ardizzone S, Giuffrida P, Giannarelli D, Massari A, Monterubbianesi R, Lenti MV, Corazza GR, Kohn A. The Time Course of Diagnostic Delay in Inflammatory Bowel Disease Over the Last Sixty Years: An Italian Multicentre Study. *J Crohns Colitis* 2017; **11**: 975-980 [PMID: 28333328 DOI: 10.1093/ecco-jcc/jjx041]
- 19 **Riedl B**, Kehler S, Werner CU, Schneider A, Linde K. Do general practice patients with and without appointment differ? Cross-sectional study. *BMC Fam Pract* 2018; **19**: 101 [PMID: 29935538 DOI: 10.1186/s12875-018-0787-5]
- 20 **Chmiel C**, Vavricka SR, Hasler S, Rogler G, Zahnd N, Schiesser S, Tandjung R, Scherz N, Rosemann T, Senn O. Feasibility of an 8-item questionnaire for early diagnosis of inflammatory bowel disease in primary care. *J Eval Clin Pract* 2019; **25**: 155-162 [PMID: 30324695 DOI: 10.1111/jep.13046]
- 21 **Danese S**, Fiorino G, Mary JY, Lakatos PL, D'Haens G, Moja L, D'Hoore A, Panes J, Reinisch W, Sandborn WJ, Travis SP, Vermeire S, Peyrin-Biroulet L, Colombel JF. Development of Red Flags Index for Early Referral of Adults with Symptoms and Signs Suggestive of Crohn's Disease: An IOIBD Initiative. *J Crohns Colitis* 2015; **9**: 601-606 [PMID: 25908718 DOI: 10.1093/ecco-jcc/jjv067]
- 22 **Khaki-Khatibi F**, Quej Q, Kashifard M, Moein S, Maniati M, Vaghari-Tabari M. Calprotectin in inflammatory bowel disease. *Clin Chim Acta* 2020; **510**: 556-565 [PMID: 32818491 DOI: 10.1016/j.cca.2020.08.025]

- 23 **Cantoro L**, Monterubbiansi R, Falasco G, Camastra C, Pantanella P, Allocca M, Cosentino R, Faggiani R, Danese S, Fiorino G. The Earlier You Find, the Better You Treat: Red Flags for Early Diagnosis of Inflammatory Bowel Disease. *Diagnostics (Basel)* 2023; **13** [PMID: 37892004 DOI: 10.3390/diagnostics13203183]

Observational Study

Prevalence of *Helicobacter pylori* infection among patients with esophageal carcinoma

Miriam López-Gómez, Maria Morales, Rebeca Fuerte, Marta Muñoz, Pedro-David Delgado-López, Jorge Francisco Gómez-Cerezo, Enrique Casado

Specialty type: Oncology

Provenance and peer review:

Invited article; Externally peer reviewed.

Peer-review model: Single blind

Peer-review report's classification

Scientific Quality: Grade A, Grade B, Grade C

Novelty: Grade A, Grade B, Grade B

Creativity or Innovation: Grade A, Grade B, Grade B

Scientific Significance: Grade A, Grade B, Grade B

P-Reviewer: El-Serafi I; Fu Z; Stan FG

Received: April 24, 2024

Revised: June 24, 2024

Accepted: July 11, 2024

Published online: August 7, 2024

Processing time: 95 Days and 14.8 Hours



Miriam López-Gómez, Department of Medical Oncology, Precision Oncology Laboratory, Infanta Sofía University Hospital, San Sebastián de los Reyes 28231, Madrid, Spain

Maria Morales, Department of Medical Oncology, Infanta Sofía University Hospital, San Sebastián de los Reyes 28702, Spain

Rebeca Fuerte, Department of Internal Medicine, Infanta Sofía University Hospital, San Sebastián de los Reyes 28703, Madrid, Spain

Marta Muñoz, Department of Pathology, Infanta Sofía University Hospital, San Sebastián de los Reyes 28702, Spain

Pedro-David Delgado-López, Department of Neurosurgery, Burgos University Hospital, Burgos 09006, Spain

Jorge Francisco Gómez-Cerezo, Department of Internal Medicine, Infanta Sofía University Hospital and Henares University Hospital Foundation for Biomedical Research and Innovation, San Sebastian de los Reyes 28702, Madrid, Spain

Enrique Casado, Department of Medical Oncology, Infanta Sofía University Hospital and Henares University Hospital Foundation for Biomedical Research and Innovation, San Sebastian de los Reyes 28702, Madrid, Spain

Co-first authors: Miriam López-Gómez and Maria Morales.

Corresponding author: Miriam López-Gómez, PhD, Doctor, Department of Medical Oncology, Precision Oncology Laboratory, Infanta Sofía University Hospital, C/Paseo Europa 34, San Sebastián de los Reyes 28231, Madrid, Spain. miriam.lopez@telefonica.net

Abstract

BACKGROUND

Helicobacter pylori (*H. pylori*) is a widespread microorganism related to gastric adenocarcinoma (AC). In contrast, it has been reported that an inverse association exists between *H. pylori* infection and esophageal carcinoma. The mechanisms underlying this supposedly protective effect remain controversial.

AIM

To determine the prevalence of *H. pylori* infection in esophageal carcinoma

patients, we performed a retrospective observational study of esophageal tumors diagnosed in our hospital.

METHODS

We retrospectively reviewed the prevalence of *H. pylori* infection in a cohort of patients diagnosed with esophageal carcinoma. Concomitant or previous proton pump inhibitor (PPI) usage was also recorded.

RESULTS

A total of 89 patients with esophageal carcinoma (69 males, 77.5%), with a mean age of 66 years (range, 26-93 years) were included. AC was the most frequent pathological variant ($n = 47$, 52.8%), followed by squamous cell carcinoma ($n = 37$, 41.6%). Fourteen ACs (29.8%) originated in the gastroesophageal junction and 33 (70.2%) in the esophageal body. Overall, 54 patients (60.7%) presented at stages III and IV. Previous *H. pylori* infection occurred only in 4 patients (4.5%), 3 with AC (6.3% of all ACs) and 1 with squamous cell carcinoma (2.7% of all squamous cell tumors). All patients with previous *H. pylori* infection had stage III-IV. Only one patient had received prior *H. pylori* eradication therapy, whereas 86 (96.6%) had received previous or concomitant PPI treatment.

CONCLUSION

In our cohort of patients, and after histologic evaluation of paraffin-embedded primary tumors, we found a very low prevalence of previous *H. pylori* infection. We also reviewed the medical history of the patients, concluding that the majority had received or were on PPI treatment. The minimal prevalence of *H. pylori* infection found in this cohort of patients with esophageal carcinoma suggests a protective role.

Key Words: *Helicobacter pylori*; Eradication; Esophageal tumor; Dysbiosis; Proton pump inhibitors; Carcinogenesis; Microbiota; Incidence

©The Author(s) 2024. Published by Baishideng Publishing Group Inc. All rights reserved.

Core Tip: *Helicobacter pylori* (*H. pylori*) is involved in gastric carcinogenesis and its eradication has become widely accepted. However, recent studies suggest that it might have a role in maintaining homeostasis in the gastroesophageal junction cells and may have a protective role in esophageal carcinogenesis. The absence of this microorganism might contribute to dysbiosis and alterations in the esophageal microenvironment which might finally be involved in the onset of esophageal tumor. We are very much concerned that the prevalence of esophageal cancer increases after the universalization of *H. pylori* eradication.

Citation: López-Gómez M, Morales M, Fuerte R, Muñoz M, Delgado-López PD, Gómez-Cerezo JF, Casado E. Prevalence of *Helicobacter pylori* infection among patients with esophageal carcinoma. *World J Gastroenterol* 2024; 30(29): 3479-3487

URL: <https://www.wjgnet.com/1007-9327/full/v30/i29/3479.htm>

DOI: <https://dx.doi.org/10.3748/wjg.v30.i29.3479>

INTRODUCTION

Esophageal cancer constitutes a relevant health problem, being the sixth cause of death attributable to cancer worldwide [1]. There are two major histological subtypes: Esophageal squamous cell carcinoma (SCC) and adenocarcinoma (AC). The incidence of AC has increased in the recent decades, currently accounting for almost half of all esophageal neoplasms [2]. Well-established risk factors for AC include Barrett's esophagus (BE), gastroesophageal reflux (GER), male sex, central obesity, older age, and tobacco smoking [3]. Interestingly, *Helicobacter pylori* (*H. pylori*) eradication with antibiotics and acid suppression therapies seem to be protective in gastric cancer [4]. *H. pylori* is a helical-shaped Gram-negative (GN) bacterium that generally colonizes the stomach early in life [5].

The estimated global prevalence of *H. pylori* infection has decreased from 58.2% (95%CI: 50.7-65.8) in the 1980-1990 decade to 43.1% (40.3%-45.9%) in the 2011-2022 period [6]. In Spain, studies report a population prevalence around 55% [7].

The prevalence of *H. pylori* infection in gastric cancer patients seems to vary among regions, with the highest and lowest figures in America and Africa, respectively (18.1%, 95%CI: 16.5-19.6 vs 9.5%, 95%CI: 5.9-13.1) [8].

However, a higher prevalence has been reported in other gastrointestinal malignancies. In a Finnish study, prevalence ranged from 100% for gallbladder cancer to 94% for ampulla of Vater cancer. Similarly, the prevalence of *H. pylori* infection in hepatocellular carcinoma has been reported to be up to 94% [9]. *H. pylori* has also been found in 86% patients with advanced colon neoplasia [10]. Proton pump inhibitors (PPIs) are classically prescribed for the treatment of acid-related gastrointestinal disorders and are part of the multidrug treatment for *H. pylori* eradication [11]. However, long-term administration of PPI can change the microbial composition in the esophagus [12] which might contribute to the development of BE and esophageal cancer. The role of *H. pylori* in the origin of gastric ACs has been thoroughly studied and its eradication has become one of the greatest challenges worldwide [13].

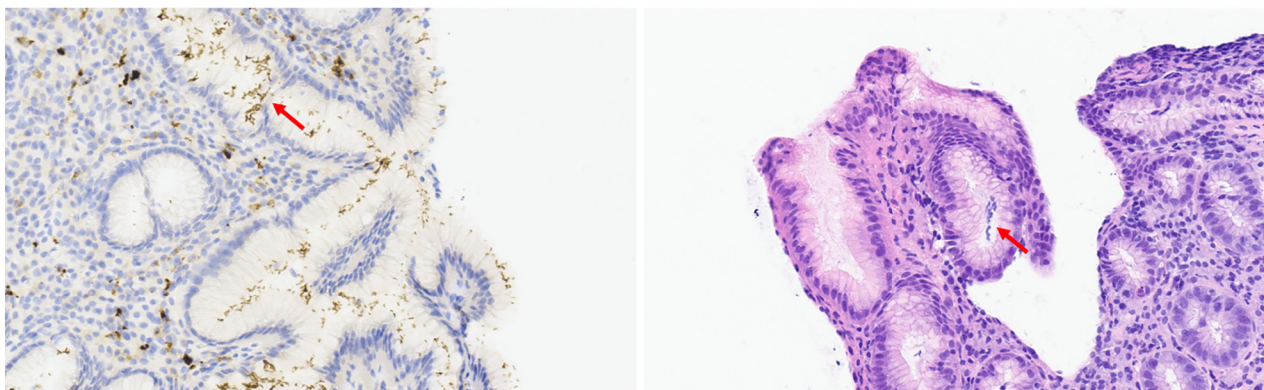


Figure 1 Red arrows show *Helicobacter pylori* in the lumen of gastric mucosa.

Interestingly, the presence of *H. pylori* infection has been associated with a reduced risk of the development of esophagus ACs[14]. The underlying mechanisms responsible for this protective effect remain unclear. Several hypotheses have been suggested: *H. pylori* induced atrophy and loss of the acid parietal cells in the antrum[15]; secondary alteration of esophageal microbiota[16]; induction of apoptosis of AC cells progressing from BE *via the* Fas apoptotic pathway[17], and ghrelin synthesis reduction, with a secondary impact on central obesity and GER[18].

Considering that *H. pylori* eradication has become a widely accepted healthcare policy in Spain, concerns about a plausible increase in esophageal cancer have grown. In this study we reviewed the prevalence of pre-existent *H. pylori* infection among patients with esophageal carcinoma and recorded which of them were on previous PPI treatment, either as part of the eradication therapy or for other reasons.

MATERIALS AND METHODS

Study design

We performed a retrospective observational study that included all patients with a previous diagnosis of esophageal or gastroesophageal junction (GEJ) cancer between February 2008 and December 2023 and were managed at our center. Local Institutional Review Board approval was obtained on June 1, 2023. All patients or relatives were informed and accepted participation by signing a written informed consent form. Patients' data were anonymized according to national regulations (RD 1720/2007, Organic Law 15/1999 on Personal Data Protection).

Patient selection

All patients over 18 years of age with a diagnosis of esophageal or GEJ cancer were included. Patients with gastric or other gastrointestinal neoplasms were excluded from the study. The incidence of *H. pylori* in gastric cancer patients diagnosed throughout the same years (2008 and 2022) were also included in the analysis.

In situ tumors or premalignant lesions were also excluded. All patients included agreed to participate in the study.

Tumor subtype and *H. pylori* infection identification

All tumors (esophageal or GEJ invasive tumors) were histologically confirmed by trained pathologists of the center. Paraffin-embedded primary tumor specimens and metastatic tumor specimens containing at least 70% of tumoral cells were selected for each patient. Specimens were reviewed and classified into three subtypes: AC, SCC, and others. The presence or absence of *H. pylori* was also confirmed by histologic examination. Definitive diagnosis was made by microscopic visualization of *H. pylori* on hematoxylin and eosin (H&E)-stained slides. Positive cases of *H. pylori* included patients with obvious *H. pylori* gastritis with characteristic inflammation and heavy bacterial load, and those with subtle *H. pylori* gastritis with less inflammation and fewer bacteria. Two examples of *H. pylori* identification are shown in **Figure 1** (gastric cancer) and **Figure 2A** (GEJ cancer). **Figure 2B** and **C** show H&E staining of GEJ and esophageal tumors.

Variables registered, endpoint and statistical analysis

In addition to the presence or absence of *H. pylori* in biopsy specimens, the following variables were recorded: Age, sex, tumor stage at diagnosis, and previous treatment with anti-acid drugs (PPIs or others, as part of *H. pylori* eradication therapy or as independent treatment). The endpoint of the study was the identification of *H. pylori* infection in patients diagnosed with esophageal cancer. Results were expressed as mean \pm SD for numerical variables, and as ratios and proportions for categorical variables, both with 95% CI.

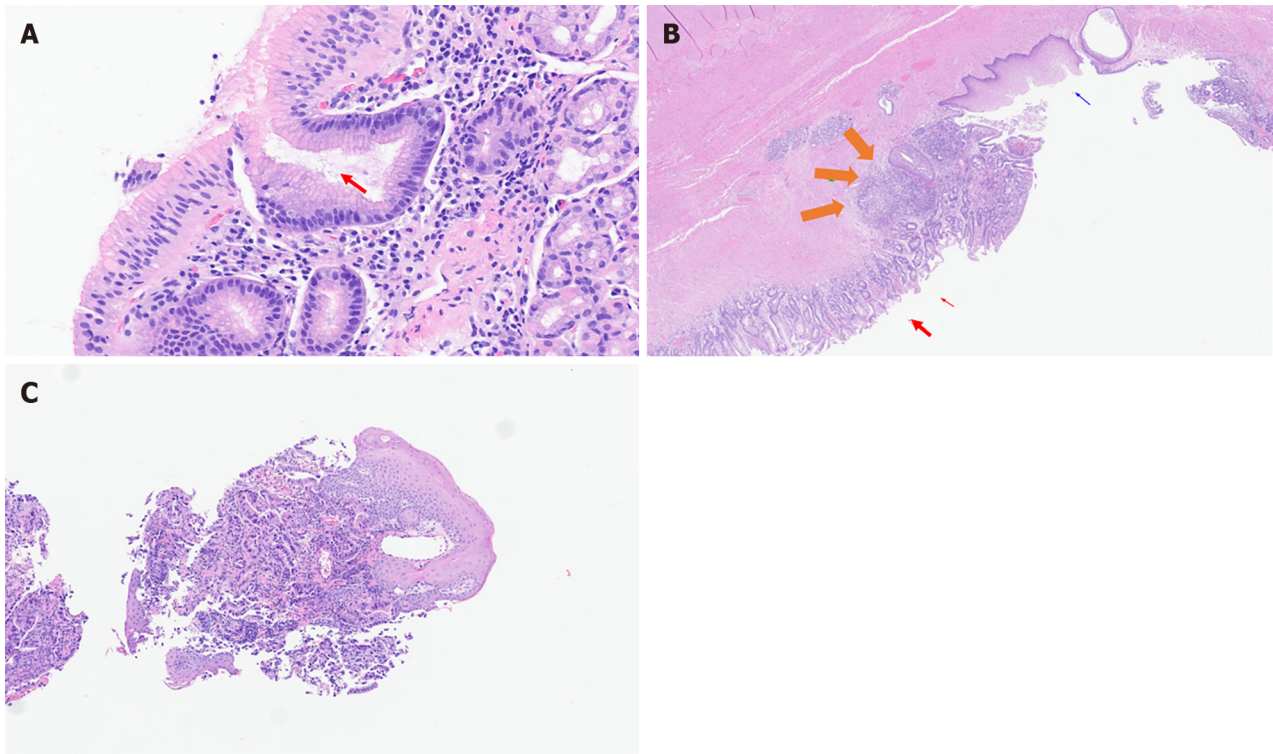


Figure 2 Gastroesophageal junction and esophageal tumors. A: Red arrow shows *Helicobacter pylori* in the lumen of an esophageal gland; B: Gastroesophageal junction (GEJ) tumor. Blue arrow shows squamous cells in normal esophageal tumors. Red arrows show Barrett's esophagus. Orange arrows show GEJ adenocarcinoma; C: Esophageal adenocarcinoma.

RESULTS

Demographic and clinical data

A total of 89 patients (77.5% males, mean age 66 years) were included in our study. Demographic and clinical data are shown in [Table 1](#).

Tumor statistics

In this cohort, AC was the most frequent histological subtype (52.8%) followed by SCC (41.6%). Neuroendocrine tumors were infrequent (5.6%). As expected, most tumors were stage III-IV at the time of diagnosis (60.7%). *H. pylori* infection was confirmed in only 4 patients (4.5%), 3 with AC and 1 with SCC. Survival among *H. pylori* positive patients did not exceed 9 months after diagnosis ([Figure 3](#)). Although only one patient had undergone previous *H. pylori* eradication therapy, 96.6% of patients had received prior PPI treatment and 35.9% ($n = 32$) had received both PPIs and other antiacid treatment (such as anti- H_2 or sucralfate). The median time from initiation of PPIs to the diagnosis of esophageal cancer was 15 months, ranging from 3 to 60 months ([Figure 4](#)). Total gastric cancer diagnoses were 431, with a rate in men/women of 269/162 (62.41% vs 37.58%). The mean age was 66 years. *H. pylori* prevalence among them was 66%.

DISCUSSION

H. pylori infection and esophageal cancer are conditions with a high geographical variability and prevalence. The purpose of this study was to analyze the prevalence of *H. pylori* in esophageal tumors in a sample of patients from a tertiary hospital in Madrid, Spain. In this cohort, less than 5% of patients with esophageal cancer tested positive for *H. pylori*, which is approximately 10 times less than the general population. Interestingly, most of them had received previous antiacid treatment, either with PPIs or with anti- H_2 drugs.

The burden due to the diagnosis of esophageal cancer is expected to rise dramatically across high-income countries, with increasing incidence rates predicted for the next decades, according to some statistical models[19].

Previous epidemiologic studies provide inconclusive data on a positive, inverse or neutral association between *H. pylori* infection and esophageal carcinoma. Although meta-analyses of observational studies favor an inverse association, these may be biased by confounders present in older studies ([Table 2](#)). Our findings are in line with this supposedly protective role of *H. pylori* infection in the genesis of esophageal carcinoma.

To date, four meta-analyses have shown an inverse association between *H. pylori* infection and esophageal cancer. Islami and Kamangar[20] reviewed 19 studies ([Table 2](#)) and found an inverse association between cytotoxin-associated gene A (CagA)-positive strains of *H. pylori* and the risk of esophageal carcinoma [odds ratio (OR) 0.41, 95%CI: 0.28-0.62].

Table 1 Baseline characteristics of all patients, *n* (%)

Number of patients	<i>n</i> = 89
Age (median, yr)	66 (26-93)
Sex	
Male	69 (77.52)
Female	20 (22.47)
Histology	
Adenocarcinoma	47 (52.80)
Squamous cell carcinoma	37 (41.57)
Others	4 (5.5)
Tumor location	
Gastroesophageal junction	33 (70.21)
Esophageal	14 (29.78)
Stage	
Stage I-II	25 (28.08)
Stage III-IV	54 (60.67)
Presence of <i>Helicobacter pylori</i>	4 (4.5)
Adenocarcinoma	3 (6.3)
Squamous cell carcinoma	1 (2.7)
Previous PPI treatments	86 (96.82)

PPI: Proton pump inhibitor.

Table 2 Studies regarding *Helicobacter pylori* infection and esophageal carcinoma

Paper characteristics				Sample characteristics			
Ref.	Country	Year	Design	Age (mean, yr)	<i>Helicobacter pylori</i> prevalence	Tumor	Location
Holleczeck <i>et al</i> [23]	Germany	2020	Cohort	62.2	47.80%	EA	Gastric cardia; esophagus esophago-gastric junction
Wu <i>et al</i> [27]	Taiwan	2009	Case-control	58.3	35.30%	ESCC	Upper, middle or lower third of the esophagus
Khoshbaten <i>et al</i> [28]	Iran	2011	Case-control	63.9 cases; 61.3 controls	41.2% ± 36.95% cases; 56.2% ± 29.5% controls	ESCC	Esophagus
Hu <i>et al</i> [29]	Taiwan	2009	Case-control	50-70	37% cases; 53% controls	ESCC	Upper, middle or lower third esophagus
Cook <i>et al</i> [30]	Finland	2010	Case-control	57.7 cases; 58.1 controls	80.28% cases; 78.16% controls	ESCC	Upper, middle, and lower third of the esophagus
Murphy <i>et al</i> [18]	Finland	2012	Case-control	57.9 cases; 57.9 controls	78.04% cases; 76.82% controls	ESCC	Esophagus

EA: Esophageal adenocarcinoma; ESCC: Esophageal squamous cell carcinoma.

A similar conclusion was stated by Zhuo *et al*[21], in a study that included 195 articles, and found a risk of developing esophageal AC among *H. pylori* infected patients of 0.58 (95%CI: 0.48-0.70) as compared with controls. Xie *et al*[22], also confirmed this inverse association in the general population (0.59, 95%CI: 0.51-0.68, and an OR of 0.56, 95%CI: 0.45-0.70 in Cag A+ strains). However, results from these meta-analyses were based on retrospective observational studies. Only one population-based prospective study[23] conducted in Germany, which included 9949 patients followed for a mean period of 13.8 years, found a 0.65-fold increase risk of developing esophageal carcinoma among *H. pylori* infected individuals.

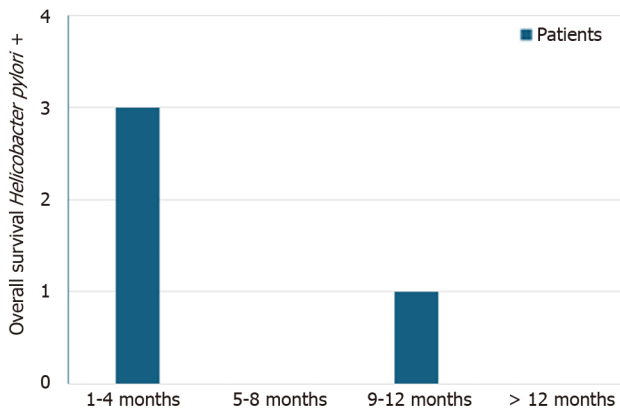


Figure 3 Survival among *Helicobacter pylori* positive patients.

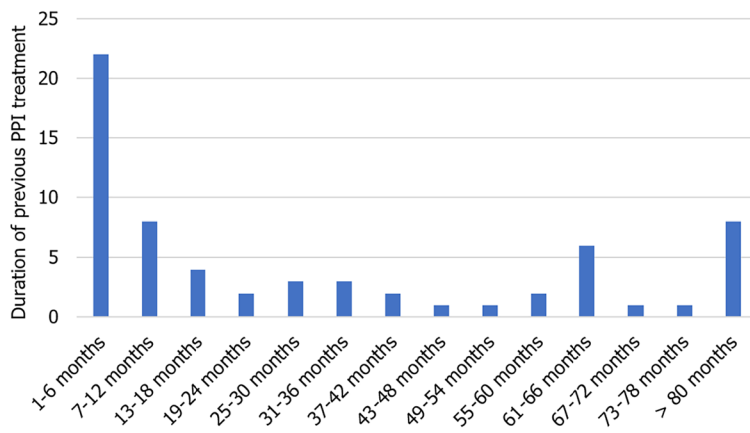


Figure 4 Duration of proton pump inhibitor treatment before cancer development. PPI: Proton pump inhibitor.

These findings support the need for further research on the inner mechanisms behind this association. Several plausible pathways have been suggested. First, *H. pylori* infection-related gastritis induces atrophy and loss of parietal cells in the stomach, resulting in a reduced reflux which decreases related-esophagitis and BE; second, *H. pylori* infection might induce apoptosis in Barrett's cells through the Fas-Caspase cascade; third, *H. pylori* could promote inflammatory responses by activating nuclear factor kappa B, that induces the production of certain cytokines and tumor necrosis factor-alpha, directly damaging the epithelial DNA by dysregulating DNA transcription factors such as the caudal type homeobox 2 (*Cdx2*); fourth, *H. pylori* infected patients have a significantly lower number of ghrelin producing cells, which has been shown to be involved in cancer development and metastasis[24].

Additionally, an interesting and promising relation between *H. pylori* infection and the esophageal microbiome has been suggested. In the normal esophageal mucosa, *Streptococcus spp.*, together with six other major phyla (*Firmicutes*, *Bacteroides*, *Actinobacteria*, *Proteobacteria*, *Fusobacteria* and *TM7*) are the most commonly found microorganisms belonging to the local microbiota. Type I microbiota, which is mainly composed of gram-positive (GP) bacteria, is typically found in the normal esophagus mucosa. In contrast, type II microbiota, enriched in GN bacteria, is associated with an abnormal esophagus. *H. pylori* infection might play a role in the shift from GP to GN-enriched environment. Previous studies have reported that *H. pylori* seems to influence gastric microbiome diversity and composition and affects species prevalence and phylogenetic diversity. In fact, esophageal tumors colonized by *H. pylori* CagA positive strains were inversely associated with the risk of developing esophageal AC. These findings suggest that the absence of *H. pylori* in the gastroesophageal mucosa might contribute to an unbalanced esophageal microbial composition that may promote carcinogenesis[25].

Similarly, PPI treatment has been suggested to alter the esophageal microbiota, by increasing species like *Firmicutes* and decreasing *Bacteroides* and *Proteobacteria*. A recent study has suggested that the long-term use of PPIs is associated with an increased risk of esophageal cancer[26], likely attributable to the colonization of non-gastric microorganisms capable of producing nitrosamines, which are known to promote both esophageal AC and SCC. In our cohort, almost 95% of patients were under PPI treatment, in line with this hypothesis. PPIs-induced reduction of esophageal gastric acid reflux might avoid the death of acid sensitive bacteria involved in the maintenance of type I microbiota. This hypothesis might be in conflict with recommending PPIs in non-dysplastic BE, aimed to decrease the risk of progression to high grade dysplasia and AC. Considering the widespread use of PPIs, we believe our findings maintain a reasonable doubt on the possible deleterious effect of this medication in the development of esophageal cancer.

This study has some limitations. Most importantly, given the observational and retrospective nature of the study, a causal relation between the lack of *H. pylori* infection and esophageal cancer cannot be established. Second, as we did not include a non-PPI treatment control group, we cannot conclude on the relation between PPI therapy and esophageal carcinogenesis. Finally, although the results of a single center study may not be extrapolated to other populations, it highlights the importance of further research on the role of *H. pylori*, and other microorganisms belonging to the local microbiota, in esophageal carcinogenesis.

CONCLUSION

The very low prevalence of *H. pylori* infection among esophageal cancer patients found in our study is consistent with previous reports suggesting that the presence of *H. pylori* might have a protective role in esophageal carcinogenesis. Several mechanisms have been proposed for this inverse association, in which esophageal mucosa dysbiosis seems to play a primary role. Future research should determine to what extent *H. pylori* infection interacts with the esophageal microbiota, establish whether this interaction is involved in the protective role of *H. pylori*, and whether PPI treatment contributes to the alteration of esophageal microbiome and eventually promotes esophageal cancer.

ACKNOWLEDGEMENTS

We acknowledge and thank the patients that participated in this study.

FOOTNOTES

Author contributions: López-Gómez M and Morales M wrote the manuscript; Morales M and Fuerte R curated the clinical data and performed the biostatistical analyses; Muñoz M selected the tumor tissue to be analyzed; Delgado-López PD drafted/edited the manuscript and reviewed the English version; Gómez-Cerezo JF and Casado E helped with clinical and scientific input and study design; López-Gómez M developed the study concept, interpreted the data and drafted/edited the manuscript; All authors edited the manuscript.

Institutional review board statement: Infanta Sofia University Hospital Institutional Review Board approval was obtained on June 1, 2023.

Informed consent statement: All study participants, or their legal guardian, provided informed written consent prior to study enrollment.

Conflict-of-interest statement: All the authors report no relevant conflicts of interest for this article.

Data sharing statement: Participants gave informed consent for data sharing at miriam.lopez@telefonica.net.

STROBE statement: The authors have read the STROBE Statement-checklist of items, and the manuscript was prepared and revised according to the STROBE Statement-checklist of items.

Open-Access: This article is an open-access article that was selected by an in-house editor and fully peer-reviewed by external reviewers. It is distributed in accordance with the Creative Commons Attribution NonCommercial (CC BY-NC 4.0) license, which permits others to distribute, remix, adapt, build upon this work non-commercially, and license their derivative works on different terms, provided the original work is properly cited and the use is non-commercial. See: <https://creativecommons.org/licenses/by-nc/4.0/>

Country of origin: Spain

ORCID number: Miriam López-Gómez [0000-0001-6019-647X](https://orcid.org/0000-0001-6019-647X); Pedro-David Delgado-López [0000-0002-9317-6958](https://orcid.org/0000-0002-9317-6958); Jorge Francisco Gómez-Cerezo [0000-0002-3288-5996](https://orcid.org/0000-0002-3288-5996); Enrique Casado [0000-0002-1279-3293](https://orcid.org/0000-0002-1279-3293).

Corresponding Author's Membership in Professional Societies: European Society of Medical Oncology, 387999; Sociedad Española de Oncología Médica.

S-Editor: Li L

L-Editor: Webster JR

P-Editor: Yu HG

REFERENCES

- 1 Ferlay J, Soerjomataram I, Dikshit R, Eser S, Mathers C, Rebelo M, Parkin DM, Forman D, Bray F. Cancer incidence and mortality worldwide: sources, methods and major patterns in GLOBOCAN 2012. *Int J Cancer* 2015; **136**: E359-E386 [PMID: [25220842](https://pubmed.ncbi.nlm.nih.gov/25220842/) DOI: [10.1002/ijc.29355](https://doi.org/10.1002/ijc.29355)]

- 10.1002/jjc.29210]
- 2 **Bird-Lieberman EL**, Fitzgerald RC. Early diagnosis of oesophageal cancer. *Br J Cancer* 2009; **101**: 1-6 [PMID: 19513070 DOI: 10.1038/sj.bjc.6605126]
 - 3 **Vakil N**, van Zanten SV, Kahrilas P, Dent J, Jones R; Global Consensus Group. The Montreal definition and classification of gastroesophageal reflux disease: a global evidence-based consensus. *Am J Gastroenterol* 2006; **101**: 1900-20; quiz 1943 [PMID: 16928254 DOI: 10.1111/j.1572-0241.2006.00630.x]
 - 4 **Quante M**, Abrams JA, Wang TC. The rapid rise in gastroesophageal junction tumors: is inflammation of the gastric cardia the underwater iceberg? *Gastroenterology* 2013; **145**: 708-711 [PMID: 23978439 DOI: 10.1053/j.gastro.2013.08.023]
 - 5 **Piscione M**, Mazzone M, Di Marcantonio MC, Muraro R, Mincione G. Eradication of *Helicobacter pylori* and Gastric Cancer: A Controversial Relationship. *Front Microbiol* 2021; **12**: 630852 [PMID: 33613500 DOI: 10.3389/fmicb.2021.630852]
 - 6 **Hooi JKY**, Lai WY, Ng WK, Suen MMY, Underwood FE, Tanyingoh D, Malfertheiner P, Graham DY, Wong VWS, Wu JCY, Chan FKL, Sung JY, Kaplan GG, Ng SC. Global Prevalence of *Helicobacter pylori* Infection: Systematic Review and Meta-Analysis. *Gastroenterology* 2017; **153**: 420-429 [PMID: 28456631 DOI: 10.1053/j.gastro.2017.04.022]
 - 7 **Li Y**, Choi H, Leung K, Jiang F, Graham DY, Leung WK. Global prevalence of *Helicobacter pylori* infection between 1980 and 2022: a systematic review and meta-analysis. *Lancet Gastroenterol Hepatol* 2023; **8**: 553-564 [PMID: 37086739 DOI: 10.1016/S2468-1253(23)00070-5]
 - 8 **Shirani M**, Pakzad R, Haddadi MH, Akrami S, Asadi A, Kazemian H, Moradi M, Kaviar VH, Zomorodi AR, Khoshnood S, Shafieian M, Tavasolian R, Heidary M, Saki M. The global prevalence of gastric cancer in *Helicobacter pylori*-infected individuals: a systematic review and meta-analysis. *BMC Infect Dis* 2023; **23**: 543 [PMID: 37598157 DOI: 10.1186/s12879-023-08504-5]
 - 9 **Murphy G**, Michel A, Taylor PR, Albanes D, Weinstein SJ, Virtamo J, Parisi D, Snyder K, Butt J, McGlynn KA, Koshiol J, Pawlita M, Lai GY, Abnet CC, Dawsey SM, Freedman ND. Association of seropositivity to *Helicobacter* species and biliary tract cancer in the ATBC study. *Hepatology* 2014; **60**: 1963-1971 [PMID: 24797247 DOI: 10.1002/hep.27193]
 - 10 **Shmueli H**, Melzer E, Braverman M, Domniz N, Yahav J. *Helicobacter pylori* infection is associated with advanced colorectal neoplasia. *Scand J Gastroenterol* 2014; **49**: 35-42 [PMID: 24164483 DOI: 10.3109/00365521.2013.848468]
 - 11 **Amir I**, Konikoff FM, Oppenheim M, Gophna U, Half EE. Gastric microbiota is altered in oesophagitis and Barrett's oesophagus and further modified by proton pump inhibitors. *Environ Microbiol* 2014; **16**: 2905-2914 [PMID: 24112768 DOI: 10.1111/1462-2920.12285]
 - 12 **Pei Z**, Yang L, Peek RM, Jr, Levine SM, Pride DT, Blaser MJ. Bacterial biota in reflux esophagitis and Barrett's esophagus. *World J Gastroenterol* 2005; **11**: 7277-7283 [PMID: 16437628 DOI: 10.3748/wjg.v11.i46.7277]
 - 13 **Polyzos SA**, Zeglinas C, Artemaki F, Douleris M, Kazakos E, Katsinelos P, Kountouras J. *Helicobacter pylori* infection and esophageal adenocarcinoma: a review and a personal view. *Ann Gastroenterol* 2018; **31**: 8-13 [PMID: 29333062 DOI: 10.20524/aog.2017.0213]
 - 14 **Thrift AP**. The epidemic of oesophageal carcinoma: Where are we now? *Cancer Epidemiol* 2016; **41**: 88-95 [PMID: 26851752 DOI: 10.1016/j.canep.2016.01.013]
 - 15 **Nie S**, Chen T, Yang X, Huai P, Lu M. Association of *Helicobacter pylori* infection with esophageal adenocarcinoma and squamous cell carcinoma: a meta-analysis. *Dis Esophagus* 2014; **27**: 645-653 [PMID: 24635571 DOI: 10.1111/dote.12194]
 - 16 **Castaño-Rodríguez N**, Goh KL, Fock KM, Mitchell HM, Kaakoush NO. Dysbiosis of the microbiome in gastric carcinogenesis. *Sci Rep* 2017; **7**: 15957 [PMID: 29162924 DOI: 10.1038/s41598-017-16289-2]
 - 17 **Jones AD**, Bacon KD, Jobe BA, Sheppard BC, Deveney CW, Rutten MJ. *Helicobacter pylori* induces apoptosis in Barrett's-derived esophageal adenocarcinoma cells. *J Gastrointest Surg* 2003; **7**: 68-76 [PMID: 12559187 DOI: 10.1016/S1091-255X(02)00129-4]
 - 18 **Murphy G**, Kamangar F, Albanes D, Stanczyk FZ, Weinstein SJ, Taylor PR, Virtamo J, Abnet CC, Dawsey SM, Freedman ND. Serum ghrelin is inversely associated with risk of subsequent oesophageal squamous cell carcinoma. *Gut* 2012; **61**: 1533-1537 [PMID: 22180062 DOI: 10.1136/gutjnl-2011-300653]
 - 19 **Arnold M**, Laversanne M, Brown LM, Devesa SS, Bray F. Predicting the Future Burden of Esophageal Cancer by Histological Subtype: International Trends in Incidence up to 2030. *Am J Gastroenterol* 2017; **112**: 1247-1255 [PMID: 28585555 DOI: 10.1038/ajg.2017.155]
 - 20 **Islami F**, Kamangar F. *Helicobacter pylori* and esophageal cancer risk: a meta-analysis. *Cancer Prev Res (Phila)* 2008; **1**: 329-338 [PMID: 19138977 DOI: 10.1158/1940-6207.CAPR-08-0109]
 - 21 **Zhuo X**, Zhang Y, Wang Y, Zhuo W, Zhu Y, Zhang X. *Helicobacter pylori* infection and oesophageal cancer risk: association studies via evidence-based meta-analyses. *Clin Oncol (R Coll Radiol)* 2008; **20**: 757-762 [PMID: 18793831 DOI: 10.1016/j.clon.2008.07.005]
 - 22 **Xie FJ**, Zhang YP, Zheng QQ, Jin HC, Wang FL, Chen M, Shao L, Zou DH, Yu XM, Mao WM. *Helicobacter pylori* infection and esophageal cancer risk: an updated meta-analysis. *World J Gastroenterol* 2013; **19**: 6098-6107 [PMID: 24106412 DOI: 10.3748/wjg.v19.i36.6098]
 - 23 **Hollecsek B**, Schöttker B, Brenner H. *Helicobacter pylori* infection, chronic atrophic gastritis and risk of stomach and esophagus cancer: Results from the prospective population-based ESTHER cohort study. *Int J Cancer* 2020; **146**: 2773-2783 [PMID: 31376284 DOI: 10.1002/ijc.32610]
 - 24 **Anderson LA**, Murphy SJ, Johnston BT, Watson RG, Ferguson HR, Bamford KB, Ghazy A, McCarron P, McGuigan J, Reynolds JV, Comber H, Murray LJ. Relationship between *Helicobacter pylori* infection and gastric atrophy and the stages of the oesophageal inflammation, metaplasia, adenocarcinoma sequence: results from the FINBAR case-control study. *Gut* 2008; **57**: 734-739 [PMID: 18025067 DOI: 10.1136/gut.2007.132662]
 - 25 **Yamamura K**, Baba Y, Nakagawa S, Mima K, Miyake K, Nakamura K, Sawayama H, Kinoshita K, Ishimoto T, Iwatsuki M, Sakamoto Y, Yamashita Y, Yoshida N, Watanabe M, Baba H. Human Microbiome *Fusobacterium Nucleatum* in Esophageal Cancer Tissue Is Associated with Prognosis. *Clin Cancer Res* 2016; **22**: 5574-5581 [PMID: 27769987 DOI: 10.1158/1078-0432.CCR-16-1786]
 - 26 **Holmberg D**, Mattsson F, Xie S, Ness-Jensen E, El-Serag H, Lagergren J. Risk of gastric and oesophageal adenocarcinoma following discontinuation of long-term proton-pump inhibitor therapy. *J Gastroenterol* 2022; **57**: 942-951 [PMID: 36258093 DOI: 10.1007/s00535-022-01930-3]
 - 27 **Wu IC**, Wu DC, Yu FJ, Wang JY, Kuo CH, Yang SF, Wang CL, Wu MT. Association between *Helicobacter pylori* seropositivity and digestive tract cancers. *World J Gastroenterol* 2009; **15**: 5465-5471 [PMID: 19916178 DOI: 10.3748/wjg.15.5465]
 - 28 **Khoshbaten M**, Zadimani A, Bonyadi MR, Mohammadzadeh M, Gachkar L, Pourhoseingholi MA. *Helicobacter pylori* infection reduces the risk of esophageal squamous cell carcinoma: a case-control study in Iran. *Asian Pac J Cancer Prev* 2011; **12**: 149-151 [PMID: 21517248]
 - 29 **Hu HM**, Kuo CH, Lee CH, Wu IC, Lee KW, Lee JM, Goan YG, Chou SH, Kao EL, Wu MT, Wu DC. Polymorphism in COX-2 modifies the inverse association between *Helicobacter pylori* seropositivity and esophageal squamous cell carcinoma risk in Taiwan: a case control study. *BMC Gastroenterol* 2009; **9**: 37 [PMID: 19463183 DOI: 10.1186/1471-230X-9-37]

- 30 **Cook MB**, Dawsey SM, Diaw L, Blaser MJ, Perez-Perez GI, Abnet CC, Taylor PR, Albanes D, Virtamo J, Kamangar F. Serum pepsinogens and *Helicobacter pylori* in relation to the risk of esophageal squamous cell carcinoma in the alpha-tocopherol, beta-carotene cancer prevention study. *Cancer Epidemiol Biomarkers Prev* 2010; **19**: 1966-1975 [PMID: 20647397 DOI: 10.1158/1055-9965.EPI-10-0270]

Basic Study

Leech *Poecilobdella manillensis* protein extract ameliorated hyperuricemia by restoring gut microbiota dysregulation and affecting serum metabolites

Xia Liu, Xing-Qiu Liang, Tian-Cai Lu, Zhe Feng, Min Zhang, Nan-Qing Liao, Feng-Lian Zhang, Bo Wang, Li-Sheng Wang

Specialty type: Gastroenterology and hepatology

Provenance and peer review:

Unsolicited article; Externally peer reviewed.

Peer-review model: Single blind

Peer-review report's classification

Scientific Quality: Grade A, Grade C

Novelty: Grade A, Grade B

Creativity or Innovation: Grade A, Grade B

Scientific Significance: Grade A, Grade C

P-Reviewer: Muntané J; Wang X

Received: March 10, 2024

Revised: June 20, 2024

Accepted: July 19, 2024

Published online: August 7, 2024

Processing time: 140 Days and 13.5 Hours



Xia Liu, Nan-Qing Liao, Feng-Lian Zhang, Bo Wang, Li-Sheng Wang, Medical College, Guangxi University, Nanning 530004, Guangxi Zhuang Autonomous Region, China

Xia Liu, Department of Traditional Chinese Medicine, HIV/AIDS Clinical Treatment Center of Guangxi (Nanning), The Fourth People's Hospital of Nanning, Nanning 530023, Guangxi Zhuang Autonomous Region, China

Xing-Qiu Liang, Department of Science and Technology, Ruikang Hospital Affiliated to Guangxi University of Chinese Medicine, Nanning 530011, Guangxi Zhuang Autonomous Region, China

Tian-Cai Lu, General Manager's Office, Guangxi Fuxinyi Biological Technology Co. Ltd., Pingnan 537300, Guangxi Zhuang Autonomous Region, China

Zhe Feng, Department of Joint and Sports Medicine, Ruikang Hospital Affiliated to Guangxi University of Chinese Medicine, Nanning 530011, Guangxi Zhuang Autonomous Region, China

Min Zhang, Department of Gerontology, Nanning Social Welfare Hospital, Nanning 530004, Guangxi Zhuang Autonomous Region, China

Corresponding author: Li-Sheng Wang, MD, PhD, Professor, Medical College, Guangxi University, No. 100 Daxue East Road, Nanning 530004, Guangxi Zhuang Autonomous Region, China. lswang@gxu.edu.cn

Abstract**BACKGROUND**

Hyperuricemia (HUA) is a public health concern that needs to be solved urgently. The lyophilized powder of *Poecilobdella manillensis* has been shown to significantly alleviate HUA; however, its underlying metabolic regulation remains unclear.

AIM

To explore the underlying mechanisms of *Poecilobdella manillensis* in HUA based on modulation of the gut microbiota and host metabolism.

METHODS

A mouse model of rapid HUA was established using a high-purine diet and potassium oxonate injections. The mice received oral drugs or saline. Additionally, 16S rRNA sequencing and ultra-high performance liquid chromatography with quadrupole time-of-flight mass spectrometry-based untargeted metabolomics were performed to identify changes in the microbiome and host metabolome, respectively. The levels of uric acid transporters and epithelial tight junction proteins in the renal and intestinal tissues were analyzed using an enzyme-linked immunosorbent assay.

RESULTS

The protein extract of *Poecilobdella manillensis* lyophilized powder (49 mg/kg) showed an enhanced anti-trioxypurine ability than that of allopurinol (5 mg/kg) ($P < 0.05$). A total of nine bacterial genera were identified to be closely related to the anti-trioxypurine activity of *Poecilobdella manillensis* powder, which included the genera of *Prevotella*, *Delftia*, *Dialister*, *Akkermansia*, *Lactococcus*, *Escherichia-Shigella*, *Enterococcus*, and *Bacteroides*. Furthermore, 22 metabolites in the serum were found to be closely related to the anti-trioxypurine activity of *Poecilobdella manillensis* powder, which correlated to the Kyoto Encyclopedia of Genes and Genomes pathways of cysteine and methionine metabolism, sphingolipid metabolism, galactose metabolism, and phenylalanine, tyrosine, and tryptophan biosynthesis. Correlation analysis found that changes in the gut microbiota were significantly related to these metabolites.

CONCLUSION

The proteins in *Poecilobdella manillensis* powder were effective for HUA. Mechanistically, they are associated with improvements in gut microbiota dysbiosis and the regulation of sphingolipid and galactose metabolism.

Key Words: Gut microbiota; Metabolism; Multi-omics; *Poecilobdella manillensis*; Sphingolipid metabolism pathway; Galactose metabolism pathway; Hyperuricemia

©The Author(s) 2024. Published by Baishideng Publishing Group Inc. All rights reserved.

Core Tip: This study reveals the novel therapeutic potential of *Poecilobdella manillensis* in treating hyperuricemia (HUA) through a dual mechanism: The direct modulation of uric acid levels and restoration of renal and intestinal barriers. Importantly, it highlights the role of proteins in *Poecilobdella manillensis* in rectifying gut microbiota dysbiosis and adjusting key metabolic pathways, most notably, sphingolipid and galactose metabolism. These findings highlight the multi-target, multi-channel effects of *Poecilobdella manillensis* treatment for HUA and provide fundamental data for the clinical use of HUA treatments.

Citation: Liu X, Liang XQ, Lu TC, Feng Z, Zhang M, Liao NQ, Zhang FL, Wang B, Wang LS. Leech *Poecilobdella manillensis* protein extract ameliorated hyperuricemia by restoring gut microbiota dysregulation and affecting serum metabolites. *World J Gastroenterol* 2024; 30(29): 3488-3510

URL: <https://www.wjgnet.com/1007-9327/full/v30/i29/3488.htm>

DOI: <https://dx.doi.org/10.3748/wjg.v30.i29.3488>

INTRODUCTION

Hyperuricemia (HUA) is a metabolic disorder characterized by abnormally elevated levels of uric acid (UA) in the bloodstream. HUA, often caused by purine metabolism disorders and UA metabolism disorders, tends to induce gout, and may also affect the urinary system[1]. A report detailing the trends in HUA and gout within China indicated that approximately 13.3% of the population is impacted by HUA, equating to around 177 million individuals[2]. Globally, the increasing incidence of HUA has resulted in it becoming one of the most common basal metabolic diseases[3]. Furthermore, accumulating evidence has shown that HUA plays a pivotal role not only in the development of gout, but also in diabetes mellitus, cardiovascular disease, hypertension, and chronic kidney disease[3]. Some studies have shown that HUA and gout are risk predictors of all-cause mortality from cardiovascular disease[4]. Given the harmful effects of HUA, there is an urgent need for a scientific understanding of the HUA pathogenesis and the identification of new therapeutic drugs.

The gut microbiota is crucial for the metabolism of HUA. Changes or imbalances in the composition of gut microbiota can lead to metabolic disorders throughout the body[5]. Approximately 70% of UA is eliminated *via* the kidneys, while the rest is primarily excreted in the feces or is further broken down by the gut microbiota[6]. A high-purine diet may influence the physiological state of the host through interactions with the gut microbiota[7]. Host metabolic function has been shown to be affected by changes in the structure and composition of the gut microbiota[8]. Exploring the pathogenesis of HUA using the gut microbiota as an entry point has become a new research hotspot worldwide. Early studies

have confirmed the relationship between the gut microbiota and metabolic changes in HUA[9-11], suggesting that changes in serum metabolism caused by the gut microbiota is a suitable strategy for HUA research.

Currently, medications for treating HUA comprise xanthine oxidase (XOD) inhibitors [such as allopurinol (AP) and febuxostat], recombinant urate oxidase (rasburicase), and promoters of UA excretion (benzbromarone)[12,13]. Although these drugs exhibit clinical efficacy, their side effects frequently restrict their usage in clinical settings. For instance, AP can provoke a deadly hypersensitivity syndrome[14], benzbromarone may cause hepatotoxicity[13], and rasburicase is known to trigger rapid hypersensitivity reactions[15,16]. Therefore, it is necessary to find valid, promising, and economical therapies for the treatment of HUA. Leeches (*Hirudo*) are part of traditional Chinese medicine, first seen in the “Shennong Materia Medica”, a pharmacological treatise published in the Eastern Han Dynasty[17]. *Poecilobdella manillensis*, commonly known as the Philippine cattle leech or medical vermiculite in Manila, belongs to the genus of medicinal vermiculite leeches[18]. This larger species of leech is widely distributed throughout Southeast Asia, including regions in China, such as Guangxi. In China, medicinal vermiculite leeches that feed on animal blood include *Poecilobdella manillensis* and *Hirudonipponia whitma*[19]. Some studies have reported that their pharmacological effects include analgesic, anti-inflammatory, platelet-inhibitory, anticoagulant, and thrombin-regulatory functions, in addition to degradative effects on the extracellular matrix[18,20,21]. Limited studies have been performed to explore the efficacy of *Poecilobdella manillensis* on HUA and gout. Dong *et al*[22] reported that *Poecilobdella manillensis* lyophilized powder significantly reduced UA levels in HUA mice, whilst also proving to be safe for use. However, the active anti-HUA components, the *in vivo* metabolic mechanisms, and the molecular mechanisms of this treatment are not fully understood. In recent years, further research on leeches has identified the main components of leeches, which include proteins, polypeptides, some small molecular compounds, and trace elements[23]. Most studies have focused on the effect of single isolated polypeptides, such as hirudin[24,25], but not a mixture of different proteins, such as the leech total protein (LTP). Therefore, the mechanism by which LTP lowers UA has not yet been clarified, and no studies on the treatment of HUA with LTP currently exist.

To the best of our knowledge, there are no metabolomics and microbiome studies on the effects of LTP in HUA animals. Here, we aimed to reveal host serum metabolic changes, in addition to gut microbial changes, in the cecal contents of HUA mice. Furthermore, we aimed to reveal to possible mechanism through a combination of gut microbiota and metabolomics analyses.

MATERIALS AND METHODS

Chemicals and reagents

Experimental leech *Poecilobdella manillensis* freeze-dried powder (Place of origin: Pingnan of Guangxi, China) was supplied by Guangxi Fuxinyi Biological Technology Co., Ltd. (Pingnan, China). Potassium oxonate (PO) (purity $\geq 98.0\%$, P137112) and AP (purity $\geq 98.0\%$) were purchased from Shanghai Aladdin Biochemical Technology Co., Ltd. (Shanghai, China). The high-purine diet consisted of mice feedstuff (100 g), yeast extract (40 g), and yeast ribonucleic acid (2 g), which were re-granulated after melting the above ingredients, supplied by Jiangsu Xietong Pharmaceutical Bio-engineering Co., Ltd. (Nanjing, China). UA (C012-2-1), XOD (A002-1-1), creatinine (CRE, C011-2-1), and blood urea nitrogen (BUN, C013-2-1) biochemical test kits were purchased from Nanjing Jiancheng Bioengineering Institute (Nanjing, China). Enzyme-linked immunosorbent assay (ELISA) kits for glucose transporter 9 (GLUT9, RX201243M), ATP-binding cassette transporter G2 (ABCG2, RX200182M), urate transporter 1 (URAT1, RX200399M), occludin (RX202826M), and zonula occludens-1 (ZO-1, RX202825M) were obtained from Quanzhou Ruixin Biotechnology Co., Ltd. (Quanzhou, China). The Enhanced bicinchoninic acid assay (BCA) Protein Assay Kit, catalogued as P0010S, was sourced from Beyotime Biotechnology, headquartered in Shanghai, China.

Extraction of LTP from *Poecilobdella manillensis* lyophilized powder

First, *Poecilobdella manillensis* lyophilized powder was dissolved in phosphate-buffered saline (PBS) at a concentration of 39 mg/mL. The extraction was then performed using the ammonium sulfate saturation precipitation technique. Gradual ammonium sulfate salting-out stages were implemented to selectively harvest crude protein within the 30%-80% range. The procedural parameters are delineated in [Supplementary Table 1](#). The protein activity of each fraction underwent meticulous examination. The methodology is outlined as follows: The solution was immersed in ammonium sulfate at 30% saturation, allowing it to rest in a refrigerated environment at 4 °C for 6 hours. Next, the solution underwent centrifugation at 8000 rpm for 20 minutes to remove precipitated impurities. These steps were repeated using 80% saturated ammonium sulfate, including centrifugation and harvesting of the resulting precipitate. The resolubilized and precipitated crude protein underwent further processing through centrifugal ultrafiltration, utilizing Millipore Amicon® Ultra 3KD tubes at 14000 rpm for 20 minutes, thereby facilitating ultrafiltration and desalination. The desalted crude protein solution (LTP) was meticulously amassed, appropriately concentrated, and stored at 4 °C[26-28].

Animals

Kunming mice (male, specific pathogen-free, 20-25 g) were provided by Tianqin Biotechnology Co., Ltd. (Changsha, China). Before the onset of the experimental procedures, all mice underwent a 1-week acclimation period in the designated animal facility, which was rigorously maintained at a temperature of 24 \pm 2 °C, a humidity level of 50% \pm 5%, and subjected to a 12 hours light/dark cycle. Throughout this preparatory phase, the subjects had unrestricted access to food and water, ensuring their physiological and psychological readiness for the forthcoming studies. All experimental procedures complied with the United Kingdom Animals (Scientific Procedures) Act 1986 and associated guidelines and

were approved by the Medical Ethics Committee of Guangxi University.

Animal treatment

For the induction of HUA and renal dysfunction, mice were provided with a high-purine diet and intraperitoneal injection of 200 μ L PO for 7 consecutive days. The high-purine diet consisted of mice feedstuff (100 g), yeast extract (40 g), and yeast ribonucleic acid (2 g), which were re-granulated after melting the above ingredients. Potassium oxyate was dissolved in 0.5% sodium carboxymethyl cellulose solution at a concentration of 52.5 mg/mL.

In the study, 36 mice were randomly allocated into four parallel groups (8-10 mice in each group), comprising a normal control group (CON), a PO-induced HUA model group (HUA), a group treated with leech *Poecilobdella manillensis* total protein extract (LTP, receiving 49 mg/kg/day *via* intragastric administration), and a positive control group (AP, receiving 5 mg/kg/day AP by intragastric administration). The CON group was provided with a normal diet and intraperitoneal injection with 200 μ L 0.5% sodium carboxymethyl cellulose, while the HUA group was provided with a high-purine diet and intraperitoneal injection with 200 μ L PO. The modeling methods adopted by the LTP group and AP group were consistent with those of the HUA group. Animal modeling and pharmacotherapeutics commenced concurrently. The protein concentrations in the leech *Poecilobdella manillensis* lyophilized Powder and LTP were determined with the BCA method[29-32]. All groups of mice were anesthetized with isoflurane after the last pharmaceutical intervention. Urine and blood samples were collected to measure UA, CRE, and BUN. Hepatic tissue supernatant (detailed methods in "Detection of hepatic XOD activity" of Materials and Methods) was employed for the assessment of XOD. The supernatant derived from kidney and jejunum tissues was utilized for the evaluation of UA transporters, including URAT1, GLUT9, and ABCG2, in addition to the epithelial tight junction proteins ZO-1 and occludin.

Urine collection

After 7 days of treatment, the mice were transferred to a clean and empty cage individually for the collection of urine, which was then centrifuged at 3500 rpm for 10 minutes. The supernatant was used for UA and CRE analyses directly.

Collection of serum and tissue samples

Animals were anesthetized using diethyl ether 1 hour after the last treatment, and blood was collected to obtain serum for the UA and CRE assays. Kidney and liver tissues were dissected quickly on ice and stored in liquid nitrogen for the following analyses.

Evaluation of UA, CRE, and BUN in the serum and urine

Blood and urine specimens were spun at 3500 rpm for 15 minutes at 4 °C to clear any sediment and extract the supernatant. UA concentrations were measured with an enzymatic colorimetric technique, as per the given guidelines. CRE levels were analyzed using a sarcosine oxidase-based CRE assay kit, following the provided instructions. Similarly, the level of BUN was assessed using a urea nitrogen assay kit following the urease method specified in the kit instructions.

Detection of hepatic XOD activity

To create a 10% liver homogenate, liver tissues were first washed with chilled PBS (0.01 mol/L, pH = 7.4) to eliminate residual blood. After weighing, the tissues were finely chopped on ice, and mixed with PBS at a specific ratio of 10 mg of tissue to 100 μ L of PBS, effectively making 1 mL of buffer equivalent to 0.1 g of tissue. Protease inhibitors were added to the PBS to prevent protein degradation. The mixture was then homogenized using a pre-cooled tissue grinder. To further break down the tissue and cells, the homogenate underwent ultrasonication according to our experimental procedures. Following homogenization, the tissues were centrifuged at 7228 rpm for 8 minutes at -4 °C to separate the supernatant. Protein concentrations were quantified using an Enhanced BCA Protein Assay Kit. Liver XOD activity was then measured using an XOD test kit, according to the instructions.

Assessment of UA transporters and epithelial tight junction proteins

For the extraction of supernatant, tissue specimens were prepared by homogenizing jejunal and kidney tissues using a pre-cooled tissue grinder, as described above ("Detection of hepatic XOD activity"). Following homogenization, the tissues were spun at 7228 rpm for 8 minutes, and the supernatant was subsequently collected at -4 °C. The analysis of UA transporters (including URAT1, GLUT9, and ABCG2) and epithelial tight junction proteins (including ZO-1 and occludin) was performed using ELISAs, following the kit instructions.

Histological examination

Renal tissues were prepared for histological analysis using hematoxylin and eosin (HE) staining: (1) Fixation and embedding: Mouse kidney tissues were longitudinally sectioned, and immediately fixed in 4% paraformaldehyde. After 72 hours, the tissues were rinsed with running water for 15 minutes, dried with sterile gauze, and placed in dehydration trays; (2) Dehydration: Tissues underwent dehydration using an increasing series of ethanol concentrations in a dehydration device. This included 75% ethanol for 4 hours, followed by 85% for 2 hours, and then 90%, 95%, and absolute ethanol stages I and II for 1.5 hours, 1 hour, and 30 minutes, respectively; (3) Clearing and infiltration: Post-dehydration, the tissues underwent clearing in xylene, which facilitates better paraffin infiltration due to its miscibility with both ethanol and paraffin. Subsequently, the tissues were infiltrated using a graded series of paraffin wax at 60 °C to ensure complete penetration; (4) Sectioning: The embedded tissues were sectioned at 4 μ m thickness using a microtome, floated in a 40 °C water bath for expansion, and mounted on adhesion slides. The slides were then dried in a 60 °C oven for 3

hours to adhere the sections; and (5) Staining: (a) Deparaffinization: Sections were deparaffinized in xylene and rehydrated through a graded series of ethanol to water; (b) Staining: Sections were stained in Mayer's hematoxylin for 5 minutes, washed, and differentiated in 1% hydrochloric acid in ethanol for 2-3 seconds. After rinsing, sections were blued in 0.6% ammonia water and then stained with 1% aqueous eosin for 5 minutes; and (c) Dehydration and clearing: Ultimately, sections underwent dehydration in alcohol, were cleared using xylene, and were mounted in neutral resin for microscopic analysis.

Untargeted metabolomics analysis using ultra-high performance liquid chromatography with quadrupole time-of-flight mass spectrometry

Metabolomics instrument: Q-Exactive Quadrupole-Orbitrap High-Resolution Mass Spectrometer (Thermo Scientific, United States), UltiMate 3000 Ultra High-Performance Liquid Chromatography System (Thermo Scientific, United States).

Chromatography conditions: The chromatographic analysis employed an ACQUITY UPLC BEH C18 column with dimensions of 50 mm by 2.1 mm and a particle size of 1.7 μm . The column was kept at a constant 30 °C, while the autosampler was cooled to 10 °C. For both positive and negative ion modes, the mobile phases were 0.1% formic acid in water (Phase A) and methanol (Phase B). The gradient elution was structured as follows: From 0 to 2 minutes, 95% Phase A; over the next 11 minutes, decreased linearly to 0% Phase A; held at 0% Phase A from 13 to 16 minutes; rapidly reverted to 95% Phase A within 0.1 minutes; and held at 95% Phase A from 16.1 to 19 minutes. The chromatography utilized a flow rate of 0.3 mL/min and an injection volume of 2 μL .

Mass spectrometry conditions: Ionization used a heated electrospray source at 350 °C. The spray voltage for negative ion mode was 3.0 kV. The transfer capillary temperature was at 320 °C, the sheath gas pressure was 35 psi, and the auxiliary gas flow was 10 psi. Full mass scan (MS) and data-dependent MS/MS scan mode was used, covering a mass range of 200 to 2000 m/z. Resolutions were 70000 for first-stage and 17500 for second-stage scans, with high-purity nitrogen as the collision gas.

Workflow for cecal microbiota analysis

Cecal content specimens were procured from the cecal regions. Genomic DNA was extracted employing the Cetyltrimethylammonium Bromide methodology[33]. After extraction, the concentration and purity of the DNA were meticulously evaluated *via* electrophoresis conducted on a 1% agarose gel, a standard procedure to ensure the integrity and quality of the genetic material for downstream applications. This step is crucial in molecular biology workflows to ascertain the suitability of DNA samples for further analyses. Following the assessment, DNA was diluted to a standard concentration of 1 ng/ μL utilizing a sterile aqueous solution for the amplification process.

Amplification of the 16S rRNA gene sequences, specifically targeting the V3-V4 regions, was achieved using primers 341F (5'-CCTAYGGGRBGCASCAG-3') and 806R (5'-GGACTACNNGGGTATCTAAT-3'), each appended with a unique barcode. The polymerase chain reaction (PCR) amplifications were executed within a reaction volume of 15 μL , incorporating Phusion® High-Fidelity PCR Master Mix, sourced from New England Biolabs, Beijing, China. This reaction mixture also included 2 $\mu\text{mol/L}$ concentrations of both the forward and reverse primers, alongside an approximate 10 ng quantity of template DNA. The thermal cycling protocol was initiated with a denaturation phase at 98 °C for 1 minute. This phase was succeeded by 30 cycles, each comprising a denaturation step at 98 °C for 10 seconds, an annealing step at 50 °C for 30 seconds, and an elongation step at 72 °C for 30 seconds. The cycling protocol was finalized with an elongation phase at 72 °C, extending for 5 minutes, to ensure the completion of DNA synthesis. This methodological approach ensures the fidelity and specificity of the amplified DNA sequences, which is integral for subsequent molecular analyses.

Following amplification, the PCR products underwent electrophoresis within a 2% agarose gel matrix, utilizing a 1X Tris-acetate-EDTA buffer, to evaluate the results of amplification. Subsequently, PCR products were pooled at equimolar concentrations and the pooled products were purified using the Universal DNA Purification Kit (TianGen, Beijing, China). The generation of sequencing libraries was meticulously conducted utilizing the NEB Next® Ultra DNA Library Prep Kit (Illumina, headquartered in San Diego, United States), adhering stringently to the guidelines provided by the manufacturer. Following library preparation, index codes were appended to facilitate the identification and multiplexing of samples. The assessment of library integrity and quality was performed using the Agilent 5400 Bioanalyzer (Agilent Technologies, California, United States), ensuring optimal library standards before sequencing. Upon satisfactory evaluation of library quality, sequencing was undertaken on the Illumina sequencing platform. This process yielded 250 bp paired-end reads, allowing for comprehensive coverage and depth of the genomic regions.

Bioinformatics and statistical analysis

Bioinformatics analysis of the gut microbiome: Bioinformatics analysis followed the "Atacama Soil Microbiome Tutorial" from Qiime2docs, supplemented with custom scripts. Raw FASTQ data were imported into QIIME2, then underwent quality control, trimming, denoising, and chimeric sequence removal using the dada2 plugin, resulting in an amplicon sequence variant feature table. The taxonomic classification used the GREENGENES 13_8 99% Operational Taxonomic Unit database, with V3-V4 region alignment *via* QIIME2 plugins, excluding mitochondrial and chloroplast DNA. Statistical tools, including ANCOM, ANOVA, and DESeq2, were used to identify differentially abundant bacteria across samples. Microbial diversity within samples (alpha diversity) and between samples (beta diversity) was assessed using QIIME2 indices and was visualized through principal coordinate analysis (PCoA). Partial least squares discriminant analysis (PLS-DA), through "mixOmics" and "vegan" R packages, respectively, explored the impact of microbiota variations and environmental factors. Spearman's rank correlations highlighted taxa associations, visualized in network plots. Functional predictions of microbial communities were estimated with Phylogenetic Investigation of

Communities by Reconstruction of Unobserved States, adhering to default parameters for consistent and reproducible analysis, in line with top-tier microbiome research standards.

Metabolomics data processing and analysis: Data processing was conducted using CD 3.1 software for peak detection, alignment, and normalization based on retention times and m/z values, forming two-dimensional data matrices. These were analyzed in MetaboAnalyst 6.0 for pattern recognition, employing the 80% rule to refine data for statistical evaluation. PLS-DA and orthogonal PLS-DA (OPLS-DA) methods were pivotal in variance analysis and identifying metabolomic differences between groups, with validation through permutation tests and K-fold cross-validation. VIP scores from OPLS-DA, indicating significant metabolite contributions, guided the identification of differential metabolites with $VIP > 1$, $P < 0.05$, and significant fold changes (FC), $FC \geq 1.5$, or $FC \leq 0.67$.

Differential metabolites were identified using the Human Metabolome Database and METLIN databases, ensuring accuracy by matching molecular mass and ionization details closely with experimental data. This facilitated the elucidation of metabolites linked to HUA. MetaboAnalyst 6.0 further explored the metabolic pathways affected by these metabolites, visualizing pathway impact and significance through bubble charts, and highlighting pathways with $P < 0.05$ as significantly altered. This comprehensive approach provided insights into the metabolites' roles and their implications in HUA, enhancing the understanding of the condition's metabolic underpinnings. PLS-DA, PCoA, and O2-PLS models were used to integrate the metabolome and microbiome datasets, which are described in detail above. The model was calculated on paired data sets; significant variables were then selected based on their correlation with the model score ($P < 0.01$).

Analysis of non-omics data: For numerical variables adhering to a normal distribution, descriptive statistics were articulated as means with standard deviations. Group comparisons were conducted using the t -test for two groups and ANOVA for more than two groups. Upon detecting significant differences between groups, the least significant difference technique was applied for subsequent pairwise comparisons. In instances where the assumption of normality was violated, descriptive statistics were presented as medians accompanied by interquartile ranges. Comparative analysis between two independent samples was conducted using the Mann-Whitney U test, whereas the Kruskal-Wallis H test facilitated comparisons across multiple groups. Upon identifying statistically significant disparities among groups, the Dunn's Sidak-Correction Factor method was employed for *post-hoc* multiple comparisons.

RESULTS

LTP ameliorated disruptions in UA and renal function in PO-induced HUA mice

The effect of LTP in terms of lowering urate was investigated in HUA mice. After 7 days of modeling, the HUA mice had considerably higher serum and urine UA and XOD levels than mice in the CON group, demonstrating that the HUA mouse model had been successfully constructed (Figure 1A-C). Compared with the HUA mice, mice in the LTP and AP groups had significantly decreased serum levels of UA ($P < 0.0001$) and liver XOD activity ($P < 0.01$) (Figure 1A and C). To assess renal function in HUA mice, serum CRE and BUN levels were analyzed. Serum CRE levels were significantly increased in the HUA mice, which were decreased by LTP ($P < 0.05$) (Figure 1D). Serum BUN levels showed a decreasing trend; however, this was not statistically significant between groups (Figure 1E). HE staining highlighted the differences in the renal morphology among the groups. The CON group exhibited well-organized tubules, clear lumens, and intact glomeruli. In contrast, the HUA model group showed severe renal damage, including tubular swelling, atrophy, and disordered epithelial alignment with disrupted glomeruli, in addition to pronounced inflammatory infiltration and vascular congestion. The LTP and AP treatment groups demonstrated significant protective effects; LTP notably reduced inflammation and restored the renal structure to that closely resembling the CON group, while AP was slightly less effective in alleviating congestion and glomerular changes (Figure 1F).

LTP promoted UA excretion by modulating urate transporters

Urate transporters are mainly responsible for UA excretion. Compared with the CON group, the concentrations of the renal tissue reabsorption transporters URAT1 and GLUT9 were elevated in the HUA group, while the concentration of the renal tissue secretory transporter ABCG2 was decreased in the HUA group. Following interventions with LTP and AP, reversals of these observations were seen in the LTP and AP groups (Figure 2A-C). Similarly, the concentrations of URAT1 and GLUT9 were upregulated in the jejunal tissues of the HUA group compared to the CON group, and there were decreases in URAT1 and GLUT9 after LTP treatment; however, these differences were not statistically significant (Figure 2D and E). The trend of ABCG2 expression in jejunal tissue was consistent with that in renal tissue (Figure 2F).

LTP ameliorated renal and intestinal barrier impairment in HUA mice

Epithelial tight junction proteins in renal and jejunal tissues were assessed to further investigate the extent of renal and intestinal barrier impairment. Compared with the CON group, the concentrations of the renal tissue epithelial tight junction proteins ZO-1 and occludin were decreased in the HUA group ($P < 0.05$) (Figure 3A and B). However, following treatment with LTP and AP, the concentrations of ZO-1 and occludin in renal tissues showed an increasing trend ($P < 0.01$) (Figure 3A and B). The concentrations of ZO-1 and occludin in jejunum tissue showed a similar trend as in renal tissue. Notably, the increase in jejunal tissue ZO-1 was statistically significant only in the LTP group ($P < 0.05$), whereas there was no statistically significant difference in the AP group ($P = 0.062$) (Figure 3C and D).

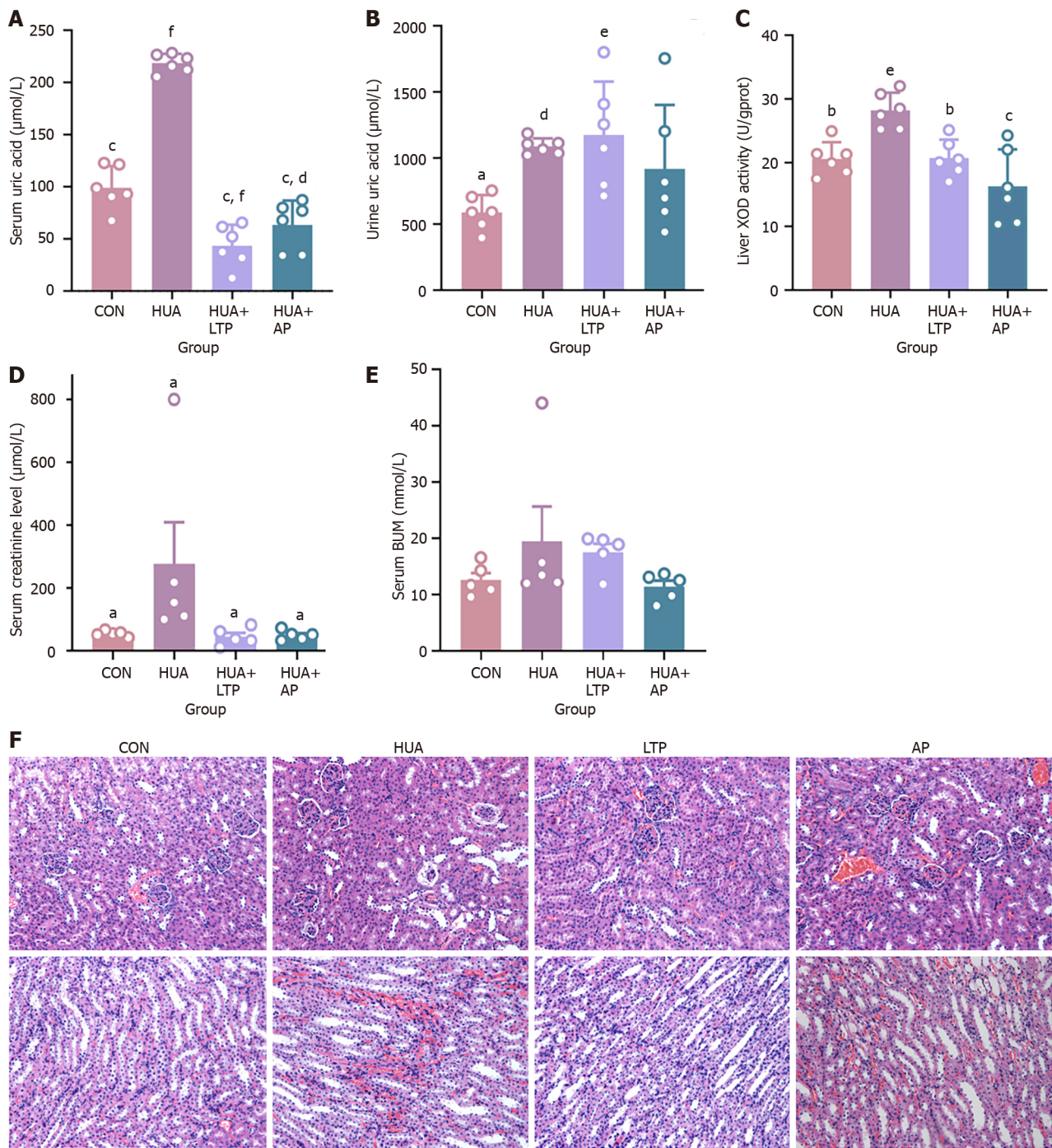


Figure 1 Effect of leech *Poecilobdella manillensis* total protein extract treatment on hyperuricemia. A: Serum uric acid levels; B: Urine uric acid levels; C: Liver xanthine oxidase activity; D: Serum creatinine levels; E: Blood urea nitrogen levels; F: Renal tissue hematoxylin and eosin staining pathology under 200 × magnification. Statistical significance determined by ANOVA is indicated as follows: ^a*P* < 0.05 vs hyperuricemia model group (HUA); ^b*P* < 0.01 vs HUA; ^c*P* < 0.001 vs HUA; ^d*P* < 0.05 vs normal control group (CON); ^e*P* < 0.01 vs CON; ^f*P* < 0.001 vs CON. CON: Normal control group; HUA: Hyperuricemia model group; AP: Allopurinol treatment group; LTP: Leech *Poecilobdella manillensis* total protein extract treatment group; XOD: Xanthine oxidase; BUN: Blood urea nitrogen.

LTP remodeled gut microbiota composition in HUA mice

To further analyze the UA-lowering potential of LTP, cecum content samples were subjected to 16S rRNA gene sequencing. Cecum microbiota communities were profiled using 16S rRNA gene V3-V4 pyrosequencing. The amount of sequencing data was sufficient to cover almost all micro-organisms, judging from the alpha rarefaction curve of all samples (Supplementary Figure 1A and B). First, the α diversity (including Shannon and Simpson indices) and β diversity were used to analyze the differences in microbial diversity within and between groups. The Shannon and Simpson indices in the HUA group were lower when compared to the CON group. However, the above indices in the LTP group were higher than those in the HUA group, with the results for Shannon’s index being statistically different (*P* < 0.05) (Figure 4A and B), suggesting that LTP could improve the richness and diversity of the gut microbiota in HUA mice. To assess the differences in gut microbial composition, PCoA and PLS-DA were performed. The PLS-DA analysis showed that the cluster of the HUA group was separated from that of the CON and LTP groups (Figure 4C, Supplementary

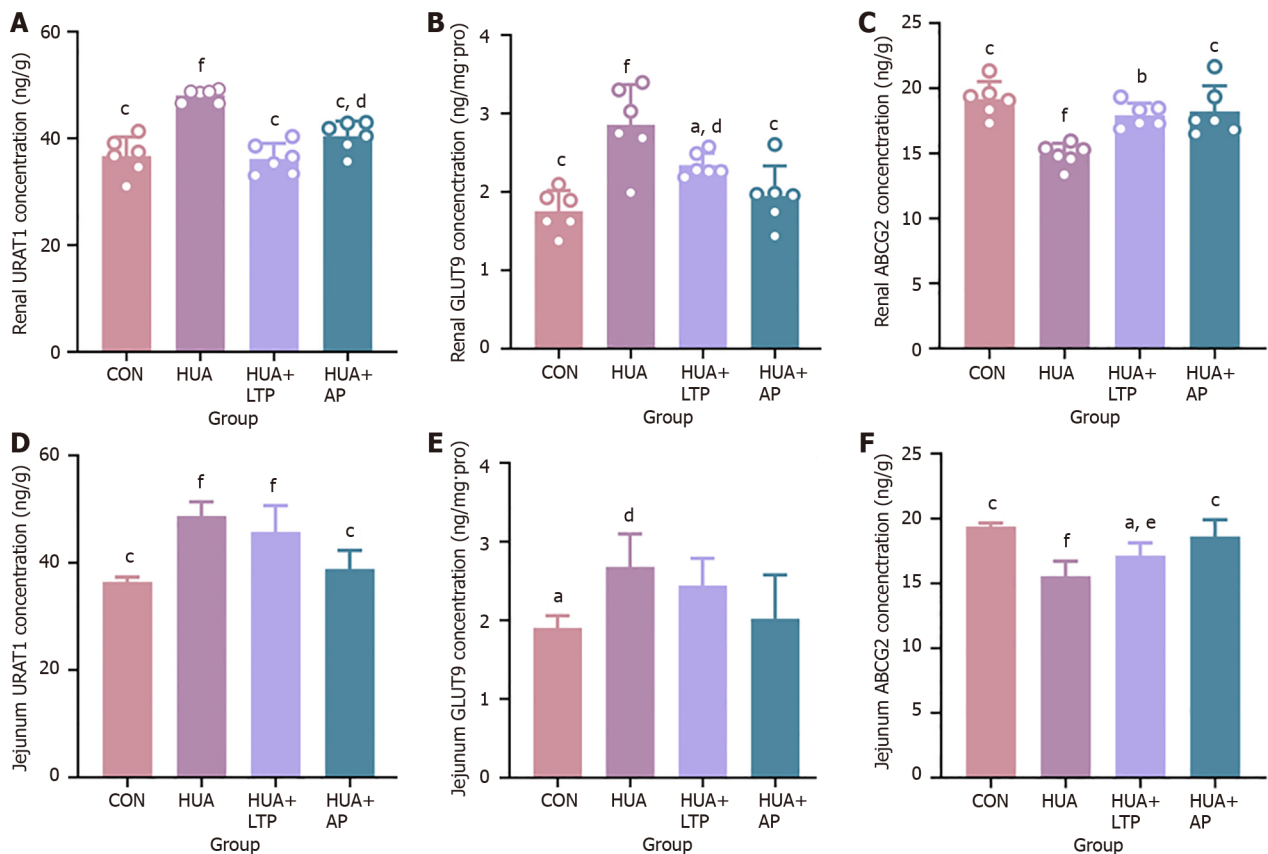


Figure 2 Effect of leech *Poecilobdella manillensis* total protein extract on facilitating uric acid excretion, evaluated by enzyme-linked immunosorbent assay. A: Renal urate transporter 1 (URAT1) concentration level; B: Renal glucose transporter 9 (GLUT9) concentration level; C: Renal ATP-binding cassette transporter G2 (ABCG2) concentration level; D: Jejenum URAT1 concentration level; E: Jejenum GLUT9 concentration level; F: Jejenum ABCG2 concentration level. Statistical significance determined by ANOVA is indicated as follows: ^a $P < 0.05$ vs hyperuricemia model group (HUA); ^b $P < 0.01$ vs HUA; ^c $P < 0.001$ vs HUA; ^d $P < 0.05$ vs normal control group (CON); ^e $P < 0.01$ vs CON; ^f $P < 0.001$ vs CON. Sample sizes: Renal tissue $n = 6$ for each group; Jejenum tissue $n = 4$ for each group. CON: Normal control group; HUA: Hyperuricemia model group; AP: Allopurinol treatment group; LTP: Leech *Poecilobdella manillensis* total protein extract treatment group; URAT1: Urate transporter 1; GLUT9: Glucose transporter 9; ABCG2: ATP-binding cassette transporter G2.

Figure 1C). PCoA plots showed that the cluster of the CON group was separated from that of the HUA group, while the LTP group was partially separated from the HUA group, and there was a significant difference ($P < 0.01$) among the three groups, as analyzed using permanova statistics (Figure 4D, Supplementary Figure 1D-G), indicating that LTP treatment altered the composition and distribution of the gut microbiota in HUA mice.

At the phylum level, the gut microbiome was dominated by *Firmicutes*, *Bacteroidota*, *Proteobacteria*, *Desulfobacterota*, *Verrucomicrobiota*, *Campilobacterota*, and *Patescibacteria*, which differed among the CON, HUA, and LTP groups (Figure 4E). Compared with the CON group, HUA group mice had a lower ratio of *Firmicutes* to *Bacteroidota* (F/B). After LTP treatment, the F/B ratio was significantly higher (Figure 5A), restoring gut microbial abundance and showing a similar microbial distribution to the CON group. The structural changes in the gut microbiota at the genus level were studied (Figures 4F and 5A-C). The absolute abundances of *Lactobacillus*, *Clostridium_sensu_stricto_1*, *Bifidobacterium*, *Prevotella*, and *Escherichia_Shigella* in the HUA group were remarkably lower than those in the CON group, while *Bacteroides*, *Alloprevotella*, and *Sphingomonas* were significantly enriched in the HUA group. LTP treatment reversed these changes and remodeled the bacterial abundance similar to that in the CON group. In addition, the LTP group showed a specific increase in the abundance of *Enterococcus*, *Dialister*, *Delftia*, *Faecalibacterium*, and *Akkermansia* (Figure 5A-C). Linear discriminant analysis effect size (LEfSe) analysis was used to compare the differences between the three groups at the phylum and genus level; with the threshold of the logarithmic linear discriminant analysis score as 4.0 and $P < 0.01$, it revealed that *Firmicutes*, *Bacteroidota*, *Proteobacteria*, and *Verrucomicrobiota* were significantly different species at the phylum level (Figure 4G). The LEfSe analysis also revealed that the abundance of *Bacteroides*, *Akkermansia*, *Escherichia_Shigella*, *Prevotella*, *Sphingomonas*, *Parabacteroides*, and *Alloprevotella* in the HUA and LTP groups significantly differed at the genus level (Figure 4H). Collectively, these results indicate that LTP modulated the gut microbiota of HUA mice, thereby alleviating PO-induced microecological dysregulation. Based on the Phylogenetic Investigation of Communities by Reconstruction of Unobserved States, the possible functions of the altered gut microbiota (CON vs HUA and HUA vs LTP) were analyzed. Figure 4I and J show the primary metabolic pathways with significant differences ($P < 0.05$).

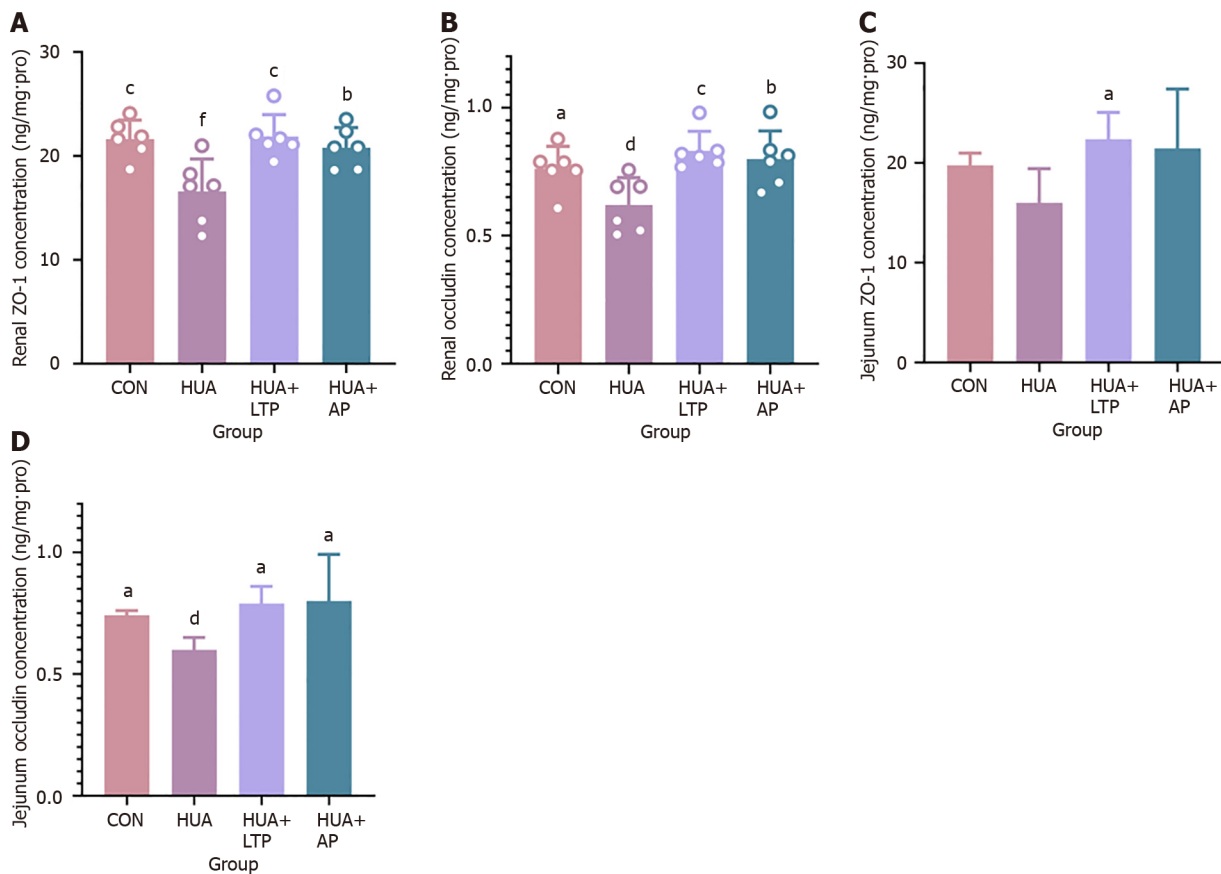
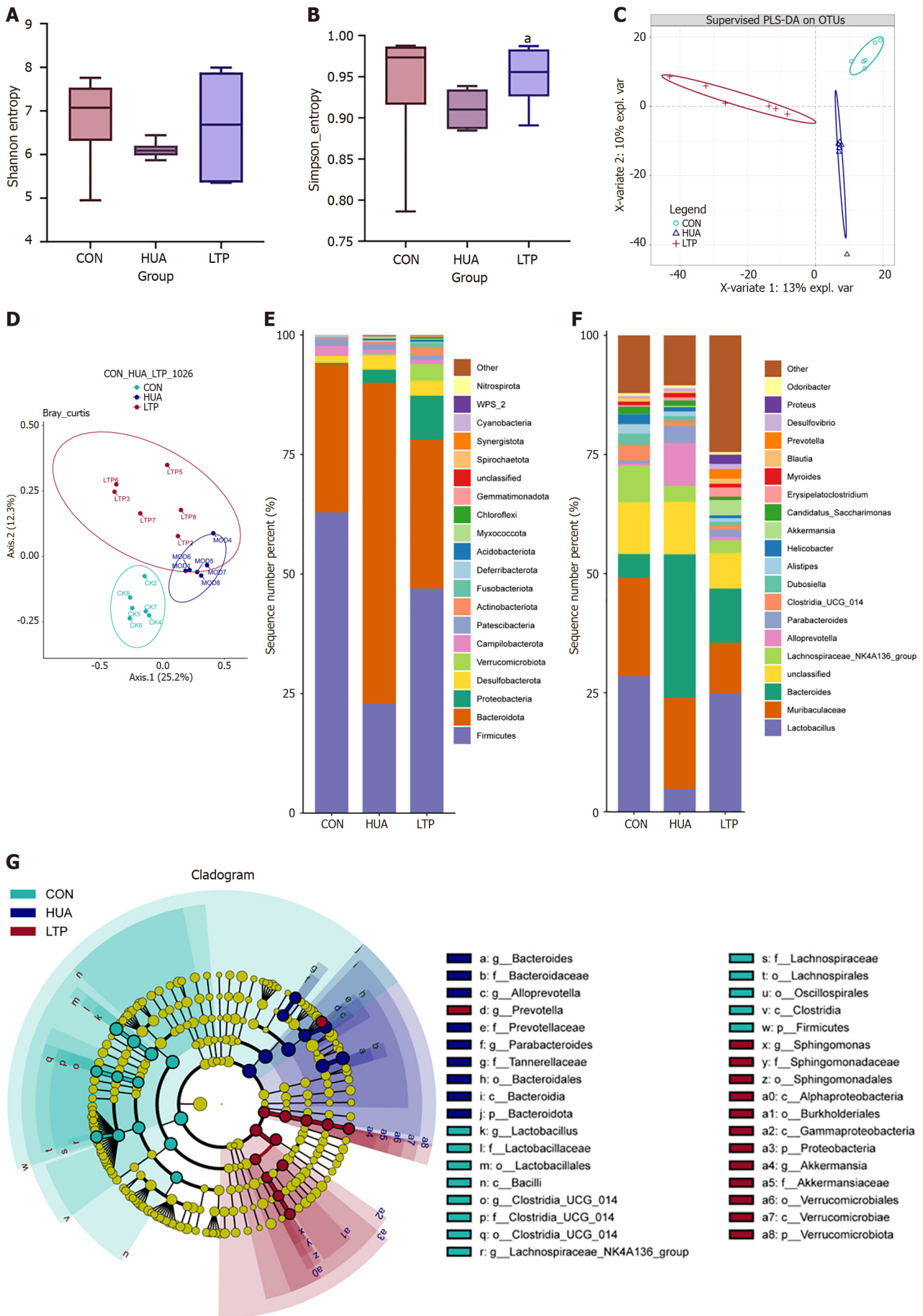


Figure 3 Effect of leech *Poecilobdella manillensis* total protein extract on epithelial tight junction proteins, evaluated by enzyme-linked immunosorbent assay. A: Renal zonula occludens-1 (ZO-1) concentration level; B: Renal occludin concentration level; C: Jejenum ZO-1 concentration level; D: Jejenum occludin concentration level. Statistical significance determined by ANOVA is indicated as follows: ^a $P < 0.05$ vs hyperuricemia model group (HUA); ^b $P < 0.01$ vs HUA; ^c $P < 0.001$ vs HUA; ^d $P < 0.05$ vs normal control group (CON); ^f $P < 0.001$ vs CON. Sample sizes: Renal tissue $n = 6$ for each group; Jejenum tissue $n = 4$ for each group. CON: Normal control group; HUA: Hyperuricemia model group; AP: Allopurinol treatment group; LTP: Leech *Poecilobdella manillensis* total protein extract treatment group; ZO-1: Zonula occludens-1.

LTP altered the serum metabolite composition in PO-induced HUA mice

We analyzed the serum metabolic profiles using ultra-high performance liquid chromatography with quadrupole time-of-flight mass spectrometry. The results of the PLS-DA score plot showed that the quality control samples were well-clustered in both positive and negative ion modes (Supplementary Figure 2A-F), indicating that the analytical method had good stability and reliability, which could be applied for the subsequent analysis of serum metabolites. As shown in the PLS-DA score plot (Figure 6A and B, Supplementary Figure 2G and H), the HUA and CON groups were separated, indicating significant differences in the metabolites of the two groups of mice. The LTP group and HUA group were separated, indicating that the LTP treatment could regulate the PO-induced alterations in serum metabolites. On the other hand, OPLS-DA was applied to further identify potential biomarkers with significant changes in concentration. The OPLS-DA results indicated a significant trend of separation in pairwise comparisons between CON and HUA groups, as well as between HUA and LTP groups (Figure 6C-F). As shown in Supplementary Table 2, using the criteria of $VIP > 1$ and $FC \leq 0.67$ or ≥ 1.50 , we screened a total of 98 common differential metabolites. The volcano map shows changes in serum metabolites between the HUA and CON groups; supplementation with LTP not only partially reversed some of these changes induced by HUA but also introduced new alterations in the serum metabolites (Figure 6G and H).

In total, 22 potential biomarkers were discovered by consulting both the Human Metabolome Database and the Kyoto Encyclopedia of Genes and Genomes (KEGG) database, as outlined in Supplementary Table 3. Heatmaps were generated to demonstrate global trends in differential metabolites between groups (Figure 7A). Sphinganine, D-glucose, L-tyrosine, ophthalmic acid, arachidonic acid, docosahexaenoic acid, 20-hydroxyeicosatetraenoic acid, and 8,11,14-eicosatrienoic acid were significantly increased in the HUA group compared to the CON group, while stearic acid and 5'-methylthioadenosine were significantly decreased. LTP treatment significantly reversed the changes in the above metabolites (Figure 7B). Further, KEGG pathway analysis of differential metabolites revealed that sphingolipid metabolism, tyrosine metabolism, primary bile acid biosynthesis, steroid hormone biosynthesis, starch and sucrose metabolism, galactose metabolism, and purine metabolism were significantly altered in the HUA group when compared with the CON group; while LTP significantly modulated cysteine and methionine metabolism, starch and sucrose metabolism, sphingolipid metabolism, galactose metabolism, and phenylalanine, tyrosine, and tryptophan biosynthesis, when compared with the HUA group (Figure 6I and J).



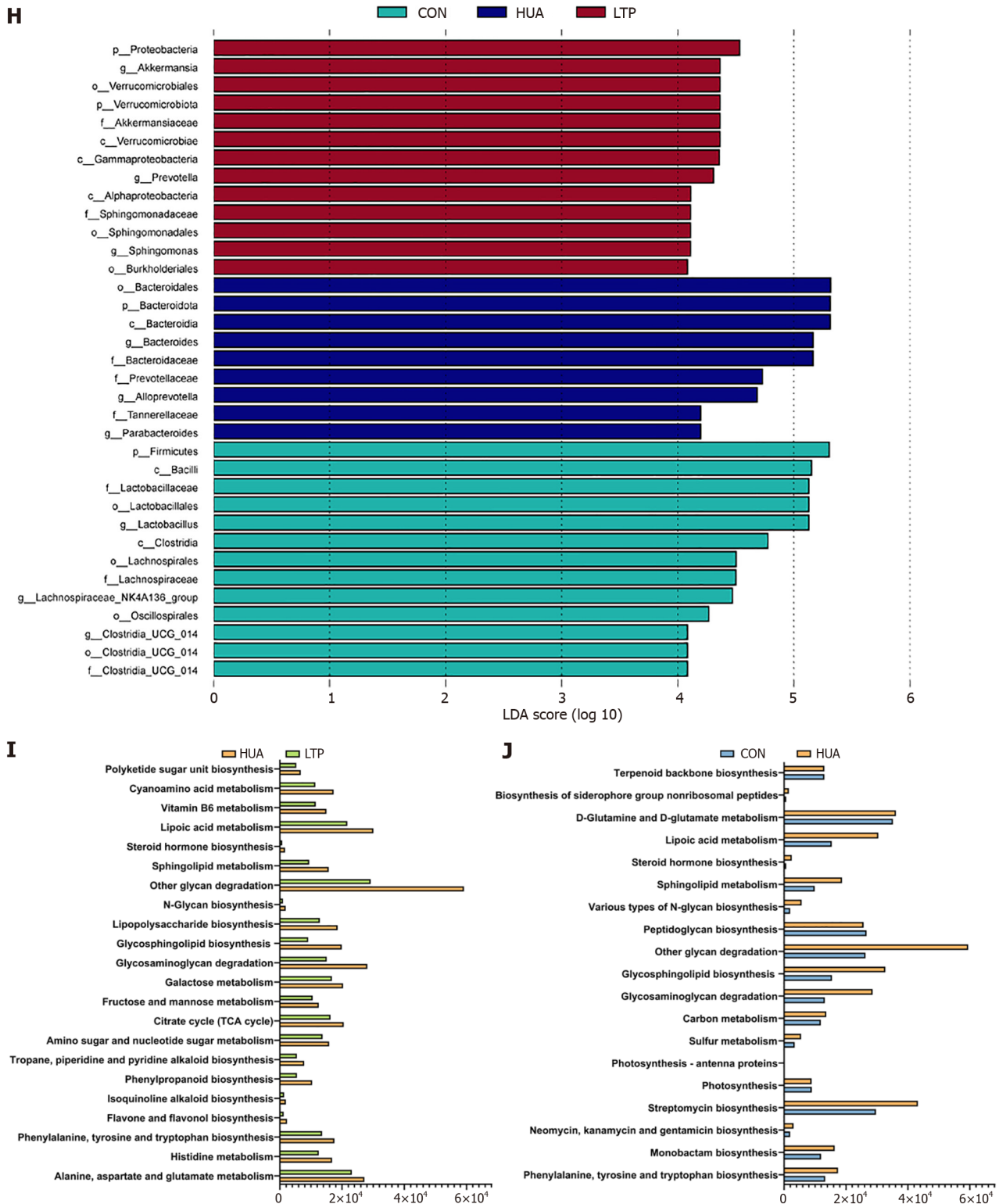
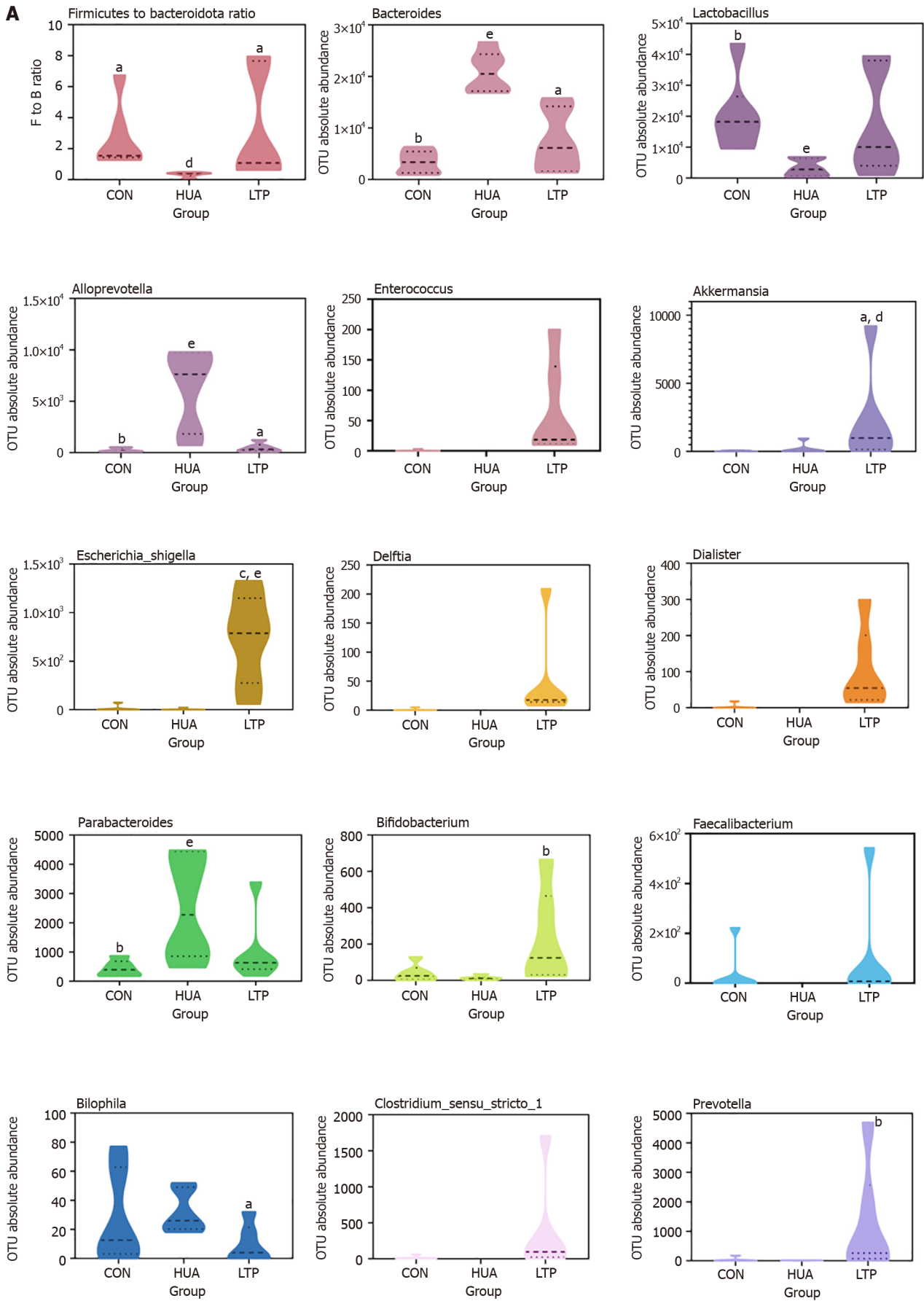


Figure 4 Leech *Poecilobdella manillensis* total protein extract alters the gut microbiota in potassium oxonate-induced hyperuricemia mice. A: Shannon index across three groups; B: Simpson index across three groups; C: Partial least squares discriminant analysis of three groups; D: Principal coordinate analysis of three groups; E: Distribution plot of relative abundance at the phylum level of bacteria; F: Distribution plot of relative abundance at the genus level of bacteria; G: Cladogram from linear discriminant analysis effect size (LEfSe) analysis identifying highly differentiated taxa from phylum to genus levels; H: Linear discriminant analysis graph from LefSe analysis identifying highly differentiated taxa from phylum to genus levels; I: Predicted functional pathways of gut microbiota in hyperuricemia model group (HUA) vs leech *Poecilobdella manillensis* total protein extract treatment group; J: Predicted functional pathways of gut microbiota in normal control group vs HUA. Statistical significance is indicated as follows: ^a*P* < 0.05 vs hyperuricemia model group. Sample size: *n* = 6 per group. CON: Normal control group; HUA: Hyperuricemia model group; LTP: Leech *Poecilobdella manillensis* total protein extract treatment group; LDA: Linear discriminant analysis.



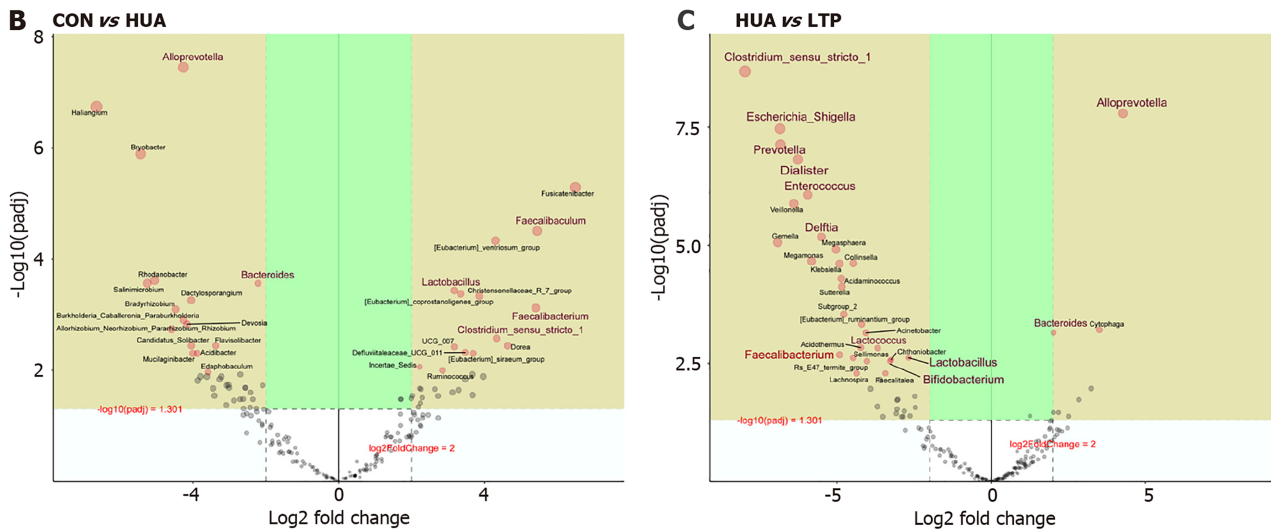


Figure 5 Effect of leech *Poecilobdella manillensis* total protein extract on vital microbial genus. A: The absolute abundance of vital microbial genera in all groups, assessed through the Kruskal-Wallis ANOVA; B and C: Significant differences between each two groups at the genus level of gut microbiota, determined by DESeq2 method [B: normal control group vs hyperuricemia model group (HUA); C: HUA vs leech *Poecilobdella manillensis* total protein extract treatment group; $n = 6$ for each group]. Statistical significance is indicated as follows: ^a $P < 0.05$ vs hyperuricemia model group (HUA); ^b $P < 0.01$ vs HUA; ^c $P < 0.001$ vs HUA; ^d $P < 0.05$ vs normal control group (CON); ^e $P < 0.01$ vs CON. CON: Normal control group; HUA: Hyperuricemia model group; LTP: Leech *Poecilobdella manillensis* total protein extract treatment group.

Correlation analysis between the gut microbiota and metabolites

When integrating the results of the microbiome and metabolome analysis, we found that the sphingolipid metabolism and galactose metabolism pathways coexisted in both the microbiota and metabolome (Figures 4I and J, 6I and J). To further elucidate the influential gut microbiota in the metabolite alterations from all groups, Pearson correlation analysis was employed to explore potential associations between gut bacterial composition and host metabolites (Supplementary Figure 3, Supplementary Tables 4 and 5). The findings indicated a substantial relationship between the LTP regulatory effects on metabolites and the abundance of *Bacteroides*, *Enterococcus*, *Faecalibacterium*, *Alloprevotella*, *Prevotellaceae_UCG_001*, *Lactococcus*, *Dialister*, *Delftia*, *Clostridium_sensu_stricto_1*, *Escherichia_Shigella*, *Dialister*, *Akkermansia*, and *Prevotella* (Figure 8). In particular, sphinganine - a metabolite within the sphingolipid metabolic pathway - exhibited significant negative correlations with *Delftia*, *Dialister*, *Clostridium_sensu_stricto_1*, *Escherichia_Shigella*, *Enterococcus*, and *Prevotella*, while indicating a notable positive correlation with *Bacteroides*. Furthermore, D-glucose - a metabolite within the galactose metabolism pathway - exhibited significant negative correlations with *Escherichia_Shigella*, *Akkermansia*, *Lactococcus*, *Enterococcus*, *Delftia*, *Dialister*, and *Prevotella*, while indicating a notable positive correlation with *Bacteroides* (Figure 8, Supplementary Tables 6 and 7). In conclusion, alterations in metabolites following LTP treatment were found to be intricately correlated with the regulation of gut microbiota, specifically *Prevotella*, *Delftia*, *Dialister*, *Akkermansia*, *Lactococcus*, *Escherichia_Shigella*, *Enterococcus*, and *Bacteroides*. Furthermore, LTP exhibited the potential to ameliorate HUA by modulating gut microbiome-dependent metabolism within the sphingolipid metabolic and galactose metabolic pathways.

Correlation analysis between gut microbiota and HUA-related parameters

To examine the relationship between the gut microbiome and HUA-related biochemical indicators, urate transporters, and epithelial tight junction proteins, the Pearson correlation coefficients were investigated. *Bifidobacterium*, *Clostridium_sensu_stricto_1*, *Enterococcus*, *Delftia*, *Escherichia_Shigella*, *Prevotella*, *Dialister*, and *Faecalibaculum* displayed strong negative correlations with serum UA and serum CRE ($P < 0.05$), while *Bacteroides*, *Alloprevotella*, *Bifidobacterium*, and *Bryobacter* showed strong positive correlations with serum UA and serum CRE ($P < 0.01$). *Delftia*, *Enterococcus*, *Lactococcus*, and *Dialister* displayed strong negative correlations with liver XOD concentration ($P < 0.01$), while *Bryobacter*, *Alloprevotella*, and *Bacteroides* displayed strong positive correlations with hepatic XOD concentration ($P < 0.01$). The results of the correlation analysis demonstrated that the absolute abundance levels of *Delftia*, *Enterococcus*, *Enterococcus*, *Clostridium_sensu_stricto_1*, *Escherichia_Shigella*, *Prevotella*, *Dialister*, *Alloprevotella*, and *Bacteroides* were closely related to the changes in renal and intestinal urate transporters and epithelial tight junction proteins. This suggests that the above gut microbiota contributed to the occurrence and recovery of HUA (Figure 9, Supplementary Table 8 and 9).

DISCUSSION

HUA has become a public health concern that needs to be solved urgently. Many of the previous studies have focused on the therapeutic effects of hirudin[24,25]; however, the associated mechanism has not been clarified, and no experiments on the reduction of UA by LTP have been reported. Based on verification of the effectiveness of *Poecilobdella manillensis*

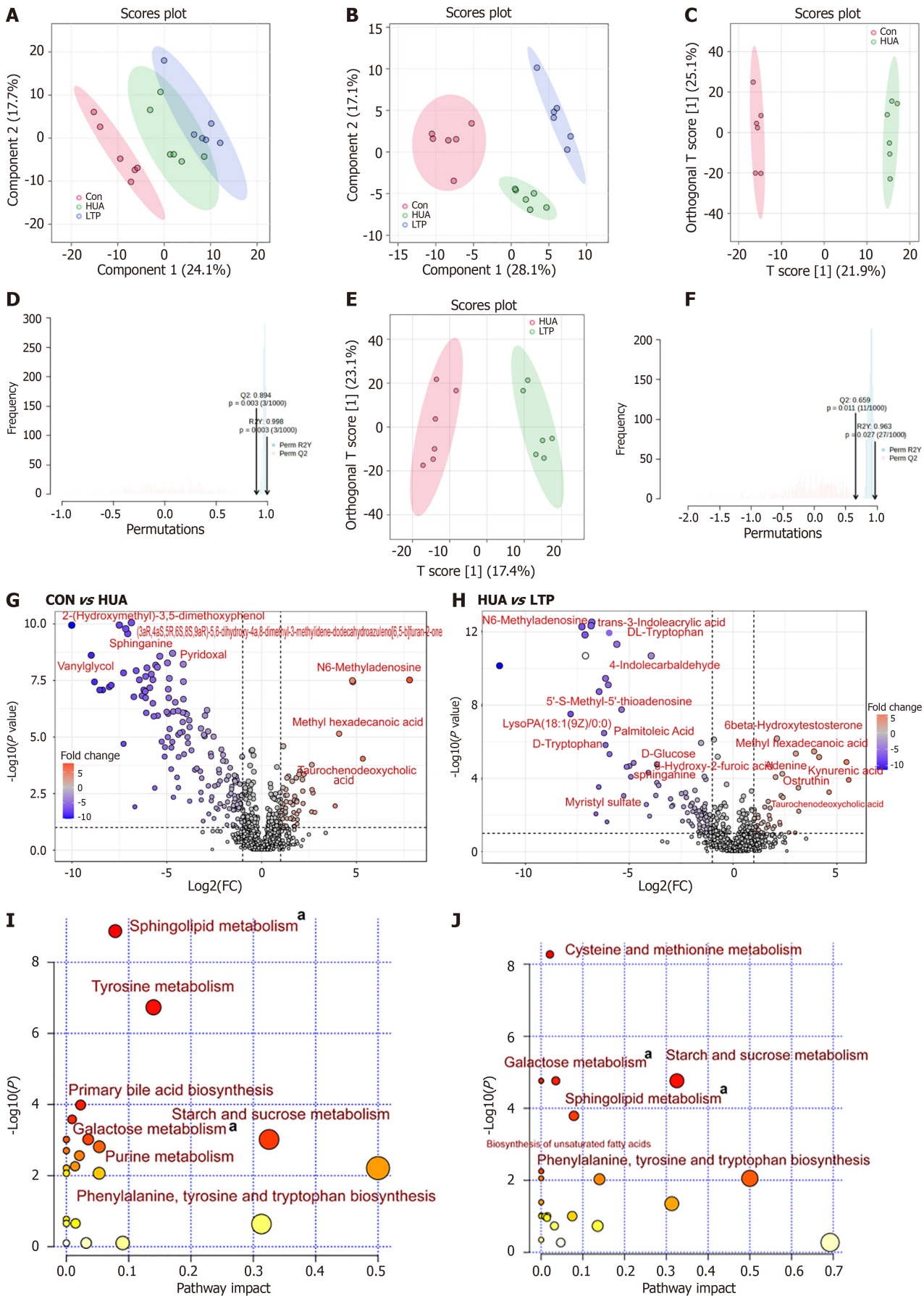


Figure 6 Leech *Poecilobdella manillensis* total protein extract alters the plasma metabolites in potassium oxonate-induced hyperuricemia mice. A and B: Partial least squares discriminant analysis (PLS-DA) score plots for normal control group (CON), hyperuricemia model group (HUA), and

leech *Poecilobdella manillensis* total protein extract treatment group (LTP) in positive and negative ion mode, respectively; C and D: Score plots and permutation tests of orthogonal PLS-DA (OPLS-DA) between the HUA and CON groups; E and F: Score plots and permutation tests of OPLS-DA between the LTP and HUA groups; G: Volcano plot showing most significant metabolites identified by univariate analysis between the HUA and CON groups; H: Volcano plot showing most significant metabolites identified by univariate analysis between the LTP and HUA groups; I: Summary plot for pathway analysis of CON vs HUA; J: Summary plot for pathway analysis of LTP vs HUA, a pathways coexisted in both the microbiota and metabolome. CON: Normal control group; HUA: Hyperuricemia model group; LTP: Leech *Poecilobdella manillensis* total protein extract treatment group; FC: Fold change.

lyophilized powder in the treatment of HUA in previous experiments, we extracted leech protein from leech *Poecilobdella manillensis* freeze-dried powder, and conducted an experiment focused on lowering UA through the administration of LTP to HUA mice. Consequently, the mechanism was expounded in relation to the gut microbiota and metabolites. We demonstrated the excellent curative potential of LTP with respect to lowering UA levels by decreasing urate synthesis and increasing renal urate excretion (summarized in Figure 10). To our knowledge, this is the first study to reveal that LTP could ameliorate the progression of HUA by re-programming the gut microbiome and metabolome.

LTP ameliorated disruptions in UA and renal function

Employing a yeast-based high-purine diet in conjunction with PO can emulate disturbances in purine metabolism, elevating UA levels and, thereby inducing an HUA model[34]. Our study employed PO alongside a yeast-based high-purine diet to successfully establish an HUA model in mice. Our findings provide evidence that LTP (as a lowering treatment for UA) induced beneficial physiological alterations in HUA-treated mice, manifesting as a noteworthy reduction in HUA-associated biochemical parameters (*e.g.*, serum UA, BUN, and CRE). Prior research has underscored the efficacy of hirudin in lowering serum UA and BUN levels and mitigating renal pathological damage[24]. Consistent with prior investigations, our study observed elevated serum CRE and BUN in the HUA mice; however, LTP treatment notably attenuated these levels, indicating that LTP ameliorated the disruptions in UA metabolism and mitigated the renal function impairment induced by HUA.

LTP enhanced UA excretion by decreasing urate synthesis and increasing renal urate excretion, thus ameliorating renal and intestinal barrier impairment

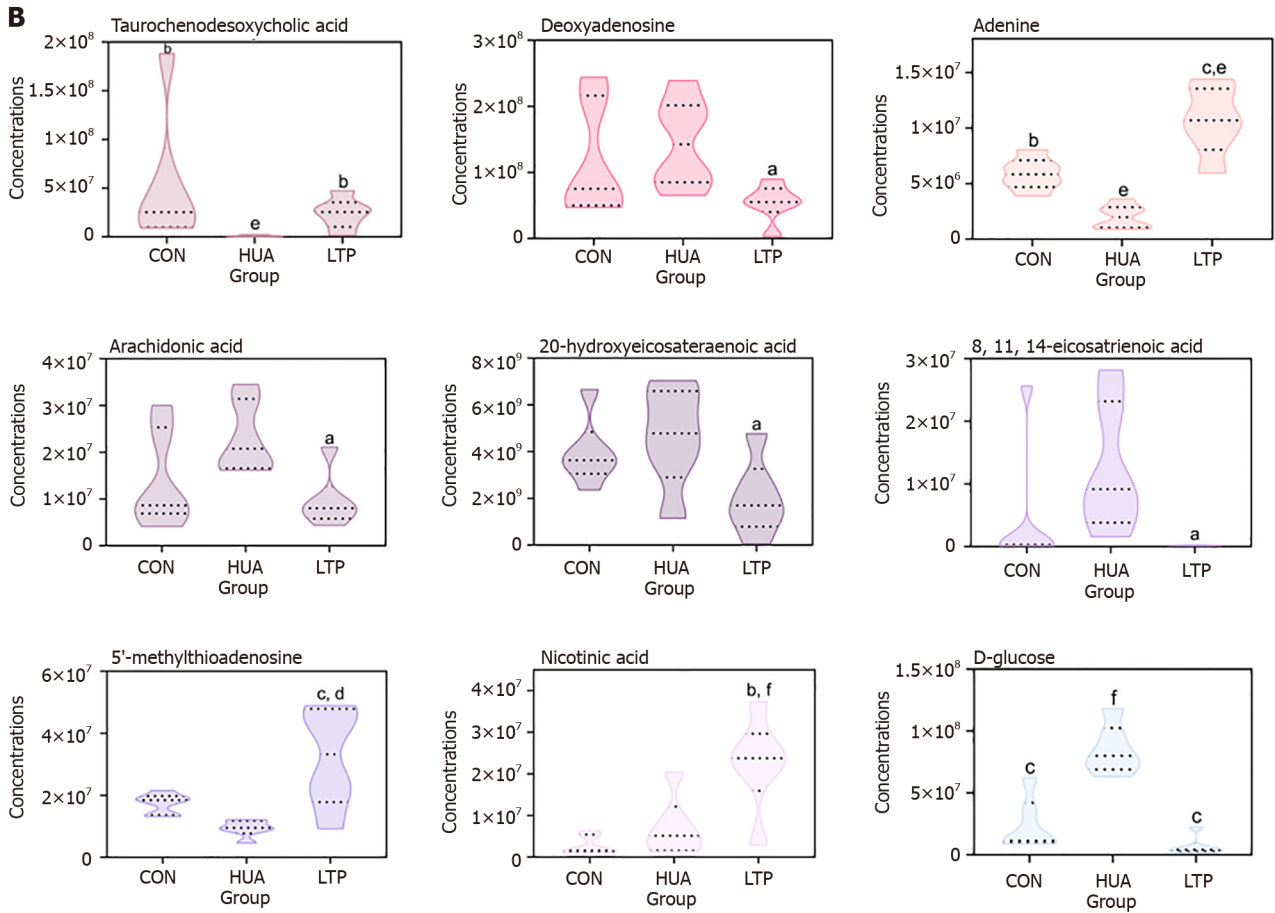
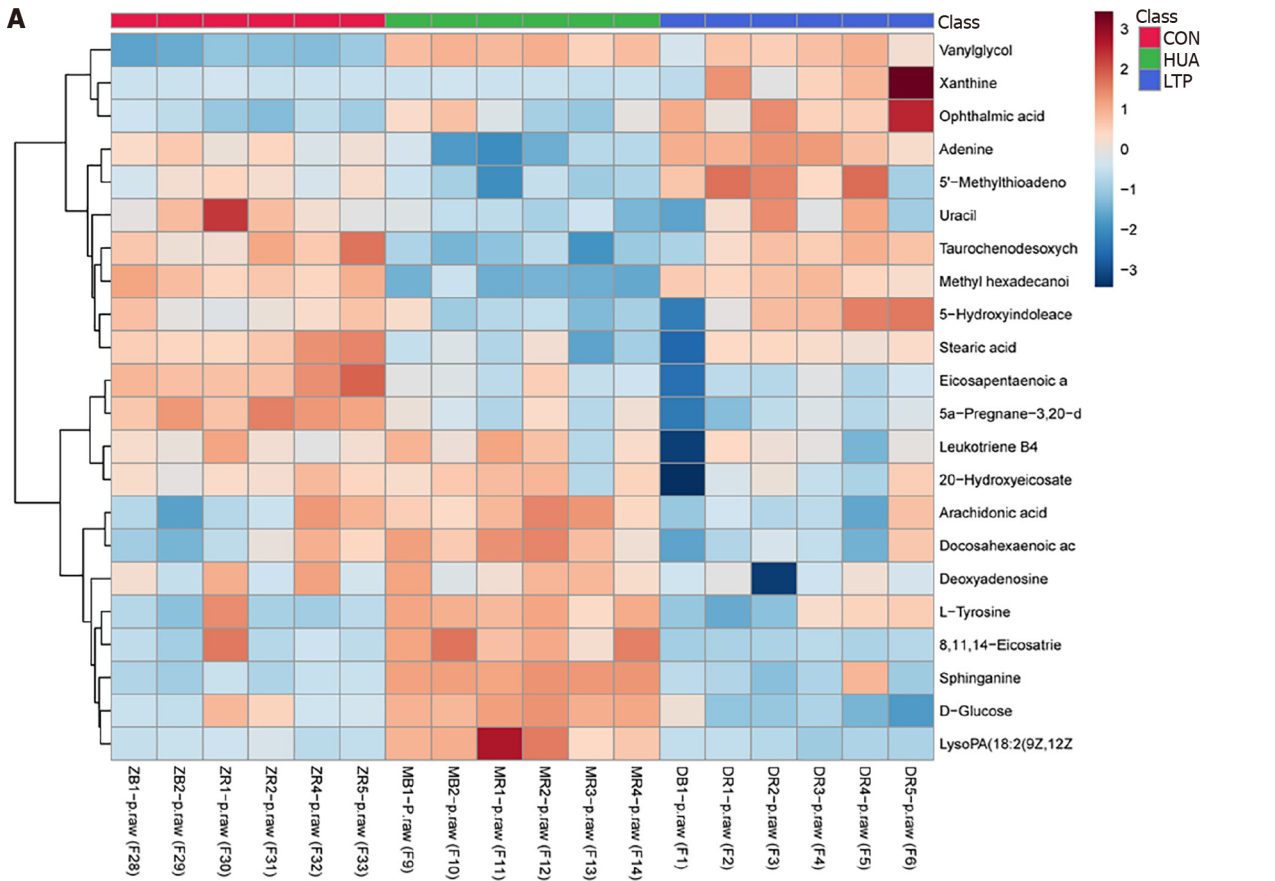
Our initial investigation into the impact of LTP on UA production unveiled its ability to attenuate XOD activity, consequently diminishing UA synthesis - a potential performance akin to AP. Our investigation highlighted that LTP not only reduced the renal concentrations of URAT1 and GLUT9 but also elevated kidney and jejunum ABCG2 proteins, in line with previous research[35]. This is related to the fact that renal UA clearance is mainly dependent on different transporters, including URAT1, GLUT9, and ABCG2[36]. Notably, the observation of the ABCG2 protein concentration in the jejunum in our study is consistent with previous reports showing that the ABCG2-encoded transporter BCRP plays a role in the gut[1]. In essence, our results delineate the dual action of LTP, *i.e.*, attenuating UA synthesis by inhibiting XOD activity and enhancing UA excretion by modulating distinct UA transporters in both the renal and intestinal domains.

Our investigation revealed decreases in ZO-1 and occludin levels in the renal tissue of HUA mice ($P < 0.05$). Following LTP treatment, a notable upward trend in the concentration of these proteins was observed ($P < 0.01$), signifying the ameliorative effect of LTP on renal barrier impairment in HUA mice. This aligns with previous findings suggesting that alterations in tight junctions play a crucial role during the repair of renal injury and participate in the pathophysiological processes involved in renal recovery[37]. The reason for this might be that aberrations in tight junctions lead to compromised integrity in the intestinal or renal epithelium, culminating in absorption and secretion disorders, consequently affecting UA excretion[38]. Likewise, our observations revealed a parallel correlation between ZO-1 and occludin within the jejunum tissue and the kidney tissue of the LTP group. However, the observed elevation of ZO-1 in the jejunum tissue of the AP group did not exhibit statistical significance. These outcomes suggest the concurrent impact of LTP on the tight junction proteins present in both the jejunum and kidney.

In this study, we particularly focused on the histological changes in liver and kidney tissues induced by the HUA model. The experimental results showed significant pathological changes in the renal interstitium of HUA mice, including swelling and atrophy of the renal tubules, irregular tubular lumens, and significant infiltration of monocytes and lymphocytes in the interstitium, which are clear signs of an inflammatory response. In contrast, the renal interstitial pathological structure of the LTP group showed a significant improvement. These observational findings confirm the potential efficacy of LTP in repairing renal barrier impairment caused by HUA.

Modulatory effects of LTP on the gut microbiota

The gut microbiome, which is often regarded as the 'second genome' acquired by the human body, constitutes a remarkably rich and functionally pivotal ecosystem, encompassing an estimated 10-100 trillion micro-organisms, including bacteria and viruses, residing within the human intestinal tract[39]. Disruptions in the structure of this intestinal flora could trigger metabolic dysregulation, which is intricately linked with HUA and gout[39]. The interplay between the intestinal flora and kidney diseases disrupts the equilibrium of gut microbes, leading to renal impairment [40]. In rat models of renal failure, a significant reduction in renal excretion triggers an adaptive discharge of UA into the intestinal lumen[41]. This process leads to marked changes in the composition and quantity of the gut microbiota[41]. In this study, our exploration of disease pathogenesis utilized the gut microbiota as a pivotal starting point. Given the intricate composition of intestinal micro-organisms, the impact of different microbial entities diverges significantly. Consequently, the efficacy of LTP in reducing UA levels cannot be solely attributed to the actions of a singular bacterium.



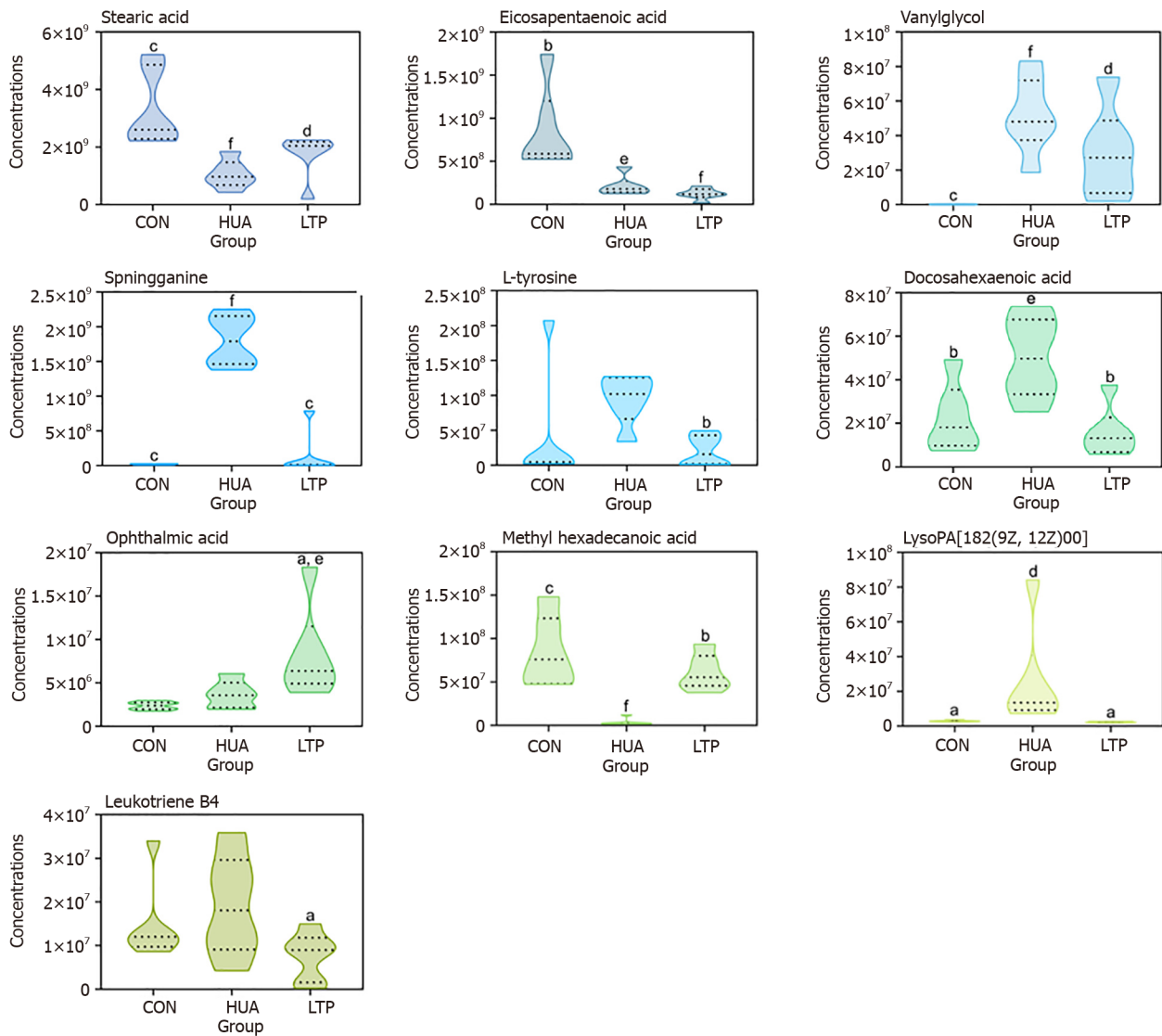


Figure 7 Effect of leech *Poecilobdella manillensis* total protein extract on vital metabolites. A: Heatmaps showing the trends in differential metabolites between groups; B: The concentrations of vital metabolites for all groups, assessed through the Kruskal-Wallis ANOVA. Statistical significance is indicated as follows: ^a $P < 0.05$ vs hyperuricemia model group (HUA); ^b $P < 0.01$ vs HUA; ^c $P < 0.001$ vs HUA; ^d $P < 0.05$ vs normal control group (CON); ^e $P < 0.01$ vs CON; ^f $P < 0.001$ vs CON. CON: Normal control group; HUA: Hyperuricemia model group; LTP: Leech *Poecilobdella manillensis* total protein extract treatment group.

Alterations in the microbiota structure have been observed in both human and animal models of HUA, notably at the phylum and genus levels[42,43]. The α - and β -diversity analyses of gut microbes conducted in this investigation showcased the capacity of LTP to enhance gut microbial diversity and influence the microbial structure in HUA mice. Specifically, at the phylum level, LTP administration led to a reduction in *Bacteroidota* and an elevation in the relative abundance of *Firmicutes*. This adjustment resulted in the restoration of the *Bacteroides* to *Firmicutes* ratio to a level akin to that in the CON group, thereby exerting a favorable influence on the restoration of the intestinal flora. These findings align with the conclusions drawn by Cao *et al*[44], emphasizing the pivotal role of the *Bacteroidetes* to *Firmicutes* ratio in preserving normal intestinal homeostasis and its association with HUA. It has been documented that *Faecalibacterium*, *Lactobacillus*, and *Bifidobacterium* represent pivotal core and physiological flora within the gastrointestinal tract of both humans and animals[45,46], which are capable of producing short-chain fatty acids, thereby fostering intestinal health through the reduction in oxidative stress, autophagic processes, and inflammation[45-47]. Additionally, *Clostridium_sensu_stricto_1* has demonstrated effective regulation of intestinal flora, being characterized as a dominant strain in cases of type 2 diabetes mellitus[48]. *Escherichia_Shigella* exhibited significant enrichment among long-lived healthy individuals[49]. Conversely, *Sphingomonas* species have been identified as opportunistic pathogens[50,51]. A study indicated that *Alloprevotella* is associated with inflammatory markers and represents a risk factor for sepsis[52]. In our study, a decline was observed in the relative abundance of *Lactobacillus*, *Faecalibacterium*, *Clostridium_sensu_stricto_1*, *Bifidobacterium*, and *Escherichia_Shigella* in HUA mice. Meanwhile, the relative abundance of *Alloprevotella* and *Sphingomonas* increased. Notably, the increase in *Alloprevotella* and *Sphingomonas*, alongside the observed changes in epithelial tight junction proteins, may suggest a potential weakening of the intestinal barrier, which could subsequently heighten the risk of intestinal inflammation and increase susceptibility to pathogenic invasion[53]. However, LTP treatment successfully reversed these shifts in the gut microbiota, notably augmenting the relative abundances of

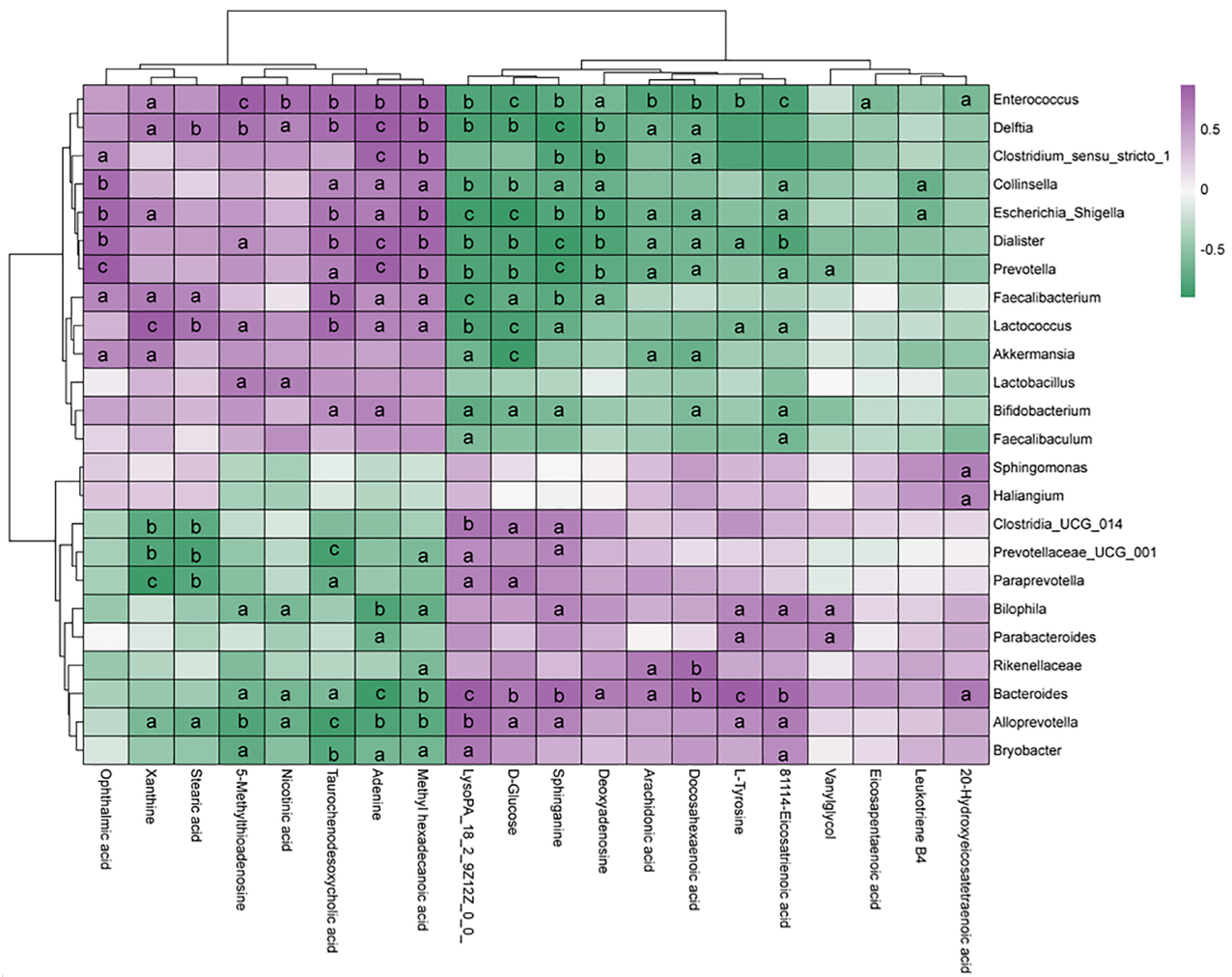


Figure 8 Correlation analysis between the gut microbiota and metabolites from hyperuricemia and leech *Poecilobdella manillensis* total protein extract groups. The R values are represented by gradient colors, where purple cells indicate positive correlations and green cells indicate negative correlations, respectively. Statistical significance is denoted as follows: ^aP < 0.05, ^bP < 0.01, ^cP < 0.001.

beneficial probiotics such as *Lactobacillus*, *Faecalibacterium*, and *Bifidobacterium*. This indicates the potential role of LTP treatment in enhancing the integrity of the intestinal barrier by increasing the concentration of tight junction proteins, which may indirectly contribute to mitigating conditions associated with gut microbiota dysbiosis. *Prevotella*, a prominent member of the gut microbiome[54], exhibited a significantly lower abundance in HUA mice and a higher abundance in CON group mice. In particular, following LTP treatment, the relative abundance of *Prevotella* notably increased. This aligns with conclusions linking *Prevotellaceae* UCG-001 to anti-inflammatory effects on immune cells and the inhibition of potential invasive pathogens[55]. *Dialister* was enriched following LTP treatment, consistent with clinical findings on beneficial bacteria related to depression[56]. *Akkermansia*, which was also notably enriched in the LTP group, belongs to a class of probiotics capable of enhancing the barrier function of the intestinal mucosa and reinforcing the host immune response[57]. In this study, the disruption of the balance of *Bacteroides* - which constituted a significant proportion in the genus - in HUA mice was evident when compared to the CON group. However, LTP intervention restored the relative abundance of *Bacteroides* to levels observed in the CON group, thus re-establishing the original balance of the gut microbiota. Spearman correlation analysis showed that *Enterococcus*, *Escherichia_Shigella*, *Delftia*, *Dialister*, *Prevotella*, and *Bacteroides* were strongly correlated with serum UA, serum CRE, liver XOD, URAT1, ABCG2, occludin, and ZO-1. In conclusion, LTP treatment not only fortified beneficial bacteria but also curtailed the relative abundance of harmful bacteria, restoring the equilibrium of intestinal microflora dominated by the largest bacterial proportion. These comprehensive analytical results highlight the dual role of LTP in the protection of both the renal and intestinal barriers, which is particularly important in addressing HUA and its complications. This finding provides an important theoretical basis for future clinical studies, especially when exploring LTP as a potential therapy for treating HUA and its related complications.

LTP demonstrated a modulatory impact on serum metabolites

Serum metabolomics analysis exhibited a notable amelioration in disturbed serum metabolism with LTP treatment. The screening process identified 22 metabolites linked with HUA, which were predominantly engaged in amino acid, lipid, and energy metabolism. Furthermore, these alterations were effectively reversed following LTP treatment in HUA mice.

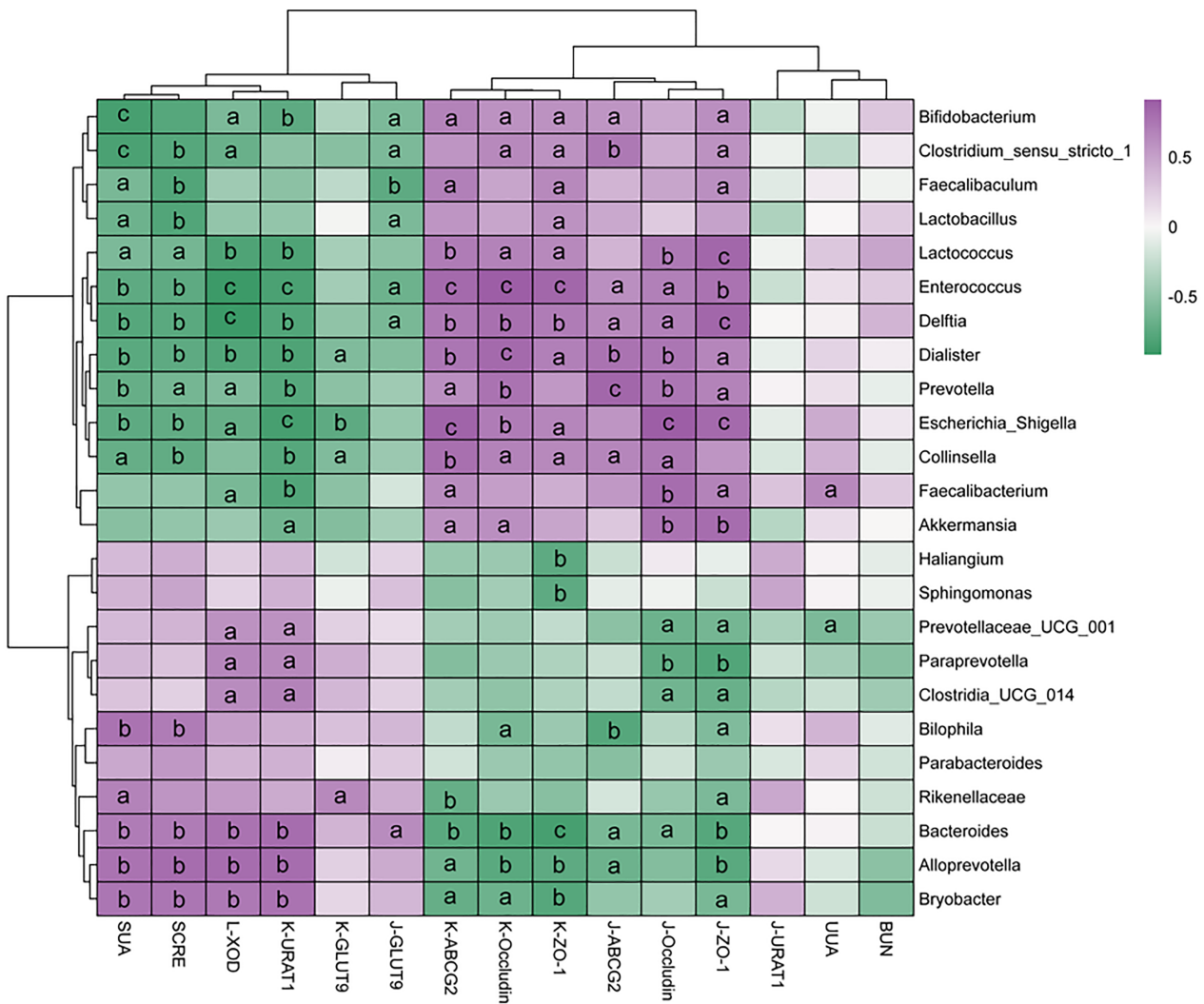


Figure 9 Correlation analysis between gut microbiota and hyperuricemia-related parameters. The R values are represented by gradient colors, where purple cells indicate positive correlations and green cells indicate negative correlations, respectively. Statistical significance is denoted as follows: ^aP < 0.05, ^bP < 0.01, ^cP < 0.001. BUN: Blood urea nitrogen; UUA: Urinary uric acid; ZO-1: Zonula occludens-1; URAT1: Urate transporter 1; GLUT9: Glucose transporter 9; ABCG2: ATP-binding cassette transporter G2; XOD: Xanthine oxidase; SCRE: Serum creatinine; SUA: Serum uric acid.

These findings highlight the metabolic pathways intertwined with HUA and the capacity of LTP to enhance pertinent markers.

LTP reversal of HUA-induced lipid metabolic alterations: In this study, we focused on the alterations in sphinganine levels in the HUA model mouse. Sphinganine, a key intermediate metabolite in the sphingolipid metabolic pathway, showed a significant increase in the serum of HUA mice. This not only suggests a potential disruption in the regulatory functions of sphingolipid metabolism but also reflects a deeper biomarker of the metabolic disorder. Previous research has shown that metabolites from sphingolipids function as signaling molecules. These molecules regulate various processes associated with immune responses and inflammation[58]. Furthermore, there is evidence linking HUA with immune reactions and inflammatory processes[59]. Therefore, the sphingolipid metabolic pathway may contribute to the onset of HUA through its effects on immunity and inflammation, potentially due to elevated sphinganine levels increasing the synthesis of ceramide, a bioactive lipid signaling molecule known to significantly influence cellular signaling and inflammation control[60]. Recent studies have demonstrated that sphingolipids from intestinal bacteria can traverse the intestinal-epithelial barrier, thereby altering the sphingolipid metabolism of the host[61].

Our findings indicate that LTP treatment significantly ameliorated the increase in sphinganine, suggesting that modulation of the sphingolipid metabolic pathway by LTP could offer potential therapeutic effects on HUA. Specifically, LTP may decrease the production of sphinganine or enhance its clearance, thus influencing UA synthesis and excretion. Future research should further explore how LTP specifically affects sphinganine and related metabolites to deepen our understanding of its regulatory mechanisms on UA levels.

Furthermore, we observed significant negative correlations between specific microbial populations in the gut microbiota - such as *Delftia*, *Dialister*, *Clostridium_sensu_stricto_1*, *Escherichia_Shigella*, *Enterococcus*, and *Prevotella* - while *Bacteroides* showed a positive correlation. This suggests that the interaction between sphingolipid metabolism and gut microbiota may play a crucial role in the therapeutic effects of LTP on HUA, primarily through the modulation of gut

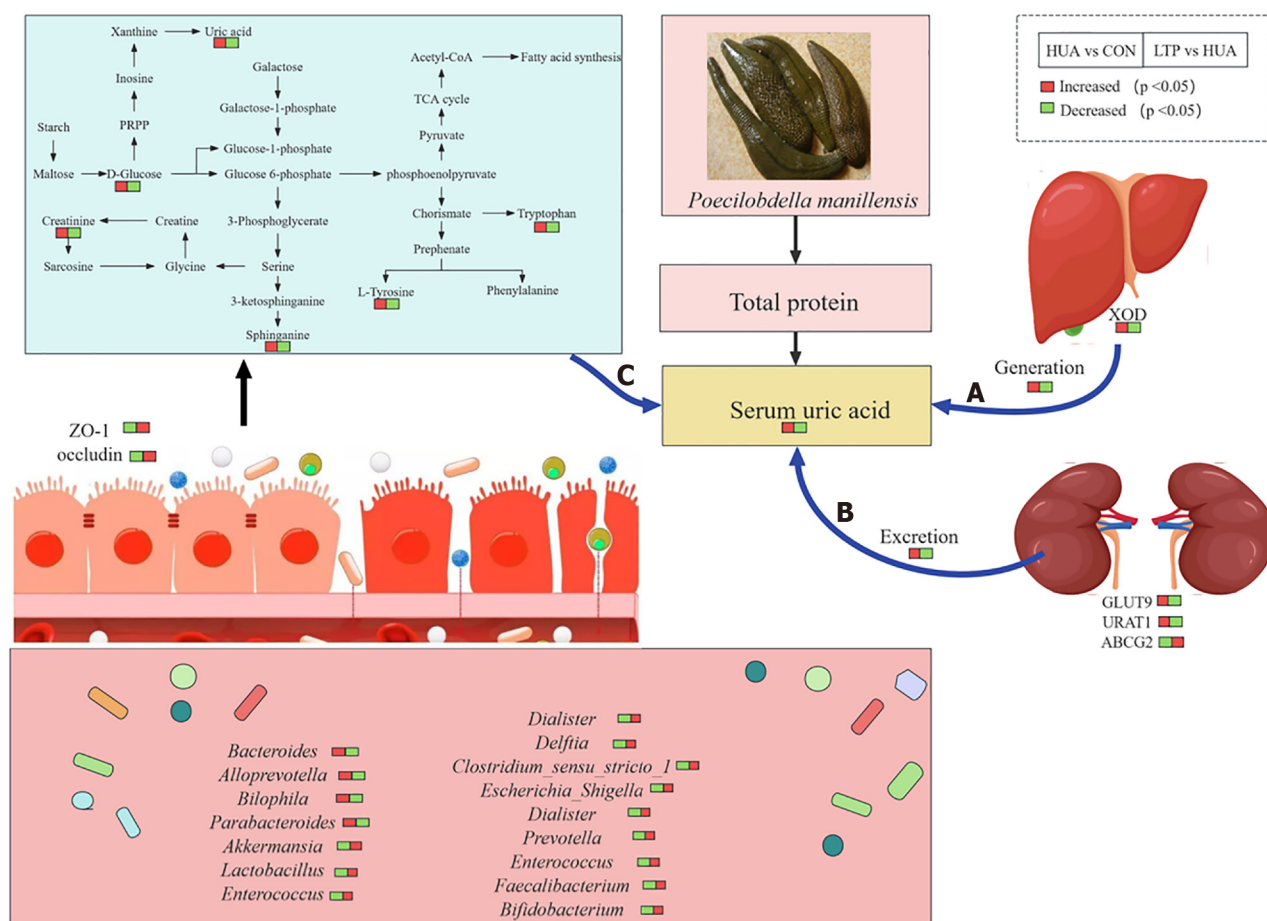


Figure 10 Mechanisms associated with treatment of *Poecilobdella manillensis* for hyperuricemia. A: decreased of uric acid generation in liver by reducing levels of xanthine oxidase; B: Reduction of uric acid excretion from kidney by regulating the expression of glucose transporter 9, urate transporter 1, and ATP-binding cassette transporter G2; C: Improvement of gut microbiota dysbiosis and regulation of sphingolipid metabolism and galactose metabolism. CON: Normal control group; HUA: Hyperuricemia model group; LTP: Leech *Poecilobdella manillensis* total protein extract treatment group; ZO-1: Zonula occludens-1; URAT1: Urate transporter 1; GLUT9: Glucose transporter 9; ABCG2: ATP-binding cassette transporter G2; XOD: Xanthine oxidase.

microbial communities affecting the sphingolipid metabolic pathway. These results not only provide new insights into the pathophysiological mechanisms of HUA but also offer a biological foundation for the development of novel therapeutic strategies based on the regulation of sphingolipid metabolism.

LTP reversed HUA-induced alterations in energy metabolism: LTP effectively reversed the disruptions in energy metabolism caused by high UA levels, as evidenced by our comprehensive functional enrichment analysis of the serum metabolome and gut microbiome. This analysis particularly highlighted the involvement of the galactose metabolism pathway, underscoring its pivotal role in mediating the therapeutic effects of LTP on HUA. LTP is suggested to exert its UA-lowering effects by modulating the gut microbiota, which, in turn, influences the galactose metabolic pathway intimately connected with glucose metabolism. This modulation may correct metabolic irregularities and restore metabolic equilibrium, offering a promising avenue for treating HUA.

In our study, elevated levels of D-glucose observed in HUA mice were significantly reduced following LTP treatment, suggesting LTP's potential role in regulating key metabolic pathways, such as the galactose metabolism pathway, alongside reducing UA levels. Although the direct link between galactose metabolism and UA levels has not been extensively documented in the literature, our findings may indicate a novel area of interest for further investigation into how specific metabolic pathways influence UA homeostasis. Notably, D-glucose - a critical metabolite within the galactose pathway - demonstrated significant correlations with various gut microbiota. It showed negative correlations with *Enterococcus*, *Escherichia Shigella*, *Lactococcus*, *Delftia*, *Dialister*, *Prevotella*, and *Akkermansia*, and a positive correlation with *Bacteroides*.

These findings suggest that shifts in D-glucose levels may influence, or be influenced by, changes in the composition of the gut microbiota. LTP selectively enhances the abundance of these microbiota, potentially through the modulation of the galactose metabolic pathway, which is linked to glucose metabolism. This highlights a complex interplay between metabolic pathways and microbiota that may be key to developing new treatments for metabolic diseases.

CONCLUSION

In conclusion, based on the results of multiple omics studies, LTP was found to play a therapeutic role in HUA by regulating gut microbial homeostasis and serum metabolites. We found that LTP might influence the gut microbiota to act on sphingolipid metabolism and galactose metabolism pathways, facilitating UA-lowering therapy. Our findings are expected to promote further research on the regulatory effects of LTP on the gut microbiome and serum metabolomics, providing new insights into microbiome-based HUA treatment strategies.

FOOTNOTES

Author contributions: Liu X, Liang XQ, Lu TC, and Wang LS designed the research study; Liu X, Liang XQ, and Wang LS performed the research and wrote the original draft; Feng Z, Zhang M, and Wang B conducted the investigations; Liu X, Zhang FL, Wang B, and Wang LS developed the methodologies; Zhang M, Liao NQ, Zhang FL, and Wang LS managed the software used; Lu TC and Wang LS acquired the funding; Lu TC, Feng Z, and Wang LS administered the project and supervised the project; Liu X, Zhang FL, and Wang B validated the results; Liu X and Wang LS reviewed and edited the manuscript. All authors have read and approved the final manuscript.

Supported by National Natural Science Foundation of China, No. 82160843.

Institutional animal care and use committee statement: All procedures involving animals were reviewed and approved by the Attitude of Animal Care & Welfare Committee of Guangxi University (No. GXU-2023-0203).

Conflict-of-interest statement: All the authors report no relevant conflicts of interest for this article.

Data sharing statement: Technical appendix, statistical code, and dataset available from the corresponding author at lswang@gxu.edu.cn.

ARRIVE guidelines statement: The authors have read the ARRIVE guidelines, and the manuscript was prepared and revised according to the ARRIVE guidelines.

Open-Access: This article is an open-access article that was selected by an in-house editor and fully peer-reviewed by external reviewers. It is distributed in accordance with the Creative Commons Attribution NonCommercial (CC BY-NC 4.0) license, which permits others to distribute, remix, adapt, build upon this work non-commercially, and license their derivative works on different terms, provided the original work is properly cited and the use is non-commercial. See: <https://creativecommons.org/licenses/by-nc/4.0/>

Country of origin: China

ORCID number: Xia Liu [0009-0007-8237-248X](https://orcid.org/0009-0007-8237-248X); Xing-Qiu Liang [0000-0003-3378-1336](https://orcid.org/0000-0003-3378-1336); Zhe Feng [0009-0005-7032-0012](https://orcid.org/0009-0005-7032-0012); Li-Sheng Wang [0000-0003-2655-0724](https://orcid.org/0000-0003-2655-0724).

S-Editor: Wang JJ

L-Editor: A

P-Editor: Yu HG

REFERENCES

- 1 **Zhao H**, Chen X, Zhang L, Meng F, Zhou L, Pang X, Lu Z, Lu Y. Lacticaseibacillus rhamnosus Fmb14 prevents purine induced hyperuricemia and alleviate renal fibrosis through gut-kidney axis. *Pharmacol Res* 2022; **182**: 106350 [PMID: [35843568](https://pubmed.ncbi.nlm.nih.gov/35843568/) DOI: [10.1016/j.phrs.2022.106350](https://doi.org/10.1016/j.phrs.2022.106350)]
- 2 **Li S**, Liu X, Jia X, Fang M, Yang Q, Gong Z. Assessment of the temporal trend and daily profiles of the dietary purine intake among Chinese residents during 2014 to 2021. *Front Nutr* 2023; **10**: 1259053 [PMID: [38024389](https://pubmed.ncbi.nlm.nih.gov/38024389/) DOI: [10.3389/fnut.2023.1259053](https://doi.org/10.3389/fnut.2023.1259053)]
- 3 **Yanai H**, Adachi H, Hakoshima M, Katsuyama H. Molecular Biological and Clinical Understanding of the Pathophysiology and Treatments of Hyperuricemia and Its Association with Metabolic Syndrome, Cardiovascular Diseases and Chronic Kidney Disease. *Int J Mol Sci* 2021; **22** [PMID: [34502127](https://pubmed.ncbi.nlm.nih.gov/34502127/) DOI: [10.3390/ijms22179221](https://doi.org/10.3390/ijms22179221)]
- 4 **McCormick N**, Lin K, Yokose C, Lu N, Zhang Y, Choi HK. Unclosing Premature Mortality Gap Among Patients With Gout in the US General Population, Independent of Serum Urate and Atherosclerotic Cardiovascular Risk Factors. *Arthritis Care Res (Hoboken)* 2024; **76**: 691-702 [PMID: [38191784](https://pubmed.ncbi.nlm.nih.gov/38191784/) DOI: [10.1002/acr.25292](https://doi.org/10.1002/acr.25292)]
- 5 **Agus A**, Clément K, Sokol H. Gut microbiota-derived metabolites as central regulators in metabolic disorders. *Gut* 2021; **70**: 1174-1182 [PMID: [33272977](https://pubmed.ncbi.nlm.nih.gov/33272977/) DOI: [10.1136/gutjnl-2020-323071](https://doi.org/10.1136/gutjnl-2020-323071)]
- 6 **Wang Z**, Li Y, Liao W, Huang J, Liu Y, Li Z, Tang J. Gut microbiota remodeling: A promising therapeutic strategy to confront hyperuricemia and gout. *Front Cell Infect Microbiol* 2022; **12**: 935723 [PMID: [36034697](https://pubmed.ncbi.nlm.nih.gov/36034697/) DOI: [10.3389/fcimb.2022.935723](https://doi.org/10.3389/fcimb.2022.935723)]
- 7 **Sun X**, Wen J, Guan B, Li J, Luo J, Li J, Wei M, Qiu H. Folic acid and zinc improve hyperuricemia by altering the gut microbiota of rats with high-purine diet-induced hyperuricemia. *Front Microbiol* 2022; **13**: 907952 [PMID: [35966674](https://pubmed.ncbi.nlm.nih.gov/35966674/) DOI: [10.3389/fmicb.2022.907952](https://doi.org/10.3389/fmicb.2022.907952)]
- 8 **Wang K**, Zhang Z, Hang J, Liu J, Guo F, Ding Y, Li M, Nie Q, Lin J, Zhuo Y, Sun L, Luo X, Zhong Q, Ye C, Yun C, Zhang Y, Wang J, Bao R, Pang Y, Wang G, Gonzalez FJ, Lei X, Qiao J, Jiang C. Microbial-host-isozyme analyses reveal microbial DPP4 as a potential antidiabetic target. *Science* 2023; **381**: eadd5787 [PMID: [37535747](https://pubmed.ncbi.nlm.nih.gov/37535747/) DOI: [10.1126/science.add5787](https://doi.org/10.1126/science.add5787)]
- 9 **Chen Y**, Pei C, Chen Y, Xiao X, Zhang X, Cai K, Deng S, Liang R, Xie Z, Li P, Liao Q. Kidney tea ameliorates hyperuricemia in mice via altering gut microbiota and restoring metabolic profile. *Chem Biol Interact* 2023; **376**: 110449 [PMID: [36921834](https://pubmed.ncbi.nlm.nih.gov/36921834/) DOI: [10.1016/j.cbi.2023.110449](https://doi.org/10.1016/j.cbi.2023.110449)]

- 10.1016/j.cbi.2023.110449]
- 10 **Wang J**, Chen Y, Zhong H, Chen F, Regenstein J, Hu X, Cai L, Feng F. The gut microbiota as a target to control hyperuricemia pathogenesis: Potential mechanisms and therapeutic strategies. *Crit Rev Food Sci Nutr* 2022; **62**: 3979-3989 [PMID: 33480266 DOI: 10.1080/10408398.2021.1874287]
 - 11 **Song S**, Lou Y, Mao Y, Wen X, Fan M, He Z, Shen Y, Wen C, Shao T. Alteration of Gut Microbiome and Correlated Amino Acid Metabolism Contribute to Hyperuricemia and Th17-Driven Inflammation in Uox-KO Mice. *Front Immunol* 2022; **13**: 804306 [PMID: 35197978 DOI: 10.3389/fimmu.2022.804306]
 - 12 **Sapankaew T**, Thadanipon K, Ruenroengbun N, Chaiyakittisopon K, Ingsathit A, Numthavaj P, Chaiyakunapruk N, McKay G, Attia J, Thakkinstian A. Efficacy and safety of urate-lowering agents in asymptomatic hyperuricemia: systematic review and network meta-analysis of randomized controlled trials. *BMC Nephrol* 2022; **23**: 223 [PMID: 35739495 DOI: 10.1186/s12882-022-02850-3]
 - 13 **Strilchuk L**, Fogacci F, Cicero AF. Safety and tolerability of available urate-lowering drugs: a critical review. *Expert Opin Drug Saf* 2019; **18**: 261-271 [PMID: 30915866 DOI: 10.1080/14740338.2019.1594771]
 - 14 **Anis TR**, Meher J. Allopurinol-Induced Stevens-Johnson Syndrome (SJS). *Clin Pharmacol* 2023; **15**: 99-105 [PMID: 37811521 DOI: 10.2147/CPAA.S427714]
 - 15 **Viel S**, Pescarmona R, Belot A, Nosbaum A, Lombard C, Walzer T, Bérard F. A Case of Type 2 Hypersensitivity to Rasburicase Diagnosed with a Natural Killer Cell Activation Assay. *Front Immunol* 2018; **9**: 110 [PMID: 29434608 DOI: 10.3389/fimmu.2018.00110]
 - 16 **Cheuk DK**, Chiang AK, Chan GC, Ha SY. Urate oxidase for the prevention and treatment of tumour lysis syndrome in children with cancer. *Cochrane Database Syst Rev* 2017; **3**: CD006945 [PMID: 28272834 DOI: 10.1002/14651858.CD006945.pub4]
 - 17 **Fan JX**, Liu JY, Gao Y, Liu SQ. [Research on the mechanism of leech preparation in the treatment of stroke]. *Yaoxve Yanjiu* 2023 [DOI: 10.13506/j.cnki.jpr.2023.01.009]
 - 18 **Wang C**, Chen M, Lu X, Yang S, Yang M, Fang Y, Lai R, Duan Z. Isolation and Characterization of Poeciguamerin, a Peptide with Dual Analgesic and Anti-Thrombotic Activity from the Poecilobdella manillensis Leech. *Int J Mol Sci* 2023; **24** [PMID: 37446275 DOI: 10.3390/ijms241311097]
 - 19 **Qiu J**, Lingna W, Jinghong H, Yongqing Z. Oral administration of leeches (Shuizhi): A review of the mechanisms of action on antiplatelet aggregation. *J Ethnopharmacol* 2019; **232**: 103-109 [PMID: 30543914 DOI: 10.1016/j.jep.2018.12.010]
 - 20 **Sig AK**, Guney M, Uskudar Guclu A, Ozmen E. Medicinal leech therapy-an overall perspective. *Integr Med Res* 2017; **6**: 337-343 [PMID: 29296560 DOI: 10.1016/j.imr.2017.08.001]
 - 21 **Rodriguez-Merchan EC**. Topical therapies for knee osteoarthritis. *Postgrad Med* 2018; **130**: 607-612 [PMID: 30156934 DOI: 10.1080/00325481.2018.1505182]
 - 22 **Dong YY**, Liu YK, Deng XL, Liang J. [Mechanism of Poecilobdella Manillensis Lyophilized Powder on Hyperuricemia Based on Network Pharmacology, RNA-seq Technology and Experimental Validation]. *Zhongguo Xiandai Yingyun Yaoxve* 2024 [DOI: 10.13748/j.cnki.issn1007-7693.20230100]
 - 23 **Grafksaia EN**, Pavlova ER, Latsis IA, Malakhova MV, Ivchenkov DV, Bashkirov PV, Kot EF, Mineev KS, Arseniev AS, Klinov DV, Lazarev VN. Non-toxic antimicrobial peptide Hm-AMP2 from leech metagenome proteins identified by the gradient-boosting approach. *Mater Des* 2022; **224**: 111364 [DOI: 10.1016/j.matdes.2022.111364]
 - 24 **Junren C**, Xiaofang X, Huiqiong Z, Gangmin L, Yanpeng Y, Xiaoyu C, Yuqing G, Yanan L, Yue Z, Fu P, Cheng P. Pharmacological Activities and Mechanisms of Hirudin and Its Derivatives - A Review. *Front Pharmacol* 2021; **12**: 660757 [PMID: 33935784 DOI: 10.3389/fphar.2021.660757]
 - 25 **Sun Y**, Wang B, Pei J, Luo Y, Yuan N, Xiao Z, Wu H, Luo C, Wang J, Wei S, Pei Y, Fu S, Wang D. Molecular dynamic and pharmacological studies on protein-engineered hirudin variants of Hirudinaria manillensis and Hirudo medicinalis. *Br J Pharmacol* 2022; **179**: 3740-3753 [PMID: 35135035 DOI: 10.1111/bph.15816]
 - 26 **Wang YP**. [Isolation and Production of Antler Plate Protein from Sika Deer and preliminary study on its Bacteriostatic Mechanism of E.coli]. Jilin Agricultural University 2021
 - 27 **Wang YT**. Study on the Purification and Characterization of Fibrinolytic Active Protein of American Cockroach. 2020
 - 28 Wang YP, Zhou YJ, Hu W. [Isolation and purification of antler plate protein from Sika deer and preliminary study on its bacteriostatic mechanism against Escherichia coli]. *Shanghai Zhongyiyao Zazhi* 2021; **55**
 - 29 **Liu J**, Gao M, He J, Wu K, Lin S, Jin L, Chen Y, Liu H, Shi J, Wang X, Chang L, Lin Y, Zhao YL, Zhang X, Zhang M, Luo GZ, Wu G, Pei D, Wang J, Bao X, Chen J. The RNA m(6)A reader YTHDC1 silences retrotransposons and guards ES cell identity. *Nature* 2021; **591**: 322-326 [PMID: 33658714 DOI: 10.1038/s41586-021-03313-9]
 - 30 **Wang J**, Zhao J, Yan C, Xi C, Wu C, Zhao J, Li F, Ding Y, Zhang R, Qi S, Li X, Liu C, Hou W, Chen H, Wang Y, Wu D, Chen K, Jiang H, Huang H, Liu H. Identification and evaluation of a lipid-lowering small compound in preclinical models and in a Phase I trial. *Cell Metab* 2022; **34**: 667-680.e6 [PMID: 35427476 DOI: 10.1016/j.cmet.2022.03.006]
 - 31 **Li K**, Lin C, Li M, Xu K, He Y, Mao Y, Lu L, Geng W, Li X, Luo Z, Cai K. Multienzyme-like Reactivity Cooperatively Impairs Glutathione Peroxidase 4 and Ferroptosis Suppressor Protein 1 Pathways in Triple-Negative Breast Cancer for Sensitized Ferroptosis Therapy. *ACS Nano* 2022; **16**: 2381-2398 [PMID: 35041395 DOI: 10.1021/acsnano.1c08664]
 - 32 **Zou Y**, Sun X, Yang Q, Zheng M, Shimoni O, Ruan W, Wang Y, Zhang D, Yin J, Huang X, Tao W, Park JB, Liang XJ, Leong KW, Shi B. Blood-brain barrier-penetrating single CRISPR-Cas9 nanocapsules for effective and safe glioblastoma gene therapy. *Sci Adv* 2022; **8**: eabm8011 [PMID: 35442747 DOI: 10.1126/sciadv.abm8011]
 - 33 **Wang H**, Zhao X, Tan L, Zhu J, Hyten D. Crop DNA extraction with lab-made magnetic nanoparticles. *PLoS One* 2024; **19**: e0296847 [PMID: 38190402 DOI: 10.1371/journal.pone.0296847]
 - 34 **Sun L**, Liu Q, Zhang Y, Xue M, Yan H, Qiu X, Tian Y, Zhang H, Liang H. Fucoidan from Saccharina japonica Alleviates Hyperuricemia-Induced Renal Fibrosis through Inhibiting the JAK2/STAT3 Signaling Pathway. *J Agric Food Chem* 2023; **71**: 11454-11465 [PMID: 37481747 DOI: 10.1021/acs.jafc.3c01349]
 - 35 **Han J**, Zuo Z, Shi X, Zhang Y, Peng Z, Xing Y, Pang X. Hirudin ameliorates diabetic nephropathy by inhibiting Gsdmd-mediated pyroptosis. *Cell Biol Toxicol* 2023; **39**: 573-589 [PMID: 34212273 DOI: 10.1007/s10565-021-09622-z]
 - 36 **Banerjee M**, Mukhopadhyay S. Gout. *N Engl J Med* 2023; **388**: e47 [PMID: 36988610 DOI: 10.1056/NEJMc2216467]
 - 37 **Xu X**, Zhang X, Gao L, Liu C, You K. Neonatal Hyperoxia Downregulates Claudin-4, Occludin, and ZO-1 Expression in Rat Kidney Accompanied by Impaired Proximal Tubular Development. *Oxid Med Cell Longev* 2020; **2020**: 2641461 [PMID: 33343804 DOI: 10.1155/2020/2641461]

- 38 **Sun H**, Li H, Yan J, Wang X, Xu M, Wang M, Fan B, Liu J, Lin N, Wang X, Li L, Zhao S, Gong Y. Loss of CLDN5 in podocytes deregulates WIF1 to activate WNT signaling and contributes to kidney disease. *Nat Commun* 2022; **13**: 1600 [PMID: 35332151 DOI: 10.1038/s41467-022-29277-6]
- 39 **Zhu C**, Niu H, Bian M, Zhang X, Zhang X, Zhou Z. Study on the mechanism of *Orthosiphon aristatus* (Blume) Miq. in the treatment of hyperuricemia by microbiome combined with metabonomics. *J Ethnopharmacol* 2023; **317**: 116805 [PMID: 37355082 DOI: 10.1016/j.jep.2023.116805]
- 40 **Ma Y**, Liu X, Wang J. Small molecules in the big picture of gut microbiome-host cross-talk. *EBioMedicine* 2022; **81**: 104085 [PMID: 35636316 DOI: 10.1016/j.ebiom.2022.104085]
- 41 **Altamura S**, Pietropaoli D, Lombardi F, Del Pinto R, Ferri C. An Overview of Chronic Kidney Disease Pathophysiology: The Impact of Gut Dysbiosis and Oral Disease. *Biomedicines* 2023; **11** [PMID: 38002033 DOI: 10.3390/biomedicines11113033]
- 42 **Halimulati M**, Wang R, Aihemaitijiang S, Huang X, Ye C, Zhang Z, Li L, Zhu W, Zhang Z, He L. Anti-Hyperuricemic Effect of Anserine Based on the Gut-Kidney Axis: Integrated Analysis of Metagenomics and Metabolomics. *Nutrients* 2023; **15** [PMID: 36839325 DOI: 10.3390/nu15040969]
- 43 **Yuan X**, Chen R, Zhang Y, Lin X, Yang X. Altered Gut Microbiota in Children With Hyperuricemia. *Front Endocrinol (Lausanne)* 2022; **13**: 848715 [PMID: 35574004 DOI: 10.3389/fendo.2022.848715]
- 44 **Cao J**, Liu Q, Hao H, Bu Y, Tian X, Wang T, Yi H. *Lactobacillus paracasei* X11 Ameliorates Hyperuricemia and Modulates Gut Microbiota in Mice. *Front Immunol* 2022; **13**: 940228 [PMID: 35874662 DOI: 10.3389/fimmu.2022.940228]
- 45 **Mao G**, Li S, Orfila C, Shen X, Zhou S, Linhardt RJ, Ye X, Chen S. Depolymerized RG-I-enriched pectin from citrus segment membranes modulates gut microbiota, increases SCFA production, and promotes the growth of *Bifidobacterium* spp., *Lactobacillus* spp. and *Faecalibaculum* spp. *Food Funct* 2019; **10**: 7828-7843 [PMID: 31778135 DOI: 10.1039/c9fo01534e]
- 46 **Martín R**, Rios-Covian D, Huillet E, Auger S, Khazaal S, Bermúdez-Humarán LG, Sokol H, Chatel JM, Langella P. *Faecalibacterium*: a bacterial genus with promising human health applications. *FEMS Microbiol Rev* 2023; **47** [PMID: 37451743 DOI: 10.1093/femsre/fuad039]
- 47 **Yi X**, Cai R, Shaoyong W, Wang G, Yan W, He Z, Li R, Chao M, Zhao T, Deng L, Yang G, Pang W. Melatonin promotes gut anti-oxidative status in perinatal rat by remodeling the gut microbiome. *Redox Biol* 2023; **65**: 102829 [PMID: 37527604 DOI: 10.1016/j.redox.2023.102829]
- 48 **Que Y**, Cao M, He J, Zhang Q, Chen Q, Yan C, Lin A, Yang L, Wu Z, Zhu D, Chen F, Chen Z, Xiao C, Hou K, Zhang B. Gut Bacterial Characteristics of Patients With Type 2 Diabetes Mellitus and the Application Potential. *Front Immunol* 2021; **12**: 722206 [PMID: 34484230 DOI: 10.3389/fimmu.2021.722206]
- 49 **Pang S**, Chen X, Lu Z, Meng L, Huang Y, Yu X, Huang L, Ye P, Chen X, Liang J, Peng T, Luo W, Wang S. Longevity of centenarians is reflected by the gut microbiome with youth-associated signatures. *Nat Aging* 2023; **3**: 436-449 [PMID: 37117794 DOI: 10.1038/s43587-023-00389-y]
- 50 **Johnson RC**, Deming C, Conlan S, Zellmer CJ, Michelin AV, Lee-Lin S, Thomas PJ, Park M, Weingarten RA, Less J, Dekker JP, Frank KM, Musser KA, McQuiston JR, Henderson DK, Lau AF, Palmore TN, Segre JA. Investigation of a Cluster of *Sphingomonas koreensis* Infections. *N Engl J Med* 2018; **379**: 2529-2539 [PMID: 30586509 DOI: 10.1056/NEJMoa1803238]
- 51 **Ryan MP**, Adley CC. *Sphingomonas paucimobilis*: a persistent Gram-negative nosocomial infectious organism. *J Hosp Infect* 2010; **75**: 153-157 [PMID: 20434794 DOI: 10.1016/j.jhin.2010.03.007]
- 52 **Chen JH**, Zeng LY, Zhao YF, Tang HX, Lei H, Wan YF, Deng YQ, Liu KX. Causal effects of gut microbiota on sepsis: a two-sample Mendelian randomization study. *Front Microbiol* 2023; **14**: 1167416 [PMID: 37234519 DOI: 10.3389/fmicb.2023.1167416]
- 53 **Yin L**, Huang G, Khan I, Su L, Xia W, Law BYK, Wong VKW, Wu Q, Wang J, Leong WK, Hsiao WLW. *Poria cocos* polysaccharides exert prebiotic function to attenuate the adverse effects and improve the therapeutic outcome of 5-FU in *Apc(Min/+)* mice. *Chin Med* 2022; **17**: 116 [PMID: 36192796 DOI: 10.1186/s13020-022-00667-8]
- 54 **Tett A**, Pasolli E, Masetti G, Ercolini D, Segata N. *Prevotella* diversity, niches and interactions with the human host. *Nat Rev Microbiol* 2021; **19**: 585-599 [PMID: 34050328 DOI: 10.1038/s41579-021-00559-y]
- 55 **Zhou X**, Zhang B, Zhao X, Lin Y, Wang J, Wang X, Hu N, Wang S. Chlorogenic acid supplementation ameliorates hyperuricemia, relieves renal inflammation, and modulates intestinal homeostasis. *Food Funct* 2021; **12**: 5637-5649 [PMID: 34018499 DOI: 10.1039/d0fo03199b]
- 56 **Chi L**, Khan I, Lin Z, Zhang J, Lee MYS, Leong W, Hsiao WLW, Zheng Y. Fructo-oligosaccharides from *Morinda officinalis* remodeled gut microbiota and alleviated depression features in a stress rat model. *Phytomedicine* 2020; **67**: 153157 [PMID: 31896054 DOI: 10.1016/j.phymed.2019.153157]
- 57 **Zhai Q**, Feng S, Arjan N, Chen W. A next generation probiotic, *Akkermansia muciniphila*. *Crit Rev Food Sci Nutr* 2019; **59**: 3227-3236 [PMID: 30373382 DOI: 10.1080/10408398.2018.1517725]
- 58 **Maceyka M**, Spiegel S. Sphingolipid metabolites in inflammatory disease. *Nature* 2014; **510**: 58-67 [PMID: 24899305 DOI: 10.1038/nature13475]
- 59 **Li D**, Yuan S, Deng Y, Wang X, Wu S, Chen X, Li Y, Ouyang J, Lin D, Quan H, Fu X, Li C, Mao W. The dysregulation of immune cells induced by uric acid: mechanisms of inflammation associated with hyperuricemia and its complications. *Front Immunol* 2023; **14**: 1282890 [PMID: 38053999 DOI: 10.3389/fimmu.2023.1282890]
- 60 **Jin J**, Lu Z, Li Y, Ru JH, Lopes-Virella MF, Huang Y. LPS and palmitate synergistically stimulate sphingosine kinase 1 and increase sphingosine 1 phosphate in RAW264.7 macrophages. *J Leukoc Biol* 2018; **104**: 843-853 [PMID: 29882996 DOI: 10.1002/JLB.3A0517-188RRR]
- 61 **Johnson EL**, Heaver SL, Waters JL, Kim BI, Bretin A, Goodman AL, Gewirtz AT, Worgall TS, Ley RE. Sphingolipids produced by gut bacteria enter host metabolic pathways impacting ceramide levels. *Nat Commun* 2020; **11**: 2471 [PMID: 32424203 DOI: 10.1038/s41467-020-16274-w]

Basic Study

Calculus bovis inhibits M2 tumor-associated macrophage polarization via Wnt/ β -catenin pathway modulation to suppress liver cancer

Zhen Huang, Fan-Ying Meng, Lin-Zhu Lu, Qian-Qian Guo, Chang-Jun Lv, Nian-Hua Tan, Zhe Deng, Jun-Yi Chen, Zi-Shu Zhang, Bo Zou, Hong-Ping Long, Qing Zhou, Sha Tian, Si Mei, Xue-Fei Tian

Specialty type: Gastroenterology and hepatology

Provenance and peer review:

Unsolicited article; Externally peer reviewed.

Peer-review model: Single blind

Peer-review report's classification

Scientific Quality: Grade B, Grade B, Grade B, Grade C, Grade C, Grade C

Novelty: Grade A, Grade B, Grade B, Grade B, Grade C, Grade C

Creativity or Innovation: Grade A, Grade B, Grade B, Grade B, Grade B, Grade C

Scientific Significance: Grade A, Grade B, Grade B, Grade B, Grade B, Grade D

P-Reviewer: Buldak L; Ricci AD; Rizzo A; Shelat VG

Received: April 9, 2024

Revised: June 5, 2024

Accepted: July 5, 2024

Published online: August 7, 2024

Processing time: 110 Days and 23.3 Hours



Zhen Huang, Lin-Zhu Lu, Qian-Qian Guo, Chang-Jun Lv, Nian-Hua Tan, Zhe Deng, Jun-Yi Chen, Sha Tian, Xue-Fei Tian, College of Integrated Chinese and Western Medicine, Hunan University of Chinese Medicine, Changsha 410208, Hunan Province, China

Zhen Huang, Lin-Zhu Lu, Qian-Qian Guo, Chang-Jun Lv, Nian-Hua Tan, Jun-Yi Chen, Si Mei, Xue-Fei Tian, Hunan Key Laboratory of Translational Research in Formulas and Zheng of Traditional Chinese Medicine, Hunan University of Chinese Medicine, Changsha 410208, Hunan Province, China

Zhen Huang, Lin-Zhu Lu, Qian-Qian Guo, Chang-Jun Lv, Nian-Hua Tan, Jun-Yi Chen, Si Mei, Xue-Fei Tian, Key Laboratory of Traditional Chinese Medicine for Mechanism of Tumor Prevention and Treatment, Hunan University of Chinese Medicine, Changsha 410208, Hunan Province, China

Fan-Ying Meng, Zi-Shu Zhang, Bo Zou, The First Clinical College of Traditional Chinese Medicine, Hunan University of Traditional Chinese Medicine, Changsha 410007, Hunan Province, China

Nian-Hua Tan, Department of Hepatology, Hunan University of Chinese Medicine, Changsha 410007, Hunan Province, China

Hong-Ping Long, Qing Zhou, The First Hospital of Hunan University of Chinese Medicine, Hunan University of Chinese Medicine, Changsha 410007, Hunan Province, China

Si Mei, Faculty of Medicine, Hunan University of Chinese Medicine, Changsha 410208, Hunan Province, China

Co-first authors: Zhen Huang and Fan-Ying Meng.

Co-corresponding authors: Si Mei and Xue-Fei Tian.

Corresponding author: Xue-Fei Tian, College of Integrated Chinese and Western Medicine, Hunan University of Chinese Medicine, No. 300 Xueshi Road, Changsha 410208, Hunan Province, China. 003640@hnuucm.edu.cn

Abstract

BACKGROUND

Calculus bovis (CB), used in traditional Chinese medicine, exhibits anti-tumor effects in various cancer models. It also constitutes an integral component of a compound formulation known as Pien Tze Huang, which is indicated for the treatment of liver cancer. However, its impact on the liver cancer tumor microenvironment, particularly on tumor-associated macrophages (TAMs), is not well understood.

AIM

To elucidate the anti-liver cancer effect of CB by inhibiting M2-TAM polarization *via* Wnt/ β -catenin pathway modulation.

METHODS

This study identified the active components of CB using UPLC-Q-TOF-MS, evaluated its anti-neoplastic effects in a nude mouse model, and elucidated the underlying mechanisms *via* network pharmacology, transcriptomics, and molecular docking. *In vitro* assays were used to investigate the effects of CB-containing serum on HepG2 cells and M2-TAMs, and Wnt pathway modulation was validated by real-time reverse transcriptase-polymerase chain reaction and Western blot analysis.

RESULTS

This study identified 22 active components in CB, 11 of which were detected in the bloodstream. Preclinical investigations have demonstrated the ability of CB to effectively inhibit liver tumor growth. An integrated approach employing network pharmacology, transcriptomics, and molecular docking implicated the Wnt signaling pathway as a target of the antineoplastic activity of CB by suppressing M2-TAM polarization. *In vitro* and *in vivo* experiments further confirmed that CB significantly hinders M2-TAM polarization and suppresses Wnt/ β -catenin pathway activation. The inhibitory effect of CB on M2-TAMs was reversed when treated with the Wnt agonist SKL2001, confirming its pathway specificity.

CONCLUSION

This study demonstrated that CB mediates inhibition of M2-TAM polarization through the Wnt/ β -catenin pathway, contributing to the suppression of liver cancer growth.

Key Words: *Calculus bovis*; M2 tumor-associated macrophage polarization; Liver cancer; Wnt/ β -catenin pathway; Tumor microenvironment

©The Author(s) 2024. Published by Baishideng Publishing Group Inc. All rights reserved.

Core Tip: *Calculus bovis* (CB), a valuable herb in traditional Chinese medicine, has shown definite anti-liver cancer effects *in vivo*. By analyzing the composition of CB and using network pharmacology for target prediction, we found that CB exhibits anti-liver cancer effects by affecting immune-related pathways in the tumor microenvironment. Through transcriptome sequencing, we further showed that regulation of the M2-type polarization of tumor-associated macrophages (TAMs) is responsible for the effects of CB. *In vitro* studies showed that modulating the Wnt/ β -catenin pathway is a crucial mechanism by which CB regulates M2 polarization of TAMs. This study provides evidence for the development of anti-liver cancer drugs.

Citation: Huang Z, Meng FY, Lu LZ, Guo QQ, Lv CJ, Tan NH, Deng Z, Chen JY, Zhang ZS, Zou B, Long HP, Zhou Q, Tian S, Mei S, Tian XF. *Calculus bovis* inhibits M2 tumor-associated macrophage polarization *via* Wnt/ β -catenin pathway modulation to suppress liver cancer. *World J Gastroenterol* 2024; 30(29): 3511-3533

URL: <https://www.wjgnet.com/1007-9327/full/v30/i29/3511.htm>

DOI: <https://dx.doi.org/10.3748/wjg.v30.i29.3511>

INTRODUCTION

Liver cancer is a global health concern that ranks sixth in prevalence and fourth in cancer-related mortality worldwide [1]. Liver cancer is highly malignant, progresses rapidly, and has a poor prognosis. The 5-year survival rate of patients with liver cancer is only 3%, severely affecting their quality of life [2]. The primary treatment options for liver cancer include surgical interventions such as liver resection or transplantation, interventional therapies, local ablation treatments, and targeted immunotherapies [3-6]. However, the application of these treatments has limitations, and the survival rate of some patients remains low even after treatment [7-10]. Therefore, there is an urgent need for novel and more effective strategies for the treatment of liver cancer [11,12]. Traditional Chinese medicine (TCM) is characterized by a

multicomponent and multi-target approach[13,14]. Studies have shown that TCM can inhibit liver cancer by regulating the tumor microenvironment (TME)[15], offering a new perspective on liver cancer treatment. Within the multifaceted TME, macrophages play a crucial role in liver cancer progression[16]. Tumor-associated macrophages (TAMs) derived from circulating monocytes can adopt the M1 or M2 phenotype in response to various TME cytokines and growth factors [17]. While M1-type TAMs exhibit anti-tumor properties driven by cytokines such as IFN- γ and TNF- α [18], M2 TAMs (M2-TAMs) support tumor growth and metastasis through pathways such as NF- κ B, IL-6/STAT3, and Wnt/ β -catenin[19-21]. These pathways also facilitate TAM-mediated tumor proliferation, invasion, and angiogenesis[22,23]. Therefore, reversing TAM polarization and targeting these pathways are promising therapeutic approaches for liver cancer.

TCM values *Calculus bovis* (CB) for its anti-tumor potential in various models[24]. Combinations of CB with Moschus have been shown to induce apoptosis in liver cancer cells such as SMMC-7721 and HepG2[25,26]. Prior research has documented the mechanisms of CB against liver cancer[27] and its ability to enhance macrophage phagocytosis while suppressing pro-inflammatory cytokine secretion and alleviating liver inflammation and injury[28]. However, the full extent of the influence of CB on the liver cancer TME, particularly on TAMs, remains elusive.

This investigation revealed that the antineoplastic effects of CB may involve the inhibition of M2-polarized TAM differentiation through the modulation of key molecular pathways. Our comprehensive *in vitro* and *in vivo* analyses aimed to elucidate the mechanisms underlying the anti-liver cancer activity of CB, including its active constituents, cellular targets, and signaling pathways. The findings demonstrated the regulatory role of CB in macrophage phenotypic plasticity and interaction with the Wnt/ β -catenin pathway within the TME. This study lays a foundation for developing CB-derived antineoplastic therapeutic strategies that inhibit M2-TAM polarization by targeting the Wnt/ β -catenin pathway to suppress liver cancer.

MATERIALS AND METHODS

Chemicals and reagents

CB (20160526-2) was obtained from Hunan Sanxiang Herbal Pieces Co., Ltd. (Hunan, China). Sorafenib was obtained from GLPbio, Inc. (Montclair, United States). HepG2 cells, fetal bovine serum (FBS), and Dulbecco's modified Eagle's medium (DMEM) were acquired from Meisen Cell Technology Co., Ltd. (Zhejiang, China). HepG2 cells were authenticated using short tandem repeats. THP-1 cells were provided by the State Key Laboratory of Macau University. The TRIzol Kit (15596026) was procured from Thermo Fisher Scientific (Massachusetts, United States). Phorbol 12-myristate 13-acetate (PMA) and the cytokines for cell induction, including IL-4 and IL-13, were procured from Sigma (Darmstadt, United States). The Cell Counting Kit-8 (CCK-8) Kit was procured from Biosharp (Anhui, China). The Annexin V-FITC/PI Apoptosis Kit was purchased from APEX BIO (Houston, TX, United States). Type I collagenase was purchased from BioFroxx (Santiago, Germany). A Protein Assay Kit was purchased from CWBIO (Jiangsu, China). NovoStart[®]SYBR qPCR SuperMix Plus, and NovoScript[®]Plus All-in-one 1st Strand cDNA Synthesis SuperMix were procured from Novoprotein Inc. (Jiangsu, China). The primary antibodies against Wnt5B (#55184-1-AP), β -catenin (#66379-1-Ig), Axin2 (#20540-1-AP), and GADPH (#66009-1-Ig), as well as HRP-conjugated affinity-pure goat anti-rabbit IgG (#SA00001-2) and multi-rab HRP-goat anti-mouse recombinant secondary antibody (#RGAM Φ 01), were acquired from Proteintech (Wuhan, China).

In vivo and in vitro analysis of CB components

Sample preparation: To prepare a CB extract, 2.0 g of CB was mixed with 30 mL of 100% methanol, followed by ultrasonication for 30 min at 250 W and 40 kHz. After ultrasonication, the mixture was allowed to settle. Next, 2 mL of the mixture was centrifuged at 8000 g at 25 °C for 5 min. The supernatant was then filtered using a 0.22 μ m microporous membrane, and 1 mL of this filtrate was reserved in an injection vial for subsequent analysis.

For serum sample preparation, 2 mL of CB-enriched serum and 2 mL of blank serum (BS) were taken separately, and each was mixed with 6 mL of 100% methanol. The mixtures were chilled in an ice bath, then centrifuged at 12000 g at 25 °C for 5 min. The supernatant was then dried using a centrifugal evaporator. The dried samples were re-dissolved in 100 μ L methanol and again centrifuged under the same conditions to ensure clarity. Finally, the purified supernatants were filtered with a 0.22 μ m microporous membrane for further examination.

Chromatography and mass spectrometry: Chromatographic analysis was conducted using an Agilent ZORBAX Eclipse Plus C18 column, applying a gradient elution method with mobile phases of acetonitrile and either 1 mL/L formic acid in water in the positive ion mode or 5 mmol/L ammonium acetate in water in the negative ion mode. The sample injection volume was 2 μ L. Subsequently, mass spectrometry (MS) was performed with both positive and negative ESI settings, utilizing a multi-reaction monitoring scanning mode and calibrated with the ESI-L Low Concentration Tuning Mix. The MS spanned m/z 100 to 1500 with a resolution of 30000, employing nitrogen as the nebulizing gas, and a drying temperature of 325 °C, capillary voltage of 4.0 kV, fragmentation voltage of 110 V, and sheath gas temperature of 350 °C were maintained.

Animal experiments

Subcutaneous transplantation tumor experiment: Male 6-wk-old *BALB/c* nude mice and Sprague-Dawley rats, supplied by Hunan Slake Jinda Laboratory Animal Company Limited (Changsha, China), were housed under specific pathogen-free conditions. All animals were maintained in an environment with a controlled 12-hour dark/light cycle at 21 \pm 2 °C and 50% \pm 10% relative humidity.

Nude mouse xenograft tumors were induced *via* subcutaneous injection of 5×10^6 HepG2 cells into the posterior side of the right forelimb. Upon reaching a tumor volume of 100 mm³, the mice were allocated into a control group receiving 9 g/L saline (0.2 mL/d orally), low-dose (L-CB), medium-dose (M-CB), and high-dose (H-CB) CB groups receiving 45.5 mg/(kg/d), 113.75 mg/(kg/d), and 227.5 mg/(kg/d) of CB, respectively, and a sorafenib group administered 20 mg/(kg/d) of sorafenib. Body weight and tumor volume were monitored at 3-d intervals. This study complied with the 1986 Animals (Scientific Procedures) Act of the United Kingdom, ensuring the ethical treatment of laboratory animals. This study was approved by the Ethical Review Committee of Experimental Animal Welfare of the Slacker Jingda Laboratory, Changsha, Hunan, China (Approval No. IACUC-SJA2022105).

Blank and drug-enriched serum preparation: In this study, the rats were allocated to a control group receiving 5 g/L sodium carboxymethyl cellulose and a CB-treated group administered a 157.5 mg/kg CB suspension. Both regimens were administered twice daily for 1 wk. After a fasting period of 12 h, the rats were anesthetized using 30 g/L pentobarbital sodium at a dose of 30 mg/kg to facilitate the subsequent collection of serum.

Network pharmacological analysis

Collection of potential targets and construction of component-target-disease networks: In this study, we identified 22 unique chemicals in CB using UPLC-EIS-Q-TOF-MS analysis. Subsequently, the TCMSP and SwissTargetPrediction tools were employed to predict biological targets, which were further refined using the UniProt database[29]. To identify liver cancer-related targets, a comprehensive search was conducted across multiple databases including DrugBank, OMIM, PharmGKB, and TTD. The obtained data were refined to eliminate redundancy and false positives. Using R software, an intersection analysis was performed between the predicted targets of the bioactive compounds of CB and those present in the liver cancer target database. This enabled us to identify potential therapeutic targets of CB against liver cancer. Finally, a "component-target-disease" interaction network was constructed using Cytoscape.

Protein interaction network construction: A protein-protein interaction (PPI) network for the identified anti-liver cancer targets of CB was established *via* the STRING database. Following this, R software was employed to quantify the frequency of these target interactions, with the results presented in a histogram format for clearer analysis and interpretation.

Analysis of Gene Ontology function and Kyoto Encyclopedia of Genes and Genomes pathway enrichment: The anti-liver cancer targets obtained from CB screening were imported into the Metascape database for Gene Ontology (GO) function analysis. Using R software as a platform, Kyoto Encyclopedia of Genes and Genomes (KEGG) enrichment analysis was performed by inputting the corresponding script commands to clarify the pathways involving the genes.

Molecular docking: To investigate the interactions between liver cancer targets and the active components of CB, we used bioinformatics tools and databases. The structures of the target proteins Wnt5B, β -catenin, and Axin2 were obtained from UniProt. These protein frameworks were prepared for molecular modeling using PyMOL software by removing water molecules and small ligands, and the refined structures were saved in PDB format. The 'component-target-disease' network, focused on 17 primary active components of CB against liver cancer, was explored using PubChem to retrieve the two-dimensional (2D) structures. The chemical structures were further refined and optimized using Chem3D software to ensure accuracy in subsequent studies. Molecular docking simulations were performed using AutoDock Vina software to assess the binding affinity between the CB components and target proteins based on the calculated binding energies. Finally, the results from molecular docking were comprehensively visualized and analyzed using PyMOL software to understand the interactions between the active compounds of CB and the respective liver cancer protein targets.

RNA extraction, RNA sequencing, and bioinformatics analysis

The TRIzol method was used to extract total RNA for quality assessment *via* electrophoresis and bioanalysis. Following RNA extraction, cDNA libraries were sequenced on an Illumina NovaSeq 6000 platform, and reproducibility was evaluated using Pearson's correlation coefficient. RNA expression levels were quantified using Subread software and normalized for gene length and sequencing depth. Differential gene expression analysis was conducted using DESeq2, followed by GO and KEGG pathway enrichment analyses using ClusterProfiler software.

Cell culture

HepG2 cells were cultured in DMEM enriched with 100 mL/L FBS and antibiotic at 37 °C in an atmosphere containing 50 mL/L CO₂, while THP-1 monocytes were similarly cultivated in RPMI-1640. For experimental purposes, PMA was applied at a concentration of 100 ng/mL for 48 h to induce THP-1 monocytes to differentiate into M ϕ macrophages. To model tumor-promoting M2 macrophages, these M ϕ macrophages were further incubated with IL-4 and IL-13, each at a concentration of 20 ng/mL, for an additional 48 h.

Preparation of conditioned medium

For preparation of M ϕ and M2 + 10% (100 mL/L) FBS conditioned media, differentiated M ϕ macrophages and M2 macrophages were cultured in DMEM containing 10% (100 mL/L) FBS and 1% (10 mL/L) penicillin-streptomycin. For M2 + 0%, 5%, 10%, and 20% (respectively equal to 0 mL/L, 50 mL/L, 100 mL/L, and 200 mL/L) CB-containing serum (CBS) conditioned media, differentiated M2 macrophages cultured in DMEM were supplemented with 0% (0 mL/L), 5% (50 mL/L), 10% (100 mL/L), and 20% (200 mL/L) CBS and 1% (10 mL/L) penicillin-streptomycin. All the above con-

ditional medium were supernatant collected after culture at 37 °C in an atmosphere containing 50 mL/L CO₂ for 24 h.

CCK-8 assay

HepG2 (5 × 10⁵ cells/mL) and THP-1 (2.5 × 10⁴ cells/mL) cells were plated in 96-well plates. After a 24-h cultivation period, media containing various concentrations of CBS (0%, 5%, 10%, and 20%, equal to 0 mL/L, 50 mL/L, 100 mL/L, and 200 mL/L, respectively) were added to the wells for THP-1 cell treatment. HepG2 cells were maintained in different conditioned medium. Cultures were incubated for an additional 24 h to assess the effects of the treatment. Then, 10 µL of CCK-8 solution was added to each well. To facilitate color development, the plates were incubated for an additional 2 h. Optical density was measured at 450 nm using a Spark multimode microplate reader (TECAN, Switzerland).

Flow cytometry

Cell apoptosis detection: HepG2 cells (5 × 10⁵ cells/mL) were inoculated into 96-well plates and incubated for 24 h. Concurrently, THP-1 monocytes, transitioned to Mφ macrophages or subsequently to M2 macrophages, were incubated with either 10% (100 mL/L) control serum or 10% (100 mL/L) CB-enriched serum. Thereafter, the HepG2 cells were treated with media conditioned with these macrophages for an additional day. Following this period, cells were harvested using 800 µL of trypsin without EDTA. Cell apoptosis and viability were analyzed by staining with propidium iodide (5 µL) and annexin V (5 µL). Stained cells were then examined using a CytoFLEX flow cytometer (Beckman, United States).

Macrophage polarization detection: Tumor tissues were minced into small pieces and treated with type I collagenase, then incubated for 1.5 h at 37 °C to facilitate digestion. The cell suspension was gently layered over a density gradient consisting of 300 and 700 mL/L Percoll solutions and centrifuged to separate the lymphocytes, which were harvested from the interface between these two layers. To generate M2-TAMs *in vitro*, cells were dissociated using trypsin without EDTA and collected. Before antibody staining, cells were blocked with anti-mouse CD16/32 antibody (TruStain FcX™) to inhibit non-specific binding, followed by staining with primary antibodies against CD45, CD11b, and F4/80 [all diluted 1:100 in 1% BSA (10 g/L BSA in PBS)] for 30 min at 4 °C. The cells were fixed and permeabilized according to the BD Cytotfix/Cytoperm kit protocol, followed by staining with an anti-CD206 antibody for intracellular marker detection. The stained samples were examined using CytoFLEX (Beckman, United States). The data were further evaluated and visualized using FlowJo software (version 10).

Cell scratch assay

HepG2 cells were inoculated into six-well plates, transfected, and subjected to various treatments. After 24 h, a pipette tip was used to draw a straight line across the cell layer and create a scratch to simulate a wound. The wells were then exposed to media supplemented with different concentrations of CB [0% (0 mL/L), 5% (50 mL/L), 10% (100 mL/L), and 20% (200 mL/L)]. Cell migration was monitored and recorded under an inverted microscope at baseline (0 hour) and after 24 h, and the scratch area was quantified using ImageJ software.

Transwell assay

Invasion and migration assays were conducted using 24-well Transwell chambers with 8 µm pores. A mixture of Matrigel and DMEM was placed in the upper chamber containing HepG2 cells, whereas the lower chamber contained DMEM with 100 mL/L FBS as an attractant. After 24 h, non-migrated cells were expunged, whereas migratory cells on the lower surface were fixed, stained, and imaged with ImageJ software to quantify migration and invasion rates.

Real-time reverse transcriptase-polymerase chain reaction

Total RNA was isolated using TRIzol reagent (Vazyme, China) and then reverse-transcribed to cDNA using the All-in-one 1st Strand cDNA Synthesis SuperMix (gDNA Purge). Real-time reverse transcriptase-polymerase chain reaction (RT-qPCR) was conducted using NovoStart® SYBR qPCR SuperMix Plus and the LightCycler® 96™ Real-Time PCR System (Roche Inc., Switzerland). Primers specifically designed for the gene sequences of interest were synthesized based on the sequences available in GenBank (Table 1). The 2^{-ΔΔCt} method was utilized to test the relative expression of each gene.

Western blot analysis

THP-1 monocytes were incubated with 10% (100 mL/L) CB-enriched serum for 24 h and then processed for protein isolation using RIPA buffer (Applygen, China). Protein levels were assessed by the BCA assay, then 50 µg protein samples was separated for Western blot analysis on a 100 mL/L SDS-PAGE gel. The membranes underwent an overnight incubation at 4 °C with primary antibodies targeting Wnt5B, Axin2, β-catenin, and GAPDH, followed by incubation with HRP-conjugated secondary antibodies. Signals were detected using an ECL kit (Biosharp Inc., Anhui, China), followed by imaging using an Amersham Imager 600. Image Pro Plus software was used to conduct band intensity analysis.

Statistical analysis

SPSS version 20.0 was used for statistical analyses. Data normality was verified using the Shapiro-Wilk test. Normally distributed datasets are shown as the mean ± SD. Analysis of variance (ANOVA) was used to evaluate group differences, followed by either SNK post hoc or Tukey's tests, depending on suitability. For two-group comparisons, the independent sample *t* test was applied. The threshold for statistical significance was set at *P* < 0.05.

Table 1 Primers used for qPCR in this study

Gene name	Forward (5' to 3')	Reverse (5' to 3')	Product Length
<i>WNT5B</i>	TCTTCATCCTCCACGGTT	CAGTTTAGGGCTTTCCTGAC	84 bp
<i>β-catenin</i>	CAACTAAACAGGAAGGGATGGAAGG	CAGATGACGAAGAGCACAGATGG	239 bp
<i>AXIN2</i>	TACACTCCTTATTTGGCGATCA	TTGGCTACTCGTAAAAGTTTGGT	151 bp
<i>CCL22</i>	ATCGCTACAGACTGCACTC	GACGGTAACGGACGTAATCAC	129 bp
<i>TGF-β</i>	GCAGGTATTGATGGCACCTCC	GGCATGCTCCAGCACAGAAG	301 bp
<i>Arg-1</i>	CTTGGCAAAAGACTTATCCTTAG	ATGACATGGACACATAGTACCTTTC	170 bp
<i>IL-10</i>	TTTAAGGGTTACCTGGGTGC	TTGATGTCGGGCTTGGTTC	98 bp
<i>GAPDH</i>	GCTGAGAACGGGAAGCTTGT	GCCAGGGGTGCTAAGCAG	299 bp

RESULTS

Analysis of pharmacodynamic material basis of CB

To examine the pharmacological components of CB, we used UPLC-Q-TOF MS for an extensive analysis. This led to the identification of 22 chemical constituents, including bilirubin, bile acids, cholesterol, and acid esters, as detailed in Table 2 and illustrated in Figure 1. *In vivo* studies revealed 11 components and their metabolites in the blood of rats treated with CB, as shown in Figure 1 and Table 2. Standardized comparisons and quantitative assessments were conducted for the selected components (Figure 1C and Tables 3 and 4). Notably, lithocholic acid was the most abundant component in the CB extract, reaching a concentration of 0.7066 mmol/L, whereas glycohyodeoxycholic acid was the most prevalent in the CB-enriched serum, with a concentration of 0.2759 mmol/L.

CB suppresses liver cancer growth *in vivo*

The anti-tumor effects of CB have been previously evaluated in animal models. Treatment with low, medium, and high doses of CB (L-CB, M-CB, and H-CB) and sorafenib significantly reduced both the size and weight of the tumors relative to the controls (Figure 2A-C). Interestingly, there was no notable impact on the body weight of the mice across all experimental groups (Figure 2D).

The anti-cancer efficacy of CB was further validated by histological analysis. As illustrated in Figure 2E, hematoxylin and eosin staining of tumor tissue revealed distinct morphological indications of tumor regression following treatment with medium and high doses of CB and sorafenib. The observed signs of regression include degenerative changes in tumor cells, reduced nucleolar staining intensity, and the presence of nuclear fragments, which are indicative of diminished malignancy post-treatment. These findings suggest that CB, particularly at medium and high doses, significantly impedes the growth of liver cancer.

Cyberpharmacology analysis of CB components for anti-liver cancer study utilizing UPLC-Q-TOF MS

Construction of a "component-target-disease" network: Following database searching, 392 possible chemical targets associated with the components of CB were discovered. Liver cancer-related targets were compiled from comprehensive databases, including DrugBank, OMIM, PharmGKB, and TTD, resulting in 6307 targets associated with liver cancer. Using R software for data analysis, we matched the targets related to the active components of CB against those associated with liver cancer. This comparative approach led to the identification of 168 potential anti-liver cancer targets using intersection analysis (Figure 3A). The constructed component-target-disease interaction network (Figure 3B) visualized the potential efficacy of CB against liver cancer, encompassing 463 edges and 184 nodes, with an average degree value of 5.04. Notably, compounds such as gelsevirine, nisinic acid, methyl cholate, 7-ketolithocholic acid, glycocholic acid, deoxyloganin, bilirubin, hyodeoxycholic acid, campechic acid A, glycohyodeoxycholic acid, and phorbol 12,13-dimyrystate were identified with degree values ≥ 10 , highlighting their significant role in the anti-liver cancer activity of CB[30].

GO analysis: We used PPI network analysis to identify the primary targets of CB in liver cancer. This analysis revealed TNF and IL-6 as central targets (Figure 3C), highlighting their significant roles in the immune response associated with liver cancer. Furthermore, GO functional analysis was conducted on these key targets to categorize their roles in biological processes, molecular functions, and cellular components. The top 20 items were statistically significant ($P < 0.01$; Figure 3D). Our findings demonstrate that the biological processes involved in liver cancer pathogenesis mainly include the regulation of the MAPK cascade signaling pathway, hormonal responses, positive regulation of cell migration and death, and secretory regulation. The cellular components associated with the pathogenesis of liver cancer predominantly comprise membrane rafts, receptor complexes, postsynaptic membranes, and cellular projection membranes.

KEGG analysis: Moreover, the core targets were analyzed, and the signaling pathways with $P < 0.01$ were chosen for visualization (Figure 3E). KEGG analysis revealed significant pathways, including the PI3K-Akt, Wnt, Rap1, and Ras pathways (Figure 3E). The Wnt pathway, which is involved in cell proliferation, differentiation, and apoptosis, has been

Table 2 Information analysis of 22 compounds in *Calculus bovis*

Number	Retention time (min)	Molecular weight	Molecular formula	Name	Serum
1	11.362	222.0905	C13H10N4	1,5-Diphenyltetrazole	√
2	13.144	374.1593	C17H26O9	Deoxyloganin	
3	14.277	352.1787	C21H24N2O3	Gelsevirine	√
4	16.133	678.5017	C40H70O8	Campechic acid A	
5	16.381	190.1205	C6H13NO6	D-Glucosaminic Acid	√
6	18.253	221.0953	C14H11N3	Isoquinoline	
7	21.631	515.2957	C26H45NO7S	Taurocholic acid	
8	22.525	408.2876	C24H40O5	Cholic acid	√
9	23.039	584.2634	C33H36N4O6	Bilirubin	√
10	23.716	465.309	C26H43NO6	Glycocholic acid	√
11	24.844	499.2968	C26H45NO6S	Taurodeoxycholic acid	√
12	25.939	256.2402	C16H32O2	Palmitic acid	
8	26.684	408.2876	C24H40O5	Cholic acid	
13	27.776	449.3141	C26H43NO5	Glycohyodeoxycholic acid	√
14	28.919	392.2927	C24H40O4	Hyodeoxycholic acid	√
15	29.765	390.277	C24H38O4	7-Ketolithocholic acid	
16	31.405	356.2715	C24H40O4	Anoxycholic acid	
17	32.051	784.5853	C24H40O4	Deoxycholic acid	
18	33.541	222.162	C14H22O2	Isobornyl methacrylate	
19	37.532	422.3032	C25H42O5	Methyl cholate	
20	37.556	280.2402	C24H40O3	Lithocholic acid	√
21	37.701	148.016	C8H4O3	Isobenzofuran-1,3-dione	
22	38.046	304.2402	C20H32O2	Arachidonic acid	√

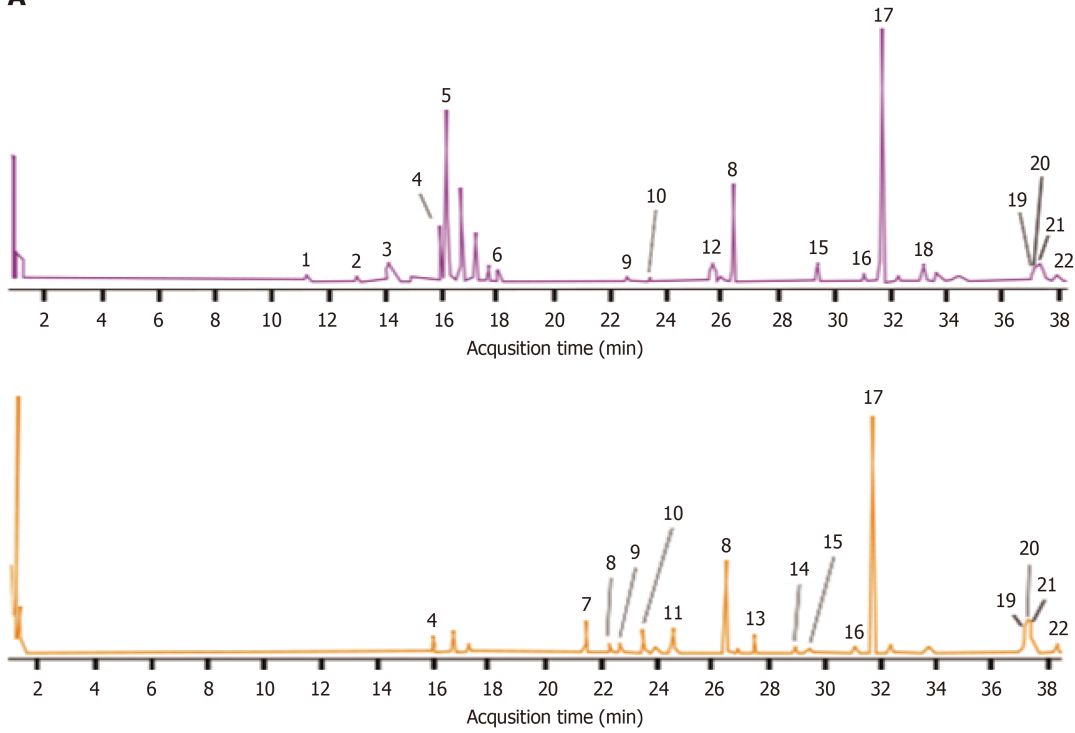
Table 3 Quantitative analysis of active components in *Calculus bovis* extract

No.	Component	Concentration of standard	Peak area of standard	Peak area of sample	Concentration of sample (mM)
1	Cholic acid	1 mg/mL	303383832.9	111239787.3	0.366663531
2	Glycohyodeoxycholic acid	1 mg/mL	263903105.5	151518620.6	0.574144894
3	Anoxycholic acid	1 mg/mL	255212724.5	84507042.75	0.331123939
4	Deoxycholic acid	1 mg/mL	303655598.9	116148310.7	0.382500145
5	Lithocholic acid	1 mg/mL	377852336.8	133498724.1	0.706618491

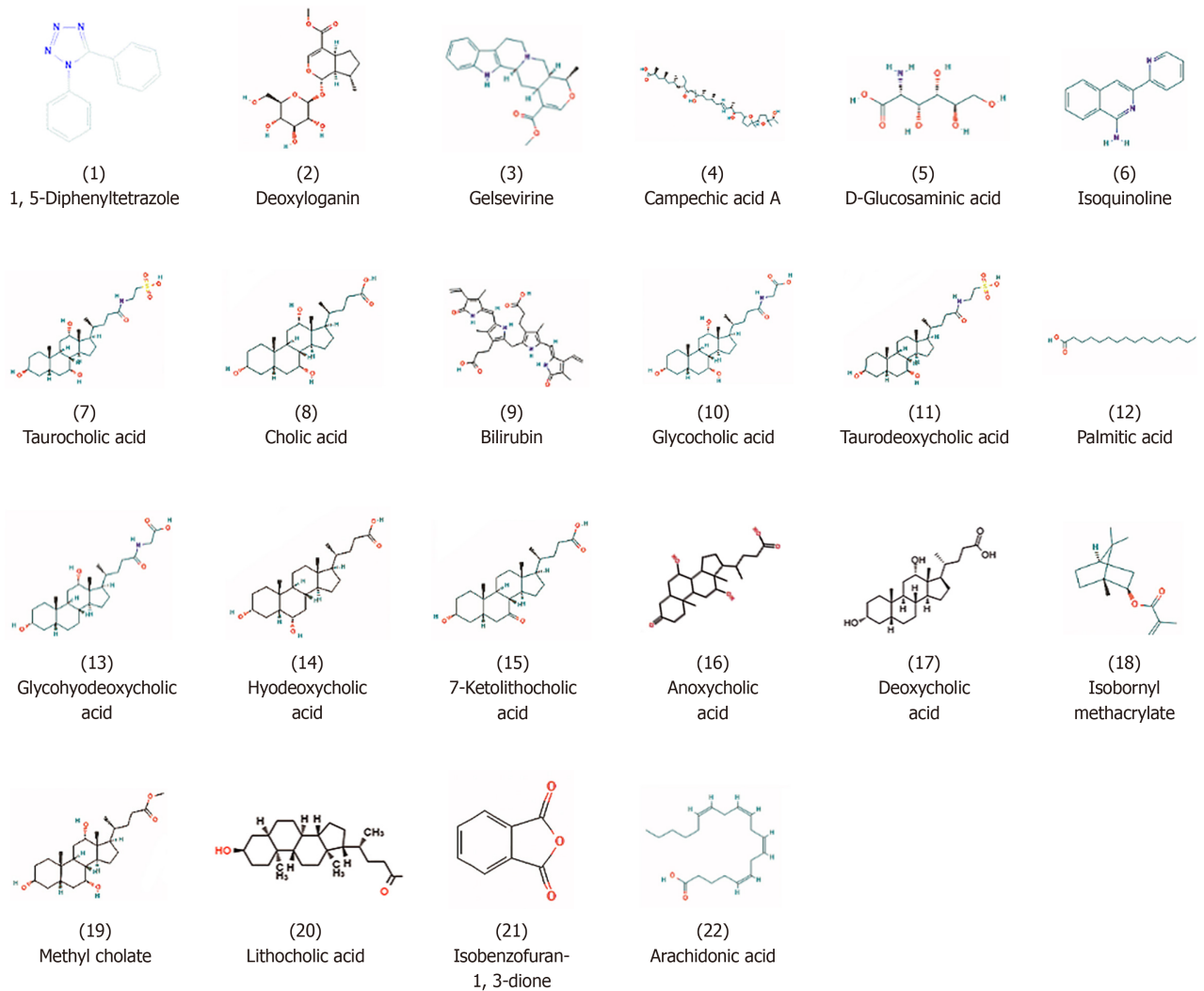
Table 4 Quantitative analysis of active components in *Calculus bovis*-enriched serum

No.	Component	Concentration of standard	Peak area of standard	Peak area of sample	Concentration of sample (mM)
1	Cholic acid	1 mg/mL	18294415.89	4577619.85	0.250219514
2	Glycohyodeoxycholic acid	1 mg/mL	14604541.97	4029834.55	0.275930225
3	Lithocholic acid	1 mg/mL	15655005.77	175178.8	0.022379909

A



B



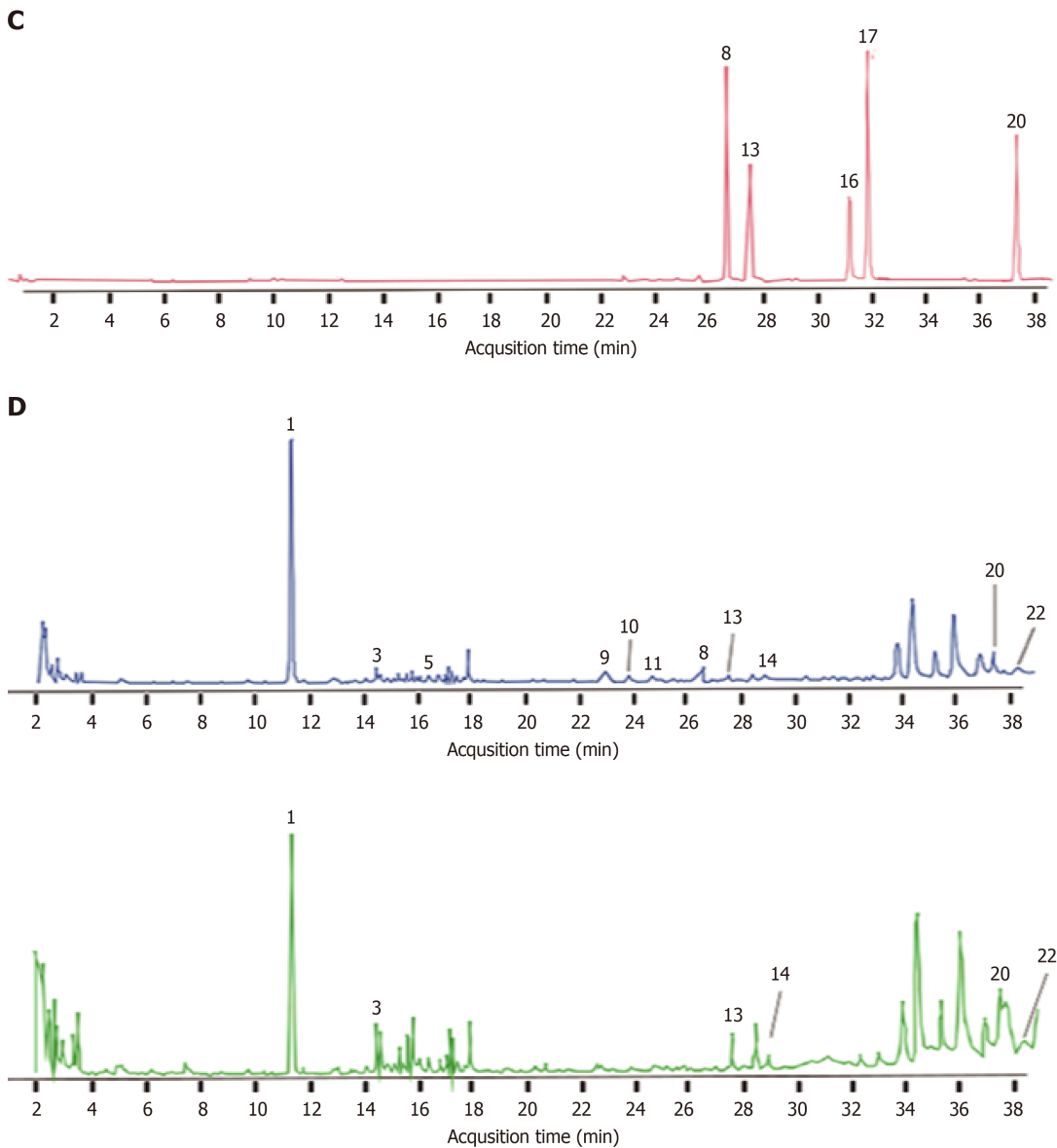


Figure 1 Analysis of pharmacodynamic material basis of *Calculus bovis*. A: Positive and negative ion chromatograms of *Calculus bovis* (CB) extract; B: Structural diagrams of 22 components of CB; C: Ion chromatogram of the standardized substances of CB extract; D: Ion chromatograms of CB-enriched serum and blank serum.

linked to cancer progression and immune system modulation. Based on these insights, further detailed investigation into the Wnt pathway was prioritized to better understand the mechanism of action of CB against liver cancer, supported by the findings of Pai *et al*[31].

Molecular docking results: The study excluded isolinolic acid from further analysis owing to the absence of a 2D structure in the database. To investigate the interactions between the target proteins associated with the Wnt signaling pathway and the active components of CB, molecular docking was conducted on the remaining 16 active components, including Wnt5B, β -catenin, and Axin2. A binding energy threshold of -5.0 kcal/mol was set as an indicator of strong affinity between the active ingredients and their target proteins. Our findings revealed that bilirubin and bile acid-like compounds such as glycocholic acid, taurodeoxycholic acid, glycohyodeoxycholic acid, hyodeoxycholic acid, and 7-ketolithocholic acid exhibited binding energies ≤ -6.5 kcal/mol with Wnt5B, β -catenin, and Axin2 proteins. This is depicted in Figure 3F and G, which demonstrate a stable binding conformation. These results suggest that CB inhibits liver cancer progression by modulating the Wnt signaling pathway.

Wnt pathway and its target molecules are involved in the effects of CB on M2-TAM

Transcriptome analysis was performed to investigate the effects of CB on gene functionality during cell migration. This analysis identified significant changes in 820 genes, including 359 genes with increased expression and 461 genes with decreased expression (Figure 4A). GO and KEGG enrichment analyses were then performed on differentially expressed genes, which indicated that the Wnt pathway is a key target of CB-mediated inhibition in liver cancer. Furthermore, CB

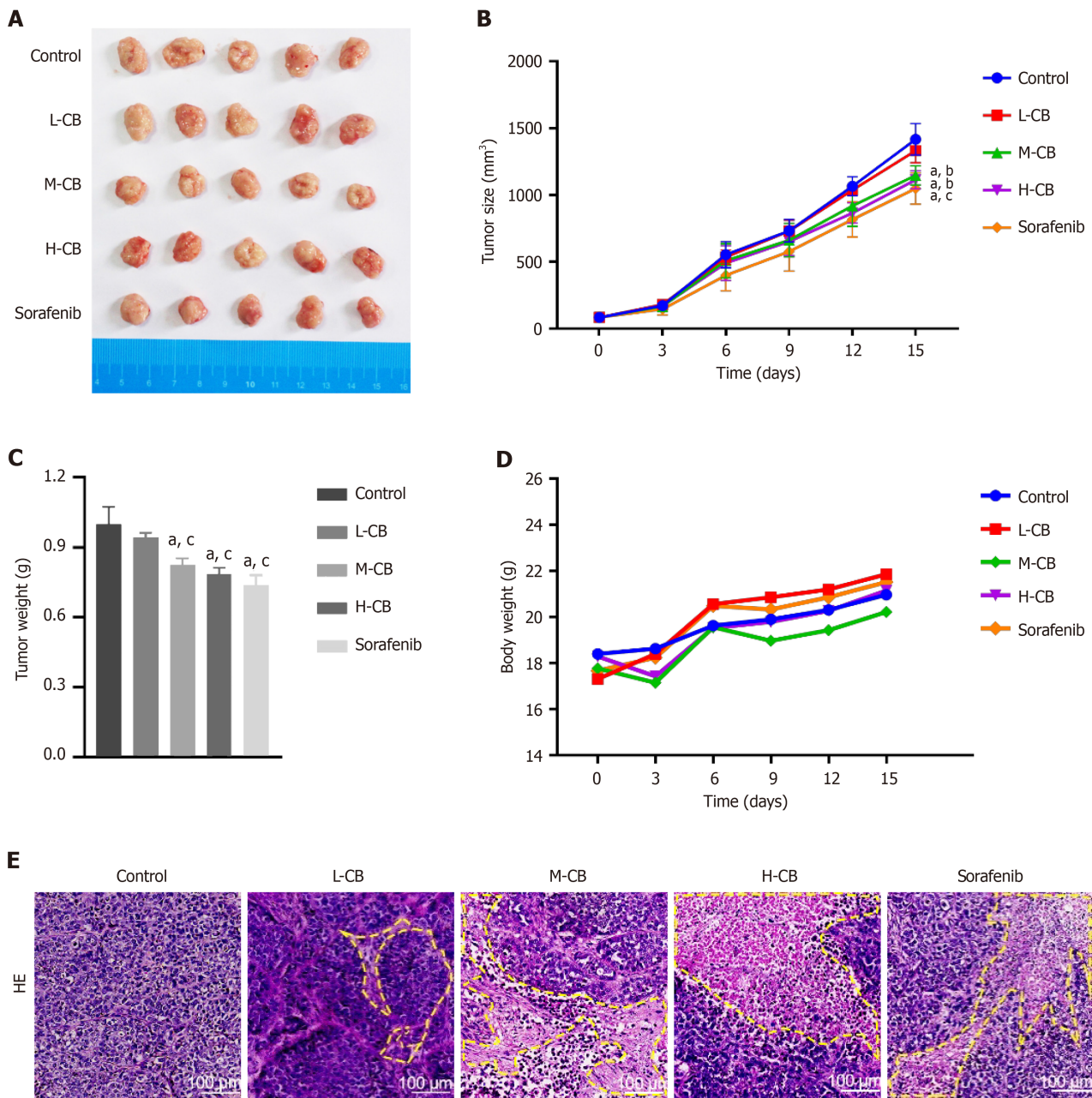


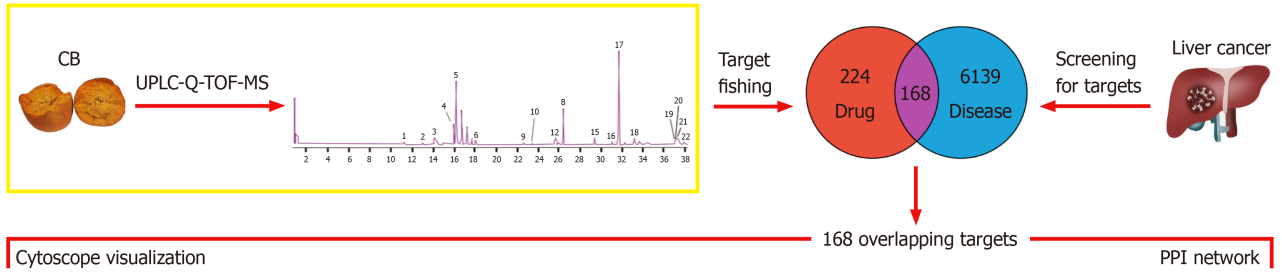
Figure 2 *In vivo* anti-tumor activity of *Calculus bovis*. A: Pictures of tumors in each group after treatment; B: Tumor size changes in each group during treatment; C: Tumor weight of each group during treatment; D: Changes in weight of mice in each group during treatment; E: Hematoxylin-eosin staining results of tumor tissue sections in each group after treatment. Control: Model group. CB: *Calculus bovis*; L-CB: Low-dose CB group; M-CB: Medium-dose CB group; H-CB: High-dose CB group; Differences were assessed using one-way ANOVA and multiple comparisons were determined using Tukey's test. ^a*P* < 0.01 vs control, ^b*P* < 0.05 vs L-CB, ^c*P* < 0.01 vs L-CB.

appeared to affect differential mRNA expression in mouse tumor tissues by targeting molecular functions and biological processes related to the Wnt pathway (Figure 4B-D). Notably, among the genes in this pathway, *CCL22* and *TGF-β*, both known for their association with M2-TAM polarization, were significantly enriched. Therefore, our results support the hypothesis that CB exerts its anti-liver cancer effects through modulation of the Wnt pathway and subsequent alteration of M2-TAM polarization.

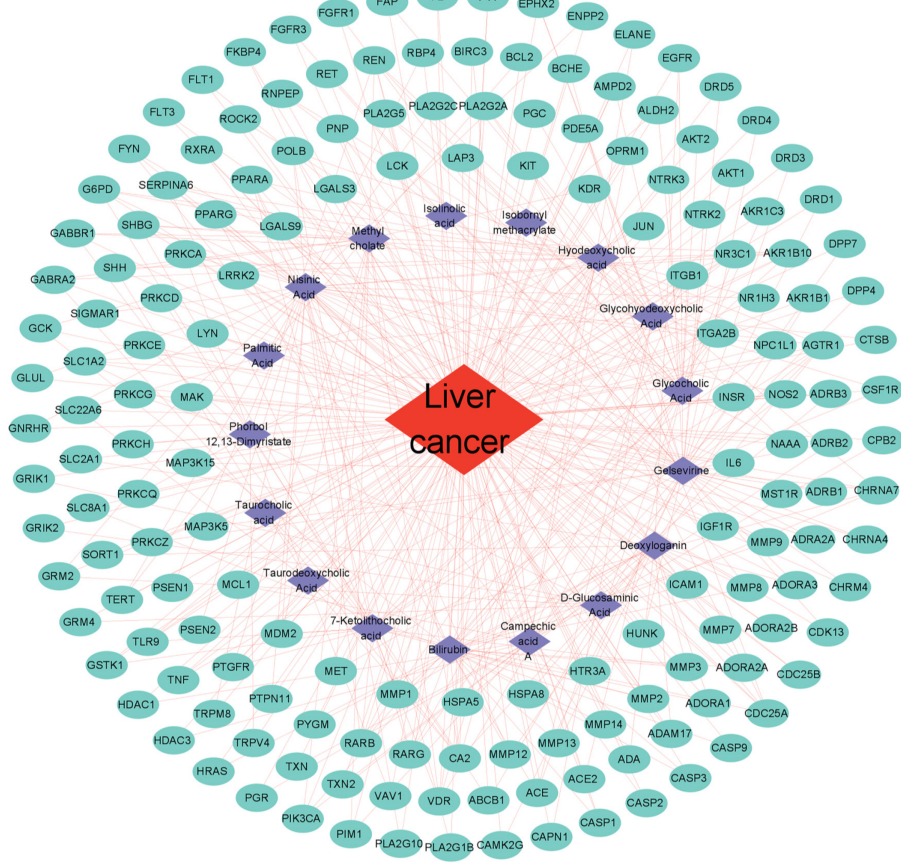
CBS inhibits M2 macrophage polarization in vitro

To assess the cytotoxic effects of CBS on THP-1 cells, we initially performed a CCK-8 assay using varying concentrations of CBS [5% (50 mL/L), 10% (100 mL/L), and 20% (200 mL/L)]. Figure 5A shows no significant effects on cell viability after exposure to CBS. Subsequently, we investigated the ability of CBS to inhibit M2 macrophage polarization stimulated by IL-13 and IL-4. Flow cytometry was used to measure CD86 and CD206 surface markers on THP-1 cells. As shown in Figure 5B, stimulation with IL-13 and IL-4 resulted in substantial upregulation of CD206 expression, confirming successful M2-TAM polarization. Furthermore, we evaluated the influence of different concentrations of BS and CBS on the mRNA expression of *CD206* in M2-TAM using RT-qPCR. Across the BS concentrations, *CD206* expression remained

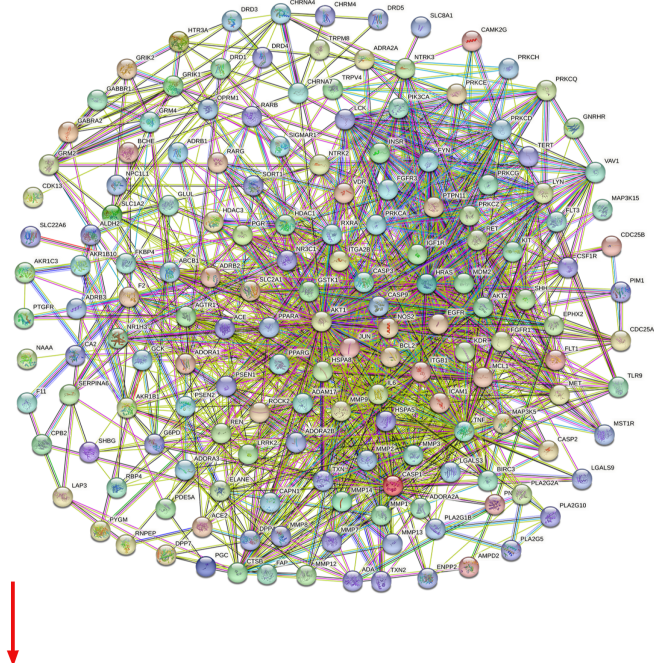
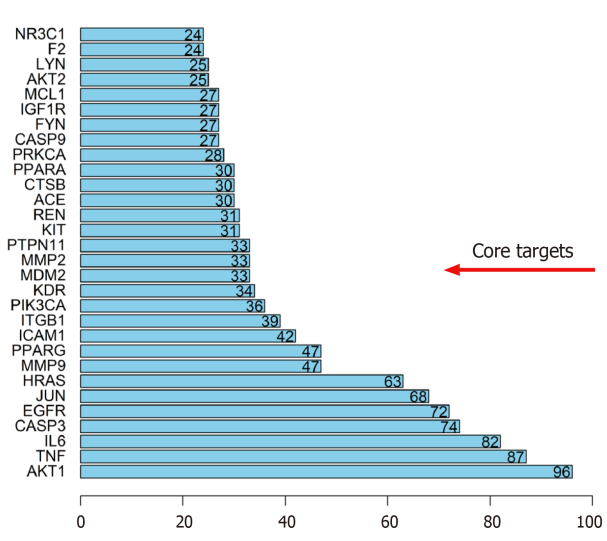
A



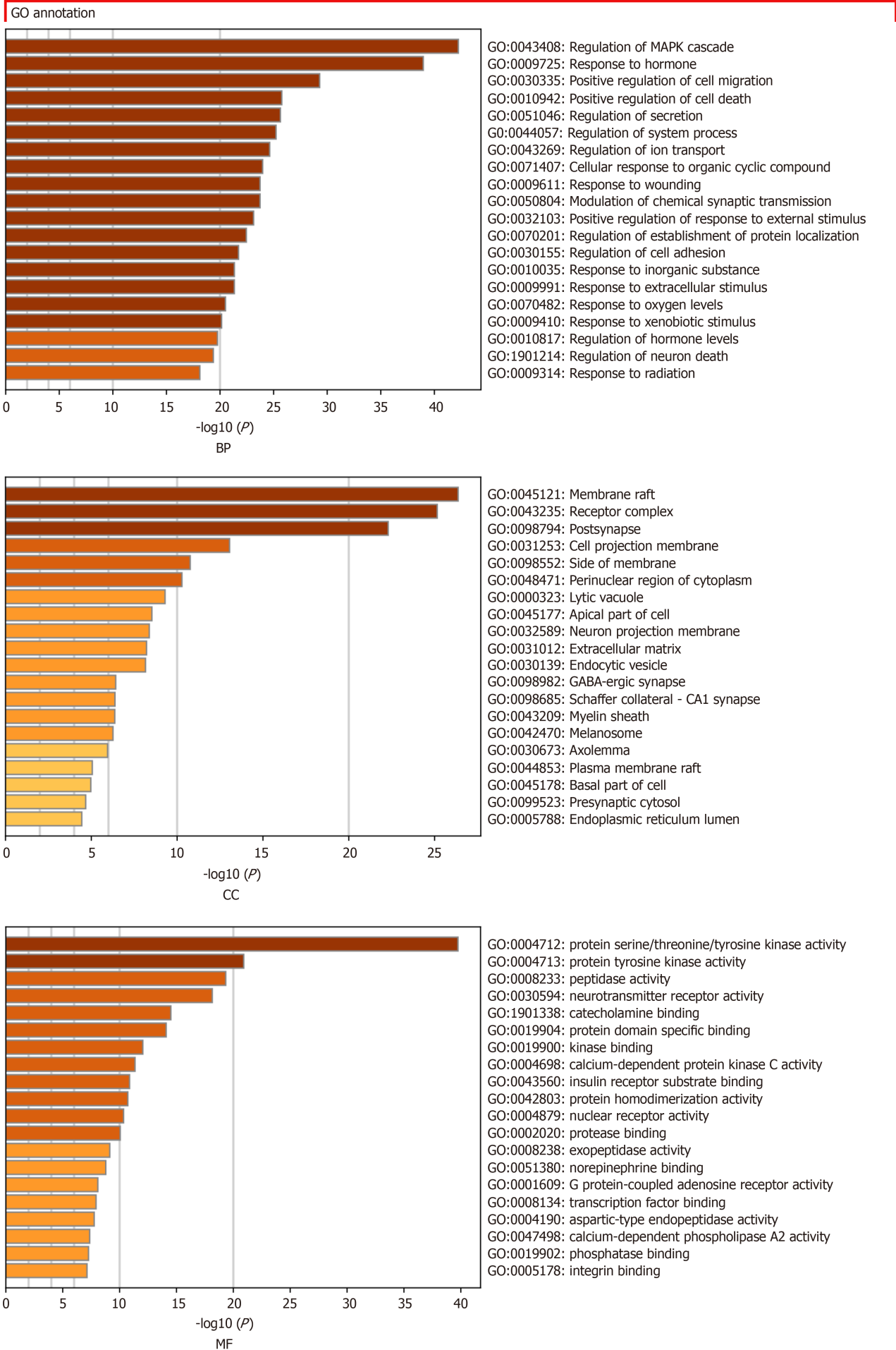
B



C



D



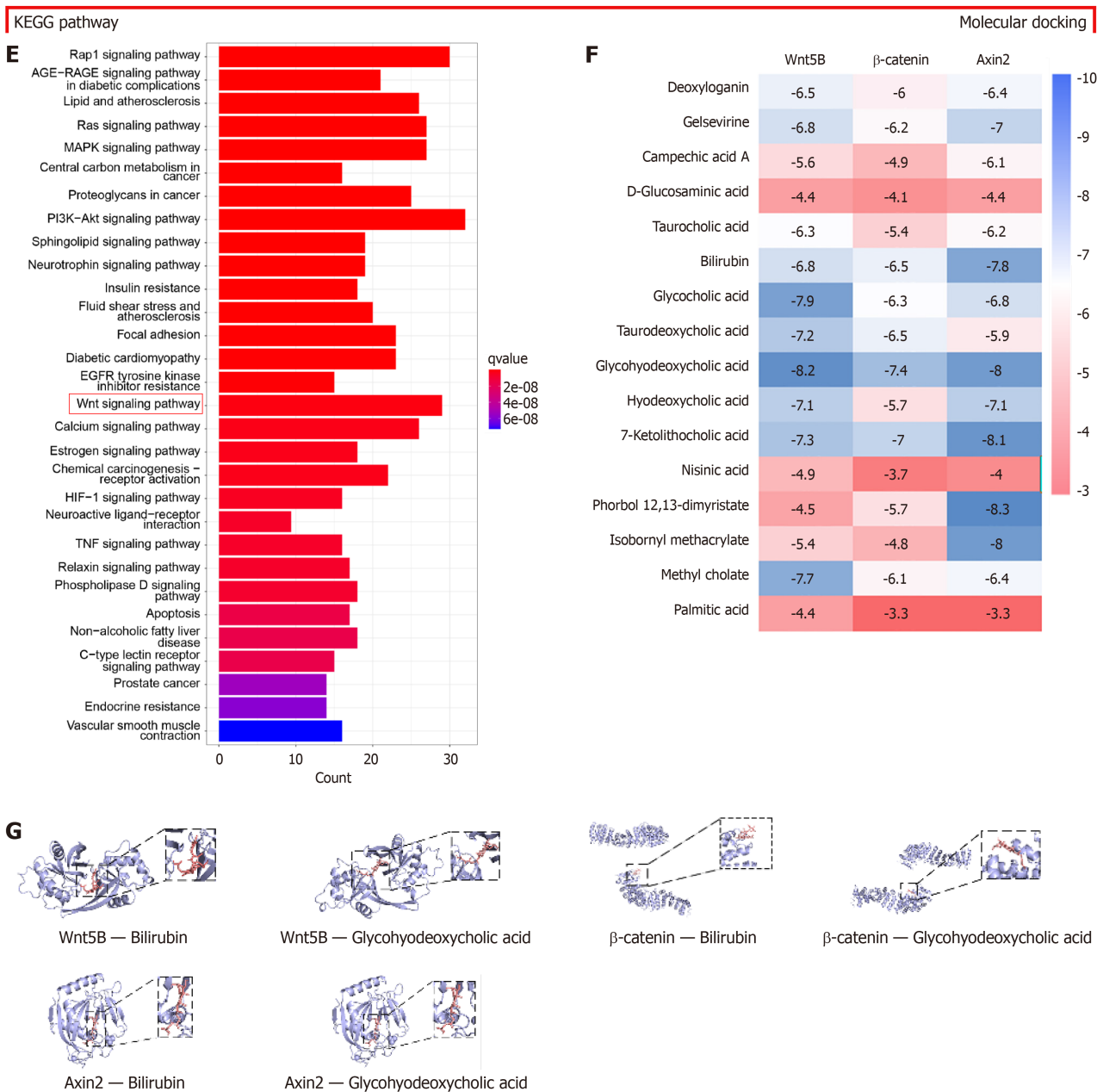


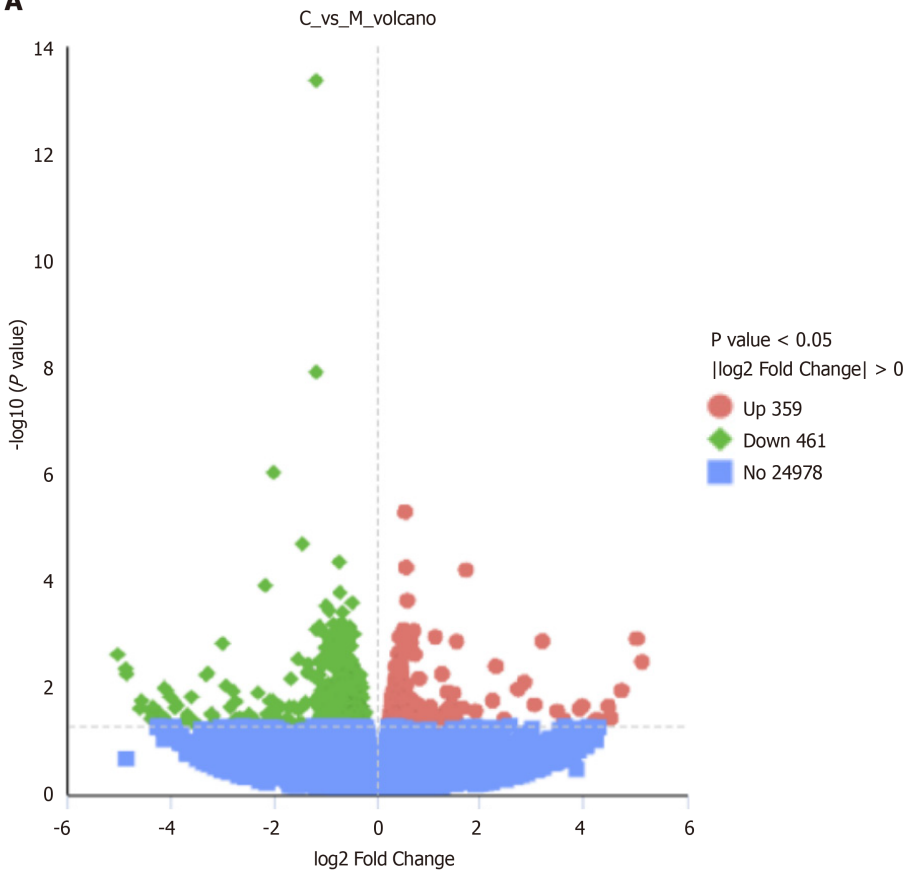
Figure 3 Cyberpharmacological study on anti-liver cancer mechanism of active components of *Calculus bovis* based on UPLC-Q-TOF-MS analysis. A: Intersection plot of potential targets of *Calculus bovis* (CB) and liver cancer targets; B: Component-target-disease interaction network of CB against liver cancer. The purple quadrilaterals represent the active components of CB; C: Protein-protein interaction network; D: Gene Ontology function analysis of CB against liver cancer; E: Kyoto Encyclopedia of Genes and Genomes pathway enrichment analysis of CB against liver cancer; F: Minimum binding energy of the active components of CB with core target proteins; G: Molecular docking diagram of some active components.

stable, with no significant alterations. However, notable differences in *CD206* mRNA expression were detected when comparing the groups treated with 10% (100 mL/L) CBS to those receiving 10% (100 mL/L) BS, as well as between the 20% (200 mL/L) CBS group and the corresponding BS group ($P < 0.01$). Treatment with both 10% and 20% (100 and 200 mL/L) CBS led to a statistically significant downregulation of *CD206* mRNA expression compared to treatment with 5% (50 mL/L) CBS; however, there was no significant difference between these two higher concentrations (Figure 5C). Consequently, 10% CBS (100 mL/L) was selected for subsequent experiments. Flow cytometry analysis demonstrated that treatment with this concentration effectively reduced *CD206* expression in M2-TAM cells (Figure 5D). Additionally, RT-qPCR analysis revealed significant reductions in mRNA levels of *CCL22*, *Arg-1*, *TGF-β2*, and *IL-10* (Figure 5E). Collectively, these findings indicate that CBS effectively inhibits M2-TAM polarization.

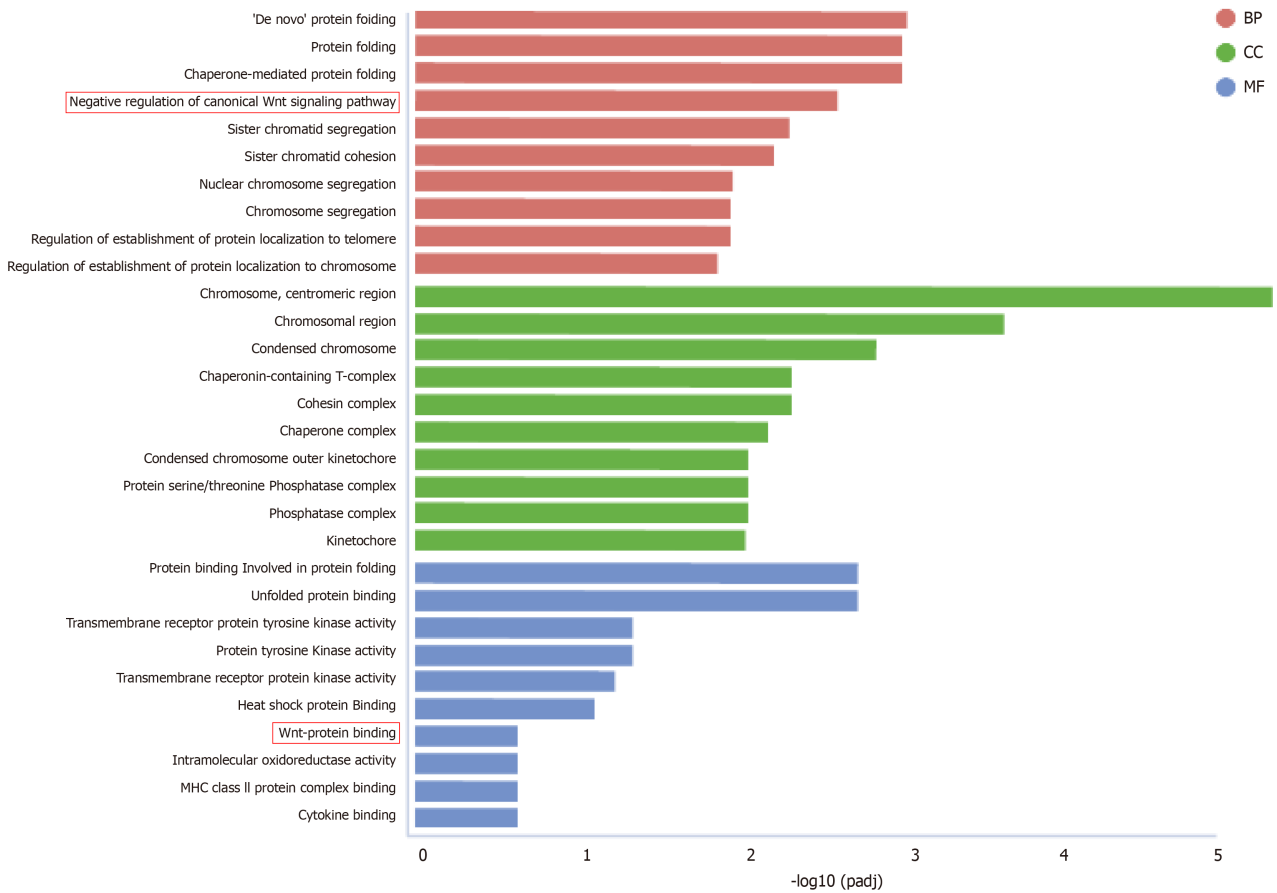
CBS mitigates the proliferative and migratory properties of liver cancer cells by suppressing TAM polarization to M2

We used the CCK-8 assay to evaluate the effects of various concentrations of CBS on HepG2 cell proliferation in a medium conditioned with M2 macrophages, which revealed notable inhibitory effects (Figure 6A). Flow cytometry analysis indicated an enhancement in the proliferation of liver cancer cells compared to Mφ macrophages. Notably, enhanced apoptosis was observed in the group treated with M2 + 10% (100 mL/L) CBS conditioned medium, in stark

A



B



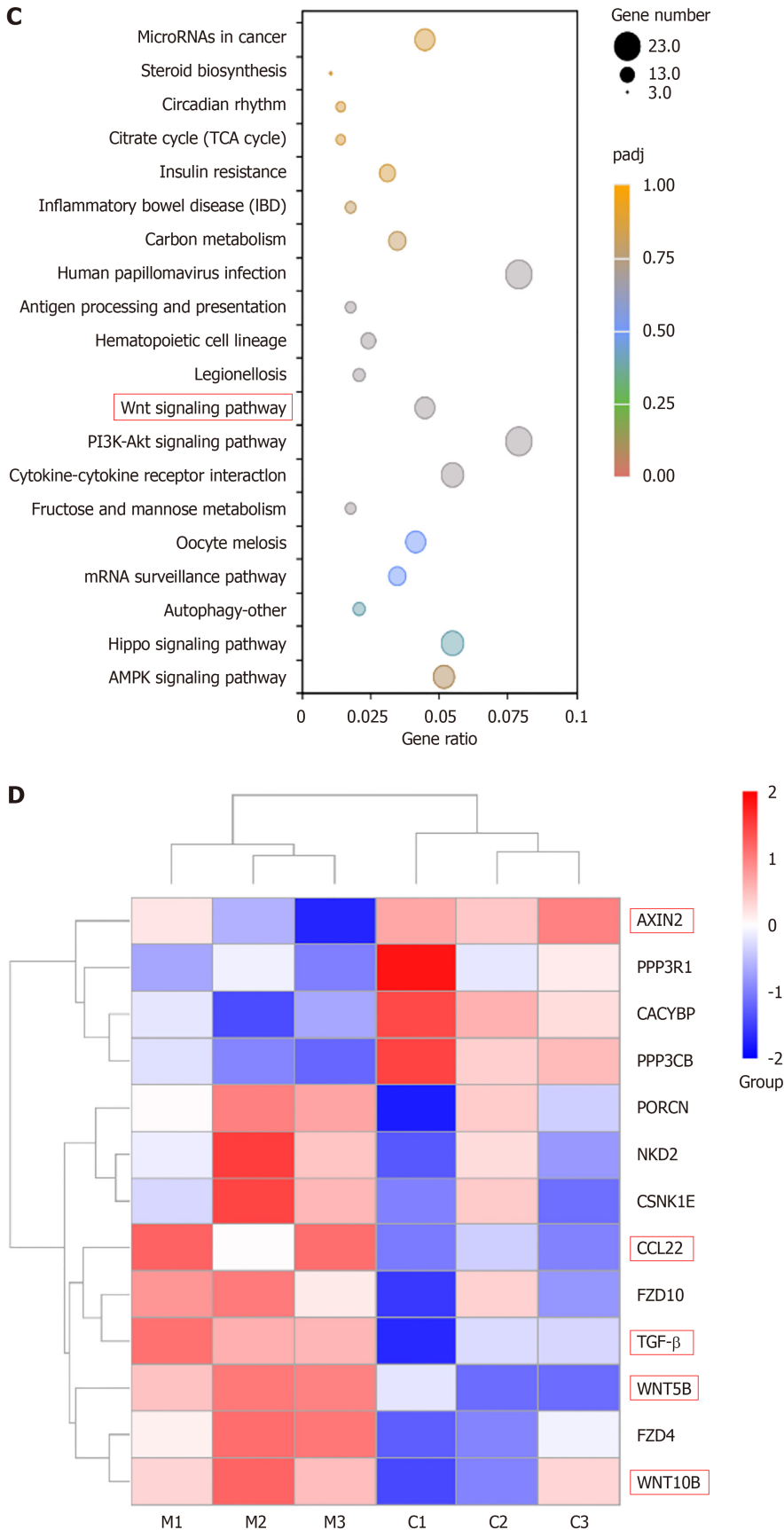


Figure 4 Differentially expressed genes between *Calculus bovis*-treated group and control group ($q < 0.05$ and $\log_2\text{FoldChange} > 0$) after transcriptome sequences were analyzed by bioinformatics. A: Differential gene volcano plot between the *Calculus bovis* (CB)-treated and control groups; B: Histogram of Gene Ontology enrichment results of differentially expressed mRNAs in the CB-treated and control groups (top 10); C: Bubble plots of Kyoto Encyclopedia of Genes and Genomes enrichment results of differentially expressed mRNAs in the CB-treated and control groups (top 20); D: Heatmap of selected genes involved in the Wnt pathway.

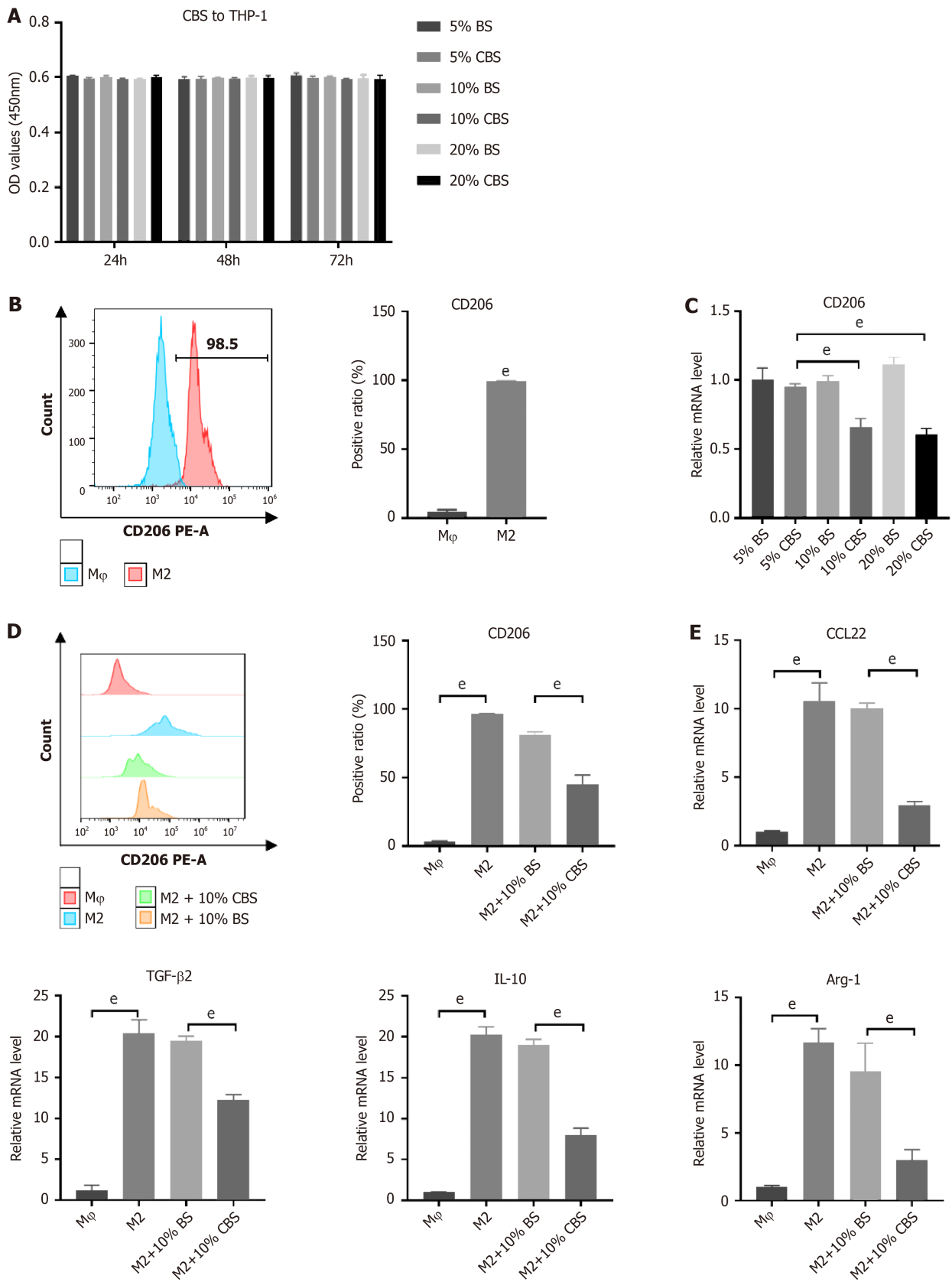


Figure 5 *Calculus bovis*-enriched serum inhibits polarization of M2 tumor-associated macrophages. A: Cytotoxicity of *Calculus bovis*-enriched serum (CBS) on THP-1 cells by Cell Counting Kit-8 assay. The blank group served as a control; B: CD206 quantification in THP-1 cells after IL-4 and IL-13 induction by flow cytometry; C: The mRNA expression levels of *CD206* after intervention of M2 tumor-associated macrophages (M2-TAMs) with different concentrations of blank serum and CBS; D: Quantification of CD206 in M2-TAMs after 10% (100 mL/L) CBS intervention by flow cytometry; E: The mRNA expression levels of *CCL22*, *TGF-β2*, *IL-10*, and *Arg-1* after 10% (100 mL/L) CBS intervention in M2-TAMs. ^a*P* < 0.05, ^a*P* < 0.01. BS: Blank serum; CBS: CB-enriched serum.

contrast to the M ϕ + 10% (100 mL/L) BS and M2 + 10% (100 mL/L) BS conditioned medium groups (Figure 6B). These results confirm that CBS not only impedes M2-TAM-induced proliferation of liver cancer cells but also significantly promotes their apoptosis. In the 24-h wound healing assay, the migratory capacity of HepG2 cells was increased when cultured with medium from the M2 + 10% (100 mL/L) BS group, compared to the M ϕ + 10% (100 mL/L) BS group. However, this enhanced migratory behavior was significantly reduced following treatment with M2 + 10% (100 mL/L) CBS-conditioned medium (Figure 6C). Similarly, the Transwell invasion assay revealed that M2 + 10% (100 mL/L) CBS-conditioned medium effectively decreased the migration rate of HepG2 cells (Figure 6D). Collectively, these findings indicate that CBS-treated M2-TAM medium considerably diminishes the cell invasion and migration capabilities of liver cancer, underscoring the potential therapeutic value of CB in halting liver cancer progression.

CBS inhibits M2-TAM polarization through the Wnt pathway

RT-qPCR and Western blot analysis showed upregulated expression of Wnt5B and β -catenin, along with a reduction in Axin2 levels, confirming the activation of the Wnt pathway (Figure 7A and B). Significantly, the inclusion of 10% (100 mL/L) CBS markedly mitigated IL-13/IL-4 induced alterations, suggesting that Wnt pathway modulation occurred in the CBS-mediated inhibition of macrophage M2 polarization. To further elucidate the effect of CBS on Wnt signaling in macrophages, we used SKL2001, a recognized activator of this pathway, in our experimental design. As depicted in Figure 7C, THP-1 cells co-treated with 10% (100 mL/L) CBS and SKL2001 showed a significant elevation in β -catenin levels compared with cells treated with 10% (100 mL/L) CBS alone. Additionally, flow cytometry analysis demonstrated that treatment with 10% (100 mL/L) CBS reduced CD206 expression by approximately 40%. Notably, simultaneous administration of SKL2001 and CBS abrogated the CBS-induced suppression of CD206 expression (Figure 7D). These findings highlight that the inhibitory effect of CBS on M2-TAM polarization predominantly operates through the downregulation of the Wnt pathway.

CB regulates M2 polarization via the Wnt pathway *in vivo* to combat liver cancer

In the subsequent *in vivo* experiments, we aimed to confirm the effects of the Wnt pathway. Consistent with our earlier findings, CB treatment resulted in significant downregulation of Wnt5B and β -catenin, alongside increased expression of Axin2 (Figure 8A and B). These findings suggest that CB suppresses Wnt pathway activity. Moreover, flow cytometry analysis indicated that CB effectively reduced the expression of the M2 macrophage marker CD206, with the most significant decrease observed in the high-dose group (Figure 8C).

DISCUSSION

Despite recent advances in treatment methods that have reduced liver cancer mortality, prognosis remains poor owing to high rates of metastasis and chemotherapy resistance. TCM can inhibit liver cancer by regulating the TME, thus providing a new perspective on liver cancer treatment. CB, a classic herb in TCM described in ancient medical texts and with thousands of years of use, is a foundational substance in compound formulations such as Xihuang Pills and Pien Tze Huang, used for treating tumors. Its immunomodulatory and anti-inflammatory effects are well documented, highlighting its medicinal significance in traditional Chinese therapeutic practices[32-34]. We hypothesized that CB inhibits tumor progression by modulating macrophages within the TME, and subsequently investigated this effect.

Antitumor experiments conducted *in vivo* and *in vitro* have demonstrated that CB significantly inhibits the progression of liver cancer. Network pharmacology and transcriptome sequencing analysis indicated enrichment of the Wnt/ β -catenin signaling pathway, suggesting that the mechanism of action of CB may involve this pathway. Previous studies have established that the Wnt signaling pathway is crucial for the pathogenesis of liver cancer[35-37], as it regulates the proliferation of liver cancer stem cells and promotes tumor growth. Our research illustrated the mechanism that CB impedes progression of liver cancer by alerting M2-TAM polarization *via* Wnt/ β -catenin pathway modulation. Detailed serum analysis revealed 11 bioactive compounds, including bilirubin, which exhibits antioxidant, anticancer, and anti-inflammatory effects as documented by Yu *et al*[26]. Bile acid-like components and acid esters, which are recognized for their roles in enterohepatic circulation and their antitumor properties[38], also contribute to the hepatoprotective profile of CB. These findings verify the multiple therapeutic effects of CB in targeting liver cancer through the interaction of its active constituents.

In the further analysis of the Wnt pathway, a significant upregulation of CCL22 and TGF- β 2 was observed among downstream molecules. The stimulation of TGF- β and Wnt/ β -catenin pathways is known to facilitate M2 macrophage polarization, which has a significant impact in connecting inflammatory and oncogenic processes. This polarization further enhances the invasion and migration of liver cancer[39]. It has been demonstrated that CCL22 exacerbates autoimmune diseases by recruiting macrophages and enhancing their effector functions. Neutralizing CCL22 leads to an altered cytokine profile within macrophages, characterized by reduced TNF- α levels and increased IL-10 levels, aligning with the characteristics of M2-TAMs[17,40]. CB may impede liver cancer progression by obstructing M2-TAM polarization *via* the Wnt/ β -catenin pathway. *In vitro*, CB-supplemented serum reduced M2-TAM markers and cytokines in THP-1 cells activated with IL-4/IL-13 for 24 h. Identification of M2-TAMs relies on their responsiveness to IL-4, IL-10, IL-13, and TGF- β , resulting in elevated levels of CD206 and Arg-1 expression[41]. Moreover, TAMs tend to secrete lower amounts of TNF- α and IL-1 β while exhibiting higher concentrations of TGF- β and IL-10[41-43]. These observations support the findings of this study.

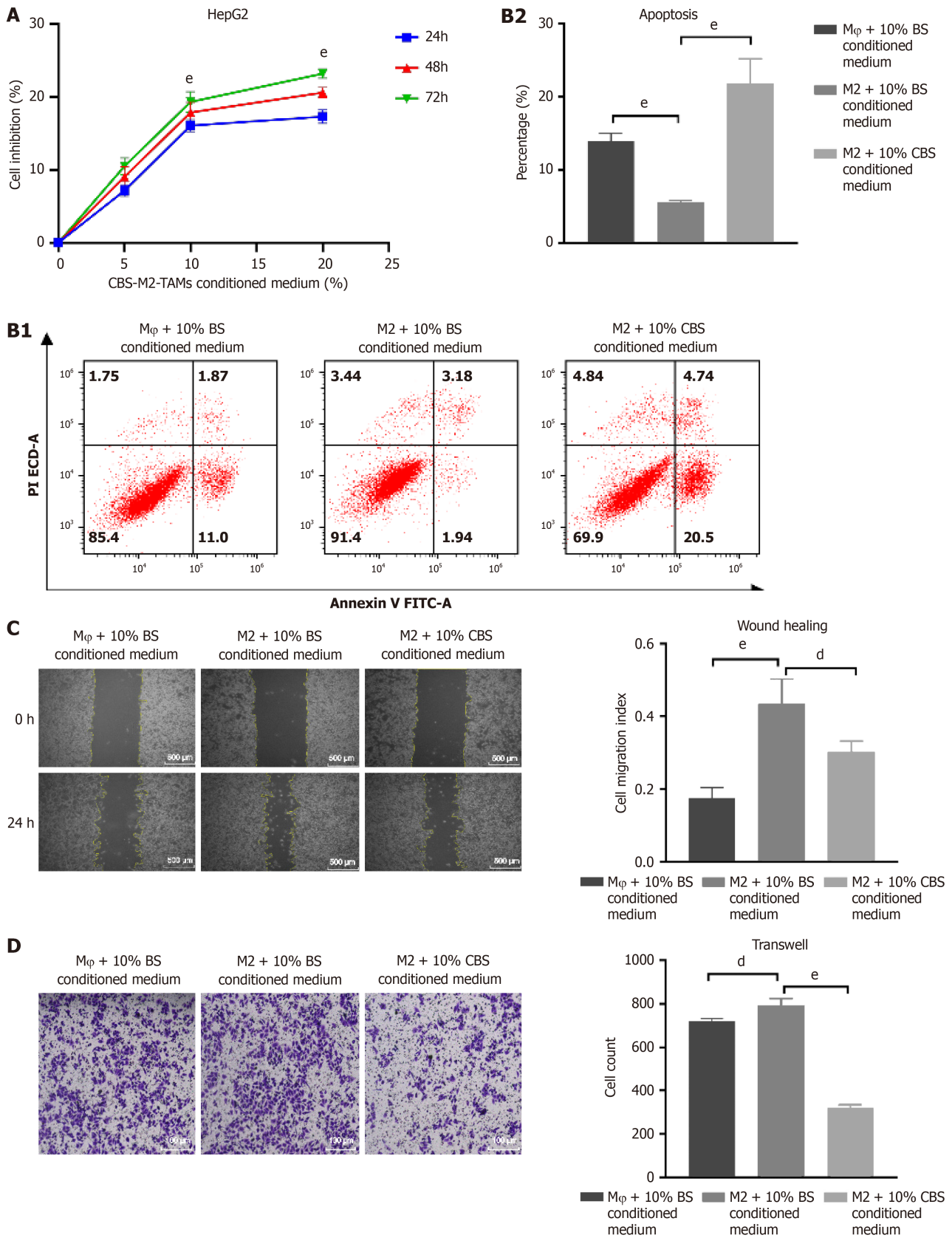


Figure 6 *Calculus bovis*-enriched serum inhibits polarization of M2 tumor-associated macrophages through the Wnt pathway and suppresses malignant behaviors of liver cancer cells. **A:** Inhibition rate of HepG2 proliferation by M2 + *Calculus bovis*-enriched serum (CBS) conditioned medium; **B:** Effect of M2 + CBS conditioned medium on HepG2 apoptosis detected by flow cytometry; **C:** Inhibitory effect of M2 + CBS conditioned medium on migration of HepG2 cells by cell scratch assay; **D:** Inhibitory effect of M2 + CBS conditioned medium on migration of HepG2 cells by Transwell assay. M2 + CBS conditioned medium: Supernatants of differentiated M2 macrophages cultured in DMEM medium enriched with CBS and penicillin-streptomycin, and the conditional media were collected after culture. ^d*P* < 0.05, ^e*P* < 0.01.

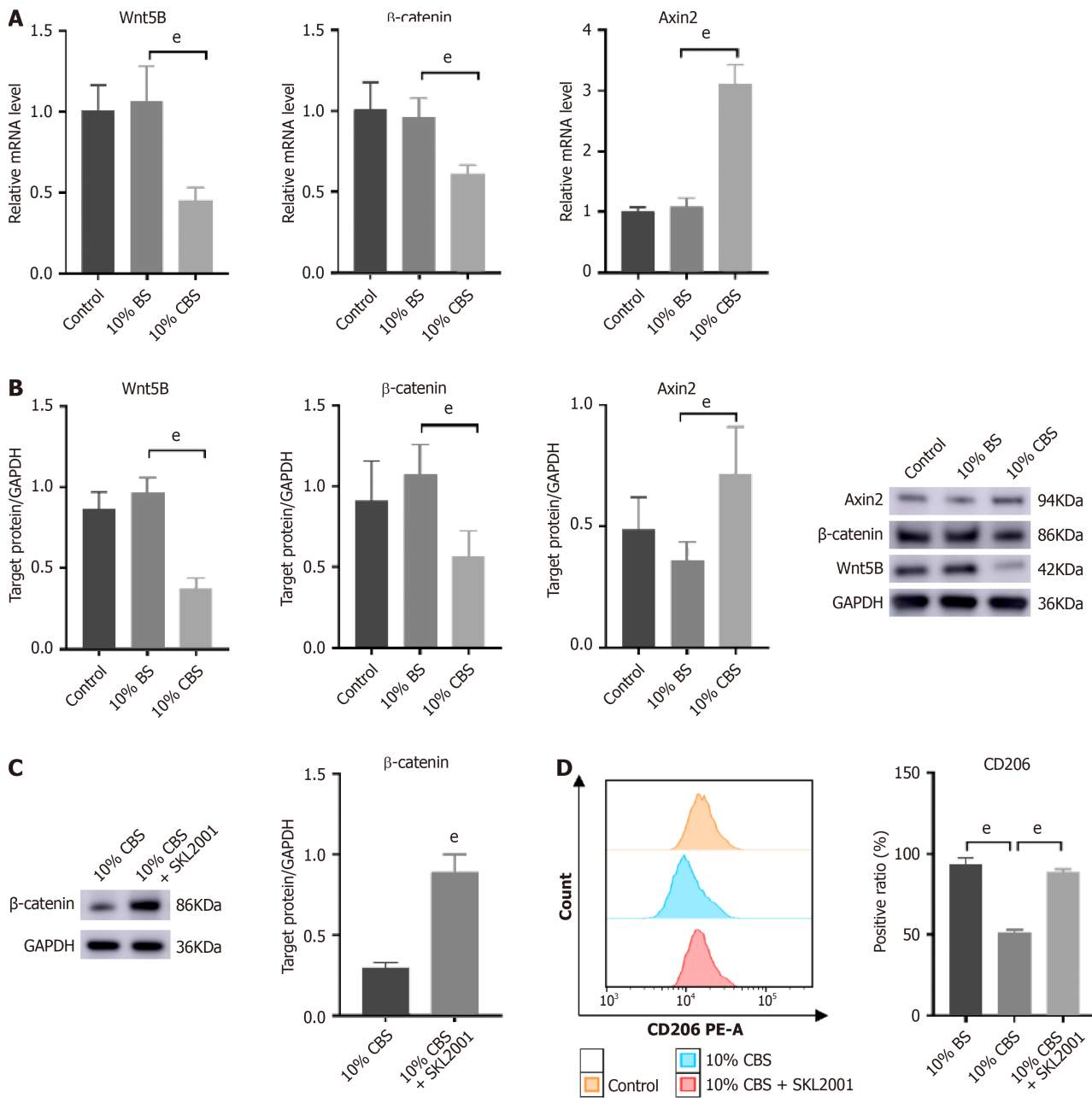


Figure 7 *Calculus bovis*-enriched serum inhibits polarization of M2 tumor-associated macrophages through the Wnt pathway to suppress against liver cancer. A: Effect of *Calculus bovis*-enriched serum (CBS) on *Wnt5B*, β -*catenin*, and *Axin2* mRNA levels in THP-1 cells detected by real-time reverse transcriptase-polymerase chain reaction; B: Effect of CBS on *Wnt5B*, β -*catenin*, and *Axin2* protein levels in THP-1 cells detected by Western blot analysis; C: Effect of the Wnt pathway agonist SKL2001 on β -*catenin* protein expression; D: Changes in CD206 detected by flow cytometry in THP-1 cells after CBS combined with SKL2001 intervention for polarization. ^e*P* < 0.01.

Research has shown that the Wnt pathway is essential to drive liver cancer progression, particularly by upregulating CCL22 and TGF- β 2, which are associated with M2 macrophage polarization[44-46]. It has been demonstrated that CB-enriched serum can inhibit M2-TAM polarization stimulated by IL-13/IL-4, reversing the switch to an M2 phenotype and reducing the invasive and migratory capabilities in liver cancer both *in vitro* and *in vivo*. Meanwhile, the presence of SKL2001 indicates that the inhibitory effects of CB on M2-TAM activation can be modulated by the Wnt/ β -catenin pathway. The weak direct killing effect on tumor cells exhibited by CB *in vitro* does not completely explain its anti-tumor effects *in vivo*. Therefore, we speculate that immunomodulation may be an important pathway for the anti-tumor activity of CB. This study is the first to demonstrate that CB inhibits liver cancer development by regulating TAM polarization, thereby enhancing our understanding of the pharmacological role of CB and offering a promising and effective treatment option for liver cancer. However, T-cell infiltration, NK cell activation, and PD-1/PD-L1 expression are factors that affect the TME, and it is not clear whether CB has a regulatory effect on them, which needs to be addressed in future studies.

We found that there are as many as 22 constituents of CB. However, it is not clear which compounds play a role in regulating macrophage polarization, and this needs to be clarified in future studies. Furthermore, the synergistic effects of these active components with clinical antitumor drugs should be investigated. In addition, new drug development

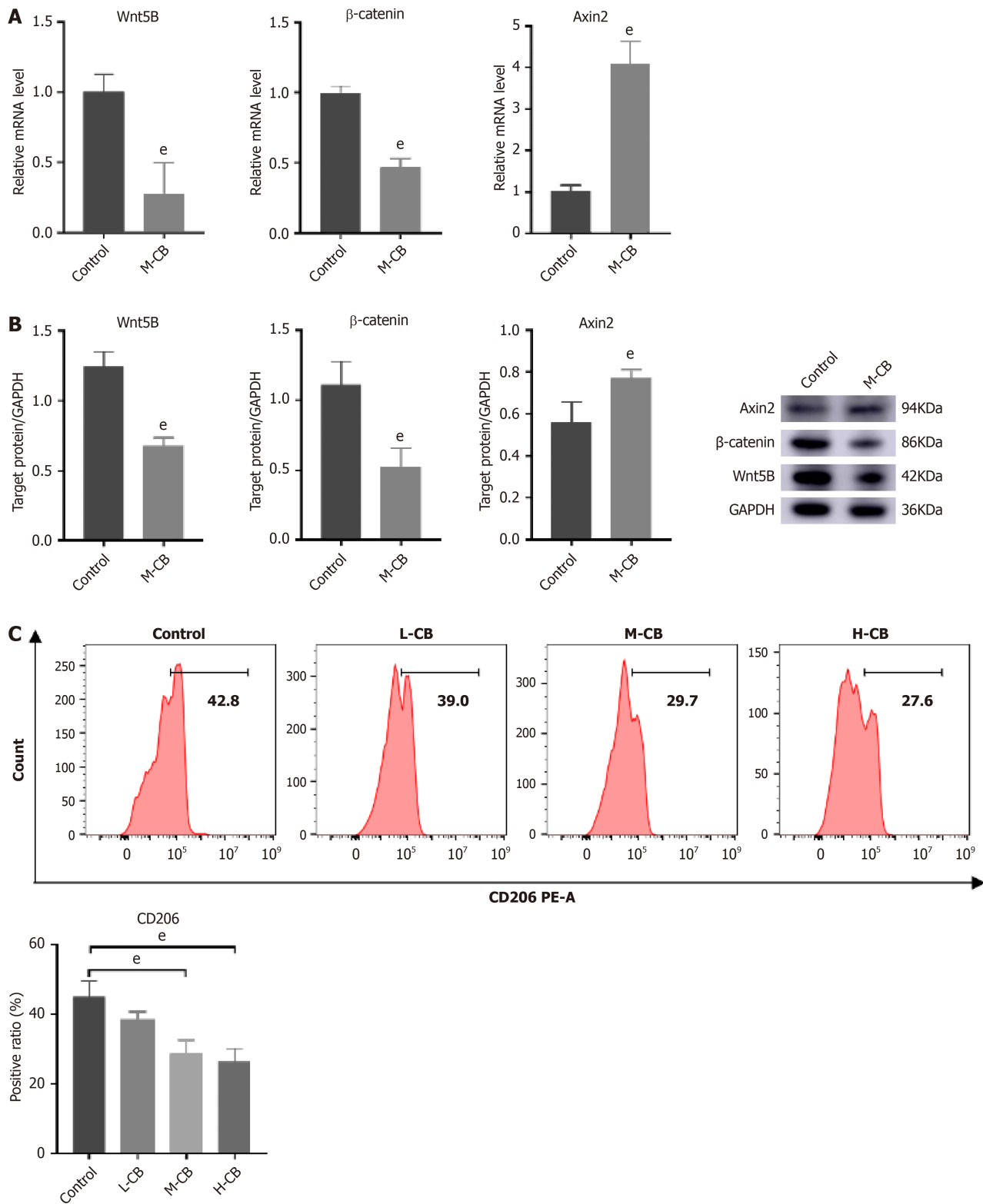


Figure 8 *In vivo* experimental validation of regulation of M2 macrophage polarization by *Calculus bovis* through the Wnt pathway. A: Quantification of mRNA expression of *Wnt5B*, β -catenin, and *Axin2* by real-time reverse transcriptase-polymerase chain reaction; B: Quantification of protein expression of *Wnt5B*, β -catenin, and *Axin2* by Western blot analysis; C: Ratio of cells expressing CD206 molecules in tumor tissues analyzed by flow cytometry. ^e*P* < 0.01.

strategies such as structural modifications and targeting system construction should be utilized to enhance the antitumor effects of the active ingredients of CB and improve their targeting properties, making them potential antitumor drugs.

CONCLUSION

CB has long been used in traditional Chinese herbal medicine for its anti-inflammatory and immunomodulatory properties to treat various tumors. The influential anti-inflammatory and immunomodulatory properties of CB make it a potential therapeutic agent against liver cancer by modulating the TME and inhibiting M2-TAM macrophage polarization through the Wnt/ β -catenin pathway (Figure 9). Its suppressive effects and ability to target the Wnt pathway offer a novel approach to cancer therapy, potentially leading to progressive advances in malignancy treatment.

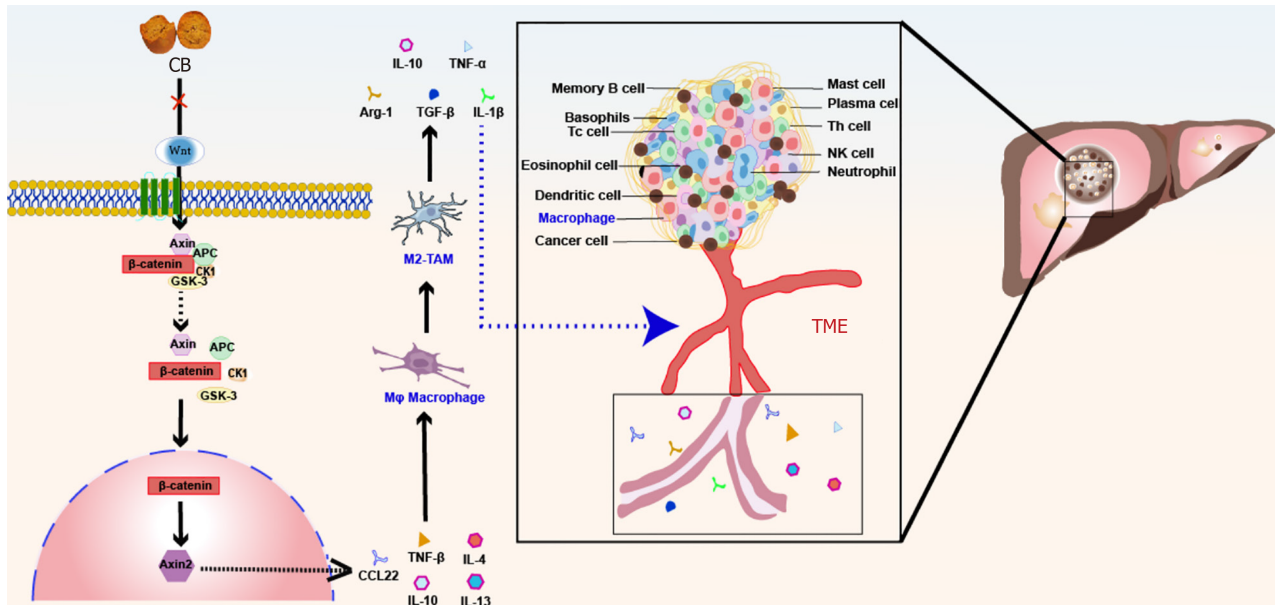


Figure 9 Schematic diagram of anti-liver cancer mechanism of *Calculus bovis*. *Calculus bovis* exerts its anti-liver cancer effect by inhibiting the Wnt/ β -catenin pathway and suppressing the polarization of M2 tumor-associated macrophage. M2-TAMs: M2 tumor-associated macrophages; TME: Tumor microenvironment.

FOOTNOTES

Author contributions: Huang Z, Meng FY, Mei S, and Tian XF designed the study; Huang Z, Meng FY, Lu LZ, Guo QQ, Deng Z, Zou B, and Long HP performed the experiments, and acquired and analyzed the data; Huang Z, Meng FY, Lu LZ, and Guo QQ prepared the figures and tables; Huang Z, Meng FY, Lu LZ, Guo QQ, Lv CJ, Tan NH, Deng Z, Chen JY, Zhang ZS, Zhou Q, Mei S, and Tian XF reviewed and edited the manuscript. All authors reviewed and approved the final version of the article. Huang Z and Meng FY are designated as co-first authors due to their nearly equal contributions across various aspects of the project, including study design, data collection and analysis, and manuscript writing. Their dedication and efforts in these crucial stages highlight their high level of collaboration and professional competence, which has ensured the smooth progress and high quality of the research. The comparable workload and impact of both authors justify their co-first author designation, reflecting their significant contributions fairly. Additionally, the research team comprises members with diverse expertise and skills across multiple disciplines. This diversity forms a solid foundation for the study, ensuring its comprehensiveness and reliability. The designation of co-first authors not only exemplifies the collaborative spirit and professional standards within the team but also enhances the scientific rigor and integrity of the paper. The reasons for designating Tian XF and Mei S as co-corresponding authors are threefold. First, both authors have made equally important contributions to the research work and have invested equal amounts of effort in writing the paper and designing the experiments. To be fair, they are listed as co-corresponding authors. Second, both authors have made significant contributions in their respective fields and have assumed different responsibilities in the paper. Their joint communication better reflects the nature of interdisciplinary cooperation. Third, having two corresponding authors provides a wider range of contact channels for readers to communicate and discuss with the research team, improving the dissemination and influence of the research work.

Supported by National Natural Science Foundation of China, No. 82074450; Education Department of Hunan Province, No. 21A0243, No. 21B0374, No. 22B0397, and No. 22B0392; Research Project of "Academician Liu Liang Workstation" of Hunan University of Traditional Chinese Medicine, No. 21YS003; Hunan Administration of Traditional Chinese Medicine, No. B2023001 and No. B2023009; and Hunan Provincial Natural Science Foundation of China, No. 2023JJ40481.

Institutional animal care and use committee statement: All animal experiments were conducted according to a protocol approved by the Ethical Review Committee of Experimental Animal Welfare at Slacker Jingda Laboratory, Changsha, Hunan (No. IACUC-SJA2022105).

Conflict-of-interest statement: The authors declare that they have no competing interests to disclose.

Data sharing statement: Dataset is available from the corresponding author at 003640@hnu cm.edu.cn. Participants gave informed consent for data sharing.

ARRIVE guidelines statement: The authors have read the ARRIVE guidelines, and the manuscript was prepared and revised according to the ARRIVE guidelines.

Open-Access: This article is an open-access article that was selected by an in-house editor and fully peer-reviewed by external reviewers. It is distributed in accordance with the Creative Commons Attribution NonCommercial (CC BY-NC 4.0) license, which permits others to distribute, remix, adapt, build upon this work non-commercially, and license their derivative works on different terms, provided the original work is properly cited and the use is non-commercial. See: <https://creativecommons.org/licenses/by-nc/4.0/>

Country of origin: China

ORCID number: Zhen Huang 0000-0002-8437-7141; Zhe Deng 0000-0002-3283-6289; Hong-Ping Long 0000-0001-8891-5851; Qing Zhou 0000-0002-9633-7542; Sha Tian 0000-0002-2557-5674; Si Mei 0000-0002-4263-1121; Xue-Fei Tian 0000-0003-4786-0844.

S-Editor: Qu XL

L-Editor: Wang TQ

P-Editor: Zhao YQ

REFERENCES

- Peng J, Lü M, Peng Y, Tang X. Global incidence of primary liver cancer by etiology among children, adolescents, and young adults. *J Hepatol* 2023; **79**: e92-e94 [PMID: 36841544 DOI: 10.1016/j.jhep.2023.02.019]
- Laface C, Fedele P, Maselli FM, Ambrogio F, Foti C, Molinari P, Ammendola M, Lioce M, Ranieri G. Targeted Therapy for Hepatocellular Carcinoma: Old and New Opportunities. *Cancers (Basel)* 2022; **14** [PMID: 36011021 DOI: 10.3390/cancers14164028]
- Muñoz-Martínez S, Iserte G, Sanduzzi-Zamparelli M, Llarch N, Reig M. Current pharmacological treatment of hepatocellular carcinoma. *Curr Opin Pharmacol* 2021; **60**: 141-148 [PMID: 34418875 DOI: 10.1016/j.coph.2021.07.009]
- Rizzo A, Ricci AD, Brandi G. Trans-Arterial Chemoembolization Plus Systemic Treatments for Hepatocellular Carcinoma: An Update. *J Pers Med* 2022; **12** [PMID: 36579504 DOI: 10.3390/jpm12111788]
- Xu B, Sun HC. Camrelizumab: an investigational agent for hepatocellular carcinoma. *Expert Opin Investig Drugs* 2022; **31**: 337-346 [PMID: 34937475 DOI: 10.1080/13543784.2022.2022121]
- Maki H, Hasegawa K. Advances in the surgical treatment of liver cancer. *Biosci Trends* 2022; **16**: 178-188 [PMID: 35732434 DOI: 10.5582/bst.2022.01245]
- Dall'Olio FG, Rizzo A, Mollica V, Massucci M, Maggio I, Massari F. Immortal time bias in the association between toxicity and response for immune checkpoint inhibitors: a meta-analysis. *Immunotherapy* 2021; **13**: 257-270 [PMID: 33225800 DOI: 10.2217/imt-2020-0179]
- Rizzo A, Mollica V, Tateo V, Tassinari E, Marchetti A, Rosellini M, De Luca R, Santoni M, Massari F. Hypertransaminasemia in cancer patients receiving immunotherapy and immune-based combinations: the MOUSEION-05 study. *Cancer Immunol Immunother* 2023; **72**: 1381-1394 [PMID: 36695827 DOI: 10.1007/s00262-023-03366-x]
- Güven DC, Sahin TK, Erul E, Rizzo A, Ricci AD, Aksoy S, Yalcin S. The association between albumin levels and survival in patients treated with immune checkpoint inhibitors: A systematic review and meta-analysis. *Front Mol Biosci* 2022; **9**: 1039121 [PMID: 36533070 DOI: 10.3389/fmolb.2022.1039121]
- Wang K, Chen Q, Shao Y, Yin S, Liu C, Liu Y, Wang R, Wang T, Qiu Y, Yu H. Anticancer activities of TCM and their active components against tumor metastasis. *Biomed Pharmacother* 2021; **133**: 111044 [PMID: 33378952 DOI: 10.1016/j.biopha.2020.111044]
- Rizzo A, Ricci AD, Brandi G. Immune-based combinations for advanced hepatocellular carcinoma: shaping the direction of first-line therapy. *Future Oncol* 2021; **17**: 755-757 [PMID: 33508960 DOI: 10.2217/fon-2020-0986]
- Rizzo A, Ricci AD, Brandi G. Systemic adjuvant treatment in hepatocellular carcinoma: tempted to do something rather than nothing. *Future Oncol* 2020; **16**: 2587-2589 [PMID: 32772560 DOI: 10.2217/fon-2020-0669]
- Rui R, Zhou L, He S. Cancer immunotherapies: advances and bottlenecks. *Front Immunol* 2023; **14**: 1212476 [PMID: 37691932 DOI: 10.3389/fimmu.2023.1212476]
- Li JJ, Liang Q, Sun GC. Traditional Chinese medicine for prevention and treatment of hepatocellular carcinoma: A focus on epithelial-mesenchymal transition. *J Integr Med* 2021; **19**: 469-477 [PMID: 34538644 DOI: 10.1016/j.joim.2021.08.004]
- Shi J, Zhu L, Tang BY, Yang WQ, Xi SY, Zhang CL, Li PF, Wang YJ, Guo KH, Huang JR, Huang CR, Yu ZX, Yu BK, Zhang CF, Zhang YM. Regulatory effect of Yinchenhao decoction on bile acid metabolism to improve the inflammatory microenvironment of hepatocellular carcinoma in mice. *J Nat Med* 2024; **78**: 633-643 [PMID: 38704807 DOI: 10.1007/s11418-024-01812-3]
- Sharma A, Seow JJW, Dutertre CA, Pai R, Blériot C, Mishra A, Wong RMM, Singh GSN, Sudhagar S, Khalilnezhad S, Erdal S, Teo HM, Khalilnezhad A, Chakarov S, Lim TKH, Fui ACY, Chieh AKW, Chung CP, Bonney GK, Goh BK, Chan JKY, Chow PKH, Ginhoux F, DasGupta R. Onco-fetal Reprogramming of Endothelial Cells Drives Immunosuppressive Macrophages in Hepatocellular Carcinoma. *Cell* 2020; **183**: 377-394.e21 [PMID: 32976798 DOI: 10.1016/j.cell.2020.08.040]
- Yunna C, Mengru H, Lei W, Weidong C. Macrophage M1/M2 polarization. *Eur J Pharmacol* 2020; **877**: 173090 [PMID: 32234529 DOI: 10.1016/j.ejphar.2020.173090]
- Sica A, Erreni M, Allavena P, Porta C. Macrophage polarization in pathology. *Cell Mol Life Sci* 2015; **72**: 4111-4126 [PMID: 26210152 DOI: 10.1007/s00018-015-1995-y]
- Yang Y, Ye YC, Chen Y, Zhao JL, Gao CC, Han H, Liu WC, Qin HY. Crosstalk between hepatic tumor cells and macrophages via Wnt/ β -catenin signaling promotes M2-like macrophage polarization and reinforces tumor malignant behaviors. *Cell Death Dis* 2018; **9**: 793 [PMID: 30022048 DOI: 10.1038/s41419-018-0818-0]
- Mano Y, Aishima S, Fujita N, Tanaka Y, Kubo Y, Motomura T, Taketomi A, Shirabe K, Maehara Y, Oda Y. Tumor-associated macrophage promotes tumor progression via STAT3 signaling in hepatocellular carcinoma. *Pathobiology* 2013; **80**: 146-154 [PMID: 23364389 DOI: 10.1159/000346196]

- 21 Cox N, Pokrovskii M, Vicario R, Geissmann F. Origins, Biology, and Diseases of Tissue Macrophages. *Annu Rev Immunol* 2021; **39**: 313-344 [PMID: 33902313 DOI: 10.1146/annurev-immunol-093019-111748]
- 22 Cronan MR, Beerman RW, Rosenberg AF, Saelens JW, Johnson MG, Oehlers SH, Sisk DM, Jurcic Smith KL, Medvitz NA, Miller SE, Trinh LA, Fraser SE, Madden JF, Turner J, Stout JE, Lee S, Tobin DM. Macrophage Epithelial Reprogramming Underlies Mycobacterial Granuloma Formation and Promotes Infection. *Immunity* 2016; **45**: 861-876 [PMID: 27760340 DOI: 10.1016/j.immuni.2016.09.014]
- 23 Fidler IJ, Schroit AJ. Recognition and destruction of neoplastic cells by activated macrophages: discrimination of altered self. *Biochim Biophys Acta* 1988; **948**: 151-173 [PMID: 3052591 DOI: 10.1016/0304-419x(88)90009-1]
- 24 Naramore S, Virojanapa A, Bell M, Jhaveri PN. Bezoar in a Pediatric Oncology Patient Treated with Coca-Cola. *Case Rep Gastroenterol* 2015; **9**: 227-232 [PMID: 26269699 DOI: 10.1159/000431217]
- 25 Dimin N, Zhe D, Yongrong W, Si M, Yongjie T, Qing Z, Xuefei T. Niu Huang (Bovis Calculus)-Shexiang (Moschus) combination induces apoptosis and inhibits proliferation in hepatocellular carcinoma via PI3K/AKT/mTOR pathway. *Digit Chin Med* 2022; **5**: 83-92 [DOI: 10.1016/j.dcm.2022.03.009]
- 26 Yu ZJ, Xu Y, Peng W, Liu YJ, Zhang JM, Li JS, Sun T, Wang P. Calculus bovis: A review of the traditional usages, origin, chemistry, pharmacological activities and toxicology. *J Ethnopharmacol* 2020; **254**: 112649 [PMID: 32068140 DOI: 10.1016/j.jep.2020.112649]
- 27 Zhang Z, Zeng P, Gao W, Wu R, Deng T, Chen S, Tian X. Exploration of the Potential Mechanism of Calculus Bovis in Treatment of Primary Liver Cancer by Network Pharmacology. *Comb Chem High Throughput Screen* 2021; **24**: 129-138 [PMID: 32772910 DOI: 10.2174/1386207323666200808172051]
- 28 Xiang D, Liu Y, Zu Y, Yang J, He W, Zhang C, Liu D. Calculus Bovis Sativus alleviates estrogen cholestasis-induced gut and liver injury in rats by regulating inflammation, oxidative stress, apoptosis, and bile acid profiles. *J Ethnopharmacol* 2023; **302**: 115854 [PMID: 36273746 DOI: 10.1016/j.jep.2022.115854]
- 29 Deng Y, Ren H, Ye X, Xia L, Liu M, Liu Y, Yang M, Yang S, Ye X, Zhang J. Integrated Phytochemical Analysis Based on UPLC-Q-TOF-MS/MS, Network Pharmacology, and Experiment Verification to Explore the Potential Mechanism of Platycodon grandiflorum for Chronic Bronchitis. *Front Pharmacol* 2020; **11**: 564131 [PMID: 33013400 DOI: 10.3389/fphar.2020.564131]
- 30 Liu H, Mohammed SAD, Lu F, Chen P, Wang Y, Liu S. Network Pharmacology and Molecular Docking-Based Mechanism Study to Reveal Antihypertensive Effect of Gedan Jiangya Decoction. *Biomed Res Int* 2022; **2022**: 3353464 [PMID: 36046450 DOI: 10.1155/2022/3353464]
- 31 Pai SG, Cameiro BA, Mota JM, Costa R, Leite CA, Barroso-Sousa R, Kaplan JB, Chae YK, Giles FJ. Wnt/beta-catenin pathway: modulating anticancer immune response. *J Hematol Oncol* 2017; **10**: 101 [PMID: 28476164 DOI: 10.1186/s13045-017-0471-6]
- 32 Miao TG, Nan YM. [Hepatocellular carcinoma immune microenvironment]. *Zhonghua Gan Zang Bing Za Zhi* 2022; **30**: 923-930 [PMID: 36299184 DOI: 10.3760/cma.j.cn501113-20220703-00365]
- 33 Gou H, Su H, Liu D, Wong CC, Shang H, Fang Y, Zeng X, Chen H, Li Y, Huang Z, Fan M, Wei C, Wang X, Zhang X, Li X, Yu J. Traditional Medicine Pien Tze Huang Suppresses Colorectal Tumorigenesis Through Restoring Gut Microbiota and Metabolites. *Gastroenterology* 2023; **165**: 1404-1419 [PMID: 37704113 DOI: 10.1053/j.gastro.2023.08.052]
- 34 Xu HB, Chen XZ, Wang X, Pan J, Yi-Zhuo Z, Zhou CH. Xihuang pill in the treatment of cancer: TCM theories, pharmacological activities, chemical compounds and clinical applications. *J Ethnopharmacol* 2023; **316**: 116699 [PMID: 37257709 DOI: 10.1016/j.jep.2023.116699]
- 35 Wang W, Smits R, Hao H, He C. Wnt/ β -Catenin Signaling in Liver Cancers. *Cancers (Basel)* 2019; **11** [PMID: 31269694 DOI: 10.3390/cancers11070926]
- 36 Long G, Wu Z, Wang D, Mi X, Hu K, Zhou L, Tang J. UCHL3 inhibits ferroptosis by stabilizing β -catenin and maintains stem-like properties of hepatocellular carcinoma cells. *Free Radic Biol Med* 2024; **212**: 162-173 [PMID: 38092274 DOI: 10.1016/j.freeradbiomed.2023.11.030]
- 37 Chen Y, Yang Y, Wang N, Liu R, Wu Q, Pei H, Li W. β -Sitosterol suppresses hepatocellular carcinoma growth and metastasis via FOXM1-regulated Wnt/ β -catenin pathway. *J Cell Mol Med* 2024; **28**: e18072 [PMID: 38063438 DOI: 10.1111/jcmm.18072]
- 38 Sen B, Aggarwal S, Nath R, Sehgal R, Singh R, Agrawal K, Shashidhara AN, Rastogi A, Bajpai M, Pamecha V, Trehanpati N, Ramakrishna G. Secretome of senescent hepatoma cells modulate immune cell fate by macrophage polarization and neutrophil extracellular traps formation. *Med Oncol* 2022; **39**: 134 [PMID: 35726030 DOI: 10.1007/s12032-022-01732-w]
- 39 Li XY, Su L, Jiang YM, Gao WB, Xu CW, Zeng CQ, Song J, Xu Y, Weng WC, Liang WB. The Antitumor Effect of Xihuang Pill on Treg Cells Decreased in Tumor Microenvironment of 4T1 Breast Tumor-Bearing Mice by PI3K/AKT-AP-1 Signaling Pathway. *Evid Based Complement Alternat Med* 2018; **2018**: 6714829 [PMID: 29849718 DOI: 10.1155/2018/6714829]
- 40 Xiang X, Wang J, Lu D, Xu X. Targeting tumor-associated macrophages to synergize tumor immunotherapy. *Signal Transduct Target Ther* 2021; **6**: 75 [PMID: 33619259 DOI: 10.1038/s41392-021-00484-9]
- 41 Cutolo M, Campitiello R, Gotelli E, Soldano S. The Role of M1/M2 Macrophage Polarization in Rheumatoid Arthritis Synovitis. *Front Immunol* 2022; **13**: 867260 [PMID: 35663975 DOI: 10.3389/fimmu.2022.867260]
- 42 Li Y, Jin K, van Pelt GW, van Dam H, Yu X, Mesker WE, Ten Dijke P, Zhou F, Zhang L. c-Myb Enhances Breast Cancer Invasion and Metastasis through the Wnt/ β -Catenin/Axin2 Pathway. *Cancer Res* 2016; **76**: 3364-3375 [PMID: 27197202 DOI: 10.1158/0008-5472.CAN-15-2302]
- 43 Wu Y, Zheng L. Dynamic education of macrophages in different areas of human tumors. *Cancer Microenviron* 2012; **5**: 195-201 [PMID: 22696271 DOI: 10.1007/s12307-012-0113-z]
- 44 Wang C, Shen N, Guo Q, Tan X, He S. YAP/STAT3 inhibited CD8(+) T cells activity in the breast cancer immune microenvironment by inducing M2 polarization of tumor-associated macrophages. *Cancer Med* 2023; **12**: 16295-16309 [PMID: 37329188 DOI: 10.1002/cam4.6242]
- 45 de Carvalho TG, Lara P, Jorquera-Cordero C, Araújo CFS, de Santana Oliveira A, Garcia VB, de Paiva Souza SV, Schomann T, Soares LAL, da Matta Guedes PM, de Araújo Júnior RF. Inhibition of murine colorectal cancer metastasis by targeting M2-TAM through STAT3/NF- κ B/AKT signaling using macrophage 1-derived extracellular vesicles loaded with oxaliplatin, retinoic acid, and Libidibia ferrea. *Biomed Pharmacother* 2023; **168**: 115663 [PMID: 37832408 DOI: 10.1016/j.biopha.2023.115663]
- 46 He S, Lu M, Zhang L, Wang Z. RSK4 promotes the macrophage recruitment and M2 polarization in esophageal squamous cell carcinoma. *Biochim Biophys Acta Mol Basis Dis* 2024; **1870**: 166996 [PMID: 38142759 DOI: 10.1016/j.bbdis.2023.166996]

Defining failure of endoluminal biliary drainage in the era of endoscopic ultrasound and lumen apposing metal stents

Faisal S Ali, Sushovan Guha

Specialty type: Gastroenterology and hepatology

Provenance and peer review: Invited article; Externally peer reviewed.

Peer-review model: Single blind

Peer-review report's classification

Scientific Quality: Grade C

Novelty: Grade B

Creativity or Innovation: Grade B

Scientific Significance: Grade B

P-Reviewer: Nicolae N

Received: April 8, 2024

Revised: May 12, 2024

Accepted: July 18, 2024

Published online: August 7, 2024

Processing time: 111 Days and 21.4 Hours



Faisal S Ali, Department of Gastroenterology, Hepatology, and Nutrition, University of Texas Health Science Center at Houston, Houston, TX 77054, United States

Sushovan Guha, Department of Clinical Sciences, Tilman J. Fertitta Family College of Medicine, University of Houston, Houston, TX 77204, United States

Corresponding author: Sushovan Guha, MD, PhD, AGAF, FASGE, Professor, Department of Clinical Sciences, Tilman J. Fertitta Family College of Medicine, University of Houston, 5055 Medical Cir, Houston, TX 77204, United States. sguha@hrgastro.com

Abstract

The role of endoscopy in pathologies of the bile duct and gallbladder has seen notable advancements over the past two decades. With advancements in stent technology, such as the development of lumen-apposing metal stents, and adoption of endoscopic ultrasound and electrosurgical principles in therapeutic endoscopy, what was once considered endoscopic failure has transformed into failure of an approach that could be salvaged by a second- or third-line endoscopic strategy. Incorporation of these advancements in routine patient care will require formal training and multidisciplinary acceptance of established techniques and collaboration for advancement of experimental techniques to generate robust evidence that can be utilized to serve patients to the best of our ability.

Key Words: Endoscopic ultrasound; Guided biliary drainage; Gallbladder; Biliary obstruction; Lumen-apposing metal stent

©The Author(s) 2024. Published by Baishideng Publishing Group Inc. All rights reserved.

Core Tip: For malignant distal biliary obstruction, endoscopic ultrasound (EUS)-guided choledochoduodenostomy is noninferior to endoscopic retrograde cholangiopancreatography (ERCP) with biliary stent placement, and can be considered as a primary drainage modality instead of a salvage method. In cases with malignant hilar biliary obstruction, combined ERCP with EUS-biliary drainage (CERES), when performed in the appropriate patient, can not only provide bilateral drainage but also establish communication of the right and left intrahepatic biliary systems through bridging intra-hepatic stenting. EUS-guided gallbladder drainage (EUS-GBD) is increasingly being recognized as a feasible and efficacious treatment modality and should be considered in the management of cholecystitis in a multidisciplinary setting. EUS-GBD can also be incorporated in the algorithm of management of distal or hilar biliary obstruction, either as a prophylactic or a therapeutic strategy.

Citation: Ali FS, Guha S. Defining failure of endoluminal biliary drainage in the era of endoscopic ultrasound and lumen apposing metal stents. *World J Gastroenterol* 2024; 30(29): 3534-3537

URL: <https://www.wjgnet.com/1007-9327/full/v30/i29/3534.htm>

DOI: <https://dx.doi.org/10.3748/wjg.v30.i29.3534>

TO THE EDITOR

Biliary interventional endoscopy refers to the ability to treat pathologies of the biliary tract through a non-surgical, endoluminal approach. The availability of fluoroscopy, coupled with endoscopic ability to access the biliary system through the ampulla of Vater, gave rise to the now well-established modality, endoscopic retrograde cholangiopancreatography (ERCP)[1]. As expertise with ERCP grew, our ability to treat and palliate expanded to encompass pathologies of the biliary system which were historically managed with surgery. While this opened new avenues, it also unveiled new challenges that highlighted the need to evolve beyond ERCP through technological innovation and novel thought to address unmet needs of patients with limited options for management of their malady. This milieu led to innovations such as endoscopic ultrasound (EUS) and development of the lumen-apposing metal stent (LAMS), both major milestones which continue to improve our ability to manage biliary pathologies.

Traditionally, failure of endoscopic biliary drainage meant failure of ERCP, subjecting patients to percutaneous biliary drainage (PTBD). Although PTBD is a valuable treatment option, one could argue that it adversely impacts patients' quality of life due to its external attachments. In the current era, the availability of EUS and LAMS have served to redefine failure of endoscopic biliary drainage, as has been highlighted by Fugazza *et al*[2], who shed light on the role of EUS-guided biliary drainage (EUS-BD) in the management of gallbladder and biliary tree pathologies.

In malignant distal biliary obstruction (MDBO), EUS-choledochoduodenostomy (EUS-CDS) historically served as a salvage modality in the setting of ERCP failure. This stepwise approach allowed expansion of endoscopic techniques available for biliary decompression in patients with MDBO. As experience with EUS-CDS grew, its technical equivalency to ERCP in the setting of MDBO became evident; EUS-CDS has now been shown to be noninferior to ERCP in the ELEMENT and DRA-MBO clinical trials[3,4], and as such one may perform EUS-CDS as a primary drainage modality in appropriately selected patients. The question of cost-effectiveness of EUS-CDS as a primary drainage modality compared to ERCP in MDBO remains to be answered. In countries where LAMS are unavailable, EUS-BD still serves a useful purpose in the setting of MDBO by providing rendezvous access to allow transpapillary biliary drainage, particularly when MDBO leads to ampullary distortion.

In cases with malignant hilar biliary obstruction (MHBO), EUS-BD can serve as an adjuvant drainage modality that is to be used alongside ERCP; the utility of combined ERCP with EUS-BD (CERES) allows applicability of EUS-BD in multiple configurations (Figure 1)[5,6]. The techniques of EUS-BD studied in the setting of MHBO can serve to prolong the efficacy of endoscopic biliary drainage, potentially delaying PTBD in appropriately selected patients, thereby preserving their quality of life. EUS-BD can also establish bilateral drainage of the liver in cases with high grade MHBO with non-communicating left and right biliary systems by performing bridging intra-hepatic stenting along with a hepaticogastrostomy[7]. Put together, these are promising avenues that warrant further exploration in randomized trials to validate the utility of EUS-BD in MHBO as has been done in the setting of MDBO.

The presence or absence of gallbladder can materially alter the course of management in the setting of biliary obstruction. In the case of both MDBO and MHBO, EUS-guided gallbladder drainage (EUS-GBD) can be performed prophylactically or therapeutically. Preliminary data on EUS-GBD addressed the utility of this technique as a rescue modality, with promising results, as summarized by Fugazza *et al*[2]. Similar to EUS-BD, the role of EUS-GBD has evolved beyond a rescue technique and carries the potential to be incorporated in the algorithm of biliary drainage in malignant cases as a prophylactic measure. Such an approach may be of utility in cases where biliary stent placement poses the risk of cystic duct obstruction and cholecystitis; in cases with MHBO, incorporating EUS-GBD can be considered an extension of CERES, allowing bilateral drainage of the biliary tree, and maintaining gallbladder outflow. The utility of EUS-GBD has been shown primarily in the setting of cholecystitis, particularly for patients who are unfit for surgery. In the current era, incorporation of a multidisciplinary team consisting of surgeons, interventional radiologists, and interventional endoscopists to drive therapeutic decision-making in the setting of acute cholecystitis should be considered standard practice in resource-rich health systems and tertiary care centers, and will serve to increase adoption of EUS-GBD in appropriately selected patients (Figure 2)[8]. Lithotripsy after EUS-GBD in patients with cholelithiasis is an additional

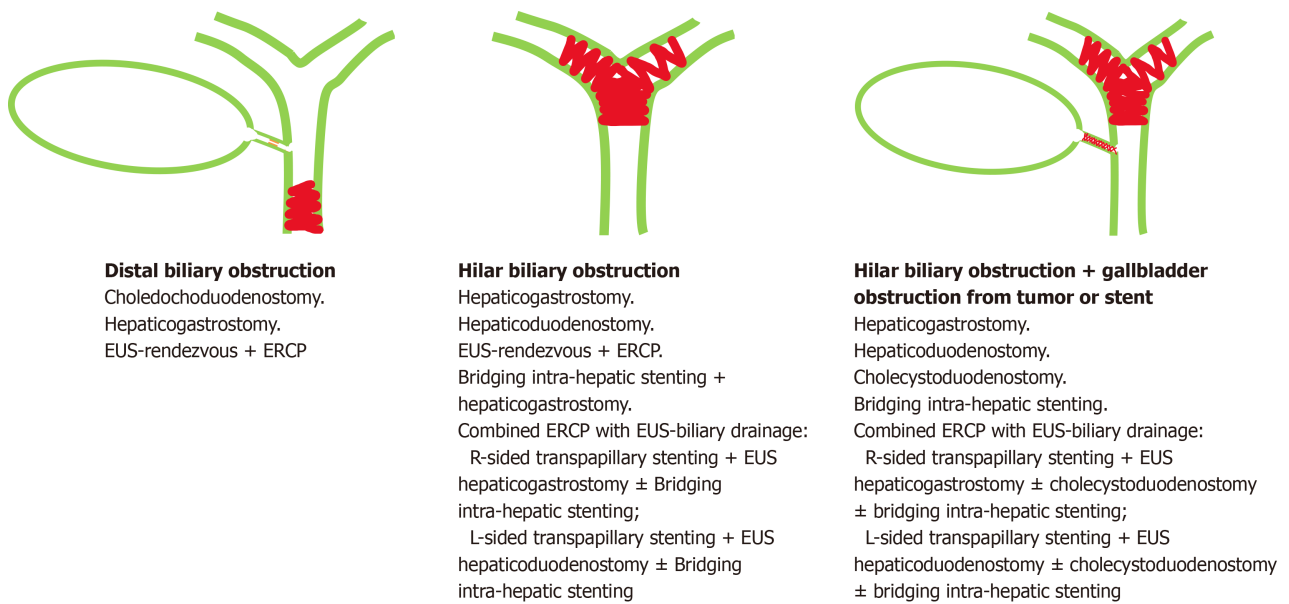


Figure 1 Role of endoscopic ultrasound-guided biliary drainage in various forms of obstruction. EUS: Endoscopic ultrasound; ERCP: Endoscopic retrograde cholangiopancreatography.

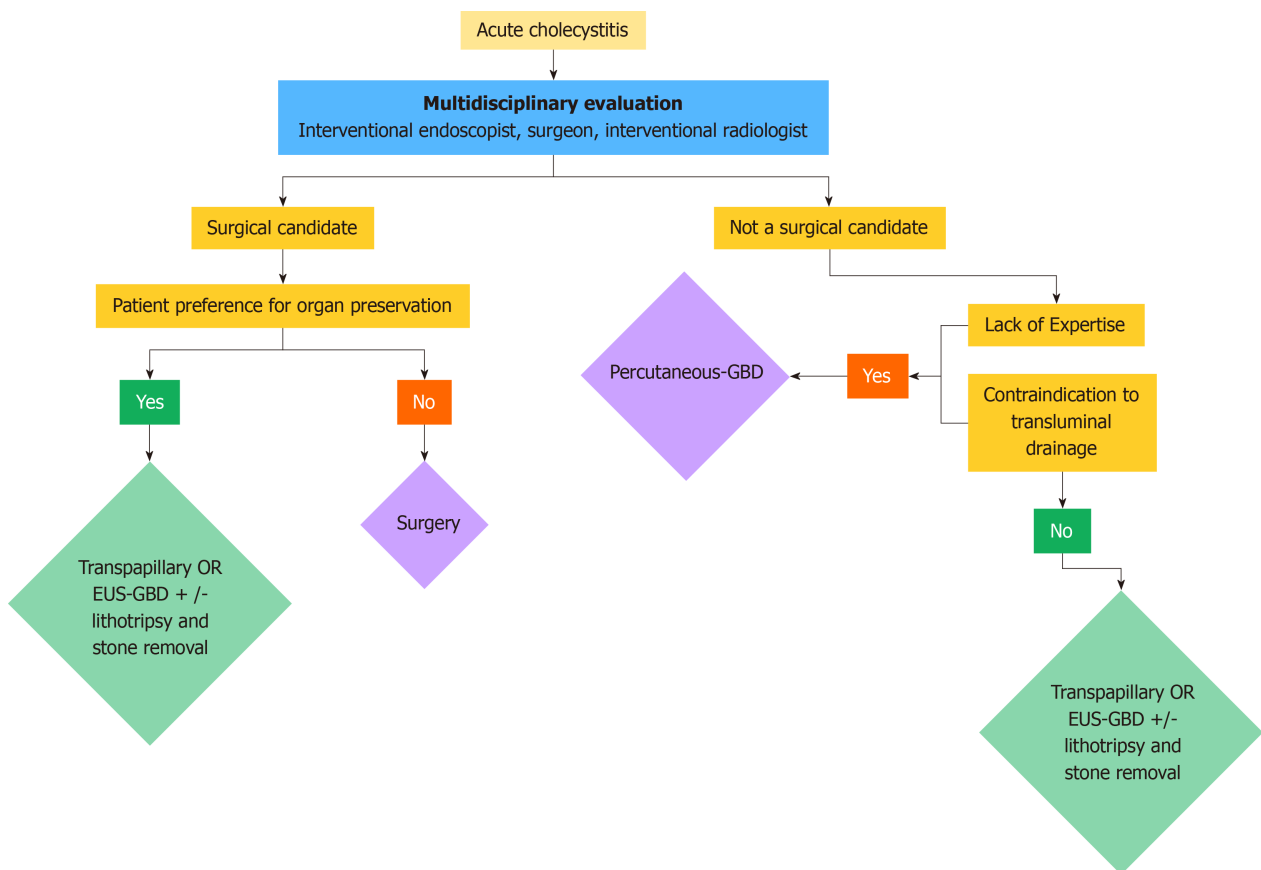


Figure 2 Potential approach to multidisciplinary management of acute cholecystitis. EUS: Endoscopic ultrasound; GBD: Gallbladder drainage.

treatment strategy that is currently in its infancy but will undoubtedly be explored in a robust manner in the near future [9]. Above all, long-term safety, reproducibility, and the ability to train proceduralists in these evolving techniques will be paramount in driving progress of therapeutic biliary endoscopy.

CONCLUSION

As the armamentarium of interventional endoscopy continues to grow, the definition of “failure” as it pertains to the ability to achieve endobiliary drainage will continue to evolve to the point where a majority of patients can be offered one of the many potential therapeutic modalities to achieve adequate biliary drainage, be it through the biliary tree or the gallbladder.

FOOTNOTES

Author contributions: Ali FS drafted the manuscript; Ali FS and Guha S contributed to the inception; Guha S participated in the final approval of this manuscript.

Conflict-of-interest statement: All the authors report no relevant conflicts of interest for this article.

Open-Access: This article is an open-access article that was selected by an in-house editor and fully peer-reviewed by external reviewers. It is distributed in accordance with the Creative Commons Attribution NonCommercial (CC BY-NC 4.0) license, which permits others to distribute, remix, adapt, build upon this work non-commercially, and license their derivative works on different terms, provided the original work is properly cited and the use is non-commercial. See: <https://creativecommons.org/licenses/by-nc/4.0/>

Country of origin: United States

ORCID number: Faisal S Ali 0000-0001-7372-5158; Sushovan Guha 0009-0001-5954-3603.

S-Editor: Wang JJ

L-Editor: A

P-Editor: Zhao YQ

REFERENCES

- 1 **Fujita R.** The History of ERCP and EUS. In: Mine T, Fujita R. *Advanced Therapeutic Endoscopy for Pancreatico-Biliary Diseases*. Tokyo: Springer, 2019
- 2 **Fugazza A, Khalaf K, Pawlak KM, Spadaccini M, Colombo M, Andreozzi M, Giacchetto M, Carrara S, Ferrari C, Binda C, Mangiavillano B, Anderloni A, Repici A.** Use of endoscopic ultrasound-guided gallbladder drainage as a rescue approach in cases of unsuccessful biliary drainage. *World J Gastroenterol* 2024; **30**: 70-78 [PMID: 38293324 DOI: 10.3748/wjg.v30.i1.70]
- 3 **Chen YI, Sahai A, Donatelli G, Lam E, Forbes N, Mosko J, Paquin SC, Donnellan F, Chatterjee A, Telford J, Miller C, Desilets E, Sandha G, Kenschil S, Mohamed R, May G, Gan I, Barkun J, Calo N, Nawawi A, Friedman G, Cohen A, Maniere T, Chaudhury P, Metrakos P, Zogopoulos G, Bessissow A, Khalil JA, Baffis V, Waschke K, Parent J, Soulellis C, Khashab M, Kunda R, Geraci O, Martel M, Schwartzman K, Fiore JF Jr, Rahme E, Barkun A.** Endoscopic Ultrasound-Guided Biliary Drainage of First Intent With a Lumen-Apposing Metal Stent vs Endoscopic Retrograde Cholangiopancreatography in Malignant Distal Biliary Obstruction: A Multicenter Randomized Controlled Study (ELEMENT Trial). *Gastroenterology* 2023; **165**: 1249-1261.e5 [PMID: 37549753 DOI: 10.1053/j.gastro.2023.07.024]
- 4 **Teoh AYB, Napoleon B, Kunda R, Arcidiacono PG, Kongkam P, Larghi A, Van der Merwe S, Jacques J, Legros R, Thawee RE, Saxena P, Aerts M, Archibugi L, Chan SM, Fumex F, Kaffes AJ, Ma MTW, Messaoudi N, Rizzatti G, Ng KKC, Ng EKW, Chiu PWY.** EUS-Guided Choledochoduodenostomy Using Lumen Apposing Stent Versus ERCP With Covered Metallic Stents in Patients With Unresectable Malignant Distal Biliary Obstruction: A Multicenter Randomized Controlled Trial (DRA-MBO Trial). *Gastroenterology* 2023; **165**: 473-482.e2 [PMID: 37121331 DOI: 10.1053/j.gastro.2023.04.016]
- 5 **Sundaram S, Dhir V.** EUS-guided biliary drainage for malignant hilar biliary obstruction: A concise review. *Endosc Ultrasound* 2021; **10**: 154-160 [PMID: 34137381 DOI: 10.4103/EUS-D-21-00004]
- 6 **Kongkam P, Tasneem AA, Rerknimitr R.** Combination of endoscopic retrograde cholangiopancreatography and endoscopic ultrasonography-guided biliary drainage in malignant hilar biliary obstruction. *Dig Endosc* 2019; **31** Suppl 1: 50-54 [PMID: 30994233 DOI: 10.1111/den.13371]
- 7 **Nakai Y, Kogure H, Isayama H, Koike K.** Endoscopic Ultrasound-Guided Biliary Drainage for Unresectable Hilar Malignant Biliary Obstruction. *Clin Endosc* 2019; **52**: 220-225 [PMID: 30472818 DOI: 10.5946/ce.2018.094]
- 8 **Irani SS, Sharzehi K, Siddiqui UD.** AGA Clinical Practice Update on Role of EUS-Guided Gallbladder Drainage in Acute Cholecystitis: Commentary. *Clin Gastroenterol Hepatol* 2023; **21**: 1141-1147 [PMID: 36967319 DOI: 10.1016/j.cgh.2022.12.039]
- 9 **Quoraishi S, Ahmed J, Ponsford A, Rasheed A.** Lessons learnt from a case of extracorporeal shockwave lithotripsy for a residual gallbladder stone. *Int J Surg Case Rep* 2017; **32**: 43-46 [PMID: 28235649 DOI: 10.1016/j.ijscr.2017.02.001]



Evaluating the role of large language models in inflammatory bowel disease patient information

Eun Jeong Gong, Chang Seok Bang

Specialty type: Gastroenterology and hepatology

Provenance and peer review: Invited article; Externally peer reviewed.

Peer-review model: Single blind

Peer-review report's classification

Scientific Quality: Grade B

Novelty: Grade A

Creativity or Innovation: Grade B

Scientific Significance: Grade B

P-Reviewer: Dai YC

Received: May 27, 2024

Revised: July 15, 2024

Accepted: July 22, 2024

Published online: August 7, 2024

Processing time: 62 Days and 23.8 Hours



Eun Jeong Gong, Chang Seok Bang, Department of Internal Medicine, Hallym University College of Medicine, Chuncheon 24253, Gangwon-do, South Korea

Corresponding author: Chang Seok Bang, MD, PhD, Associate Professor, Doctor, Department of Internal Medicine, Hallym University College of Medicine, Sakju-ro 77, Chuncheon 24253, Gangwon-do, South Korea. csbang@hallym.ac.kr

Abstract

This letter evaluates the article by Gravina *et al* on ChatGPT's potential in providing medical information for inflammatory bowel disease patients. While promising, it highlights the need for advanced techniques like reasoning + action and retrieval-augmented generation to improve accuracy and reliability. Emphasizing that simple question and answer testing is insufficient, it calls for more nuanced evaluation methods to truly gauge large language models' capabilities in clinical applications.

Key Words: Crohn's disease; Ulcerative colitis; Inflammatory bowel disease; Chat generative pre-trained transformer; Large language model; Artificial intelligence

©The Author(s) 2024. Published by Baishideng Publishing Group Inc. All rights reserved.

Core Tip: This commentary evaluates the article by Gravina *et al* on ChatGPT's potential in providing medical information for inflammatory bowel disease patients. While promising, it highlights the need for advanced techniques like reasoning + action and retrieval-augmented generation to improve accuracy, emphasizing that simple question-and-answer testing is insufficient for evaluating large language models' true capabilities.

Citation: Gong EJ, Bang CS. Evaluating the role of large language models in inflammatory bowel disease patient information. *World J Gastroenterol* 2024; 30(29): 3538-3540

URL: <https://www.wjgnet.com/1007-9327/full/v30/i29/3538.htm>

DOI: <https://dx.doi.org/10.3748/wjg.v30.i29.3538>

TO THE EDITOR

We are writing to express our thoughts on the recently published article by Gravina *et al*[1]. Gravina *et al*[1] assessed the capability of large language models (LLMs) like ChatGPT to provide plausible medical information to patients with inflammatory bowel disease (IBD). Despite identifying several limitations, the authors concluded that there is significant potential in using LLMs for this purpose[1].

One of the key insights from the article is the potential for ChatGPT to offer immediate and accessible information to patients. The authors correctly note that this could be particularly beneficial in providing preliminary guidance and answering common queries that patients may have about their condition. This aligns with the increasing trend of patients seeking health information online before consulting their healthcare providers.

However, the study also underscores significant limitations, such as the potential for outdated or inaccurate information. Given that medical knowledge is continuously evolving, it is crucial for artificial intelligence (AI) tools like ChatGPT to have mechanisms for regular updates to ensure the information provided is current and evidence-based[1]. This is especially important for chronic conditions like IBD, where treatment guidelines and best practices frequently change.

A pertinent question arises: Can LLMs truly perform inference? Current AI-based agents utilizing LLMs operate by either generating answers directly or referring to external tools if the LLM itself cannot provide an answer. These agents determine the necessary information, redefine the questions, call appropriate tools to extract information, analyze the extracted data, and iterate this process as needed to reach a final answer. This pattern, known as reasoning + action, closely mimics human problem-solving by iteratively refining questions and seeking relevant tools rather than merely retrieving similar past solutions[2].

The effectiveness of such an approach often hinges on prompt engineering. Enhanced prompt engineering can significantly improve the accuracy of LLM-generated answers by aligning queries more closely with the model's trained data and inference capabilities. Therefore, evaluating LLMs based on selected questions often reflects their proficiency in leveraging search tools to produce desired answers. Advanced prompt engineering techniques can potentially yield more accurate responses, indicating that simple question-and-answer testing might not fully capture an LLM's capabilities[3].

Moreover, the retrieval-augmented generation (RAG) technique enhances traditional LLMs by enabling real-time retrieval of external data not included in the training dataset, thus generating answers that integrate the latest information. This approach helps prevent hallucination and allows the model to utilize a broader knowledge base. However, standardized performance evaluation of these advanced techniques remains challenging due to the limited benchmarks available, making it difficult to assess using only a few representative questions[4].

Another important point raised by the authors is the issue of contextual understanding and empathy, which AI currently lacks. The physician-patient relationship is built on trust and understanding, and while AI can provide factual information, it cannot replace the nuanced, empathetic communication that healthcare providers offer. This aspect is particularly vital for managing chronic diseases that significantly impact patients' quality of life[1].

The authors' recommendation for further refinement and alignment of AI outputs with reliable medical databases is essential. Such improvements could enhance the accuracy and reliability of AI-generated medical information, making it a more robust tool for both patients and healthcare providers.

Despite these challenges, there is no doubt that LLMs, equipped with sophisticated learning datasets and RAG capabilities, hold promise for clinical application. However, evaluating their potential solely based on simple question-answer accuracy is inadequate. It is essential to consider the advanced techniques and iterative processes that significantly enhance the precision and reliability of LLM-generated medical information.

In conclusion, the article by Gravina *et al*[1] provides valuable insights into the current capabilities and limitations of AI in gastroenterology. While promising, further refinement and a more nuanced evaluation approach are crucial for realizing the full potential of AI in healthcare. Continued research and development, combined with rigorous validation against established medical standards, will be essential.

FOOTNOTES

Author contributions: Gong EJ and Bang CS contributed to conceptualization, methodology, investigation and wrote the original draft; Bang CS reviewed and edited the draft, and contributed to supervision; All authors have read and agreed to the published version of the manuscript.

Conflict-of-interest statement: The authors declare that they have no conflict of interest.

Open-Access: This article is an open-access article that was selected by an in-house editor and fully peer-reviewed by external reviewers. It is distributed in accordance with the Creative Commons Attribution NonCommercial (CC BY-NC 4.0) license, which permits others to distribute, remix, adapt, build upon this work non-commercially, and license their derivative works on different terms, provided the original work is properly cited and the use is non-commercial. See: <https://creativecommons.org/licenses/by-nc/4.0/>

Country of origin: South Korea

ORCID number: Eun Jeong Gong 0000-0003-3996-3472; Chang Seok Bang 0000-0003-4908-5431.

S-Editor: Fan M

L-Editor: A

P-Editor: Yu HG

REFERENCES

- 1 **Gravina AG**, Pellegrino R, Cipullo M, Palladino G, Imperio G, Ventura A, Auletta S, Ciamarra P, Federico A. May ChatGPT be a tool producing medical information for common inflammatory bowel disease patients' questions? An evidence-controlled analysis. *World J Gastroenterol* 2024; **30**: 17-33 [PMID: [38293321](#) DOI: [10.3748/wjg.v30.i1.17](#)]
- 2 **Verma M**, Bhambri S, Kambhampati S. On the Brittle Foundations of ReAct Prompting for Agentic Large Language Models. 2024 Preprint. Available from: arXiv 2405. 13966 [DOI: [10.48550/arXiv.2405.13966](#)]
- 3 **Kim HJ**, Gong EJ, Bang CS. Application of Machine Learning Based on Structured Medical Data in Gastroenterology. *Biomimetics (Basel)* 2023; **8**: 512 [PMID: [37999153](#) DOI: [10.3390/biomimetics8070512](#)]
- 4 **Guinet G**, Omidvar-Tehrani B, Deoras A, Callot L. Automated Evaluation of Retrieval-Augmented Language Models with Task-Specific Exam Generation. 2024 Preprint. Available from: arXiv 2405. 13622 [DOI: [10.48550/arXiv.2405.13622](#)]



Published by **Baishideng Publishing Group Inc**
7041 Koll Center Parkway, Suite 160, Pleasanton, CA 94566, USA
Telephone: +1-925-3991568
E-mail: office@baishideng.com
Help Desk: <https://www.f6publishing.com/helpdesk>
<https://www.wjgnet.com>

